SCALING FISH ENERGETICS FROM INDIVIDUALS TO COMMUNITIES

Coral reef in Taveuni, Fiji. Photo credit: João Paulo Krajewski

Diego Barneche Rosado, BSc, MSc

Department of Biological Sciences
Macquarie University
Sydney, Australia

Principal Supervisor: Dr. Andrew P. Allen
Co-Supervisor: Dr. John Alroy

This thesis is presented for the degree of Doctor of Philosophy

November 2015

Esta tese é dedicada ao meu amado sobrinho e afilhado,

João Victor Petry Rosado.

TABLE OF CONTENTS

LIST OF FIGURES AND TABLES

Tables

STATEMENT OF CANDIDATE

I certify that the work in this thesis entitled "*Scaling fish energetics from individuals to communities*" has not previously been submitted for a degree nor has it been submitted as part or requirements for a degree to any other university or institution other than Macquarie University.

I also certify that the thesis is an original piece of research and it has been written by me. Any help and assistance that I have received in my research work and the preparation of the thesis itself have been appropriately acknowledged. In addition, I certify that all information sources and literature used are indicated in thesis.

Diego Barneche Rosado

42621445

SUMMARY

Two distinct biological currencies – energy and materials – are essential to life because both are required for the maintenance, growth, and reproduction of organisms. Modelling ecological phenomena on the basis of these currencies therefore holds potential for developing a deeper understanding of how the availability of energy and materials in the environment constrains life, in all its diversity, across space and time. In this dissertation, I use the Metabolic Theory of Ecology (MTE) as a framework to explore how individual energetics influences biological processes at distinct levels of organization, from individuals to communities. Particularly, I explore how body mass, environmental temperature, and other variables constrain (*i*) metabolic rates and growth rates of individuals, and thereby influence (*ii*) densities of populations at different trophic levels and (*iii*) the standing biomass and energy fluxes of communities that differ substantially in species diversity. I use fishes to address these questions because they encompass the highest species richness among vertebrates, they encompass more than seven orders of magnitude in body mass, and they occupy diverse habitats that vary substantially in thermal regime across the globe. At the individual level, MTE predictions are generally well supported, although deviations attributable to differences among taxa are clearly noted. By contrast, at the population and community levels, while I do find evidence of energetic constraints, deviations from MTE-derived predictions are frequently observed, highlighting the importance of factors other than individual energetics. I conclude by discussing the implications of these findings to climate change biology and ecosystem dynamics, and highlight avenues for future research.

ACKNOWLEDGEMENTS

I will be forever grateful to my amazing mentor, Andrew Allen, for the continuous support he provided me during my candidature. Thanks for teaching me the great value of theory and quantitative approaches in ecology, and how to be careful and critical of my own research. Most importantly, you have been a great role model of supervision and collaboration, presenting a great balance between guidance, counseling and collaboration.

I also thank my parents, sister and brother who have always been supportive of my choices in life even if this meant being apart for so long. Thanks for giving me all the tools to achieve my personal goals. My dear and loving wife, Priscila, who has always been there for me. You shared this PhD journey showing unconditional love and care, making my personal life happy and pleasant at all times. You are truly the most amazing person in my life. Thanks for putting up with my late hours, long trips away from home and work stress. I love you very much!

I owe a big thanks to many people at Macquarie who have taught me so much during this candidature. Matthew Kosnik, thanks for inviting me to so many field trips, greatly improving my diving skills. Thanks also for being a responsible and caring field coordinator - this has been an invaluable learning experience. Daniel Falster and Remko Duursma, thanks for providing me with the amazing opportunity to work on BAAD. Dan, you have been an amazing boss and collaborator, always fair and honest. It has certainly been the greatest academic experience outside my PhD project. Thanks to Rich Fitzjohn for being a great coding guru, always willing to help. I would also like to thank Josh Madin and John Alroy, who have both provided me with academic guidance at times during my candidature. Thanks to the amazing admin staff from the Biological Sciences Department, who were always ready and willing to help with a big smile on their faces: Marie, Laura, Veronica, Teresa, Sharyon and Anne Marie. Big thanks to Marie Herberstein and Tracy Rushmer who have provided

invaluable structural and financial support, particularly during the final few months of my candidature.

I thank my research collaborators who have been key in the development of this thesis: Sergio Floeter, Michel Kulbicki, Enrico Rezende, Alan Friedlander, Valeriano Parravicini, Cadu Ferreira, the GASPAR working group, and LBMM and LECAR folks. None of this would have been possible without your insightful and supportive collaboration. I also thank Greg Wilson and the Software Carpentry community for providing me with the amazing opportunity to learn how to be and act as a volunteer instructor. This partnership has certainly made a huge impact in the way I conduct my research.

Special thanks to my friends and colleagues down under: Adam Wilkins, Alex and Louise Bush, Daniel and Yian Noble, Joseph Maina, Julieta Martinelli, Lara Ainley, Linda Armbrecht, Marcela Diaz, Nick Chan, Osmar Luiz, Silvia Pineda, Toni Mizerek, and Wander and Stefanie Godinho. Thanks for sharing both happy and frustrating times during this PhD experience. Finally, I thank my great Brazilian friends Raphael Aggio and Mauricio Cantor who, despite the long distance, have been ‘Skypely’ present throughout this journey.

INTRODUCTION

Ecological systems exhibit bewildering complexity and diversity at all levels of organisation, from cells to ecosystems. The quantitative models aimed at explaining the structure and dynamics of such systems are much simpler by comparison because most processes and variables must be ignored for problems to remain mathematically tractable (Marquet *et al.* 2014). As a consequence, even if predictions of an ecological model are generally supported by data, the fraction of the variance "explained" by the model is often quite modest. Thus, an inherent tension exists between ecological data and models, which raises questions about the role of mathematical theory in Ecology (Barneche & Allen 2015), as exemplified by earlier (e.g. Peters 1991; Cyr & Walker 2004) and more recent discussions (e.g. Hurlbert & Stegen 2014; Marquet *et al.* 2014, 2015; Houlahan *et al.* 2015; Kearney *et al.* 2015).

Despite these issues, theory has an important role to play in Ecology. In particular, expressing hypotheses in mathematical terms generally allows for more rigorous tests of their logic (Servedio *et al.* 2014). Consequently, predictions can serve as quantitative benchmarks for comparison against empirical data in order to determine whether one or more assumptions have been violated (Harte 2004). Thus, adopting a theoretical framework as part of the process of discovery arguably allows for more rapid scientific advancement in Ecology by sharpening both deductive and inductive reasoning (Marquet *et al.* 2014).

An essential step in the development of ecological theory involves determining what variables/processes are essential to include as model parameters, and what details can be ignored. What constitutes an essential variable may be partly a matter of personal taste, but also varies to some extent depending on the specific question being addressed. For example, across the diversity of life, body size alone, which encompasses more than 15 orders of magnitude from bacteria to whales, explains the vast majority of the variance in individual metabolic rate (Brown *et al.* 2004; DeLong *et al.* 2010). However, for a more taxonomically

and spatially restricted community (e.g. a grassland), the range of variation in body size is often much smaller, and hence the fraction of variation in biological rates that is attributable to variables other than body size, is likely to be far greater (Tilman *et al.* 2004).

It has recently been argued that, rather than focusing on the number of model parameters per se, researchers should instead focus on developing ecological theories that are "efficient", meaning that they yield a large number of predictions per "free" parameter that must be estimated from data (Harte 2004; Kearney *et al.* 2015; Marquet *et al.* 2015). Moreover, to the extent possible, these predictions should arise from "first principles", defined as theoretically empirically and well-established law-like postulates that apply to processes in a particular domain (Scheiner & Willig 2008). First principles from chemistry and physics, such as energy- and mass- balance, are of particular relevance in the development of efficient ecological theories because they apply to all ecological phenomena, regardless of taxon, ecosystem, or level of biological organisation (Sterner & Elser 2002; Brown *et al.* 2004; Kooijman 2009).

Energy represents a useful currency for the development of efficient ecological theory because the process of living necessarily entails the transformation of energy and materials (Reiners 1986). At the individual level, the rate at which an organism undertakes energy transformation, i.e. its "pace of life" (Kleiber 1961), is its metabolic rate, which is defined as the rate of energy transformation for fitness enhancing processes of survival, growth and reproduction (Brown *et al.* 2004). Given the fundamental importance of metabolic rate, it is perhaps not surprising that two competing theory frameworks currently under development attempt to link individuals to ecosystems based on individual metabolic rate: the Metabolic Theory of Ecology (MTE) (West *et al.* 1997; Gillooly *et al.* 2001; Brown *et al.* 2004) and the Dynamic Energy Budget Theory (DEB) (Kooijman 2001, 2009).

The single most important determinant of metabolic rate across the diversity of life is body size (Thompson 1917; Murray 1926; Huxley 1932; Kleiber 1932; Brown *et al.* 2000).

For almost a century, there has been an ongoing debate about why metabolic rate, B, generally exhibits power-function scaling with body mass, M, meaning that $B \propto M^{\alpha}$, and why this scaling relation is generally sublinear, meaning that the exponent is bounded such that $0 < \alpha < 1$ (Thompson 1917; Murray 1926; Huxley 1932; Kleiber 1932; Peters 1983; Brown *et al.* 2000; Kooijman 2009). Early researchers proposed surface-to-volume arguments (Thompson 1917; Murray 1926; Huxley 1932) and biomechanical arguments (McMahon 1975; McMahon & Kronauer 1976) to account for this sub-linear scaling, both of which yield a predicted exponent of $\alpha = 2/3$. However, the current weight of evidence suggests that the exponent for the size scaling, α, is closer to 3/4 than 2/3 (Kleiber 1932, 1961; Peters 1983; Schmidt-Nielsen 1984; Savage *et al.* 2004b), highlighting the need for further theoretical work. The most notable effort along these lines is the model of West *et al.* (1997), which predicts 3/4-power scaling by assuming that metabolic rate is constrained by the geometry of distribution networks within the body (e.g. circulatory system) that have been optimised for energy and material exchange. The model itself has been met with controversy (e.g. Dodds *et al.* 2001), but thus far remains the only explanation that has been proposed to account for the ubiquity of 3/4-power body-size scaling relationships in Biology. It has also served to rekindle interest in biological scaling from both a theoretical (Banavar *et al.* 1999; Kolokotrones *et al.* 2010), and empirical perspective (Glazier 2005; White & Seymour 2005; Reich *et al.* 2006), and has inspired development of the MTE (Brown *et al.* 2004).

After accounting for size, the second most important determinant of individual metabolic rate across the diversity of life is temperature (Crozier 1924) through its exponential effects on biochemical reaction rates (Gillooly *et al.* 2001, 2002). While endothermic birds and mammals maintain relatively high and constant internal body temperatures, mostly between ~35–45 ˚C (Clarke & Rothery 2008), body temperatures vary quite substantially among ectotherms (i.e. ~0-45 ˚C, excluding thermophiles), which comprise

the bulk of the Earth's biodiversity. Within the range of temperatures at which a given ectotherm normally operates, metabolic rates and growth rates typically exhibit an exponential temperature dependence that is well characterised using the Boltzmann equation (Gillooly *et al.* 2001, 2002). This exponential-type response implies that, holding body size constant, ectotherms will have energetic requirements that vary in a predictable way both spatially with climate regime and temporally with season.

This thesis uses the MTE as a framework to explore the effects of energetics on fish individuals, populations, and communities. While the issue of whether MTE or DEB is more efficient is debatable (Kearney *et al.* 2015; Marquet *et al.* 2015), MTE models generally have fewer parameters, including the allometric-size scaling exponent for metabolic rate, α, the temperature activation energy for metabolic rate, E_r, and the size- and temperature-corrected metabolic rate, $b_o(T_c)$. While $b_o(T_c)$ varies between species and habitats (Brown *et al.* 2004), and thus represents a free parameter (but see Gillooly *et al.* 2005), α is predicted to be ~0.75 following an optimal fractal-like distribution of nutrients within the body (West *et al.* 1997), and E_r is predicted to be ~0.65 eV for heterotrophs based on the average activation energies of metabolic reactions in the respiratory complex (Gillooly *et al.* 2001, 2002; Savage *et al.* 2004a). Based largely on these few parameters, MTE has been extended to predict a variety of phenomena including individual-level rates of metabolism (Gillooly *et al.* 2001) and growth (Gillooly *et al.* 2002), population-level abundance and rates of increase (Savage *et al.* 2004a), ecosystem-level rates of carbon flux and turnover (Allen *et al.* 2005), and even rates of DNA evolution (Gillooly *et al.* 2005). Nevertheless, the theory as currently developed possesses important limitations, some of which are addressed as part of this PhD thesis.

In Chapter 1, I characterise the scaling of fish metabolic rates at the individual level and use this model to explore constraints on energetics at higher levels of organisation. As part of this work, I present evidence of a general temperature optimum for fish metabolic rate,

and fit a temperature response function with more parameters than the Boltzmann expression typically used in MTE models. I then scale up this new metabolic rate model from individuals to reef-fish communities in order to test predictions about: (1) how energy flux scales with temperature; (2) how biomass, after correcting for size effects, is constrained by net primary productivity and environmental temperature; (3) how size-corrected biomass is partitioned among distinct trophic groups.

In Chapter 2, the individual-level metabolic-rate model developed in Chapter 1 is scaled up to populations of reef fishes in order to test how density is constrained by trophic group, body size, temperature, species richness, and sampling area. Models are fitted and evaluated using hierarchical quantile regression in order to characterise the differential effects of the above-mentioned variables on rare versus abundant species. In doing so, I explicitly evaluate the energetic-equivalence hypothesis of MTE and, more generally, assess the relative importance of energetics versus ecological factors as determinants of population density.

Finally, in Chapter 3, I characterise overall trends in size and temperature scaling of fish growth rates. I show how this scaling can be combined with the scaling of metabolic rates to inform how much energy organisms must expend in the production of biomass. This quantity has thus far received relatively little attention in the literature, but nevertheless represents a fundamental quantity for understanding constraints on the efficiency of energy transfer across trophic levels, ultimately influencing the shape of trophic pyramids.

Throughout this PhD thesis, I make extensive use of statistical models to test mathematical predictions yielded from MTE. These models have been fit using two distinct statistical approaches, maximum likelihood and Bayesian inference. Maximum likelihood, as the name suggests, maximises the likelihood function to yield *deterministic* point estimates of model parameters. The likelihood function quantifies the chances of obtaining the observed data given a set of parameter values (Bolker 2008). Bayesian inference, by contrast, treats

model parameters as random, and therefore represents parameters using posterior distributions. This shift in perspective allows the investigator to focus on the effect sizes of parameters, and whether they are biologically relevant (Gelman *et al*. 2013), rather than on the significance levels of parameters (i.e. *P*-values) (Gerrodette 2011). While the estimated Baeysian *posterior* distribution of a parameter can be influenced by *prior* beliefs, if the prior probability distribution of a given parameter is uninformative over the likelihood region, and the dataset is large, the mean of the Bayesian posterior distribution is roughly equivalent to the maximum likelihood estimate (Kruschke 2014). Thus, the two competing methods become largely equivalent. For this thesis, I have chosen to perform model fitting using both maximum likelihood and Bayesian methods. I have done this, in part, because Bayesian approaches are relatively new to Ecology. Additionally, fitting the same models using these two distinct approaches, and then comparing the model fits, as I did, aided in ensuring that model convergence had been achieved.

I make use of standard statistical approaches that allow parameters to vary among taxa or environments (O'Connor *et al.* 2007; Yvon-Durocher & Allen 2012; Yvon-Durocher *et al.* 2012; Barneche *et al.* 2014). These so-called mixed (or hierarchical) models allow one to attribute the source of variance of a given parameter to a random variable (e.g. family or species) instead of treating it as overall model residual. Using this approach, I am able to quantify differences in scaling parameters among taxa in a statistically sound manner while characterising overall trends. By explicitly accounting for scaling differences among taxa, modelling approaches such as the one used here may help to resolve controversies surrounding the generality of metabolic scaling relationships (Agutter & Wheatley 2004; Hirst *et al.* 2014).

REFERENCES

Agutter, P. & Wheatley, D. (2004). Metabolic scaling: consensus or controversy? *Theoretical Biology and Medical Modelling*, 1, 13.

Allen, A.P., Gillooly, J.F. & Brown, J.H. (2005). Linking the global carbon cycle to individual metabolism. *Functional Ecology*, 19, 202–213.

Banavar, J.R., Maritan, A. & Rinaldo, A. (1999). Size and form in efficient transportation networks. *Nature*, 399, 130–132.

Bolker, B.M. (2008). *Ecological Models and Data in R*. 508th edn. Princeton University Press, pp. 396.

Barneche, D.R. & Allen, A.P. (2015). Embracing general theory and taxon-level idiosyncrasies to explain nutrient recycling. *Proceedings of the National Academy of Sciences*, in press.

Barneche, D.R., Kulbicki, M., Floeter, S.R., Friedlander, A.M., Maina, J. & Allen, A.P. (2014). Scaling metabolism from individuals to reef-fish communities at broad spatial scales. *Ecology Letters*, 17, 1067–1076.

Brown, J.H., Gillooly, J.F., Allen, A.P., Savage, V.M. & West, G.B. (2004). Toward a metabolic theory of ecology. *Ecology*, 85, 1771–1789.

Brown, J.H., West, G.B. & Enquist, B.J. (2000). Scaling in biology: patterns and processes, causes and consequences. In: *Scaling in biology* (eds. Brown, J.H. & West, G.B.). Oxford University Press, pp. 1–24.

Clarke, A. & Rothery, P. (2008). Scaling of body temperature in mammals and birds. *Functional Ecology*, 22, 58–67.

Crozier, W.J. (1924). On the possibility of identifying chemical processes in living matter. *Proceedings of the National Academy of Sciences of the United States of America*, 10, 461–464.

Cyr, H. & Walker, S.C. (2004). An illusion of mechanistic understanding. *Ecology*, 85, pp. 1802–1804.

DeLong, J.P., Okie, J.G., Moses, M.E., Sibly, R.M. & Brown, J.H. (2010). Shifts in metabolic scaling, production, and efficiency across major evolutionary transitions of life. *Proceedings of the National Academy of Sciences*, 107, 12941–12945.

Dodds, P.S., Rothman, D.H. & Weitz, J.S. (2001). Re-examination of the "3/4-law" of metabolism. *Journal of Theoretical Biology*, 209, 9–27.

Gelman, A., Carlin, J.B., Stern, H.S., Dunson, D.B., Vehtari, A. & Rubin, D.B. (2013). *Bayesian data analysis*. Chapman & hall/CRC texts in Statistical Science. 3rd edn. Chapman & Hall / CRC, London, pp. 675.

Gerrodette, T. (2011). Inference without significance: measuring support for hypotheses rather than rejecting them. *Marine Ecology*, 32, 404–418.

Gillooly, J.F., Allen, A.P., West, G.B. & Brown, J.H. (2005). The rate of DNA evolution: Effects of body size and temperature on the molecular clock. *Proceedings of the National Academy of Sciences of the United States of America*, 102, 140–145.

Gillooly, J.F., Brown, J.H., West, G.B., Savage, V.M. & Charnov, E.L. (2001). Effects of size and temperature on metabolic rate. *Science*, 293, 2248–2251.

Gillooly, J.F., Charnov, E.L., West, G.B., Savage, V.M. & Brown, J.H. (2002). Effects of size and temperature on developmental time. *Nature*, 417, 70–73.

Glazier, D.S. (2005). Beyond the '3/4-power law': variation in the intra-and interspecific scaling of metabolic rate in animals. *Biological Reviews*, 80, 611–662.

Harte, J. (2004). The value of null theories in ecology. *Ecology*, 85, pp. 1792–1794.

Hirst, A.G., Glazier, D.S. & Atkinson, D. (2014). Body shape shifting during growth permits tests that distinguish between competing geometric theories of metabolic scaling. *Ecology Letters*, 17, 1274–1281.

Houlahan, J.E., McKinney, S.T. & Rochette, R. (2015). On theory in ecology: another perspective. *BioScience*.

Hurlbert, A.H. & Stegen, J.C. (2014). When should species richness be energy limited, and how would we know? *Ecology Letters*, 17, 401–413.

Huxley, J.S. (1932). *Problems on relative growth*. Methuen, London, pp. 276.

Kearney, M.R., Domingos, T. & Nisbet, R. (2015). Dynamic energy budget theory: An efficient and general theory for ecology. *BioScience*.

Kleiber, M. (1932). Body size and metabolism. *Hilgardia*, 6, 315–353.

Kleiber, M. (1961). *The fire of life: An introduction to animal energetics*. John Wiley & Sons, New York, pp. 454.

Kolokotrones, T., Savage, V., Deeds, E.J. & Fontana, W. (2010). Curvature in metabolic scaling. *Nature*, 464, 753–756.

Kooijman, S. (2001). Quantitative aspects of metabolic organization: a discussion of concepts. *Philosophical Transactions of the Royal Society of London B: Biological Sciences*, 356, 331–349.

Kooijman, S.A.L.M. (2009). *Dynamic energy budget theory for metabolic organisation*. 3rd edn. Cambridge University Press, Cambridge, pp. 532.

Kruschke, J.K. (2014). *Doing Bayesian data analysis: A tutorial with R, JAGS, and stan*. 2nd edn. Academic Press, pp. 776.

Marquet, P.A., Allen, A.P., Brown, J.H., Dunne, J.A., Enquist, B.J. & Gillooly, J.F. *et al.* (2014). On theory in ecology. *BioScience*, 64, 701–710.

Marquet, P.A., Allen, A.P., Brown, J.H., Dunne, J.A., Enquist, B.J. & Gillooly, J.F.*et al.* (2015). On the importance of first principles in ecological theory development. *BioScience*, 65, 342–343.

McMahon, T.A. (1975). Allometry and biomechanics: limb bones in adult ungulates. *American Naturalist*, 109, 547–563.

McMahon, T.A. & Kronauer, R.E. (1976). Tree structures: deducing the principle of mechanical design. *Journal of Theoretical Biology*, 59, 443–466.

Murray, C.D. (1926). The physiological principle of minimum work: I. the vascular system and the cost of blood volume. *Proceedings of the National Academy of Sciences*, 12, 207–214.

O'Connor, M.I., Bruno, J.F., Gaines, S.D., Halpern, B.S., Lester, S.E. & Kinlan, B.P. *et al.* (2007). Temperature control of larval dispersal and the implications for marine ecology, evolution, and conservation. *Proceedings of the National Academy of Sciences*, 104, 1266–1271.

Peters, R.H. (1983). *The ecological implications of body size*. Cambridge University Press, Cambridge, pp. 329.

Peters, R.H. (1991). *A critique for ecology*. Cambridge University Press, Cambridge, pp. 366.

Reich, P.B., Tjoelker, M.G., Machado, J.-L. & Oleksyn, J. (2006). Universal scaling of respiratory metabolism, size and nitrogen in plants. *Nature*, 439, 457–461.

Reiners, W.A. (1986). Complementary models for ecosystems. *The American Naturalist*, 127, pp. 59–73.

Savage, V.M., Gillooly, J.F., Brown, J.H., West, G.B. & Charnov, E.L. (2004a). Effects of body size and temperature on population growth. *The American Naturalist*, 163, 429–441.

Savage, V.M., Gillooly, J.F., Woodruff, W.H., West, G.B., Allen, A.P. & Enquist, B.J. *et al.* (2004b). The predominance of quarter-power scaling in biology. *Functional Ecology*, 18, 257–282.

Scheiner, S. & Willig, M. (2008). A general theory of ecology. *Theoretical Ecology*, 1, 21–28.

Schmidt-Nielsen, K. (1984). *Scaling: Why is animal size so important?* Cambridge University Press, Cambridge, pp. 256.

Servedio, M.R., Brandvain, Y., Dhole, S., Fitzpatrick, C.L., Goldberg, E.E. & Stern, C.A. *et al.* (2014). Not just a theory-the utility of mathematical models in evolutionary biology. *PLoS Biology*, 12, e1002017.

Sterner, R.W. & Elser, J.J. (2002). *Ecological stoichiometry: the biology of elements from molecules to the biosphere*. Princeton University Press, Princeton, pp. 464.

Thompson, D.W. (1917). *On growth and form*. Cambridge University Press, Cambridge, pp. 793.

Tilman, D., HilleRisLambers, J., Harpole, S., Dybzinski, R., Fargione, J. & Clark, C. *et al.* (2004). Does metabolic theory apply to community ecology? It's a matter of scale. *Ecology*, 85, 1797–1799.

West, G.B., Brown, J.H. & Enquist, B.J. (1997). A general model for the origin of allometric scaling laws in biology. *Science*, 276, 122–126.

White, C.R. & Seymour, R.S. (2005). Allometric scaling of mammalian metabolism. *Journal of Experimental Biology*, 208, 1611–1619.

Yvon-Durocher, G. & Allen, A.P. (2012). Linking community size structure and ecosystem functioning using metabolic theory. *Philosophical Transactions of the Royal Society B: Biological Sciences*, 367, 2998–3007.

Yvon-Durocher, G., Caffrey, J.M., Cescatti, A., Dossena, M., Giorgio, P. del & Gasol, J.M. *et al.* (2012). Reconciling the temperature dependence of respiration across timescales and ecosystem types. *Nature*, 487, 472–476.

ESTIMATED PROPORTION OF CONTRIBUTION TO ARTICLES

Co-authored and submitted chapters	Extent of intellectual input by the candidate (%)				
	Study concept and design	Acquisition of data *	Analysis and interpretation of data	Drafting of manuscript	Critical revision
Chapter 1: 'Scaling metabolism from individuals to reef-fish communities at broad spatial scales'	70%	40%	80%	100%	50%
Chapter 2: 'Energetic and ecological constraints on population density'	70%	40%	80%	100%	50%
Chapter 3: 'Quantifying the energetics of fish growth and its implications for energy transfer between trophic levels'	70%	100%	80%	90%	50%

* My collaborators have provided me with reef-fish community structure data. Although I happen to have collected parts of it as well, it only accounts for less than 2% of the total database. The major challenge was to compile and standardise the database for the purposes of Chapters 1 and 2, which I have been doing since 2010.

OTHER RELEVANT PUBLICATIONS DURING CANDIDATURE

1) Hachich, N.F., Bonsall, M.B, Arraut, E.M., **Barneche, D.R.,** Lewinsohn, T.M. & Floeter, S.R. (2015). Island biogeography: patterns of marine shallow-water organisms in the Atlantic Ocean. *Journal of Biogeography*, 421, 871–1882.

2) **Barneche, D.R.** & Allen, A.P. (2015). Embracing general theory and taxon-level idiosyncrasies to explain nutrient recycling. **Invited commentary** to *Proceedings of the National Academy of Sciences*, 112, 6248–6249.

3) Falster, D.S., Duursma, R.A., Ishihara, M.I., **Barneche, D.R.,** FitzJohn, R.G., Vårhammar, A. *et al.* (2015). BAAD: A Biomass and allometry database for woody plants. *Ecology*, 96, 1445.

4) Luiz, O.J., Mendes, T.C., **Barneche, D.R.,** Ferreira, C.G.W., Noguchi, R., Villaça, R.C. *et al.* (2015). Community structure of reef fishes on a remote oceanic island: the relative influence of abiotic and biotic variables. *Marine and Freshwater Research*, 66, 739–749.

5) Anderson, A.B., Bonaldo, R.M., **Barneche, D.R.,** Hackradt, C.W., Félix-Hackradt, F.C., García-Chartón, J.A. *et al.* (2014). Recovery of grouper assemblages indicates effectiveness in a Marine Protected Area in Southern Brazil. *Marine Ecology Progress Series*, 514, 207–215.

6) Lobato, F.L., **Barneche, D.R.,** Siqueira, A.C., Liedke, A.R., Lindner, A., Pie, M.R. *et al.* (2014). Diet and diversification in the evolution of coral reef fishes. *PLoS One*, 9, e102094.

CHAPTER 1

SCALING METABOLISM FROM INDIVIDUALS TO REEF-FISH COMMUNITIES AT BROAD SPATIAL SCALES

Published as: Barneche, D.R., Kulbicki, M., Floeter, S.R., Friedlander, A.M., Maina, J., Allen, A.P. (2014). Scaling metabolism from individuals to reef-fish communities at broad spatial scales. *Ecology Letters*, 17, 1067–1076. doi: 10.1111/ele.12309 (with post-publication corrections).

1.1 ABSTRACT

Fishes contribute substantially to energy and nutrient fluxes in reef ecosystems, but quantifying these roles is challenging. Here, we do so by synthesising a large compilation of fish metabolic-rate data with a comprehensive database on reef-fish community abundance and biomass. Individual-level analyses support predictions of Metabolic Theory after accounting for significant family-level variation, and indicate that some tropical reef fishes may already be experiencing thermal regimes at or near their temperature optima. Comparisons of estimated fluxes among trophic groups highlight striking differences in resource use by communities in different regions, perhaps partly reflecting distinct evolutionary histories, and support the hypothesis that piscivores receive substantial energy subsidies from outside reefs. Our study demonstrates one approach to synthesising individual- and community-level data to establish broad-scale trends in contributions of biota to ecosystem dynamics.

1.2 INTRODUCTION

Reef fishes are a diverse group of vertebrates, comprising > 6000 species (Parravicini *et al.* 2013). They play key roles in the flow of energy and nutrients through many reef ecosystems (Polovina 1984; Arias-González *et al.* 1997; Bozec *et al.* 2004), but quantifying these roles, and how they may be affected by future climate change, remains an important research challenge (Wilson *et al.* 2010). An essential step in meeting this challenge entails characterising the trophic structures and energy fluxes of reef-fish communities, and how they vary with broad-scale gradients in key variables such as temperature and productivity.

Metabolic rate is a fundamental determinant of an organism's contribution to energy and nutrient flux in an ecosystem (Brown *et al.* 2004; Allen *et al.* 2005). The metabolic rate per unit body mass (i.e. mass-specific rate) generally declines with body mass, but increases with temperature (Gillooly *et al.* 2001; Brown *et al.* 2004). Consequently, given that the energy flux of a community is equal to the sum of the individual metabolic rates (Allen *et al.* 2005), changes in temperature, size structure and/or standing biomass of a given community may affect its energetics and resource use, and hence its contribution to ecosystem structure and function (Sandin *et al.* 2008; Mora *et al.* 2011; McDole *et al.* 2012). Conversely, communities that are distinct with respect to these variables may be energetically similar (Fig. 1.1). The Metabolic Theory of Ecology (MTE; Brown *et al.* 2004) yields predictions for how community abundance, biomass and energy flux should change with size structure, temperature and ecosystem productivity (Allen *et al.* 2005; Yvon-Durocher & Allen 2012; Trebilco *et al.* 2013), but there have been few attempts to test such predictions (but see López-Urrutia *et al.* 2006; O'Connor *et al.* 2009; McDole *et al.* 2012), particularly at broad spatial scales.

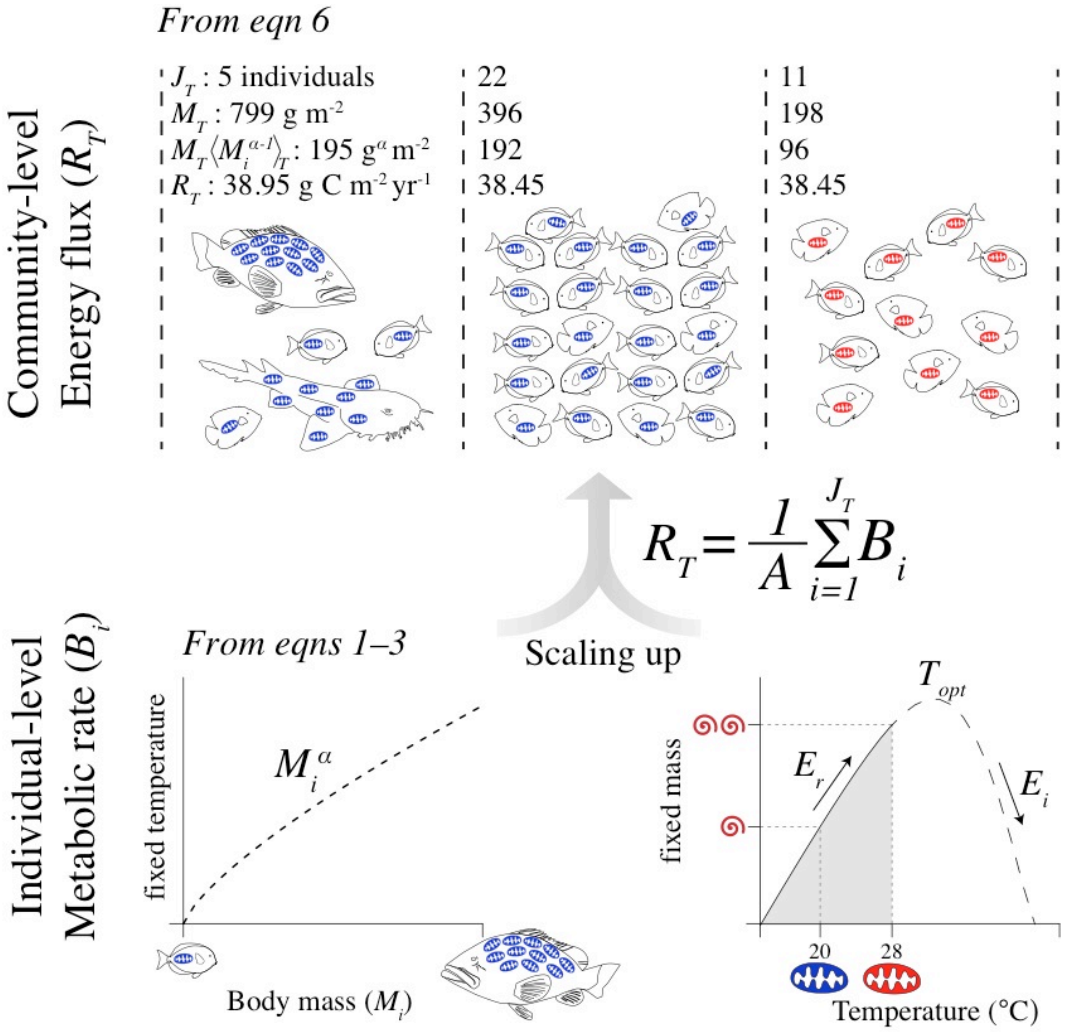

Figure 1.1. Scaling from individual-level metabolic rate (B_i) to total community-level respiration (R_T). Individual-level rates (lower graphs) exhibit sub-linear power-function scaling with body mass (M_i), implying that the scaling exponent α is < 1 and that respiratory capacity (depicted as mitochondria) per unit body mass declines as size increases. Effects of temperature on rates are exponential well below the optimum. In the hypothetical example, ATP turnover per mitochondrion (spirals) doubles from 20 °C (blue) to 28 °C (red). Community-level flux (in 1 m^2 area, upper graphs) is similar despite the fact that communities differ in number of individuals (J_T), standing biomass (M_T), size-corrected biomass ($M_T\langle M_i^{\alpha-1}\rangle_T$) and temperature. From left to right, the first and second communities differ in size structure, but are very similar in $M_T\langle M_i^{\alpha-1}\rangle_T$ and environmental temperature (20 °C), and therefore equivalent in terms of respiration. The third community has low M_T, but is found at 28 °C, and therefore respires similarly. Equations 1–6 are detailed in Materials and Methods.

Here, we use MTE as a framework to synthesise individual- and community-level data and analyses (Fig. 1.1) to estimate energy fluxes and trophic structures of reef-fish communities and how they change along broad gradients of temperature and productivity.

Our approach builds on other recent studies that use MTE to quantify the energetics of marine communities and ecosystems (López-Urrutia *et al.* 2006; O'Connor *et al.* 2009; McDole *et al.* 2012), and a much larger body of earlier work that yielded predictions on ecosystem dynamics by summing metabolic rates of individuals (e.g. Polovina 1984). The community-level database we use encompasses 49 reef sites in eight regions, 455,818 individuals and 1,169 species. While a number of studies have assessed spatial gradients in biomass and abundance for reef fishes (e.g. Mora *et al.* 2011), to our knowledge, no studies have attempted to quantify energy fluxes of reef-fish communities at such broad spatial scales.

Our analysis entails two distinct components. First, we quantify metabolic rates of fish and their primary determinants and, in so doing, test three predictions of MTE (hypotheses H1–H3 detailed in Methods). Second, we scale up the individual-level scaling relationships to first estimate energy fluxes of communities (e.g. Allen *et al.* 2005; Yvon-Durocher *et al.* 2012) (Fig. 1.1), and then derive and test predictions on how community-level energy flux should vary with temperature and net primary productivity (NPP) if specific community- and ecosystem-level assumptions are upheld (hypotheses H4–H5). For this second component, we synthesise individual- and community-level data and analyses using a Bayesian approach, building on recent work (Yvon-Durocher & Allen 2012).

1.3 MATERIALS AND METHODS

1.3.1 Individual-level hypotheses

Hypothesis H1: Metabolic rate will increase sub-linearly with body mass according to a power function with a scaling exponent $\alpha \approx 0.75$.

The single best predictor of metabolism across the diversity of life is body mass (Gillooly *et al.* 2001; Brown *et al.* 2004), which varies by > 6 orders of magnitude among reef fishes

(Froese & Pauly 2012). The effect of individual body mass, M_i (g), on metabolic rate, B_i (g C d^{-1}), can be characterised by a power function of the form

$$B_i = B_o M_i^{\alpha}, \quad (1)$$

where B_o is a metabolic normalisation (g C $g^{-\alpha}$ d^{-1}) that varies among taxa and with other variables (Brown *et al.* 2004). The dimensionless scaling exponent a is generally < 1 for metazoans, indicating sub-linear scaling with body mass, and also varies among metazoan taxa, with an average of ~0.75 (Savage *et al.* 2004). Previous analyses suggest that basal metabolic rates of fish may exhibit a somewhat steeper size scaling (i.e. $\alpha \approx 0.80$; Clarke & Johnston 1999). Here, we assess the scaling of routine metabolic rate, which corresponds to the rate of energy expenditure required by a fish in the field to sustain survival, growth and reproduction.

Hypothesis H2: Metabolic-rate temperature dependence can be approximated by the Boltzmann relationship with an activation energy $E_r \approx 0.6–0.7$ eV at temperatures below the optimum, T_{opt}.

Another key determinant of metabolic rate is temperature. In general, metabolic rate exhibits a unimodal response (Huey & Stevenson 1979) such that the effects of temperature are positive and exponential at temperatures well below the temperature optimum owing to biochemical kinetics (Gillooly *et al.* 2001), but negative above this optimum owing to protein denaturation and/or other processes that compromise biological function (bottom right plot of Fig. 1.1). Here, we model these effects of temperature on the metabolic normalisation, B_o from eqn 1, using the following expression (see Appendix I),

$$B_o = b_o(T_c)e^{E_r\left(\frac{1}{kT_c} - \frac{1}{kT}\right)}I(T) \quad (2)$$

$$I(T) = \left(1 + \left(\frac{E_r}{E_i - E_r}\right)e^{E_i\left(\frac{1}{kT_{opt}} - \frac{1}{kT}\right)}\right)^{-1}, \quad (3)$$

where $b_o(T_c)$ is the value of the metabolic normalisation at some arbitrary absolute temperature T_c (K), and k is Boltzmann's constant (8.62×10^{-5} eV K^{-1}). In this expression, the Boltzmann relationship, $e^{E_r\left(\frac{1}{kT_c} - \frac{1}{kT}\right)}$, describes temperature-induced enhancement of rates using an activation energy, E_r (eV), consistent with previous MTE work (Gillooly *et al.* 2001; Allen *et al.* 2005), whereas $I(T)$ characterises declines in rates above T_{opt} using an inactivation parameter E_i (Schoolfield *et al.* 1981). The existence of a temperature optimum implies that $E_i > E_r$. Previous work indicates that E_r varies among taxonomic groups, with an average of ~0.65 eV, which corresponds closely to the average activation energy of metabolic reactions in the respiratory complex (Gillooly *et al.* 2001). In the absence of temperature inactivation, this value for E_r would imply a ~3.3-fold increase in individual energy flux over the range of temperatures experienced by reef fishes (~18–32 °C). However, if the upper bound of this range is at or near the temperature optimum for reef-fish species, as suggested by some recent work (Gardiner *et al.* 2010), the overall temperature response will be weaker. We can evaluate this hypothesis by statistically comparing models fitted with and without the inactivation term, $I(T)$, in eqns 2 and 3.

Hypothesis H3: The size- and temperature-corrected rate of metabolism, $b_o(T_c)$, is independent of average thermal regime.

While the exponential effects of temperature on biochemical reaction rates have long been recognised, organisms utilise diverse physiological mechanisms to maintain homeostasis in different thermal regimes (Hochachka & Somero 2002). Consequently, some have argued

that physiological acclimation and/or evolutionary adaptation may allow organisms that occupy distinct thermal regimes to modulate acute temperature effects, as expressed in eqns 2 and 3, through changes in $b_o(T_c)$ (Clarke & Fraser 2004). We can evaluate this hypothesis by fitting a function of the form

$$b_o(T_c) = \overline{b_o(T_c)} e^{E_a\left(\langle \frac{1}{kT} \rangle - \frac{1}{kT_c}\right)}, \quad (4)$$

where $\overline{b_o(T_c)}$ is the size- and temperature-corrected metabolic rate of an organism whose average thermal regime is $\langle 1/kT_c \rangle$, and E_a characterises any changes in this rate with average thermal regime, $\langle 1/kT \rangle$. We refer to E_a as an adaptation parameter (rather than an activation energy) because it cannot be justified based on simple biochemical kinetics. Nevertheless, it provides a useful benchmark for comparison with the activation energy, E_r, in eqns 2 and 3 above. The evolutionary adaptation hypothesis, as articulated by Clarke & Fraser (2004), proposes that $b_o(T_c)$ is generally higher for taxa adapted to cooler environments, implying that $E_a > 0$ in eqn 4. By contrast, if $E_a \approx 0$, $b_o(T_c)$ is essentially independent of thermal regime, as assumed in the original MTE formulation (Gillooly *et al.* 2001), meaning that temperature scaling of rates is similar within and among taxa. Distinguishing between these alternative hypotheses is particularly relevant here because the existence of temperature adaptation ($E_a > 0$) would imply that the overall temperature-induced enhancement of rates for communities that occupy warmer environments is weaker than would be predicted based solely on the activation energy E_r.

Testing hypotheses H1–H3

The predicted effects of body size ($\alpha \approx 0.75$), temperature ($E_r \approx 0.6$–0.7 eV) and thermal regime ($E_a \approx 0$ eV) can be evaluated by combining eqns 1–4 and then taking logarithms to yield

$$\ln B_i = \ln\overline{b_o(T_c)} + \alpha \ln M_i + E_a\left(\left\langle\frac{1}{kT}\right\rangle - \frac{1}{kT_c}\right) + E_r\left(\frac{1}{kT_c} - \frac{1}{kT}\right) - \ln\left(1 + \left(\frac{E_r}{E_i - E_r}\right)e^{E_i\left(\frac{1}{kT_{opt}} - \frac{1}{kT}\right)}\right). \quad (5)$$

We evaluate these predictions using metabolic-rate data compiled in FishBase (Froese & Pauly 2012), along with additional reef-fish data compiled from the recent literature (Appendix I). The FishBase data we analyse include all measurements of routine metabolic rate that have accompanying size and temperature data, except measurements denoted as being taken under stressful conditions. To allow for the assessment of differences among families in the temperature scaling of rates (described below), we only include data from families with at least five metabolic-rate measurements over at least a 5 °C temperature range. Data for two families (Carangidae and Coryphaenidae) were, however, excluded because preliminary analyses indicated that they were outliers with respect to scaling behaviour, and therefore prevented statistical models (described below) from converging on stable parameters estimates. In total, our compilation of metabolic-rate data encompasses 2,036 measurements taken from 43 families and 207 species of marine and freshwater fish, including 40 reef-fish species.

Effects of size and temperature were assessed by fitting eqn 5 to metabolic-rate data using non-linear mixed-effects modelling in the R package *lme4* (version 1.1-8) (Bates *et al.* 2015, Tables AI.2–AI.3). During model fitting, thermal regime (E_a) and temperature

inactivation (E_i) were treated as having fixed effects. Thermal acclimation occurs, by definition, at the level of taxon (e.g. Houde 1989; Clarke & Johnston 1999), and therefore it must be treated as fixed effect for mathematical reasons. Treating temperature inactivation as a random effect would require extensive data beyond the temperature optimum. However, insufficient data exist to undertake such an analysis for fish (see Appendix I). Moreover, this slope beyond the optimum (i.e. E_i) was not of primary interest for this study because we would not expect fish to be observed frequently in this state in nature, as it represents a stressed, functionally compromised condition.

Size (α), temperature activation (E_r), optimum temperature (T_{opt}) and the size- and temperature-corrected rate ($\ln\overline{b_o(T_c)}$) were treated as having both fixed effects and random effects that varied by family ($\Delta\alpha$, ΔE_r, ΔT_{opt}, $\Delta\ln\overline{b_o(T_c)}$). Random effects were assumed to be normally distributed, with means of 0, so the fixed effects α, E_r, T_{opt}, and $\ln\overline{b_o(T_c)}$ correspond to family-level averages. Given that thermal regime, $\langle 1/kT \rangle$, was calculated based on the average of the inverse absolute temperature measurements for each family, our approach is mathematically similar to the one described by van de Pol & Wright (2009) for distinguishing within- vs. between-group effects using mixed-effects models.

A parsimonious model that included only the most informative parameters was constructed using maximum likelihood (Zuur *et al.* 2009) (Table AI.2). This parsimonious model was then refitted using a Bayesian procedure by calling *JAGS* (version 3.4.0) from the R package *R2jags* (version 0.05-03) (Su & Yajima 2015) to determine posterior distributions and associated 95% credible intervals (CIs) for the fitted parameters (R code available at https://github.com/dbarneche/ELEBarneche). A key advantage of the Bayesian approach for this analysis was that it allowed us to assess how statistical uncertainties in our estimates for the size and temperature scaling of fish metabolic rates influenced the precision of community-level estimates of size-corrected biomass and energy flux (see hypotheses H4–H5

below). When fitting the models in both *JAGS* and *lme4*, rather than estimate E_r directly, we instead estimated the transformed quantity E_r', where $E_r = E_i/(1 + e^{-E_r'})$, to ensure that $E_i > E_r$ in eqn 5 (Tables AI.3–AI.4).

1.3.2 Community-level hypotheses

> *Hypothesis H4: Holding ecosystem net primary productivity constant, size-corrected biomass should decline with increasing temperature.*

Community-level flux is equal to the sum of the individual fluxes. Thus, annual respiratory carbon flux for a heterotroph community comprised of J_T individuals in an ecosystem of area A, R_T (g C m^{-2} year^{-1}), equals the sum of the time-integrated individual-level respiration rates, $\int_{t=0}^{t=\tau} B_i\,(t)dt$, over the time interval t = 0 day to $t = \tau$ = 365 days,

$$R_T = (1/A)\sum_{i=1}^{J_T}\int_{t=0}^{t=\tau} B_i\,(t)dt$$

$$= \tau\ b_o(T_c)\ M_T\langle M_i^{\alpha-1}\rangle_T\ \langle e^{E_r\left(\frac{1}{kT_c}-\frac{1}{kT}\right)} I(T)\rangle_\tau \qquad (6)$$

where $\langle e^{E_r\left(\frac{1}{kT_c}-\frac{1}{kT}\right)} I(T)\rangle_\tau$ is time-averaged temperature kinetics (Yvon-Durocher *et al.* 2012), which is calculated by integrating temperature variation through time, $T(t)(= (1/\tau)\int_{t=0}^{t=\tau} e^{E_r\left(\frac{1}{kT_c}-\frac{1}{kT(t)}\right)} I(T(t))dt)$. Community-level size structure is characterised as $M_T\langle M_i^{\alpha-1}\rangle_T = (1/A)\sum_{i=1}^{J_T} M_i^{\alpha}$, where M_T is total community biomass per unit area $(= (1/A)\sum_{i=1}^{J_T} M_i)$, and $\langle M_i^{\alpha-1}\rangle_T$ is the *biomass-weighted* average for $M_i^{\alpha-1}(= \left(\sum_{i=1}^{J_T} M_i^{\alpha}\right)/\left(\sum_{i=1}^{J_T} M_i\right))$ (Allen *et al.* 2005).

We refer to the product $M_T\langle M_i^{\alpha-1}\rangle_T$ as 'size-corrected biomass' because size correction, by $\langle M_i^{\alpha-1}\rangle_T$, accounts for declines in mass-specific metabolic rate, B_i/M_i, with

increasing size. This size-related decline is, in turn, predicted by MTE to reflect declines in respiratory capacity (Allen & Gillooly 2009). Consequently, $M_T\langle M_i^{\alpha-1}\rangle_T$ is predicted to be proportional to the total respiratory capacity of the community on a per-unit-area basis (Yvon-Durocher & Allen 2012). Thus, calculation of size-corrected biomass facilitates comparisons of respiratory capacity and energy flux among communities that differ in size structure and standing biomass (Fig. 1.1).

To derive hypothesis H4 using eqn 6, we note that the reef-fish community garners some fraction, ε_T, of annual NPP, N_T, meaning that $\varepsilon_T N_T = R_T$, and therefore that

$$\ln M_T\langle M_i^{\alpha-1}\rangle_T = \ln[\varepsilon_T / b_o(T_c)] + \ln N_T - \ln\langle e^{E_r\left(\frac{1}{kT_c} - \frac{1}{kT}\right)} I(T)\rangle_\tau. \quad (7)$$

Holding temperature constant, eqn 7 predicts a proportional increase in total size-corrected biomass with NPP owing to greater food availability, implying a slope of 1 for the second term, $\ln N_T$. Holding NPP constant, it predicts an inverse relationship with time-averaged temperature kinetics owing to increases in per-individual metabolic demands, implying a slope of -1 for the third term. Importantly, these predictions only hold if the fraction of that carbon consumed by the fish community, ε_T, and the size- and temperature-corrected metabolic rate, $b_o(T_c)$, are both independent of thermal regime, and if reefs are relatively closed systems with respect to the production and consumption of reduced carbon. The closed-system assumption, in particular, may not hold true (Hamner *et al.* 1988; Hatcher 1990), but nevertheless provides a point of departure for deriving and testing predictions. Thus, eqn 7 provides a useful benchmark for assessing the extent to which one or more of these assumptions have been violated.

Hypothesis H5: Size-corrected biomass should be lowest at the highest trophic level.

Energy is lost from the system as energy is transferred between trophic levels (Lindeman 1942). Owing to these losses, if reef fishes consumed only autotrophs or other fish occurring on the reef, the fraction of reef NPP garnered by piscivorous fish (ε_{Pi}) would be constrained by energy balance to be lower than that of herbivorous fish (ε_H), meaning that $\varepsilon_{Pi}/\varepsilon_H < 1$. Complications arise, however, because reef fishes consume diverse prey items other than autotrophs and fish, including gastropods and zooplankton. Moreover, higher trophic levels, particularly top predators such as sharks, may receive substantial energy subsidies from outside the system (Trebilco *et al.* 2013).

Despite these complications, we can extend eqn 7 to empirically assess whether energy fluxes of piscivores, R_{Pi}, are lower than those of herbivores, R_H, using data on size-corrected biomass,

$$\ln\frac{R_{Pi}}{R_H} = \ln\frac{M_{Pi}\langle M_i^{\alpha-1}\rangle_{Pi}}{M_H\langle M_i^{\alpha-1}\rangle_H} < 0, \tag{8}$$

where $M_{Pi}\langle M_i^{\alpha-1}\rangle_{Pi}(=(1/A)\sum_{i=1}^{J_{Pi}} M_i^{\alpha})$ is the size-corrected biomass for J_{Pi} piscivorous individuals in a defined area A, and $M_H\langle M_i^{\alpha-1}\rangle_H(=(1/A)\sum_{i=1}^{J_H} M_i^{\alpha})$ is the size-corrected biomass for J_H herbivorous individuals in this same area. Importantly, productivity, N_T, and time-averaged temperature kinetics, $\langle e^{E_r\left(\frac{1}{kT_c}-\frac{1}{kT}\right)} I(T)\rangle_\tau$, both drop out of eqn 8, assuming that the temperature dependence of respiration is the same for different trophic groups. Consequently, ratios of size-corrected biomass for pairs of trophic groups can be meaningfully compared among communities that differ in size structure, NPP and temperature. These ratios provide a useful, albeit indirect, means of assessing the importance of prey items other than fish. If, for example, the size-corrected biomass of invertivores was

higher than that of herbivores in a given community, this would represent direct evidence that the fishes garner more of their energy from invertebrates than from direct consumption of NPP.

Testing hypotheses H4–H5

We evaluated hypotheses H4–H5 using community-level data on reef-fish abundances and body lengths collected from 49 sites (islands, atolls and coastal contiguous reefs), including 14 sites in the South-western Atlantic and its oceanic islands, 1 site in the Caribbean, 2 sites in the Tropical Eastern Atlantic, 1 site in the Tropical Eastern Pacific, 4 sites in the Central Pacific, 2 sites in the South-eastern Pacific and 25 sites in the South Pacific (Table AI.5). Each species was assigned to one of five trophic groups (herbivores, omnivores, planktivores, invertivores and piscivores) using information in the published literature, online databases and expert judgment (Appendix I).

Community-level estimates of size-corrected biomass were inferred from the abundance and body length data by first estimating wet weights of individuals using power-function length-weight conversion formulas compiled from the literature and online databases (Appendix I). Fluxes were then estimated by combining size-corrected biomass values with weekly estimates of mean annual sea-surface temperature obtained from the CorTAD database between 1997 and 2007 (Selig *et al.* 2010).

Estimates of ecosystem-level reef NPP are scarce in the literature (Gattuso *et al.* 1998; Naumann *et al.* 2013). Indeed, we are aware of only one study that has estimated it (Odum & Odum 1955). Although many reef studies have reported estimates of net community productivity (NCP; Hatcher 1990), NCP does not represent the total energy available to the heterotrophic community. Rather it is the fixed carbon that remains after heterotrophic consumption (= gross ecosystem photosynthesis – total ecosystem respiration). Consequently, we evaluated hypothesis H4 for planktivorous fish (i.e. pelagic consumers) using estimates of

pelagic NPP (hereafter, N_P, g C m^{-2} $year^{-1}$) derived from SeaWIFS (Behrenfeld & Falkowski 1997). Cautious interpretation is, however, warranted because planktivores may obtain primary production from a larger area owing to oceanic currents (Hamner *et al.* 1988). Data from Abrolhos (South-western Atlantic) were excluded from this analysis because no planktivores were recorded. Uncertainties in the scaling relationships of individual-level metabolic rates were accounted for by calculating size-corrected biomass, $M_T\langle M_i^{\alpha-1}\rangle_T$, time-averaged temperature kinetics, $\langle e^{E_r\left(\frac{1}{kT_c}-\frac{1}{kT}\right)}I(T)\rangle_\tau$, and community flux, R_T (in g C m^{-2} $year^{-1}$), based on the joint posterior distribution for E_r, E_i, T_{opt}, α and $\ln\overline{b_o(T_c)}$ (E_a was not significant, see Results), as determined using Bayesian methods in *JAGS*.

We evaluated whether the size-corrected biomass of planktivores increased with N_P, and declined with increasing time-average temperature kinetics (hypothesis H4), using standard multiple regression. Two-tailed *t*-tests were used to assess whether the observed slopes differed from expected values. ANCOVA was used to assess whether log ratios of size-corrected biomass (eqn 8) varied in response to temperature and among trophic groups (hypothesis H5). Overall differences in community structure among regions, as indexed by trophic-specific log ratios of size-corrected biomass, were assessed using MANOVA, as is the standard procedure for analysing differences in compositional data (Aitchison 2003). Due to a lack of planktivores, Abrolhos was also excluded from this analysis.

1.4 RESULTS AND DISCUSSION

1.4.1 Individual-level hypotheses H1–H3

The parsimonious metabolic-rate model yields estimates for the overall size- and temperature-scaling relationships — representing family-level averages — that closely match MTE predictions (Tables 1.1, AI.2–AI.4; Figs. 1.2, AI.1–AI.5). Consistent with hypothesis H1, the

overall effect of size, characterised by the scaling exponent α, is statistically indistinguishable from 0.75, implying sub-linear scaling (i.e. $\alpha < 1$), which provides theoretical justification for 'size-correcting' biomass at the community level. Consistent with hypothesis H2, the activation energy, E_r, is statistically indistinguishable from the predicted range ~0.6–0.7 eV. Consistent with hypothesis H3, the adaptation parameter E_a is not significant (likelihood ratio test: χ^2 = 1.98; d.f. = 1; P = 0.160; Table AI.2), and is therefore excluded from the parsimonious model (Tables 1.1, AI.2–AI.3). Thus, size- and temperature-corrected rates appear to be largely independent of thermal regime.

Importantly, however, the temperature inactivation term $I(T)$ (eqn 3) is highly significant (likelihood ratio test: χ^2 = 20.06; d.f. = 6; P = 0.003), yielding evidence of a temperature optimum (T_{opt}) for metabolic rates of fish (Fig. AI.5). By incorporating these parameters into the metabolic-rate model, our analysis expands upon early MTE efforts that described the temperature dependence of biological rates based solely on the Boltzmann relationship (e.g. Gillooly *et al.* 2001; Brown *et al.* 2004; Allen & Gillooly 2009), consistent with other recent MTE work (e.g. Amarasekare & Savage 2012). Only a small subset of the observations in our dataset were taken at temperatures higher than our average estimated T_{opt} of ~33°C (0.5%, n = 10 observations). This limits the predictive power of our model, and highlights the need for more comprehensive studies focusing on the full temperature-driven performance curves for different taxa (e.g. Rombough 1994; Pörtner *et al*. 2007).

Table 1.1. Average estimates and 95% credible intervals (of Bayesian posterior distributions) for fixed-effects parameters in the parsimonious model (model F2 in Table AI.2; see Table AI.4 for estimates of random effects, and Fig. AI.1 for the residual plot). Fixed-effect parameters include: α, the (family-level) average for the mass dependence of metabolic rate; E_r, the average for the temperature dependence of metabolic rate; $\ln\overline{b_o(T_c)}$, the average for the size-corrected metabolic rate at temperature T_c = 20 °C; T_{opt}, the temperature optimum of fish metabolism and E_i, the inactivation energy describing the rate of decline in metabolic rate at temperatures > T_{opt}.

Parameter	**Estimate**	**2.5% CI**	**97.5% CI**
Fixed effects			
Size, α	0.758	0.674	0.842
Activation energy, E_r (eV)	0.595	0.427	0.886
Normalisation, $\ln\overline{b_o(T_c)}$ (g C g^{α} d^{-1})	-5.709	-5.967	-5.249
Temperature optimum, T_{opt} (K)	306.263	301.789	313.923
Inactivation energy, E_i (eV)	2.020	1.240	3.115

Of particular relevance, our estimate for the family-level average for T_{opt}, 33 °C (95% CI: 29–41 °C, Table 1.1), overlaps with the maximum temperature observed in our sampled tropical reefs (maximum temperature at the sampled sites from CorTAD: 32.55 °C). Analyses of standard metabolic-rate data yield further evidence of a temperature optimum of similar magnitude (Fig. AI.6). These findings represent independent evidence that at least some marine fish taxa are already experiencing thermal regimes at or near their temperature optima (Gardiner *et al.* 2010), perhaps constraining the capacity of fish communities (and reef ecosystems more generally) to respond to climate change (Rummer *et al.* 2014). Still, it is important to recognise that clear evidence of an optimum is only observed for a subset of the families included in our analysis, which have data that span a wide temperature range (e.g. Centrarchidae, Cyprinidae, Sparidae; Fig. AI.2). Moreover, the data in our analysis encompass a mixture of short-term acute temperature responses and longer-term temperature acclimation, which can occur over multiple generations (Donelson *et al.* 2012). Thus, our findings highlight the need for further investigations on the biochemical mechanisms and timescales of temperature acclimation and adaptation in fish.

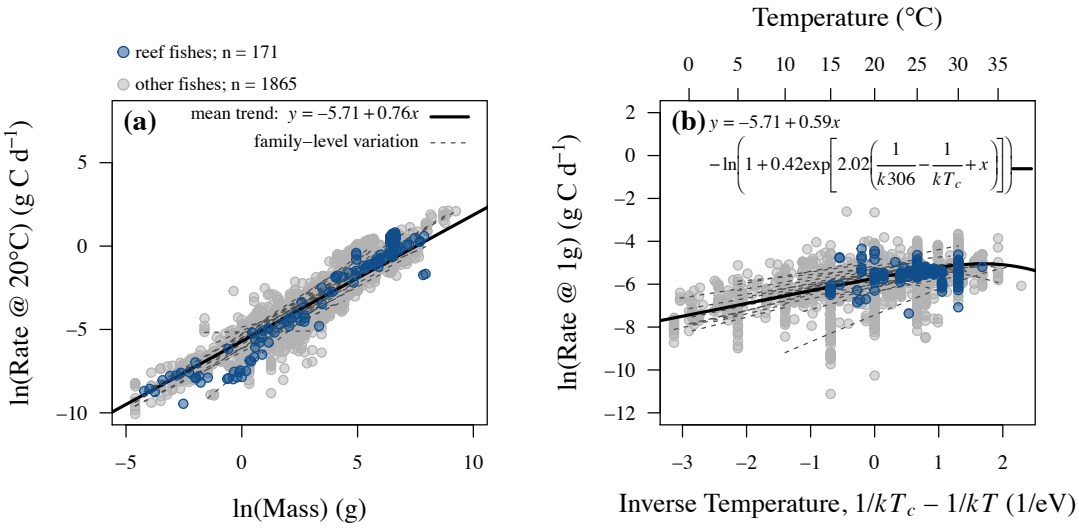

Figure 1.2. Scaling of routine metabolic rates of fish with respect to (a) body size and (b) temperature. Parameter estimates (listed in Table 1.1) were obtained using Bayesian methods. The effect of temperature on routine metabolic rate was controlled for in (a) by standardising the temperature measures, T (in K), to T_c = 293.15 K (= 20 °C) based on family-level temperature scaling relationships, where k is the Boltzmann constant (8.62×10^{-5} eV K^{-1}). The effect of body mass was controlled for in (b) by standardising measures to 1 gram based on the family-level size scaling relationships. The size-corrected rate at temperature T_c, $\ln\overline{b_o(T_c)}$ = -5.71 g C $g^{-\alpha}$ d^{-1}, corresponds to an average across families. See Fig. AI.1 for the residual plot.

After accounting for overall trends using fixed effects, our model reveals substantial family-level variation in size scaling ($\Delta\alpha$), temperature scaling (ΔE_r, ΔT_{opt}) and size- and temperature-corrected rates $\Delta\ln\overline{b_o(T_c)}$ (Figs. 1.2, AI.2). Thus, while our metabolic-rate model supports MTE predictions for fish as a group, it also quantifies deviations from general trends by incorporating random effects attributable to taxonomy. For example, our estimate of 0.58 for the standard deviation of $\Delta\ln\overline{b_o(T_c)}$ (Table AI.4) implies that metabolic rate varies, on average, by about 3-fold ($\approx e^{2\times0.58}$) among families after accounting for size and temperature. By explicitly accounting for such deviations, modelling approaches such as ours may help to resolve controversies surrounding the generality of metabolic scaling relationships (e.g. Agutter & Wheatley 2004). While the parsimonious model does indicate family-level deviations from α and E_r, 81% of the families had 95% CIs for size-scaling exponents that included the predicted 0.75, and 98% of families had 95% CIs for activation

energies that included 0.6–0.7 eV. And, notably, scaling relationships for reef fishes are similar to those of other species (Fig. 1.2, blue circles).

1.4.2 Community-level hypotheses H4–H5

Propagation of the uncertainties from the individual-level metabolic-rate model to community-level estimates of size-corrected biomass demonstrates that this source of uncertainty introduces error of small magnitude in the estimates of $\ln M_T \langle M_i^{\alpha-1} \rangle_T$ relative to variation among sites (represented by 95% CI bars in Fig. AI.8). Posterior distributions were therefore averaged to obtain the community-level estimates used in subsequent analyses.

In disagreement with hypothesis H4 (eqn 7), the logarithm of size-corrected biomass for planktivores ($\ln M_P \langle M_i^{\alpha-1} \rangle_P$) is not correlated with time-averaged temperature kinetics ($\ln \langle e^{E_r\left(\frac{1}{kT_c} - \frac{1}{kT}\right)} I(T) \rangle_\tau$) or near-pelagic NPP ($\ln N_P$) in a multiple regression analysis (F = 0.84, P = 0.44). However, after excluding from our analysis six coastal sites in the South-western Atlantic (below 17°S), all of which are exceptionally turbid (Fig. AI.9), size-corrected biomass increases significantly ($P < 0.001$) and approximately proportionally with N_P, in agreement with hypothesis H4, as indicated by a log–log slope near 1 from the multiple regression model (1.71, *t*-test: P = 0.08; Fig. 1.3). These findings are consistent with microcosm studies showing increases in biomass with productivity (O'Connor *et al.* 2009). They also suggest that planktivore abundances on reefs are constrained by N_P provided that turbidity is not so high that it hampers planktivore feeding (Johansen & Jones 2013). More generally, they suggest that, despite evidence indicating that local, site-specific hydrodynamics can influence food availability to reef planktivores (Hamner *et al.* 1988), N_P is nevertheless a useful proxy of food availability for reef planktivores at broad spatial scales. Excluding the six turbid sites, the log–log slope of the relationship between size-corrected biomass and time-averaged temperature kinetics is also highly significant in the multiple

regression model (P = 0.004), but substantially steeper than the predicted -1 (-8.22, t-test: P = 0.01), implying that planktivorous reef fishes garner a progressively smaller fraction of N_P as water temperature increases (Fig. 1.3c).

Community trophic structure, as indexed by four log ratios of size-corrected biomass (piscivore-to-herbivore, invertivore-to-herbivore, planktivore-to-herbivore and omnivore-to-herbivore, following eqn 8), differs significantly between regions (MANOVA: $P < 0.0001$; Fig. 1.4), indicating striking differences in resource use among reef-fish communities. For example, size-corrected biomass of planktivores is proportionally higher in the Tropical Eastern Atlantic (63%) than the other regions (≤ 17%; Fig. 1.4), supporting the idea that plankton can be important energy resources to reef fishes (Hamner *et al.* 1988). Remarkably, these differences in trophic structure are uncorrelated with temperature regime (ANCOVA: P = 0.691; Fig. AI.8), suggesting primary roles for unmeasured environmental factors (e.g. benthic NPP, Naumann *et al*. 2013) and historical factors related to divergent evolutionary histories of distinct fish faunas (Bellwood & Wainwright 2002; Kulbicki *et al.* 2013). In addition, fishing pressure varies considerably among the sites included in our analysis, and can alter community structure (Jackson *et al.* 2001; Sandin *et al.* 2008; Mora *et al.* 2011; Friedlander *et al.* 2013) in diverse ways (Kronen *et al.* 2012). Disentangling human impacts requires careful selection of sites along disturbance gradients (e.g. Sandin *et al.* 2008; McDole *et al.* 2012), and may be informed by the energetic approach adopted here.

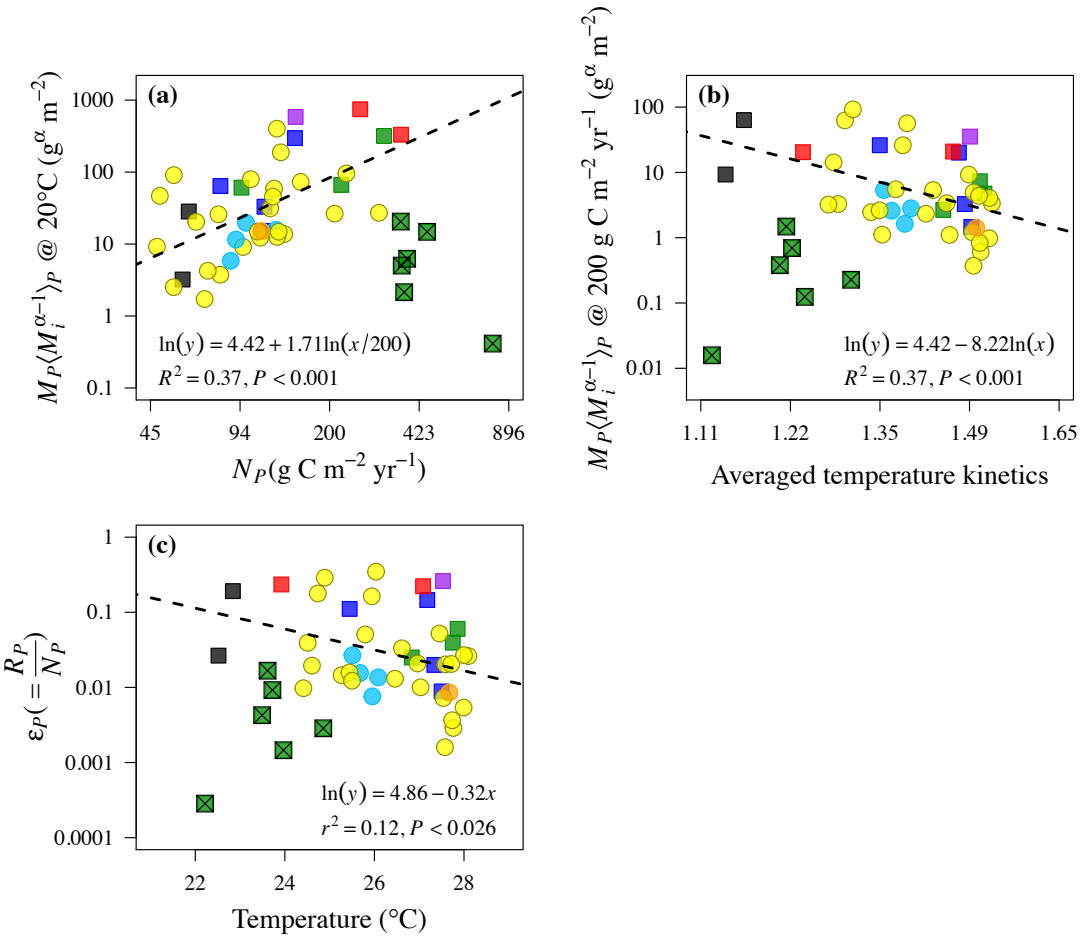

Figure 1.3. Relationships of size-corrected biomass of planktivores to (a) pelagic net primary production and (b) time-averaged temperature kinetics. (c) Estimated fraction of pelagic net primary productivity respired by planktivores plotted as a function of mean annual temperature. The fitted models and associated statistics depicted in the figure were estimated using multivariate (in a and b) and bivariate (in c) OLS (ordinary least squares) regression, excluding six exceptionally turbid sites (Fig. AI.9) denoted by 'X' (n = 42 sites). The model intercept in panels a and b corresponds to the estimated logarithm of size-corrected biomass for a planktivore community receiving 200 g C m^{-2} $year^{-1}$ at 20 °C. Colours are used to denote sites in different regions: South Pacific (yellow), Central Pacific (light blue), South-eastern Pacific (black), Tropical Eastern Pacific (purple), Caribbean (orange), South-western Atlantic (green), South-western Atlantic oceanic islands (blue), Tropical Eastern Atlantic (red). Coral-dominated reefs are depicted as circles and rock-dominated reefs are depicted as squares.

Size-corrected biomass also differed among trophic groups, as indicated by significant differences in the averages of the four log ratios (one-way ANOVA: $P < 0.0001$). Consistent with hypothesis H5, the piscivore-to-herbivore log ratio (eqn 8), as well as the planktivore-to-herbivore log ratio, had averages < 0 (two-sided *t*-tests: both $P < 0.0001$), meaning that size-

corrected biomass values (and hence energy fluxes) of both groups were less than those of herbivores. However, the mean omnivore-to-herbivore and invertivore-to-herbivore log ratios were not significantly different from 0 (two-sided *t*-tests: $P = 0.31$ and $P = 0.95$ respectively). *Post hoc* analyses [Tukey HSD (Honestly Significant Difference)] of pair-wise differences among log ratios allow us to construct an average 'stoichiometry' of size-corrected biomass: 3.79 invertivores; 2.79 herbivores; 2.56 omnivores; 0.97 piscivores; 1 planktivore. Thus, in terms of size-corrected biomass, and hence energetics, our results suggest that, on average, invertivores are the most important trophic group in reef-fish communities. These findings indicate that reef-fish communities generally obtain more energy from consumption of invertebrates than from direct consumption of NPP. The importance of invertivores in many of the communities analysed here, particularly those in the south-western Atlantic (Fig. 1.4), may in part be attributable to trophic cascades due to removal of top predators, with subsequent release of prey, including invertivores (Anderson *et al.* 2014). However, quantifying these impacts within our energetic framework will require detailed data on actual rates of reef fish harvesting and other anthropogenic effects (e.g. McDole *et al.* 2012), which are virtually inexistent at large spatial scales (but see Teh *et al*. 2013; MacNeil *et al.* 2015).

Notably, our calculated stoichiometry for size-corrected biomass implies that, on average, energy flux by piscivores is only ~2.88-fold lower than that of herbivores (i.e. $2.88 \approx 2.79/0.97$). This difference is markedly less than would be predicted if piscivorous reef fish directly or indirectly obtained all of their energy from herbivorous reef fish: assuming a difference of > 2 trophic-position units between herbivores and piscivores (Hussey *et al.* 2014) and a Lindeman (1942) efficiency of ~0.10 between adjacent trophic levels, the predicted difference would be > 100-fold (i.e. $> 0.10^2$). Given that our size-corrected biomass estimates already account for changes in energy use and biomass turnover related to size, body size alone appears insufficient to account for the observation that some pristine reefs are 'top-heavy', with most biomass in large, apex predators (Sandin *et al.* 2008; Friedlander *et al.*

2013). Rather, our results support the hypothesis that such top-heavy pyramids arise primarily because higher trophic levels receive substantially greater energetic subsidies from sources other than reef fish (Trebilco *et al.* 2013). Contributing factors may include high mobility for large piscivores (Werry *et al.* 2014), which may allow them to garner more energy from areas outside the reef.

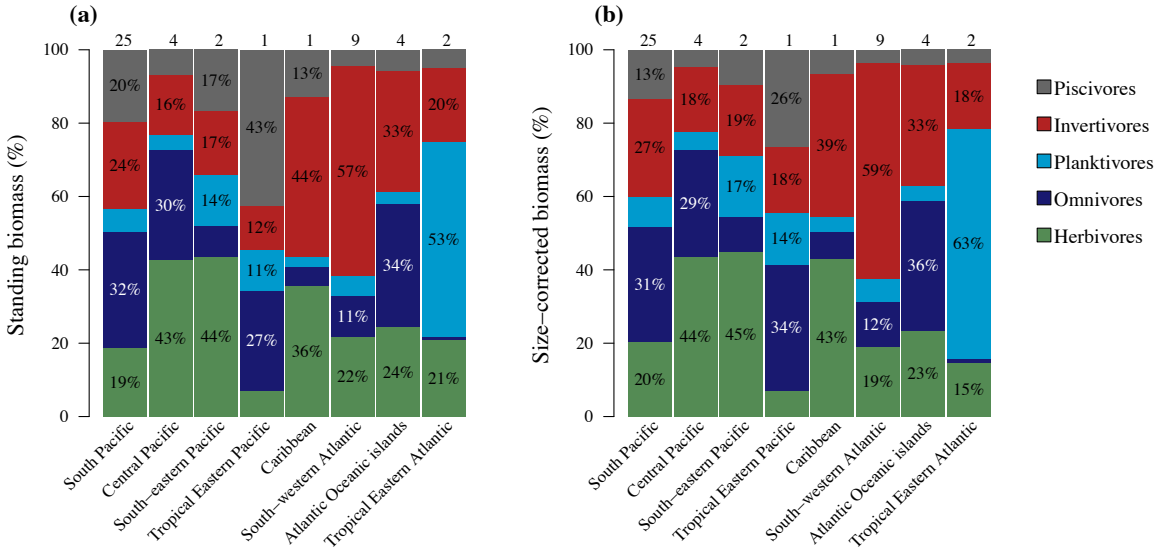

Figure 1.4. Average percentage allocations of (a) standing biomass and (b) size-corrected biomass among trophic groups for communities in different biogeographic regions. Means of each trophic group were calculated based on log ratios using MANOVA. Numbers on top of the bars indicate the number of sites sampled in each biogeographic region. Only percentages higher than 10% are labelled.

More detailed inspection of our size-corrected biomass estimates highlights the importance of size correction for broad-scale comparative analyses. For instance, the percentage standing biomass of piscivores is very high (43%) at the quasi-pristine Isla del Coco (only site in the Tropical Eastern Pacific, Fig. 1.4a). This pattern reflects the relatively high abundance of large predators, such as the hammerhead shark *Sphyrna lewini* (average biomass of 29.5 kg/sampled individual), which comprises 4% of the standing biomass, but only 2% of the size-corrected biomass. Conversely, the territorial damselfish *Stegastes arcifrons* (average biomass of 0.078 kg/individual) contributes 9% of the standing biomass,

but 15% of size-corrected biomass. Consequently, after size correction, relative biomass of piscivores at Isla del Coco becomes significantly smaller (Fig. 1.4b). These calculations support the assertion that smaller, more abundant fish (e.g. Gobiidae) are often the primary contributors to energy flux in reef-fish communities (Ackerman *et al.* 2004; Depczynski *et al.* 2007).

Total respiratory fluxes of fish communities (eqn 6) are significantly different among regions (Appendix I); however, these differences appear not to be driven by temperature (Fig. 1.5). These respiratory flux estimates are conservative because they exclude contributions of nocturnal fish and of fish < 10 cm (Fig. AI.7). Still, they exceed estimates of pelagic NPP for 6 of the 49 sites, consistent with observations that the vast majority of primary production on reefs is benthic in origin (Polovina 1984; Naumann *et al.* 2013) and that reef productivity is often substantially higher than the surrounding oceans (Hatcher 1990; Gattuso *et al*. 1998). Understanding constraints on the dynamics of reef ecosystems will require far more extensive data on reef NPP, which is estimated using an approach similar to the one adopted here by first characterising the photosynthetic rates and metabolic demands of autotrophic individuals, and then scaling these fluxes up to entire reef ecosystems (e.g. Odum & Odum 1955; Naumann *et al.* 2013). Thus, the hierarchical statistical approach adopted here, which entails scaling from individuals to ecosystems by explicitly incorporating both idiosyncratic random effects (e.g. taxonomy) and general physiological constraints (e.g. body size, temperature), may prove useful for other groups and applications.

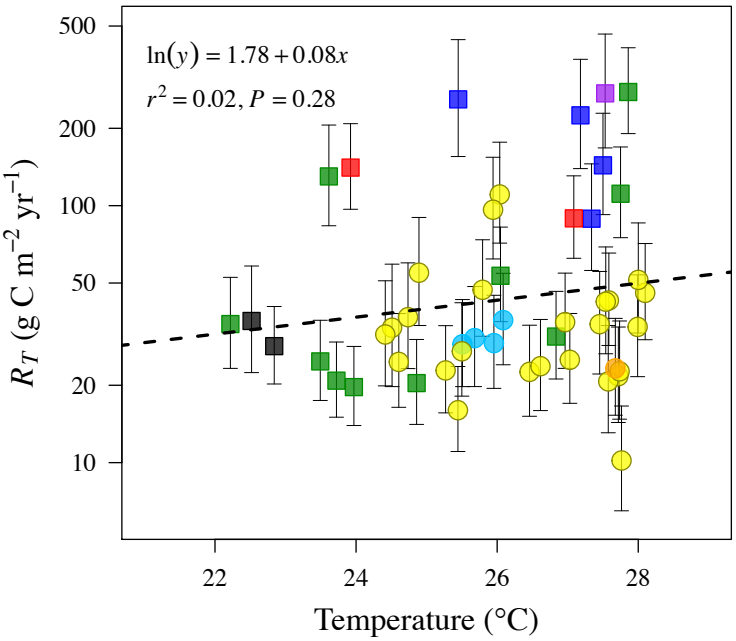

Figure 1.5. Relationships of mean annual sea surface temperature to total estimated respiratory flux of fish communities. The fitted dashed line and associated statistics were estimated using OLS regression (n = 49 sites). The fitted slope implies a ~1.6-fold increase in rates from 22 °C to 28 °C (i.e. $e^{0.08 \times (28-22)} \approx 1.6$). Colours are used to denote sites in different regions: South Pacific (yellow), Central Pacific (light blue), South-eastern Pacific (black), Tropical Eastern Pacific (purple), Caribbean (orange), South-western Atlantic (green), South-western Atlantic oceanic islands (blue) and Tropical Eastern Atlantic (red). Coral-dominated reefs are depicted as circles, and rock-dominated reefs are depicted as squares. Variation in estimates of community-level flux introduced by statistical uncertainties in the size-temperature scaling of metabolic rate are represented by 95% CI bars in the figure.

1.5 CONCLUSIONS

Our study demonstrates how individual- and community-level data can be combined to identify important broad-scale trends in energy flux (Fig. 1.1). At the individual level, our analyses highlight both the generality of MTE predictions with regard to the size and temperature scaling of metabolic rate, as well as the limitations of these predictions when applied to particular taxonomic groups (Table 1.1). Our broad-scale comparative approach also yields evidence of a temperature optimum in metabolic rate at ~33 °C for many fish taxa (Fig. 1.2), and thereby reinforces and extends previous work suggesting that at least some

tropical reef fishes are already experiencing temperatures near their thermal optima. At the community level, our study highlights the importance and utility of size correction to assess broad-scale gradients in energy flux within and among trophic levels and communities (Fig. 1.3). Accounting for size in this way reveals striking differences in trophic structure among communities in different oceanic regions (Fig. 1.4). Finally, by quantifying community-level energy flux, our approach yields important constraints on ecosystem dynamics (Fig. 1.5).

1.6 ACKNOWLEDGEMENTS

We thank V Parravicini for helping with trophic categorisation of reef fishes, EL Rezende for insights into individual-level analyses, all field assistants who helped collecting the data throughout the years and JF Bruno and two anonymous reviewers for insightful feedback on previous versions of this manuscript. This project was supported by Macquarie University (PhD scholarship to D.R.B.), Australian Research Council's Discovery Projects funding scheme (DP0987218 to A.P.A.), CESAB-FRB (Fondation pour la Recherche en Biodiversité), through the GASPAR program, SISBIOTA-Mar (PI: S.R. Floeter CNPq 563276/2010-0 and FAPESC 6308/ 2011-8), CAPES, Marinha do Brasil, Instituto Laje Viva and the National Geographic Society. The authors declare no conflict of interest.

1.7 REFERENCES

Ackerman, J.L., Bellwood, D.R. & Brown, J.H. (2004). The contribution of small individuals to density-body size relationships: examination of energetic equivalence in reef fishes. *Oecologia*, 139, 568–571.

Agutter, P. & Wheatley, D.N. (2004). Metabolic scaling: consensus or controversy? *Theoretical Biology and Medical Modelling*, 1, 13.

Aitchison, J. (2003). *The statistical analysis of compositional data*. Blackburn Press, Caldwell, New Jersey, pp. 416.

Allen, A.P. & Gillooly, J.F. (2009). Towards an integration of ecological stoichiometry and the metabolic theory of ecology to better understand nutrient cycling. *Ecology Letters*, 12, 369–384.

Allen, A.P., Gillooly, J.F. & Brown, J.H. (2005). Linking the global carbon cycle to individual metabolism. *Functional Ecology*, 19, 202–213.

Amarasekare, P. & Savage, V. (2012). A framework for elucidating the temperature dependence of fitness. *The American Naturalist*, 179, 178–191.

Anderson, A.B., Bonaldo, R.M., Barneche, D.R., Hackradt, C.W., Félix-Hackradt, F.C., García-Chartón, J.A. *et al.* (2014). Recovery of grouper assemblages indicates effectiveness in a Marine Protected Area in Southern Brazil. *Marine Ecology Progress Series*, 514, 207–215.

Arias-González, J.E., Delesalle, B., Salvat, B. & Galzin, R. (1997). Trophic functioning of the Tiahura reef sector, Moorea Island, French Polynesia. *Coral Reefs*, 16, 231–246.

Bates, D., Maechler, M., Bolker, B. & Walker, S. (2015). *lme4:* Linear mixed-effects models using Eigen and S4. R package version 1.1-8. Available at http://www.CRAN.R-project.org/package=lme4.

Behrenfeld, M.J. & Falkowski, P.G. (1997). Photosynthetic rates derived from satellite-based chlorophyll concentration. *Limnology and Oceanography*, 42, 1–20.

Bellwood, D.R. & Wainwright, P.C. (2002). The history and biogeography of fishes on coral reefs. In: *Coral reef fishes: dynamics and diversity in a complex ecosystem* (ed. Sale, P.F.). Academic Press, San Diego, pp. 5–32.

Bozec, Y.-M., Gascuel, D. & Kulbicki, M. (2004). Trophic model of lagoonal communities in a large open atoll (Uvea, Loyalty Islands, New Caledonia). *Aquatic Living Resources*, 17, 151–162.

Brown, J.H., Gillooly, J.F., Allen, A.P., Savage, V.M. & West, G.B. (2004). Toward a metabolic theory of ecology. *Ecology*, 85, 1771–1789.

Clarke, A. & Fraser, K.P.P. (2004). Why does metabolism scale with temperature? *Functional Ecology*, 18, 243–251.

Clarke, A. & Johnston, N.M. (1999). Scaling of metabolic rate with body mass and temperature in teleost fish. *Journal of Animal Ecology*, 68, 893–905.

Depczynski, M., Fulton, C.J., Marnane, M.J. & Bellwood, D.R. (2007). Life history patterns shape energy allocation among fishes on coral reefs. *Oecologia*, 153, 111–120.

Donelson, J.M., Munday, P.L., McCormick, M.I. & Pitcher, C.R. (2012). Rapid transgenerational acclimation of a tropical reef fish to climate change. *Nature Climate Change*, 2, 30–32.

Friedlander, A.M., Ballesteros, E., Beets, J., Berkenpas, E., Gaymer, C.F., Gorny, M. *et al.* (2013). Effects of isolation and fishing on the marine ecosystems of Easter Island and Salas y Gómez, Chile. *Aquatic Conservation: Marine and Freshwater Ecosystems*, 23, 515–531.

Froese, R. & Pauly, D. (2012). FishBase. World Wide Web electronic publication. Available at http://www.fishbase.org, (Version 12/2012). Last accessed 20 February 2015.

Gardiner, N.M., Munday, P.L. & Nilsson, G.E. (2010). Counter-gradient variation in respiratory performance of coral reef fishes at elevated temperatures. *PLoS ONE*, 5, e13299.

Gattuso, J.P., Frankignoulle, M. & Wollast, R. (1998). Carbon and carbonate metabolism in coastal aquatic ecosystems. *Annual Review of Ecology and Systematics*, 29, 405–434.

Gillooly, J.F., Brown, J.H., West, G.B., Savage, V.M. & Charnov, E.L. (2001). Effects of size and temperature on metabolic rate. *Science*, 293, 2248–2251.

Hamner, W.M., Jones, M.S., Carleton, J.H., Hauri, I.R. & Williams, D.M. (1988). Zooplankton, planktivorous fish, and water currents on a windward reef face: Great Barrier Reef, Australia. *Bulletin of Marine Science*, 42, 459–479.

Hatcher, B.G. (1990). Coral reef primary productivity. a hierarchy of pattern and process. *Trends in Ecology & Evolution*, 5, 149–155.

Houde, E.D. (1989). Comparative growth, mortality, and energetics of marine fish larvae: temperature and implied latitudinal effects. *Fishery Bulletin*, 87, 471–495.

Huey, R.B. & Stevenson, R. (1979). Integrating thermal physiology and ecology of ectotherms: a discussion of approaches. *American Zoologist*, 19, 357–366.

Hussey, N.E., MacNeil, M.A., McMeans, B.C., Olin, J.A., Dudley, S.F., Cliff, G. *et al.* (2014). Rescaling the trophic structure of marine food webs. *Ecology Letters*, 17, 239–250.

Jackson, J.B.C., Kirby, M.X., Berger, W.H., Bjorndal, K.A., Botsford, L.W., Bourque, B.J. *et al.* (2001). Historical overfishing and the recent collapse of coastal ecosystems. *Science*, 293, 629–637.

Johansen, J.L. & Jones, G.P. (2013). Sediment-induced turbidity impairs foraging performance and prey choice of planktivorous coral reef fishes. *Ecological Applications*, 23, 1504–1517.

Kronen, M., Pinca, S., Magron, F., McArdle, B., Vunisea, A., Vigliola, L. *et al.* (2012). Socio-economic and fishery indicators to identify and monitor artisanal finfishing pressure in pacific island countries and territories. *Ocean & Coastal Management*, 55, 63–73.

Kulbicki, M., Parravicini, V., Bellwood, D.R., Arias-González, E., Chabanet, P., Floeter, S.R. *et al.* (2013). Global biogeography of reef fishes: a hierarchical quantitative delineation of regions. *PLoS ONE*, 8, e81847.

Lindeman, R.L. (1942). The trophic-dynamic aspect of ecology. *Ecology*, 23, 399–417.

López-Urrutia, Á., San Martin, E., Harris, R.P. & Irigoien, X. (2006). Scaling the metabolic balance of the oceans. *Proceedings of the National Academy of Sciences*, 103, 8739–8744.

MacNeil, M.A., Graham, N.A.J., Cinner, J.E., Wilson, S.K., Williams, I.D., Maina, J. *et al*. (2015). Recovery potential of the world's coral reef fishes. *Nature*, 520, 341–344.

McDole, T., Nulton, J., Barott, K.L., Felts, B., Hand, C., Hatay, M. *et al.* (2012). Assessing coral reefs on a Pacific-wide scale using the microbialization score. *PLoS ONE*, 7, e43233.

Mora, C., Aburto-Oropeza, O., Bocos, A.A., Ayotte, P.M., Banks, S., G. Bauman, *et al.* (2011). Global human footprint on the linkage between biodiversity and ecosystem functioning in reef fishes. *PLoS Biology*, 9, e1000606.

Naumann, M.S., Jantzen, C., Haas, A.F., Iglesias-Prieto, R. & Wild, C. (2013). Benthic primary production budget of a Caribbean reef lagoon (Puerto Morelos, Mexico). *PLoS ONE*, 8, e82923.

O'Connor, M.I., Piehler, M.F., Leech, D.M., Anton, A. & Bruno, J.F. (2009). Warming and resource availability shift food web structure and metabolism. *PLoS Biol*ogy, 7, e1000178.

Odum, H.T. & Odum, E.P. (1955). Trophic structure and productivity of a windward coral reef community on Eniwetok Atoll. *Ecological Monographs*, 25, 291–320.

Parravicini, V., Kulbicki, M., Bellwood, D.R., Friedlander, A.M., Arias-Gonzalez, J.E., Chabanet, P. *et al.* (2013). Global patterns and predictors of tropical reef fish species richness. *Ecography*, 36, 1254–1262.

van de Pol, M. & Wright, J. (2009). A simple method for distinguishing within- versus between-subject effects using mixed models. *Animal Behaviour*, 77, 753–758.

Polovina, J. (1984). Model of a coral reef ecosystem. *Coral Reefs*, 3, 1–11.

Pörtner, H.O. & Knust, R. (2007). Climate change affects marine fishes through the oxygen limitation of thermal tolerance. *Science*, 315, 95–97.

Rombough, P.J. (1994). Energy partitioning during fish development: additive or compensatory allocation of energy to support growth? *Functional Ecology*, 8, 178–186.

Rummer, J.L., Couturier, C.S., Stecyk, J.A.W., Gardiner, N.M., Kinch, J.P., Nilsson, G.E. *et al.* (2014). Life on the edge: thermal optima for aerobic scope of equatorial reef fishes are close to current day temperatures. *Global Change Biology*, 20, 1055–1066.

Sandin, S.A., Smith, J.E., DeMartini, E.E., Dinsdale, E.A., Donner, S.D., Friedlander, A.M. *et al.* (2008). Baselines and degradation of coral reefs in the northern Line Islands. *PLoS ONE*, 3, e1548.

Savage, V.M., Gillooly, J.F., Woodruff, W.H., West, G.B., Allen, A.P., Enquist, B.J. *et al.* (2004). The predominance of quarter-power scaling in biology. *Functional Ecology*, 18, 257–282.

Schoolfield, R., Sharpe, P. & Magnuson, C. (1981). Non-linear regression of biological temperature-dependent rate models based on absolute reaction-rate theory. *Journal of Theoretical Biology*, 88, 719–731.

Selig, E.R., Casey, K.S. & Bruno, J.F. (2010). New insights into global patterns of ocean temperature anomalies: implications for coral reef health and management. *Global Ecology and Biogeography*, 19, 397–411.

Su, Y.-S. & Yajima, M. (2015). *R2jags:* A package for running *JAGS* from R. R package version 0.05-03.

Teh, L.S.L., Teh, L.C.L. & Sumaila, U.R. (2013). A global estimate of the number of coral reef fishers. *PLoS ONE*, 8, e65397.

Trebilco, R., Baum, J.K., Salomon, A.K. & Dulvy, N.K. (2013). Ecosystem ecology: size-based constraints on the pyramids of life. *Trends in Ecology & Evolution*, 28, 423–431.

Werry, J.M., Planes, S., Berumen, M.L., Lee, K.A., Braun, C.D. & Clua, E. (2014). Reef-fidelity and migration of tiger sharks, *Galeocerdo cuvier*, across the Coral Sea. *PLoS ONE*, 9, e83249.

Wilson, S.K., Adjeroud, M., Bellwood, D.R., Berumen, M.L., Booth, D., Bozec, Y.-M. *et al.* (2010). Crucial knowledge gaps in current understanding of climate change impacts on coral reef fishes. *The Journal of Experimental Biology*, 213, 894–900.

Yvon-Durocher, G. & Allen, A.P. (2012). Linking community size structure and ecosystem functioning using metabolic theory. *Philosophical Transactions of the Royal Society B: Biological Sciences*, 367, 2998–3007.

Yvon-Durocher, G., Caffrey, J.M., Cescatti, A., Dossena, M., del Giorgio, P., Gasol, J.M. *et al.* (2012). Reconciling the temperature dependence of respiration across timescales and ecosystem types. *Nature*, 487, 472–476.

Zuur, A.F., Ieno, E.N., Walker, N.J., Saveliev, A.A. & Smith, G.M. (2009). *Mixed effects models and extensions in ecology with R*. Springer, New York, pp. 574.

CHAPTER 2

ENERGETIC AND ECOLOGICAL CONSTRAINTS ON POPULATION DENSITY

Submitted as: Barneche, D.R., Kulbicki, M., Floeter, S.R., Friedlander, A.M., Allen, A.P. Energetic and ecological constraints on population density (submitted to *Proceedings of Royal Society of London B: Biological Sciences* in August 2015).

2.1 ABSTRACT

Population ecology has classically focused on pairwise species interactions, hindering the description of general patterns and processes of population abundance at large spatial scales. Here we use the Metabolic Theory of Ecology as a framework to formulate and test a model that yields predictions linking population density to the physiological constraints of body size and temperature on individual metabolism, and the ecological constraints of trophic structure and species richness on energy partitioning among species. Our model was tested by applying a novel Bayesian quantile regression approach to a comprehensive reef-fish community database, from which we extracted density data for 5609 populations spread across 49 sites around the world. Our results indicate that population density declines markedly with increases in community species richness and that, after accounting for richness, energetic constraints are manifested most strongly for the most abundant species, which generally are of small body size and occupy lower trophic groups. Overall, our findings suggest that, at the global scale, factors associated with community species richness are the major drivers of variation in population density. Given that populations of species-rich tropical systems exhibit markedly lower maximum densities, they may be particularly susceptible to stochastic extinction.

2.2 INTRODUCTION

The abundance of any given species population is influenced by myriad factors including, but not limited to, interspecific competition, habitat suitability and disturbance regime. Nevertheless, population abundance is ultimately constrained by the availability of energy and resources in the environment (Lindeman 1942; Peters 1983; Brown *et al.* 2004; Allen *et al.* 2005). Still, it remains unclear to what extent these energetic constraints can be used to predict abundances of particular species populations at particular sites (Tilman *et al.* 2004). We note that population density, rather than population abundance, is more appropriate for assessing energetic requirements because energy flows through a community on a per-unit-area, and individuals of a given species must harvest energy locally from their surroundings to meet their energetic requirements.

Body size is often a focus of this debate because of its primary role in determining metabolic rates, and hence resource demands, of individuals (Brown *et al.* 2004). The influence of body size on population density (expressed as individuals per unit area or volume) has been investigated using two distinct approaches (White *et al.* 2007): (1) global size-density relationships (GSDRs) among multiple species and sites, (2) local size-density relationships (LSDRs) among multiple species at the same site. White *et al.* (White *et al.* 2007) note that GSDRs often exhibit stronger correlations than LSDRs. This discrepancy may reflect the fact that GSDRs are typically derived from population-level studies (White *et al.* 2007), which may focus predominantly on sites where the focal species are relatively abundant (Cotgreave 1993).

A useful point of departure for investigating the role of body size in constraining population density is the energetic equivalence rule (EER) (Damuth 1987). The EER is an empirical generalisation, based primarily on GSDRs (Damuth 1987; White *et al.* 2007), that

population density, D_p, often varies with individual body mass, M_i, as $D_p \propto M_i^{-\alpha}$, where $\alpha \approx 3/4$. Given that individual metabolic rate scales as $B_i \propto M_i^{\alpha}$ for multicellular organisms (Peters 1983; Brown *et al.* 2004; Savage *et al.* 2004; Barneche *et al.* 2014), the EER is so named because it implies that population-level energy flux, $D_p B_i$, is independent of body size, i.e. $D_p B_i \propto M_i^0$. Evidence for and against the EER has been presented (Damuth 1987; Allen *et al.* 2002; Isaac *et al.* 2013), which raises more general questions about the extent to which energetic constraints on individuals can be used to predict population densities.

Trophic level may also constrain population density because only a fraction of the energy assimilated at one trophic level (perhaps ~10%) is transferable to higher trophic levels owing to energy losses through respiration and other processes (Lindeman 1942). Thus, in closed systems, total abundances are expected to be higher for herbivores than for secondary and tertiary consumers if other variables such as body size are held constant. This so-called 10% rule is consistent with data from some pelagic food webs (e.g. Sheldon *et al.* 1977; Pauly & Christensen 1995). However, in open systems, trophic-level effects may be obscured by external energy subsidies. For example, on reefs, subsidies to pelagic consumers (Hamner *et al.* 1988; Trebilco *et al.* 2013) may help explain why total abundances of piscivorous and other carnivorous fish, relatively to herbivores, are far higher than what would be predicted based on the 10% rule even after controlling for body size (Barneche *et al.* 2014).

In some food webs, particularly pelagic communities, trophic level may be determined largely by body size, rather than by species identity (Kerr & Dickie 2001). In such systems, frequency distributions of body size for all individuals comprising communities, $f(M_i)$, often adhere to power-function probability distributions with scaling exponents, s, that are steeper than that of metabolic rate (i.e. $f(M_i) \propto M_i^{-s}$, where $s > \alpha$) (Kerr & Dickie 2001; Jennings & Mackinson 2003; Reuman *et al.* 2009). For such size "spectra" (Kerr & Dickie 2001), theory predicts that $s \approx \alpha + 1/4$ if there is a 10% energy transfer efficiency between trophic levels,

and predators consume prey that are 4-orders of magnitude smaller in size (Brown & Gillooly 2003; Trebilco *et al.* 2013). However, a key assumption of size-spectrum theory – that body size is tightly and positively correlated with trophic level – is questionable for some communities, such as reef fishes (Fig. AII.1). For example, in the Indo-Malaysian Archipelago, the benthic herbivorous fish *Bolbometopon muricatum* is 59-fold larger than the piscivore *Synodus variegatus* (46 kg versus 780 g). Size-spectrum theory also assumes a closed system, and therefore does not account for the fact that reef-fish communities consume two distinct classes of resources (benthic, pelagic), the latter of which may be heavily subsidised by external sources (e.g. Hamner *et al.* 1988; Trebilco *et al.* 2013; Barneche *et al.* 2014).

Another potential constraint on population density is community species richness, which exhibits broad-scale correlations with indices of environmental energy availability, particularly temperature and ecosystem primary production (Currie *et al.* 2004). Most biological communities are comprised of relatively few abundant species and many rare species, with maximum abundance per species and variation in abundance among species generally decreasing with increasing species richness (Hubbell 2001). Theoretical explanations for this pattern involve some combination of deterministic (e.g. resource partition, species interactions) and stochastic processes (Hubbell 2001). Regardless of the underlying mechanisms, if total community abundance is held constant at some carrying capacity dictated by total energy availability in the environment (Allen *et al.* 2005), average density per species must decline with increasing species richness (Allen *et al.* 2002).

In this study, we assess the relative importance of individual- (body size), population- (trophic group), and community- and ecosystem-level attributes (temperature, species richness, area) in determining population densities of both rare and abundant species in communities. In so doing, we evaluate the general hypothesis that energetic constraints on

population density are manifested most strongly for the most abundant species because they garner the largest fractions of the energy and resources used by the community (McGill *et al.* 2007), and are therefore most likely to be limited by energy and resource availability (Blackburn *et al.* 1992; White *et al.* 2007). Our approach is timely given the increasing recognition that abundant taxa represent only a small fraction of all species present in a community, yet account for a large fraction of the biomass and energy turnover in many ecosystems (Gaston 2010, 2011; ter Steege *et al.* 2013). Using the Metabolic Theory as a framework (Brown *et al.* 2004), we first derive null expectations for population density under the assumption of energetic equivalence with respect to multiple variables, including body size, and then use these null expectations as quantitative benchmarks for comparison.

We evaluate these null expectations using one of the most comprehensive datasets of reef-fish community structure currently available (Barneche *et al.* 2014). Our approach explicitly bridges the gap between the GSDR and LSDR approaches because we analyse local-scale community-level data collected from global collections of sites using quantile regression (Cade & Noon 2003), which is capable of separately characterising density trends for rare and abundant taxa. Reef fishes are ideal study organisms because they encompass high total species richness (> 6000 species) and variation in richness among sites (~50 for temperate reefs to ~3000 for some tropical reefs) (Parravicini *et al.* 2013), they can occupy diverse habitats, and they vary substantially in body mass (> 6 orders of magnitude: ~0.1 g to ~500 kg), trophic mode, and thermal regime (~17-30˚C minimum monthly average SST) (Froese & Pauly 2012; Parravicini *et al.* 2013).

2.3 MATERIALS AND METHODS

2.3.1 Predictions Under Energetic Equivalence

The relationship of individual metabolic rate, B_i (g C d^{-1}), to body mass, M_i (g), is generally described by a power function of the form (Peters 1983; Brown *et al.* 2004; Savage *et al.* 2004)

$$B_i = B_o M_i^{\alpha}, \quad (1)$$

where B_o is a metabolic normalisation (g C $g^{-\alpha}$ d^{-1}) that varies among taxa and environments (Brown *et al.* 2004), and with other variables, particularly temperature (Gillooly *et al.* 2001; Barneche *et al.* 2014). Among fishes, the dimensionless scaling exponent α is ~0.75 (Barneche *et al.* 2014), which is similar in magnitude to values observed for other multi-cellular taxa (Peters 1983; Savage *et al.* 2004). Recent work (Barneche *et al.* 2014) indicates that, for fishes, the temperature dependence of B_o can be characterised as

$$B_o = b_o(T_s)K(T), \quad (2)$$

where b_o is the value of the metabolic normalisation at some arbitrary absolute temperature for standardisation, T_s (K),

$$K(T) = e^{E_r\left(\frac{1}{kT_s} - \frac{1}{kT}\right)}\left(1 + \left(\frac{E_r}{E_i - E_r}\right)e^{E_i\left(\frac{1}{kT_{opt}} - \frac{1}{kT}\right)}\right)^{-1}, \quad (3)$$

and k is Boltzmann's constant (8.62×10^{-5} eV K^{-1}). In eqn 3, the temperature dependence of kinetics, $K(T)$, is the product of two terms: a Boltzmann term, $e^{E_r(1/kT_s - 1/kT)}$, that characterises temperature-induced enhancement of rates below the temperature optimum, T_{opt} (K), using an activation energy, E_r (eV); and an inactivation term, $\left(1 + \left(\frac{E_r}{E_i - E_r}\right) e^{E_i\left(\frac{1}{kT_{opt}} - \frac{1}{kT}\right)}\right)^{-1}$, that characterises declines in rates above T_{opt} using an inactivation energy, E_i (Schoolfield *et al.* 1981). For fishes, E_r, E_i and T_{opt} vary significantly among taxa (see Chapter 1), with respective family-level averages of about 0.6 eV, 2 eV, and 33˚C (Barneche *et al.* 2014).

Population-level respiratory flux is equal to the sum of the individual metabolic rates (Allen *et al.* 2005). The annual respiratory flux per unit area, R_p (g C ha^{-1} yr^{-1}), for a population comprised of J_p individuals in a community of area A_c (ha) can therefore be calculated by integrating flux over the time interval $t = 0$ d to $t = \tau = 365$ d to yield

$$R_p = \frac{1}{A_c}\left[\sum_{i=1}^{J_p}\int_{t=0}^{t=\tau} B_i\,(t)dt\right] =$$

$$= D_p\langle B_i\rangle_p = D_p b_o \tau\ \langle M_i^{\alpha}\rangle_p\ \langle K(T)\rangle_c, \qquad (4)$$

where $D_p \equiv J_p/A_c$ is population density (individuals ha^{-1}) and $\langle B_i\rangle_p = b_o\tau\ \langle M_i^{\alpha}\rangle_p\ \langle K(T)\rangle_c$ is the average annual respiratory flux for individuals comprising the population. The latter quantity is calculated based on average size-corrected body mass, $\langle M_i^{\alpha}\rangle_p$ $\left(= (1/J_p)\left[\sum_{i=1}^{J_p} M_i^{\alpha}\right]\right)$ (Yvon-Durocher & Allen 2012; Barneche *et al.* 2014), and time-averaged

temperature kinetics, $\langle K(T)\rangle_c$ $\left(= (1 / \tau) \int_{t=0}^{t=\tau} K\,(T(t))dt\right)$, by allowing temperature to vary through time, $T(t)$, while holding population density and the distribution on body sizes constant.

Eqn 4 can therefore be rearranged to demonstrate how population density, D_p, is effected by the average size-corrected body mass, $\langle {M_i}^{\alpha}\rangle_p$, and time-averaged temperature kinetics, $\langle K(T)\rangle_c$, on population density, D_p,

$$D_p \propto \left[\langle M_i^{\alpha}\rangle_p\right]^{-1}\ [\langle K(T)\rangle_c]^{-1}, \tag{5}$$

if annual respiratory flux, R_p, is independent of these variables. In this expression, $\langle {M_i}^{\alpha}\rangle_p$ and $\langle K(T)\rangle_c$ both take scaling exponents of -1 because population density will decline inversely with increases in per-individual metabolic demands. Thus, these -1 values represent benchmarks for assessing if populations that differ in their body-size distributions and temperature kinetics are equivalent with respect to energy use. Here we note that the EER is typically evaluated using raw arithmetic averages for body mass (White *et al.* 2007), which entails an approximation that becomes less accurate as variation in body size increases (Savage 2004). Eqn 5, by contrast, does not entail this approximation, and is therefore preferable for evaluating the EER, if size-frequency data are available (Allen *et al.* 2002) (Fig. AII.2).

Eqn 5 is derived based solely on effects of individual energetics on population density; however, such effects may be modified by other variables. For example, in a closed system at steady state, population density may differ among trophic groups, g, even after controlling for body size, because total energy availability is lower at higher trophic levels (Lindeman 1942). Density estimates are also expected to vary with community species richness and area, S_c and

A_c, because average population density is equal to $J_c/(A_c S_c)$ for a community comprised of J_c individuals and S_c species (Allen *et al.* 2002), and S_c increases non-linearly with A_c (Rosenzweig 1995; Harte *et al.* 2009). Here we statistically assess the effects of these variables by fitting the following expression

$$\ln D_p = \ln\widetilde{D_p} + \ln\Delta_g + \beta_M \ln\left[\frac{\langle M_i^{\alpha}\rangle_p}{\langle\widetilde{M_i^{\alpha}}\rangle_p}\right] + \beta_K \ln\left[\frac{\langle K(T)\rangle_c}{\langle\widetilde{K(T)}\rangle_c}\right] + \beta_S \ln\left[\frac{S_c}{\widetilde{S_c}}\right] + \beta_A \ln\left[\frac{A_c}{\widetilde{A_c}}\right], \quad (6)$$

which assumes power-function scaling relations for the effects of average size-corrected body mass, temperature kinetics, richness, and area (respectively quantified by the scaling exponents β_M, β_K, β_S and β_A). Treatment of richness and area effects in this way is consistent with species-area relationships, which are often characterised using scaling exponents *z* as $S_c \propto A_c^z$ (Rosenzweig 1995); however, such functions are only approximations because *z* varies among systems and with spatial scale (Harte *et al.* 2009). A diagnostic plot of the model residuals suggests that the model, taken as a whole, provides a reasonable fit to the data (Fig. AII.3). For our analysis, effects of trophic group are standardised by separately estimating Δ_g for each group (g) subject to the constraint that the product of the estimates $\prod\Delta_g$ = 1. Effects of other variables are standardised using the median estimate of average size-corrected body mass for the 5609 populations included in our analysis ($\langle\widetilde{M_i^{\alpha}}\rangle_p$ = 28 $g^{0.76}$, corresponding to $M_i = \langle\widetilde{M_i^{\alpha}}\rangle_p^{\,1/\alpha}$ = 80 g), and the median estimates of temperature kinetics ($\langle\widetilde{K(T)}\rangle_c$ = 1.40), community species richness ($\widetilde{S_c}$ = 84 species) and sampling area ($\widetilde{A_c}$ = 0.656 ha) for the 49 communities included in our analysis. Consequently, the *normalised density*, $\widetilde{D_p}$ (individuals ha^{-1}), corresponds to the estimated population density for a typical trophic group at these standardised values.

Eqns 1–6 provide a useful framework for assessing energetic equivalence (or lack thereof) among populations with respect to multiple variables, as demonstrated by combining the expressions for energy flux (eqn 4) and population density (eqn 6)

$$R_p \propto \Delta_g \langle M_i^{\alpha} \rangle_p^{\beta_M+1} \langle K(T) \rangle_c^{\beta_K+1} S_c^{\beta_S} A_c^{\beta_A}. \quad (7)$$

For example, energetic equivalence with respect to trophic group for reef fishes would be indicated by identical estimates of $\Delta_g = 1$ for herbivores, invertivores, omnivores, piscivores and planktivores. Energetic equivalence with respect to body size and temperature would be indicated by values of -1 for β_M and β_K, respectively, following eqn 5. Thus, values > -1 for one or both of these fitted parameters would indicate that larger-bodied (and/or warmer) populations garner relatively more energy. By contrast, energetic equivalence with respect to species richness and area would be indicated by slopes of 0 for β_S and β_A, respectively.

2.3.2 Model Fitting Procedure

We fit eqn 6 to empirical data using quantile regression, a flexible and robust technique that entails few statistical assumptions (Cade & Noon 2003). Here we use *mixed-effects* quantile regression, which is widely known in Statistics and Economics, but which has thus far been used in only a handful of Ecology studies (e.g. Alhamzawi *et al.* 2011; Fornaroli *et al.* 2015). We implement this regression technique using a hierarchical Bayesian procedure (Yu & Moyeed 2001; Geraci & Bottai 2007) in order to determine posterior distributions and associated 95% credible intervals (CIs) for the fitted parameters. Analyses were conducted using *JAGS* version 3.4.0 and the R package *R2jags* version 0.5-6 (Su & Yajima 2015) in R version 3.2.1 (R Core Team 2015) (see Appendix II for detailed explanation and *JAGS* code).

We adopt this mixed-effects methodology in order to allow the normalised density, $\ln\widetilde{D_p}$ in eqn 6, to vary among sites. We do so by treating it as the sum of two parameters,

$$\ln\widetilde{D_p} = \langle\ln\widetilde{D_p}\rangle + \Delta_c\langle\ln\widetilde{D_p}\rangle, \quad (8)$$

a fixed effect, $\langle\ln\widetilde{D_p}\rangle$, corresponding to an average among communities for the normalised density, and a random effect, $\Delta_c\langle\ln\widetilde{D_p}\rangle$, corresponding to a community-level deviation from this average. In our model, community-level random effects, $\Delta_c\langle\ln\widetilde{D_p}\rangle$, are assumed to be normally distributed with a mean of 0. Treating $\ln\widetilde{D_p}$ in this way allows us to control for the potential effects of other unmeasured variables (e.g. sampling protocol, ecosystem productivity, habitat quality) that might otherwise lead to correlated residuals at the community level. All of the other fitted parameters – $\ln\Delta_g$, β_M, β_K, β_S and β_A – were treated as having only fixed effects for the model presented in the main text.

In order to assess whether determinants of population density varied with density, we fit a series of 30 quantile regression models, corresponding to 30 different quantiles, q, in order to derive distinct predictions for rare (q = 0.15) to abundant species (q = 0.95). For example, setting q = 0.95, the fitted quantile regression model yields predictions for a density threshold that is exceeded by only 5% of species. Note that, because the normalised density is allowed to vary among communities in our analysis, following eqns 6 and 8, this threshold corresponds to 5% of species *at a given site*. Estimates of density for rare species are particularly sensitive to sampling artefacts (McGill *et al*. 2007, Harte & Storch 2009); our quantile regression approach explicitly excludes these species from the analysis by considering only density quantiles ≥ 0.15. Quantile regression is useful for modelling heteroscedastic (e.g. constrained) relationships among variables because parameter estimates

are allowed to vary by quantile, perhaps due to the competing effects of different processes (Cade & Noon 2003). If, for example, energetic constraints on population density were greater for more abundant taxa, we would expect the slopes β_M and β_K to become more negative at high values of q.

We analysed community-level data collected from 49 communities (islands, atolls and coastal contiguous reefs) using standardised belt transects in which divers tallied the numbers, species identities, and body lengths of all fish (Appendix II; Barneche *et al.* 2014). To minimise bias associated with visual surveys of reef fish (e.g. Broke 1982; Edgar *et al*. 2004), observations were collected by teams of researchers with extensive training.

Body masses were inferred from body lengths by estimating the wet weights of individuals using length-weight conversion formulas. Each species was assigned to one of five trophic groups (herbivores, omnivores, planktivores, invertivores, piscivores) as described in Barneche *et al.* (2014). Community-level estimates of temperature kinetics, $\langle K(T)\rangle_c$, were calculated based on weekly satellite estimates of mean annual sea-surface temperature (Selig *et al.* 2010). Community-level estimates of richness, S_c, were calculated as the total numbers of species sampled over the entire sampling area, A_c. Because species richness is known to be sensitive to sampling (Rosenzweig 1995), prior to analysis, we compared our measure of diversity (the total number of species sampled) to the Chao diversity metric, which is known to be more robust to sampling artefacts (Gotelli & Colwell 2010). We obtained a high correlation for the two measures (r = 0.98, d.f. = 47, t = 37.27, $P <$ 0.0001; Fig. AII.5), indicating that our proxy for species diversity is robust for the purposes of this analysis. We also note that our community-level samples represent 'snapshots' of communities that are highly dynamic through different time scales (Sale & Douglas 1984;

Irigoyen *et al*. 2013) and these temporal effects should be captured as unexplained residual variation in our model.

2.4 RESULTS

Quantile regression analyses indicate that population density varies markedly among taxa within communities, as indicated by an 191-fold increase in the average normalised density (=$e^{\langle \ln \widetilde{D_p} \rangle}$) from about 3 ind. ha^{-1} for relatively rare species (q = 0.15) to 481 ind. ha^{-1} for relatively abundant species (q = 0.95) (Fig. 2.1a). An increase in $\langle \ln \widetilde{D_p} \rangle$ with q is expected, on a mathematical basis, because higher quantiles correspond to more abundant taxa, and the parameter $\langle \ln \widetilde{D_p} \rangle$ represents the intercept of the fitted model (eqns 6 and 8). Our mixed-model approach also characterises deviations in normalised densities from the average, $\langle \ln \widetilde{D_p} \rangle$, as random effects, $\Delta_c \langle \ln \widetilde{D_p} \rangle$ (eqns 6 and 8). The estimated standard deviation of these random effects, sd[$\Delta_c \langle \ln \widetilde{D_p} \rangle$], imply that normalised densities vary on average about 1.58-fold ($\approx e^{2\times 0.23}$) among communities for rare species (sd[$\Delta_c \langle \ln \widetilde{D_p} \rangle$] = 0.23 at q = 0.15) and about 4.48-fold ($\approx e^{2\times 0.75}$) among communities for abundant species (sd[$\Delta_c \langle \ln \widetilde{D_p} \rangle$] = 0.75 at q = 0.95) (Fig. AII.4).

Importantly, all of the parameters used to characterise the effects of predictor variables (with the exception of temperature kinetics) vary significantly between rare (q = 0.15) and abundant (q = 0.95) species (Figs. 2.1b–f). These findings indicate that determinants of population density vary significantly with density. Thus, they support our use of quantile regression over more traditional statistical methods that assume homoscedastic relationships among variables.

Our analysis yields two lines of evidence in support of the hypothesis that energetic constraints on population density are most pronounced for the most abundant species. First,

differences in the normalised densities among trophic groups are not statistically significant for rare species (lower quantiles; Fig. 2.1b), but become highly significant for abundant species judging by the non-overlapping 95% CIs for the estimates of differences at larger quantiles (grey areas of the figure). Second, the body-size effect, represented by the slope β_M, becomes steeper moving towards more abundant species (higher quantiles; Fig. 2.1c), indicating a constrained (i.e. wedge-shaped) relationship of body size to density (Fig. 2.2).

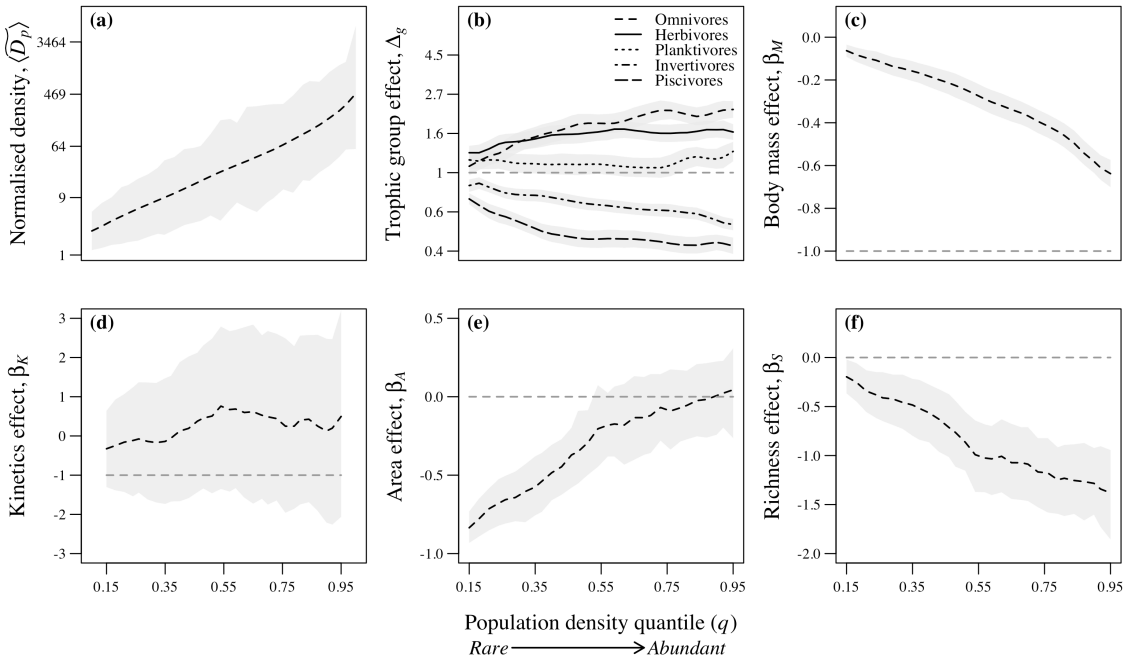

Figure 2.1. Relationships of parameter estimates (from eqns 6 and 8) to density quantiles for parameters used to characterise effects of (a) normalised population density, (b) trophic group, (c) size-corrected body mass, (d) temperature kinetics, (e) sampling area, and (f) species richness. Dashed lines represent averages of posterior distributions, and shading represents 95% credible intervals.

Despite some evidence of energetic constraints, our analysis yields no evidence of energetic equivalence. First, regarding trophic group, the observed differences in the density normalisations (characterised by Δ_g) imply that population densities (and hence energy fluxes, following eqn 7) are greater for omnivores, herbivores, and planktivores (in that order)

than for invertivores and piscivores, after controlling for other variables (Fig. 2.1b). Regarding average size-corrected body mass, even for the most abundant species (q = 0.95), the fitted slope is far shallower than -1 (-0.64; 95% CI: -0.70 to -0.57; Fig. 2.1c). Similar results are obtained if size-density relationships are instead allowed to vary among communities (Fig. AII.6). Thus, despite the fact that population density declines with increasing size-corrected body mass (Fig. 2.3a), population energy flux actually increases with body size (Fig. 2.3b). Regarding temperature kinetics, the 95% CIs for the slope overlap the values of both -1 and 0 at all density quantiles (Fig. 2.1d). Thus, for the reef communities considered here, which encompass a predicted ~1.37-fold increase in temperature kinetics moving from warm temperate (mean annual sea surface temperature of 22˚C) to tropical communities (mean annual sea surface temperature of 28˚C), population densities appear to be essentially independent of thermal regime after accounting for other variables.

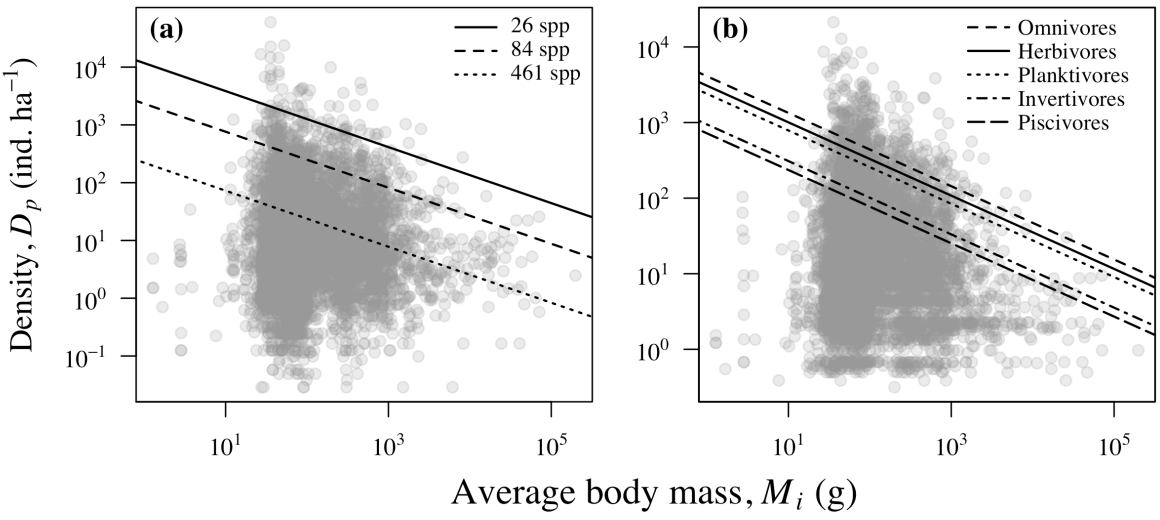

Figure 2.2. Relationship of standardised population density to body mass (grey circles), along with predicted effects (lines) at the highest density quantile (q = 0.95) for (a) species richness, and (b) trophic groups. Population density values have been standardised differently in (a) and (b) to graphically depict partial effects of variables of interest after accounting for temperature (standardised to median temperature in a and b), sampling area (standardised to median area in a and b), trophic group (standardised in a), and species richness (standardised to median species richness in b) (see Methods for median values). Average size-corrected body mass, $\langle M_i^{\alpha} \rangle_p$, has been transformed ($= \langle M_i^{\alpha} \rangle_p^{1/\alpha}$ into body-mass units (g) for plotting.

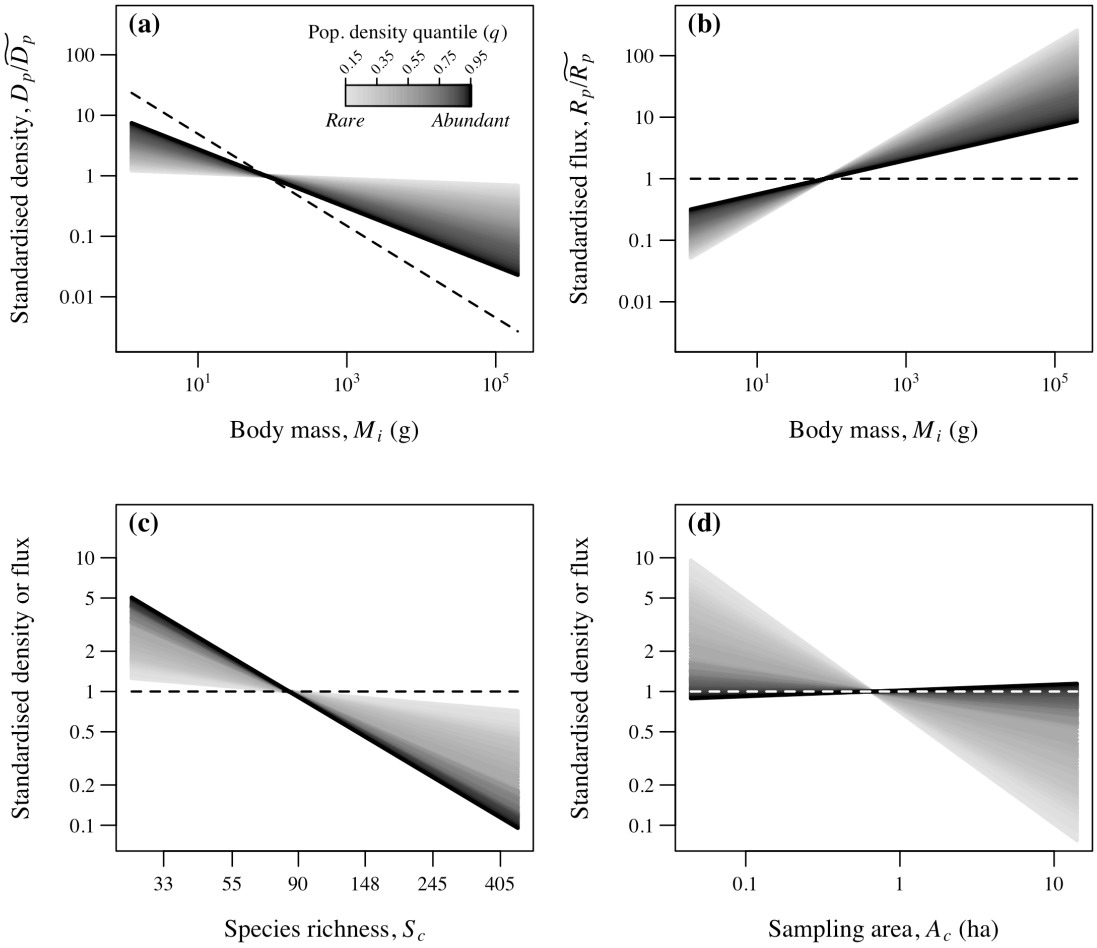

Figure 2.3. Estimated effects of (a–b) size-corrected body mass, (c) species richness, and (d) sampling area on population density and energy flux (eqns 6–7). Dashed lines (black in a–c, white in d) represent expectations based on the assumption of energetic equivalence. Grey-scale lines represent predictions of quantile regression models fitted to different population density quantiles, q, that encompass rare (light grey, q = 0.15) to abundant species (black, q = 0.95) (see Fig. 2.1 for parameter estimates of quantile regression models at different q values). Population densities, D_p (eqn 6), and fluxes, R_p (eqn 7), have been standardised as D_p / $\widetilde{D_p}$ and R_p / $\widetilde{R_p}$, respectively. Therefore, the y axes represent N-fold deviations from $\widetilde{D_p}$ and/or $\widetilde{R_p}$, both of which were estimated from the quantile regression models based on median values for size-corrected body mass ($\langle\widetilde{M_i^{\alpha}}\rangle_p$ = 28 $g^{0.76}$), temperature kinetics ($\langle\widetilde{K(T)}\rangle_c$ = 1.40), community species richness ($\widetilde{S_c}$ = 84 species) and sampling area ($\widetilde{A_c}$ = 0.656 ha) (see Methods). Average size-corrected body mass, $\langle M_i^{\alpha}\rangle_p$, has been transformed ($= \langle M_i^{\alpha}\rangle_p^{1/\alpha}$) into body-mass units (g) for plotting.

Our findings indicate that ecological constraints of species richness (i.e. competition) on population density were also strongest on the most abundant species. Specifically, after accounting for the variables described above (trophic group, body size, or temperature; Figs.

2.1b–d), and for sampling area (Fig. 2.1e), species richness had a pronounced negative effect on population density (characterised by β_S; Figs. 2.1f,2.3c), particularly for the most abundant species (β_S at q = 0.95: -1.38; 95% CI: -1.85 to -0.94). The magnitude of this slope implies an ~53-fold decline in population density $\left(= (26/461)^{\beta_S}\right)$ attributable to species richness moving from the lowest- to the highest-richness community (26 to 461 species). This effect of richness on population densities of abundant species (q = 0.95) is substantially greater than the ~18-fold effect of average size-corrected body mass $\left(= (8.9/841)^{\beta_M}\right)$ over a range encompassing 99% of the $\langle {M_i}^{\alpha} \rangle_p$ values (8.9 to 841 g^{α}) (Fig. 2.2a) and the 5.7-fold variation attributable to trophic group $\left(= e^{\max(\ln\Delta_g)-\min(\ln\Delta_g)} = e^{0.81-(-0.93)}\right)$ (Figs. 2.1b,2.2b).

2.5 DISCUSSION

Overall, results of our statistical analysis – which simultaneously assesses individual-, population-, and community-level determinants of population density for both rare and abundant species – indicate that there are many ways to achieve rarity (Gaston 1994), but that high population density is associated with a particular combination of energetic and ecological factors. The highest densities are achieved by populations of organisms that are small bodied, and that occur at lower trophic levels in communities with low species richness. With respect to energetics, our results provide some support for effects on population density attributable to trophic group, which constrains the total energy available at different trophic levels (Lindeman 1942), and to body size, which may constrain density through its effects on energetic demands of individuals (Damuth 1987; Allen *et al.* 2002; Brown *et al.* 2004). Importantly, however, the magnitudes of these effects are inconsistent with energetic equivalence, in agreement with other recent studies (e.g. Reuman *et al.* 2009; Isaac *et al.* 2013). In particular, our results indicate that, on average, energy fluxes of abundant taxa (q =

0.95) increase with body size (Fig. 2.3b). Our findings also indicate that the strength of energetic constraints varies considerably with relative density, as indexed by the density quantile (Fig. 2.3). Overall, the energetic variables considered here appear to be of limited utility for predicting the abundances of most species.

While trophic group was found to be an important determinant of population density, the arrangement of trophic groups was not as expected based on simple Lindeman-efficiency arguments. In particular, omnivore populations, rather than herbivore populations, achieved the highest densities, as indexed by Δ_g (Figs. 2.1b,2.2b). Moreover, among abundant taxa (q = 0.95), densities of piscivore populations were only about 4-fold lower than those of herbivores, and not two orders of magnitude lower, as would be predicted based on a 10% Lindeman efficiency if piscivores were separated from herbivores by two trophic levels (i.e. 0.10^2 = 100-fold). In this respect, the population-level findings presented here reinforce the results of a recent community-level analysis conducted using these reef-fish data (Barneche *et al.* 2014), and thus lend further support to the argument that piscivores receive substantial energy subsidies from outside the reef (Trebilco *et al.* 2013; Barneche *et al.* 2014). Overall, these findings highlight that trophic constraints most likely operate at spatial scales encompassing both the reef and its surroundings, and at taxonomic scales encompassing not only fish, but also invertebrates and unicells.

When interpreting our findings regarding trophic groups, it is important to note that our analysis assigns each species to one trophic group, regardless of size, and therefore does not account for any ontogenetic shifts in resource use. Although our analysis encompasses only juveniles and adults > 10 cm length – stages at which dietary shifts may occur primarily through shifts in prey size rather than prey type (e.g. McCormick 1998) – we cannot discount the possibility that ontogenetic shifts in resource use influence the observed effects of trophic

groups on population density. Moreover, our simplified energetic, bottom-up, approach does not account for other ecological effects such as top-down controls (e.g. predation), which would induce mortality (and therefore affect the abundance) of lower trophic groups. Still, it is important to note that the population-level analyses conducted here, along with complementary community-level analyses of reef-fish data (Trebilco *et al.* 2013; Barneche *et al.* 2014), suggest that energy fluxes of larger-bodied reef fishes are far higher than would be predicted by size-spectrum theory (Kerr & Dickie 2001). While these findings do not by themselves contradict a key basic assumption of size-spectrum theory – that body size plays a key role in governing trophic interactions – they do suggest that one or more of the assumptions in current models (e.g. closed-system assumption, common resource-pool assumption) must be relaxed to account for the complexity of trophic interactions in reef systems.

Comparison of the population-level results presented here with those of the community-level analysis using the same data (Barneche *et al.* 2014) highlights important differences between population- and community-level trends. For instance, invertivores were found to be the most abundant trophic group at the community level (Barneche *et al.* 2014), but were significantly less abundant than herbivores, omnivores and planktivores at the population level (Fig. 2.1b). These seemingly disparate findings can be reconciled by noting that invertivores are generally the most diverse trophic group of fish in reef ecosystems (Parravicini *et al.* 2013). Moreover, omnivores had higher normalised densities than herbivores, perhaps because they utilise multiple resources both within and outside the reef, including benthic net primary productivity (via herbivory), invertebrates on both reef substratum and sandy banks, and external plankton resources (e.g. Kavanagh & Olney 2006; Behrens & Lafferty 2007; Luiz *et al.* 2015).

Our findings highlight that estimates of population density are sensitive to the spatial scale of sampling, and that the magnitude of this sampling effect is substantially greater for rare than abundant taxa (Figs. 2.1e,2.3d). Abundant species are expected to be relatively ubiquitous across space, so estimates of their densities are expected and observed to be relatively insensitive to sampling area. By contrast, rare species are more likely to be spatially restricted, so one expects to encounter more of them, each with progressively lower estimates of density (D_p), as community sampling area, A_c, increases (Rosenzweig 1995). Here we address this issue statistically, by explicitly incorporating area, and its differential effects on density estimates of abundant versus rare species, using quantile regression. We view our approach as complementary to that of Damuth (1987), which involves estimating *ecological densities* of populations, i.e. abundances of populations in areas comprised entirely of suitable habitat. Our method of estimating population density implicitly assumes that all sampled hard-bottom reef area is suitable habitat, and thus may underestimate ecological densities, particularly for some microhabitat-specific species such as gobies and clownfishes. Applying the ecological density concept in reef systems would be challenging because tropical reef fishes often exhibit a high degree of specialization in terms of resource use, and resources availability often exhibits substantial fine-scale spatial heterogeneity (Belmaker 2009).

Remarkably, our results indicate that effects of species richness on densities of the abundant taxa are of comparable or even greater magnitude than those attributable to body size (Fig. 2.2). While richness appeared to significantly constrain the densities of rare taxa (e.g. q = 0.15) as well, its effects were relatively weak (Figs. 2.1f,2.3c). Undoubtedly, these findings reflect a nearly ubiquitous feature of species abundance distributions (McGill *et al.* 2007): as species richness goes up, abundances of taxa become more equitable, due in part to reductions in the abundances of abundant taxa (Fig. AII.7) (Currie & Fritz 1993; Niklas *et al.*

2003). Still, it is remarkable that our analysis indicates that effects of species richness on population density are of equal or greater magnitude than those of body size given that size varies by 6 orders of magnitude (0.05 g to 192 kg) for the species included in our analysis. These findings suggest that, at the broadest spatial scales, the population densities of reef fishes are, to a large extent, governed by broad-scale factors associated with species richness rather than by local-scale ecological factors and intrinsic attributes of species. Given that species-rich reef fish communities exhibit substantially lower maximum populations densities (Fig. 2.2a), they may be generally more susceptible to local stochastic extinction (Lande *et al.* 2003).

2.6 CONCLUSIONS

Here we assess the relative roles of energetics and ecology in influencing population density at broad spatial scales. Our results indicate that rarity may be achieved in many ways, but there are very few ways for a species to be abundant (Fig. 2.2). These results were obtained by separately assessing determinants of population density of rare and abundant species using a quantile regression approach (Fig. 2.1). Although our results identify energetics as an important determinant of density for abundant species, we find no evidence for energetic equivalence among different reef-fish populations (Fig. 2.3), and community species richness appears to be the key variable explaining differences in densities of abundant taxa at broad spatial scales. These findings are broadly consistent with empirical findings from other communities such as plants and mammals (Currie & Fritz 1993; Johnson 1998; Niklas *et al.* 2003), and highlight the need for further theoretical work that explicitly links population abundance to community species richness and macroevolutionary dynamics (e.g. Reuman *et al.* 2014). Further work will be necessary to incorporate effects of other ecological variables,

such as overfishing, habitat destruction and pollution, which are likely contributing to changes in abundance, and which may differentially affect species that vary in size and occur at different trophic levels.

2.7 ACKNOWLEDGEMENTS

This project was supported by Macquarie University (PhD scholarship to D.R.B.), Australian Research Council's Discovery Projects funding scheme (DP0987218 to A.P.A.), CESAB-FRB (Fondation pour la Recherche en Biodiversité), through the GASPAR program, SISBIOTA-Mar (CNPq 563276/2010-0 and FAPESC 6308/2011-8 to SRF), CAPES, Marinha do Brasil, Instituto Laje Viva and the National Geographic Society.

2.8 REFERENCES

Alhamzawi, R., Yu, K., Vinciotti, V. & Tucker, A. (2011). Prior elicitation for mixed quantile regression with an allometric model. *Environmetrics*, 22, 911–920.

Allen, A.P., Brown, J.H. & Gillooly, J.F. (2002). Global biodiversity, biochemical kinetics, and the energetic-equivalence rule. *Science*, 297, 1545–1548.

Allen, A.P., Gillooly, J.F. & Brown, J.H (2005). Linking the global carbon cycle to individual metabolism. *Functional Ecology*, 19, 202–213.

Barneche, D.R., Kulbicki, M., Floeter, S.R., Friedlander, A.M., Maina, J. & Allen, A.P. (2014). Scaling metabolism from individuals to reef-fish communities at broad spatial scales. *Ecology Letters*, 17, 1067–1076.

Behrens, M.D & Lafferty, K.D. (2007). Temperature and diet effects on omnivorous fish performance: implications for the latitudinal diversity gradient in herbivorous fishes. *Canadian Journal of Fisheries and Aquatic Sciences*, 64, 867–873.

Belmaker, J. (2009). Species richness of resident and transient coral-dwelling fish responds differentially to regional diversity. *Global Ecology and Biogeography*, 18, 426–436.

Blackburn, T.M., Lawton, J.H. & Perry, J.N. (1992). A method of estimating the slope of upper bounds of plots of body size and abundance in natural animal assemblages. *Oikos*, 65, 107–112.

Brock, R.E. (1982). A critique of the visual census method for assessing coral reef fish populations. *Bulletin of Marine Sciences*, 32, 269–276.

Brown, J.H. & Gillooly, J.F. (2003). Ecological food webs: High-quality data facilitate theoretical unification. *Proceedings of the National Academy of Sciences*, 100, 1467–1468.

Brown, J.H., Gillooly, J.F., Allen, A.P., Savage, V.M. & West, G.B. (2004). Toward a metabolic theory of ecology. *Ecology*, 85, 1771–1789.

Cade, B.S. & Noon, B.R. (2003). A gentle introduction to quantile regression for ecologists. *Frontiers in Ecology and the Environment*, 1, 412–420.

Cotgreave, P. (1993). The relationship between body size and population abundance in animals. *Trends in Ecology & Evolution*, 8, 244–248.

Currie, D.J. & Fritz, J.T. (1993). Global patterns of animal abundance and species energy use. *Oikos*, 67, 56–68.

Currie, D.J., Mittelbach, G.G., Cornell, H.V., Field, R., Guégan, J.-F., Hawkins, B.A. *et al.* (2004). Predictions and tests of climate-based hypotheses of broad-scale variation in taxonomic richness. *Ecology Letters*, 7, 1121–1134.

Damuth, J. (1987). Interspecific allometry of population density in mammals and other animals: the independence of body mass and population energy-use. *Biological Journal of the Linnean Society*, 31, 193–246.

Edgar, G.J., Barrett, N.S. & Morton, A.J. (2004). Biases associated with the use of underwater visual census techniques to quantify the density and size-structure of fish populations. *Journal of Experimental Marine Biology and Ecology*, 308, 269–290.

Fornaroli, R., Cabrini, R., Sartori, L., Marazzi, F., Vracevic, D., Mezzanotte, V. *et al.* (2015). Predicting the constraint effect of environmental characteristics on macroinvertebrate density and diversity using quantile regression mixed model. *Hydrobiologia*, 742, 153–167.

Froese, R. & Pauly, D. (2012). FishBase. World Wide Web electronic publication. Available at http://www.fishbase.org, (Version 12/2012). Last accessed 20 February 2015.

Gaston, K.J. (1994). *Rarity*. Population and community biology series. Chapman & Hall, California, pp. 205.

Gaston, K.J. (2010). Valuing common species. *Science*, 327, 154–155.

Gaston, K.J. (2011). Common ecology. *BioScience*, 61, 354–362.

Geraci, M. & Bottai, M. (2007). Quantile regression for longitudinal data using the asymmetric Laplace distribution. *Biostatistics*, 8, 140–154.

Gillooly, J.F., Brown, J.H., West, G.B., Savage, V.M. & Charnov, E.L. (2001). Effects of size and temperature on metabolic rate. *Science*, 293, 2248–2251.

Gotelli, N.J. & R.K. Colwell. (2010). Estimating species richness. In: *Biological Diversity: Frontiers in Measurement and Assessment*. (eds. Magurran, A.E. & McGill, B.J.). Oxford University Press, Oxford. pp. 39–54.

Hamner, W.M., Jones, M.S., Carleton, J.H., Hauri, I.R. & Williams, D.M. (1988). Zooplankton, planktivorous fish, and water currents on a windward reef face: Great Barrier Reef, Australia. *Bulletin of Marine Science*, 42, 459–479.

Harte, J., Smith, A.B. & Storch, D. (2009). Biodiversity scales from plots to biomes with a universal species–area curve. *Ecology Letters*, 12, 789–797.

Hubbell, S.P. (2001). *The unified neutral theory of biodiversity and biogeography*. Princeton University Press, Princeton, New Jersey, pp. 448.

Irigoyen, A.J., Galván, D.E., Venerus, L.A. & Parma, A.M. (2013). Variability in Abundance of Temperate Reef Fishes Estimated by Visual Census. *PLoS ONE*, 8, e61072.

Isaac, N.J.B., Storch, D. & Carbone, C. (2013). The paradox of energy equivalence. *Global Ecology and Biogeography*, 22, 1–5.

Jennings, S. & Mackinson, S. (2003). Abundance-body mass relationships in size-structured food webs. *Ecology Letters*, 6, 971–974.

Johnson, C.N. (1998). Rarity in the tropics: latitudinal gradients in distribution and abundance in Australian mammals. *Journal of Animal Ecology*, 67, 689–698.

Kavanagh, K.D. & Olney, J.E. (2006). Ecological correlates of population density and behavior in the circumtropical black triggerfish *Melichthys niger* (Balistidae). *Environmental Biology of Fishes*, 76, 387–398.

Kerr, S.R. & Dickie, L.M. (2001). *The biomass spectrum: a predator-prey theory of aquatic production*. Columbia University Press, New York, pp. 352.

Lande, R., Engen, S. & Saether, B.-E. (2003). *Stochastic population dynamics in ecology and conservation*. Oxford Series in Ecology and Evolution, pp. 224.

Lindeman, R.L. (1942). The trophic-dynamic aspect of ecology. *Ecology*, 23, 399–417.

Luiz, O.J., Mendes, T.C., Barneche, D.R., Ferreira, C.G.W., Noguchi, R., Villaça, R.C. *et al.* (2015). Community structure of reef fishes on a remote oceanic island: the relative influence of abiotic and biotic variables. *Marine and Freshwater Research*, 66, 739–749.

McCormick, M.I. (1998). Ontogeny of diet shifts by a microcarnivorous fish, *Cheilodactylus spectabilis*: relationship between feeding mechanics, microhabitat selection and growth. *Marine Biology*, 132, 9–20.

McGill, B.J., Etienne, R.S., Gray, J.S., Alonso, D., Anderson, M.J., Benecha, H.K. *et al.* (2007). Species abundance distributions: moving beyond single prediction theories to integration within an ecological framework. *Ecology Letters*, 10, 995–1015.

Niklas, K.J., Midgley, J.J. & Rand, R.H. (2003). Size-dependent species richness: trends within plant communities and across latitude. *Ecology Letters*, 6, 631–636.

Parravicini, V., Kulbicki, M., Bellwood, D.R., Friedlander, A.M., Arias-Gonzalez, J.E., Chabanet, P. *et al.* (2013). Global patterns and predictors of tropical reef fish species richness. *Ecography*, 36, 1254–1262.

Pauly, D. & Christensen, V. (1995). Primary production required to sustain global fisheries. *Nature*, 374, 255–257.

Peters, R.H. (1983). *The ecological implications of body size*. Cambridge University Press, Cambridge, pp. 329.

R Core Team (2015). *R: a language and environment for statistical computing*. R Foundation for Statistical Computing, Vienna, Austria.

Reuman, D.C., Gislason, H., Barnes, C., Mélin, F. & Jennings, S. (2014). The marine diversity spectrum. *Journal of Animal Ecology*, 83, 963–979.

Reuman, D.C., Mulder, C., Banasek-Richter, C., Blandenier, M.-F.C., Breure, A.M., Hollander, H.D. *et al.* (2009). Allometry of body size and abundance in 166 food webs. *Advances in Ecological Research*, 41, 1–44.

Rosenzweig, M.L. (1995). *Species diversity in space and time*. Cambridge University Press, Cambridge, pp. 436.

Sale, P.F. & Douglas, W.A. (1984). Temporal Variability in the Community Structure of Fish on Coral Patch Reefs and the Relation of Community Structure to Reef Structure. *Ecology*, 65, 409–422.

Savage, V.M. (2004). Improved approximations to scaling relationships for species, populations, and ecosystems across latitudinal and elevational gradients. *Journal of Theoretical Biology*, 227, 525–534.

Savage, V.M., Gillooly, J.F., Woodruff, W.H., West, G.B., Allen, A.P., Enquist, B.J. *et al.* (2004). The predominance of quarter-power scaling in biology. *Functional Ecology*, 18, 257–282.

Schoolfield, R., Sharpe, P. & Magnuson, C. (1981). Non-linear regression of biological temperature-dependent rate models based on absolute reaction-rate theory. *Journal of Theoretical Biology*, 88, 719–731.

Selig, E.R., Casey, K.S. & Bruno, J.F. (2010). New insights into global patterns of ocean temperature anomalies: implications for coral reef health and management. *Global Ecology and Biogeography*, 19, 397–411.

Sheldon, R.W., Jr., W.H.S. & Paranjape, M.A. (1977). Structure of pelagic food chain and relationship between plankton and fish production. *Journal of the Fisheries Research Board of Canada*, 34, 2344–2353.

ter Steege, H., Pitman, N.C.A., Sabatier, D., Baraloto, C., Salomão, R.P. & Guevara, J.E.*et al.* (2013). Hyperdominance in the amazonian tree flora. *Science*, 342.

Su, Y.-S. & Yajima, M. (2015).*:* A package for running *JAGS* from R. R package version 0.5-6.

Tilman, D., HilleRisLambers, J., Harpole, S., Dybzinski, R., Fargione, J., Clark, C. *et al.* (2004). Does metabolic theory apply to community ecology? It's a matter of scale. *Ecology*, 85, 1797–1799.

Trebilco, R., Baum, J.K., Salomon, A.K. & Dulvy, N.K. (2013). Ecosystem ecology: size-based constraints on the pyramids of life. *Trends in Ecology & Evolution*, 28, 423–431.

White, E.P., Ernest, S.M., Kerkhoff, A.J. & Enquist, B.J. (2007). Relationships between body size and abundance in ecology. *Trends in Ecology & Evolution*, 22, 323–330.

Yu, K. & Moyeed, R.A. (2001). Bayesian quantile regression. *Statistics & Probability Letters*, 54, 437–447.

Yvon-Durocher, G. & Allen, A.P. (2012). Linking community size structure and ecosystem functioning using metabolic theory. *Philosophical Transactions of the Royal Society B: Biological Sciences*, 367, 2998–3007.

CHAPTER 3

QUANTIFYING THE ENERGETICS OF FISH GROWTH AND ITS IMPLICATIONS FOR ENERGY TRANSFER BETWEEN TROPHIC LEVELS

3.1 ABSTRACT

The capacity of organisms to allocate total metabolic energy to growth is a fundamental ecological process that constrains all levels of biological organisation, from individuals to ecosystems. We here characterise the mass and temperature dependencies of growth rates and metabolic rates of marine and freshwater fishes in order to estimate how much energy different species expend in producing a unit of biomass, E_m. We do so by using a mechanistic model of ontogenetic growth, which is based on first principles of allometry and mass and energy balance. Theoretical predictions are tested using two different datasets, corresponding to distinct ontogenetic stages. Using these data, we show empirically that E_m varies substantially between species. We also show theoretically that E_m is a primary determinant of the efficiency of energy transfer across trophic levels. In so doing we demonstrate the importance of characterising individual-level energetics in order to understand constrains on the dynamics of food webs and ecosystems.

3.2 INTRODUCTION

Organisms must expend energy to gather, consume, and transform the materials necessary to produce biomass (Ashworth 1969; Millward *et al.* 1976; Hawkins *et al.* 1989). The rate of biomass production is therefore fundamental at multiple biological levels. At the individual level, it influences fitness by constraining how quickly an organism reaches maturity and subsequently produces offspring (Brown *et al.* 1993). At the population level, it constrains the intrinsic rate of population increase (Savage *et al.* 2004a). At the community level, it constrains how much energy and materials can flow to the next trophic level in a food web (Clarke *et al.* 1946; Nixon *et al.* 1986; Iverson 1990; Calbet & Saiz 2005; Conti & Scardi 2005; Pauly & Palomares 2005; Andersen *et al.* 2009; Chassot *et al.* 2010; Irigoien *et al.* 2013). And, at the ecosystem level, the fraction of assimilated energy lost in producing that biomass (through respiration) limits the total heterotrophic metabolism, and hence the number of trophic levels, that can be supported in a food web (Elton 1927; Lindeman 1942; Pauly & Christensen 1995).

Despite its theoretical importance, we still lack a comprehensive understanding of the energetics of growth. Such an understanding would be helpful on a practical level because knowing how long wild fish stocks take to achieve maturity, and how much food they need to do so, is crucial for establishing sustainable yields in fisheries management (Pauly *et al.* 2002). For example, management decisions for different fish stocks across ocean basins may be improved by investigating how growth energetics varies among species and with environmental changes in variables such as temperature. While there have been extensive empirical work documenting determinants of fish growth (e.g. Wood 1932; Kinne 1960; Laurence 1975, 1978; Hogendoorn 1983; Kiørboe *et al.* 1987; Finn *et al.* 1995; Imsland *et al.* 1995; Burel *et al.* 1996; Secor & Gunderson 1998; Hansen & Herbing 2009), these studies

have typically focused on how one or few species at a particular life stage respond to a particular set of environmental conditions. With few notable exceptions (see, for example, Pauly & Pullin 1988; Houde 1989; Charnov & Gillooly 2004), there has been little attempt to generalise determinants of biomass production across fish as a group within a theoretical framework.

Theoretical work on the mechanisms underlying growth dynamics (see Jones 1976; Parry 1983 and references listed therein for fish studies) has focused primarily on understanding why individuals tend to follow a sigmoid growth trajectory over ontogeny such that mass-specific growth rate is rapid during early life stages, but slows down as individuals approach an asymptotic adult size. More than half a century ago, Ludwig von Bertalanffy (1938) proposed that these sigmoid growth trajectories arise because the overall rate of catabolism increases more rapidly with size than the rate of anabolism. While the mechanistic basis of this model (hereafter VGBM) has been questioned (Banavar *et al.* 2002; West *et al.* 2002), the VGBM generally provides a good statistical fit to ontogenetic growth data, and is therefore frequently employed in fisheries science (Jones 1976; Pauly 1980; Weatherley *et al.* 1987). Importantly, however, VGBM is generally fitted using fish length data, rather than mass data (see Appendix II), which is unfortunate given that growth is fundamentally an energetic process, and that the energetic costs of growth are related to changes in mass (Hou *et al.* 2008).

West *et al.* (2001) have proposed an ontogenetic growth model (OGM; see also Gillooly *et al.* 2002; Moses *et al.* 2008) that is based on first principles of mass and energy balance. The OGM yields predictions on ontogenetic growth trajectories by partitioning the overall metabolic rate of an organism into growth and maintenance components. Due to this partitioning, the OGM predicts that growth rates are inextricably linked to the size- and temperature-dependencies of metabolic rate, consistent with empirical data (Pauly & Pullin

1988; Houde 1989; Atkinson 1994; Gillooly *et al.* 2001, 2002; Brown *et al.* 2004; O'Connor *et al.* 2007). Although the OGM can be mathematically similar to the VGBM (Makarieva *et al.* 2004), its conceptual foundation is fundamentally different because, while growth is an anabolic process, maintenance in the OGM involves both anabolism and catabolism, e.g. protein turnover fuelled by respiration. Of particular relevance, the OGM reveals the importance of a particular parameter, E_m, which is the amount of energy expended in respiration to produce a fixed quantity of biomass. As we will return to in the Discussion, this quantity is of particular relevance to understanding food web dynamics because it directly constrains the efficiency of energy transfer between trophic levels.

In this study, we use the OGM as a framework to help in understanding the mass and temperature dependence of growth rates for marine and freshwater fishes, and to estimate variation among species in the parameter E_m. In so doing, we quantify the fraction of total metabolic energy allocated to biomass production across different species at differing life stages and temperature regimes, and explore whether this fraction exhibits mass and temperature dependencies. Fishes are excellent model organism for this purpose because they encompass the highest species richness among vertebrates, they range over > 7 orders of magnitude in body mass (~0.1 g to ~34 × 10^6 g), and they occupy diverse habitats that vary substantially in thermal regime across the globe (~0–40˚C) (Froese & Pauly 2012).

3.3 MATERIALS AND METHODS

3.3.1 Theory

The OGM (West *et al.* 2001) is derived based on energy balance for an organism of mass m with a metabolic rate of B, and a growth rate per unit time, t, of dm/dt,

$$B = E_m \frac{dm}{dt} + B_m m \quad . \qquad (1)$$

In this expression, the first term on the right-hand side, $E_m dm/dt$ is the energy allocated to growth, where E_m (J g^{-1}) is the energy expended in producing biomass. The second term, $B_m m$, is the energy allocated to maintenance, where B_m (g C g^{-1} d^{-1}) is the energy per unit mass expended in maintenance metabolism, which is assumed to scale with adult asymptotic mass, M, but that is independent of m.

The OGM assumes that the parameters E_m and B_m remain constant over ontogeny. Consequently, eqn 1 can be rearranged to yield an expression for the ontogenetic growth rate

$$\frac{dm}{dt} = \frac{B}{E_m} - \frac{B_m}{E_m} m = \frac{B}{E_m}\left[1 - \left(\frac{m}{M}\right)^{1-\alpha}\right] = x m^{\alpha} f(m, M) \quad . \qquad (2)$$

In this expression,

$$B = b_o(T) m^{\alpha}, \qquad (3)$$

where B is the metabolic rate of an individual (g C d^{-1}), $b_o(T)$ is a normalisation constant independent of body mass that varies across species and with absolute body temperature (Barneche *et al.* 2014), T (K), α is a dimensionless mass-scaling exponent, which is theoretically predicted to take a value of 0.75 in the fractal-like distribution model of West *et al.* (1997), $x \equiv b_o(T)/E_m$, and $f(m, M) = [1 - (m/M)^{1-\alpha}]$ is the fraction of metabolic energy that is allocated to growth. This fraction approaches 0 as the organism approaches its asymptotic size, M, at which point all metabolic energy is allocated to maintenance (i.e. $B =$

$B_m M$), leaving no surplus energy to support further growth. Asymptotic adult mass, M, is functionally dependent on B_m such that $M \equiv [B_m / b_o(T)]^{1/(\alpha-1)}$. The OGM does not explicitly account for biomass production for reproduction; rather, this energy is implicitly included as part of maintenance costs.

In the OGM, the temperature dependence of growth rate is governed by the effects of temperature on metabolic rate normalisation, $b_o(T)$ (Gillooly *et al.* 2002). Initial applications of the model characterised this temperature dependence using the Boltzmann relationship

$$b_o(T) = b_o(T_s) e^{\frac{E_r}{k}\left(\frac{1}{T_s} - \frac{1}{T}\right)} \quad , \tag{4}$$

where $b_o(T_s)$ is a normalisation constant independent of mass and temperature (g C $g^{-\alpha}$ d^{-1}) at some arbitrary standardised temperature, T_s (K), E_r (eV) is an activation energy (~0.6–0.7 eV), and k is the Boltzmann constant (8.62×10^{-5} eV K^{-1}) (Gillooly *et al.* 2001). Combining eqns 3–4 yields an expression

$$B = b_o(T_s) m^{\alpha} e^{\frac{E_r}{k}\left(\frac{1}{T_s} - \frac{1}{T}\right)} \tag{5}$$

for the combined effects of body mass and temperature on metabolic rate (Gillooly *et al.* 2001).

For this study, we used the Boltzmann relation (eqn 4) to characterise the temperature dependence of metabolic rate (eqn 5) and of growth rate (eqn 7, below) for simplicity and consistency across different analyses. In reality, however, numerous studies have presented evidence for temperature optima in metabolic rates and growth rates of fishes (e.g. Clarke & Johnston 1996; Pörtner & Knust 2007; Handeland *et al.* 2008; Gardiner *et al.* 2010;

Neuheimer *et al.* 2011). Barneche *et al.* (2014), for example, presented evidence that metabolic rates of fish exhibit an average temperature optimum of ~33˚C at the family level (see Chapter 1). Given this temperature optimum, it is not surprising that the estimated activation energy for metabolic rate, E_r, is lower if the metabolic rate data analysed by Barneche *et al.* (2014) are fitted using the Boltzmann temperature relation than if they are fitted using a more complex temperature response function that incorporates a temperature optimum (0.48 eV versus 0.59 eV) (see Appendix III). The growth-rate data included in this study (Datasets I and II, described below) yielded little evidence of temperature optima at the species level (Dataset I, Fig. AIII.2) or the family level (Dataset II, Fig. AIII.3), perhaps in part due to narrow temperature ranges within taxa, justifying the use of the simpler Boltzmann relation (Table AIII.1).

Eqn 2 can be rearranged to yield an expression that can be used to estimate E_m:

$$E_m = B\frac{dt}{dm}f(m,M) \quad . \tag{6}$$

In practice, calculating E_m using eqn 6 requires ontogenetic growth data in order to estimate $f(m,M)$. In the absence of such data, an upper bound estimate for E_m, $E_m^\star$, can be calculated using estimates of growth rate taken early in ontogeny

$$E_m^\star \approx B\frac{dt}{dm} \quad , \tag{7}$$

when the total mass of an individual is negligible compared to the asymptotic adult mass, $m << M$, because, in this case, $f(m,M) \approx 1$ (Moses *et al.* 2008).

Interpretation of E_m requires recognition that its magnitude does not correspond to the combustion energy (i.e. chemical-energy content) of assimilated biomass (Makarieva *et al.* 2004); rather, it corresponds to the sum of all direct and indirect energy costs that an individual must expend in producing biomass. The direct costs of synthesising biomass may, in fact, be lower than the combustion energy because, for example, proteins may be constructed from pre-formed amino acids assimilated from food. The indirect costs include other processes that are not directly related to biomass production, but that are nevertheless essential for this production to occur (e.g. digestion). While disentangling and quantifying the processes contributing to E_m would be challenging, the overall magnitude of E_m can nevertheless be quantified based on eqns 6–7.

3.3.2 Assessing the mass and temperature dependence of growth rates

We assessed the mass and temperature dependence of growth rates, dm/dt, by fitting a function of the same form as that for metabolic rate (eqn 5),

$$\frac{dm}{dt} = g_o(T_s) m^{\gamma} e^{\frac{E_g}{k}\left(\frac{1}{T_s}-\frac{1}{T}\right)} \quad , \tag{8}$$

where $g_o(T_s)$ is a normalised growth rate that is independent of mass and temperature (g $g^{-\gamma}$ d^{-1}), γ is a dimensionless mass-scaling exponent, and E_g (eV) is an activation energy. The OGM predicts that $\gamma = \alpha$, and that $E_g = E_r \approx 0.65$ eV, implying that E_m is independent of body mass and temperature. Importantly, it also predicts that $g_o(T_s) = f(m, M) b_o(T)/E_m$, and is therefore higher for organisms at earlier ontogenetic stages, which correspond to lower values for m/M. We characterised the mass and temperature dependence of growth rates, and estimated E_m using two different datasets (Datasets I and II). As discussed below, Dataset I is

comprised of compiled estimates of growth rates and metabolic rates of marine and freshwater fishes at early ontogenetic stages ($m/M \approx 0$), implying that $f(m, M) \approx 1$. By contrast, Dataset II yields estimates at the ontogenetic stage when growth rate is maximal ($m/M \approx 0.30$), implying that $f(m, M) \approx 0.25$.

3.3.3 Datasets

3.3.3.1 Dataset I

Dataset I comprises 275 direct paired measurements of metabolic rate (g C d^{-1}) and growth rate (g d^{-1} of wet mass) for eggs (n = 25), larvae (n = 163), juveniles (n = 86) and young adults (n = 1). These data encompass 30 species of marine and freshwater fishes that have body masses of 9 μg – 1,982 g and temperatures of 3 – 36˚C (Appendix III). Because this dataset contains measurements taken early in ontogeny, meaning that $m/M \approx 0$, paired measurements of metabolic and growth rates were used to obtain upper-bound estimates for the energy expended in growth, $E_m^\star$ (eqn 7).

3.3.3.2 Dataset II

Dataset II was obtained from FishBase (Froese & Pauly 2012). It contains 2,211 sets of parameter estimates, corresponding to 2,211 ontogenetic growth curves, that were obtained by fitting the von Bertalanffy growth model (VGBM) (von Bertalanffy 1957; Pauly 1980) to age and size data collected from 400 species of marine and freshwater fishes. These data encompass 52 families and a temperature range of -0.9–30˚C (Appendix III). As is the tradition in fisheries science, these ontogenetic growth trajectories are characterised using *length*, rather than mass, which is not ideal. To obtain mass-based estimates of growth, we combined these length-based data with species-specific mass-length conversion equations, as described in Appendix III. We then calculated 2,211 estimates of optimum (i.e. maximum)

growth rate, g_{opt}, and mass at optimum growth rate, m_{opt}. As demonstrated in the Appendix III, these estimates correspond to a fixed ontogenetic stage, $m_{opt}/M \approx 0.30$, and are therefore ideal for making interspecific comparisons. These growth rate data were first used to estimate the size and temperature dependence of growth rate across species (eqn 8). A subset of these data were then combined with the metabolic rate data analysed by Barneche *et al.* (2014) in order to estimate E_m for 19 families. The E_m estimates were calculated at the family level using eqn 6 and family-specific estimates for α, E_r, $b_o(T_s)$, γ, E_g and $g_o(T_s)$ (see Statistical analyses below; Appendix III).

3.3.4 Statistical analyses

The size and temperature dependencies of growth rates were estimated by fitting eqn 8 to log-transformed data,

$$\ln\frac{dm}{dt} = \ln g_o(T_s) + \gamma \ln m + \frac{E_g}{k}\left(\frac{1}{T_s} - \frac{1}{T}\right) \quad . \qquad (9)$$

Following Barneche *et al.* (2014), we fit eqn 9 using a Bayesian procedure by calling *JAGS* version 3.4.0 from the R package *R2jags* version 0.05-03 (Su & Yajima 2015) in order to derive posterior distributions and associated 95% credible intervals (CIs) for the fitted parameters (Table 3.1). A mixed-effects modelling approach was adopted for this analysis because Dataset I is heterogeneous in structure, with species often having distinct ranges of body mass and temperature, and with substantial variation in the numbers of observations per species (i.e. one observation for *Anarhichas minor* to 47 observations for *Oncorhynchus tshawytscha*). To help control for this heterogeneity, for the analysis of Dataset I, the mass- and temperature-corrected growth rate ($\ln g_o(T_s)$) was treated as having both a fixed effect

that varied among different life stages (eggs, yolk-sac larvae, larvae without yolk, larvae undefined, juveniles, adult) ($\Delta\theta$), and a random effect that varied by species ($\Delta\ln g_o(T_s)$). Similar results are obtained if data are aggregated at the family level. The effects of mass (characterised by γ) and temperature (characterised by E_g) were treated as fixed due to insufficient ranges for these variables within species. By contrast, for the analysis of Dataset II, mass, temperature, and the mass- and temperature-corrected growth rate were all treated as having both fixed effects (γ, E_g, $\ln g_o(T_s)$), corresponding to family-level averages, and random effects that varied by family ($\Delta\gamma$, ΔE_g, $\Delta\ln g_o(T_s)$). In both analyses, random effects were assumed to be normally distributed, with means of 0. The fitted parameters were assigned priors that were vague (i.e. locally uniform over the region supported by the likelihood) (Kruschke 2014). The posterior distributions of model parameters were estimated using Markov chain Monte Carlo (MCMC) methods by constructing three chains of 1,000,000 steps each, including 500,000-step burn-in periods. Chains were thinned using a 250-step interval, so a total of 6,000 steps were retained to estimate posterior distributions (i.e. 3 × (1,000,000 - 500,000)/250 = 6,000).

We fit another mixed-effects model in *JAGS* in order to assess the temperature dependence of $E_m^\star$ for Dataset I:

$$\ln E_m^\star \approx \ln\beta_0 + \Delta\ln\beta_0 + \frac{(\beta_1 + \Delta\beta_1)}{k}\left(\frac{1}{T_s} - \frac{1}{T}\right) \quad , \qquad (10)$$

where, β_0 and β_1 are respectively the intercept and slope that vary between species ($\Delta\beta_0$ and $\Delta\beta_1$). Posterior distributions were estimated following the exact same technical specifications (e.g. vague priors, number of chains, burn-in periods) described above.

3.4 RESULTS AND DISCUSSION

The analyses of Datasets I and II yield contrasting estimates for the mass and temperature dependencies of growth rates and metabolic rates (Fig. 3.1, Tables 3.1,AIII.1). The average mass dependencies of growth rates and metabolic rates, characterised by the scaling exponents γ and α, respectively, are somewhat steeper than 0.75 early in ontogeny (Dataset I), but statistically indistinguishable from 0.75 towards intermediate ontogenetic stages (Dataset II) (Fig. 3.1a,c). These results are consistent with previous estimates of metabolic rates for fish larvae (Clarke & Johnston 1999). They reinforce the idea that the scaling of biological rates early in ontogeny may be steeper than the canonical value of '3/4' that is generally assumed by Metabolic Theory (West *et al.* 1997; Savage *et al.* 2004b). It is important to note, however, that the model of West *et al.* (1997), in fact, predicts positive deviations from 3/4-power scaling if size range encompasses very small organisms that have vascular distribution networks with only a few levels of branching. Evaluating this more detailed model would require data on aorta and capillary diameters, and the numbers of branching generations from aorta to capillary (West *et al*. 1997; 2001).

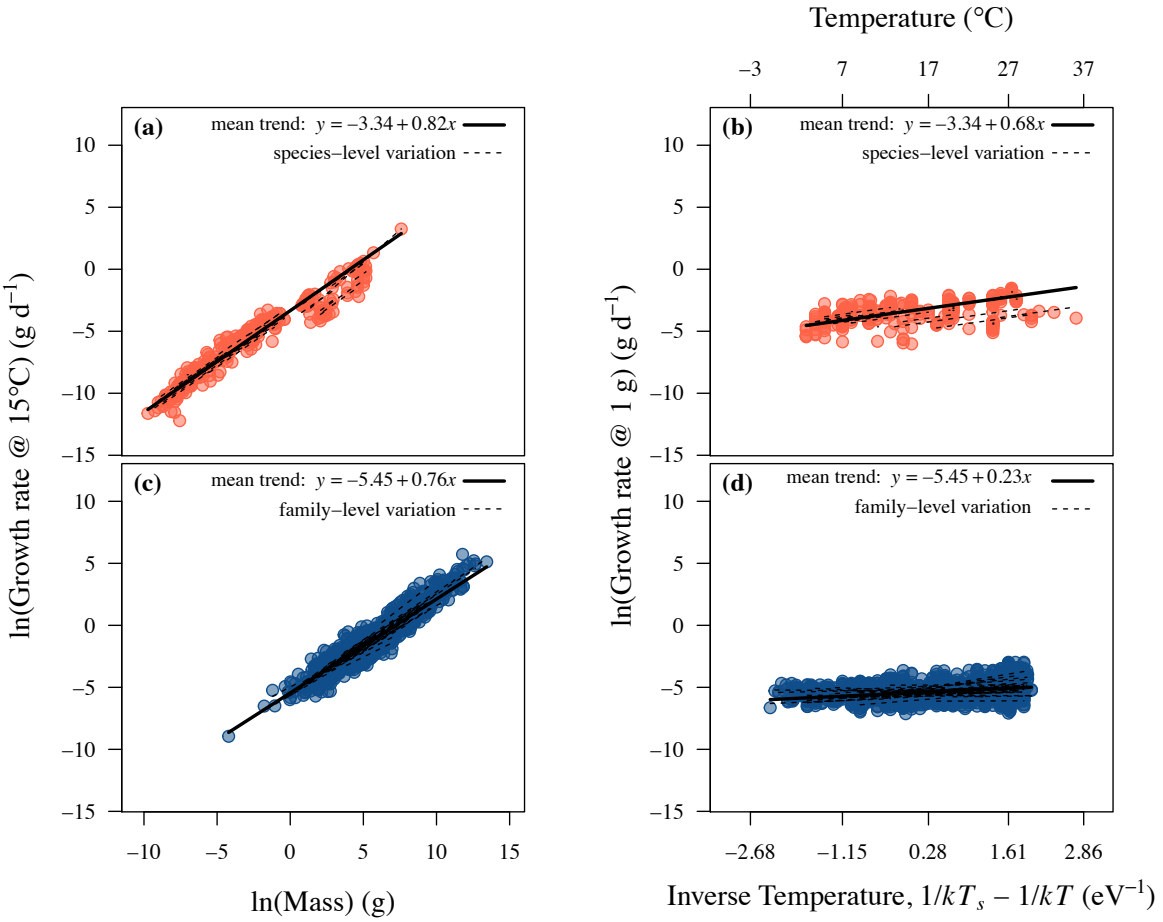

Figure 3.1. Scaling of growth rates of fish with respect to (a,c) body mass and (b,d) temperature for Datasets I (a,b) and II (c,d). Parameter estimates (listed in Table 3.1) were obtained using Bayesian methods. The effect of temperature on growth rate was controlled for in (a,c) by standardising the temperature measures, T (in K), to T_s = 288.15 K (= 15 ˚C) based on temperature scaling relationships, where k is the Boltzmann constant (8.62×10^{-5} eV K^{-1}). The effect of body mass was controlled for in (b,d) by standardising measures to 1 gram based on the mass scaling relationships. The mass-corrected rates at temperature T_s, $\ln g_o(T_s)$ (-3.34 g g $^{-\gamma}$ d^{-1} (Dataset I) and -5.45 g g $^{-\gamma}$ d^{-1} (Dataset II)), correspond to averages across species and families respectively. In (c,d) growth rates are optimum growth rates (g_{opt}) and mass is mass at optimum growth rates m_{opt}.

Table 3.1. Point estimates and 95% credible intervals (as determined using Bayesian methods) for fitted parameters in the growth rate models. Fixed-effect parameters include: γ, the average for the mass-dependence of growth rate; E_g, the average for the temperature dependence of growth rate; $\ln g_o(T_s)$, the average for the mass-corrected growth rate at temperature T_s = 15˚C; $\Delta\theta$ (Dataset I only), deviations from $\ln g_o(T_s)$ for different ontogenetic stages. Random-effects include the variance for species- (Dataset I) and family-level (Dataset II) variation in size-corrected rates at T_s ($\Delta\ln g_o(T_s)$), as well as variance for family-level size dependence ($\Delta\gamma$) and temperature dependence ΔE_g.

	Dataset I			Dataset II		
Parameter	**Mean**	**2.5% CI**	**97.5% CI**	**Mean**	**2.5% CI**	**97.5% CI**
Fixed effects						
Mass, γ	0.82	0.76	0.88	0.76	0.70	0.81
Activation energy, E_g (eV)	0.68	0.51	0.87	0.23	0.12	0.34
Normalisation, $\ln g_o(T_s)$ (g $g^{-\gamma}$ d^{-1})	-3.34	-3.76	-2.91	-5.45	-5.63	-5.26
$\Delta\theta$ eggs	0.22	-0.49	0.96	-	-	-
$\Delta\theta$ yolk-sac larvae	0.07	-0.55	0.72	-	-	-
$\Delta\theta$ larvae without yolk	-0.26	-0.72	0.17	-	-	-
$\Delta\theta$ larvae undefined	-0.21	-0.82	0.39	-	-	-
$\Delta\theta$ juveniles	-0.56	-1.07	-0.03	-	-	-
$\Delta\theta$ adult	0.74	-0.50	1.99	-	-	-
Random effects						
Variance of $\Delta\gamma$	-	-	-	0.03	0.02	0.05
Variance of ΔE_g	-	-	-	0.10	0.06	0.16
Variance of $\Delta\ln g_o(T_s)$	0.54	0.22	1.07	0.20	0.09	0.39
Covariance of $\Delta\gamma$ and ΔE_g	-	-	-	0.00	-0.02	0.01
Covariance of $\Delta\gamma$ and $\Delta\ln g_o(T_s)$	-	-	-	-0.03	-0.07	0.00
Covariance of $\Delta\ln g_o(T_s)$ and ΔE_g	-	-	-	0.00	-0.07	0.06

The average temperature dependence of growth rates differs between Datasets I and II. While it is statistically indistinguishable from the predicted 0.6–0.7 eV range for Dataset I (average for E_g: 0.68 eV; 95% CI: 0.50–0.87 eV), consistent with previous estimates of temperature dependence of developmental times in fishes (Pauly & Pullin 1988; Gillooly *et al.* 2002; O'Connor *et al.* 2007), it is significantly shallower than this value for Dataset II (average for E_g: 0.23 eV; 95% CI: 0.12–0.34 eV). This unexpected low temperature dependence may be due to errors in age estimation, which can vary systematically with temperature regime, because most age estimates were obtained using indirect methods, such as counting rings of scales or otoliths, which can be biased (Campana 2001), particularly under strong seasonality (Jones 1976). Alternatively, this weak temperature dependence may be a statistical artefact of errors introduced by estimating masses from length-weight functions. Finally, it is possible that the weaker temperature dependence for the field data is a

real biological pattern, reflecting differences in how laboratory-grown (Dataset I) and field-grown (Dataset II) fish respond to temperature, perhaps owing to differences in food availability. Despite these discrepancies between Datasets I and II, the mass dependencies of growth rates for Datasets I and II are reasonably well approximated by a single allometric function that spans ~10 orders of magnitude in body mass (Fig. 3.2), but only after controlling for differences in ontogenetic stage by expressing growth rates as $(dm/dt)f(m,M)$, assuming $f(m,M) = 1$ for Dataset I and $f(m,M) = [1-(m_{opt}/M)^{(1-0.76)}] \approx 0.24$ for Dataset II (assuming $m_{opt}/M \approx 0.32$ – see Appendix III), following the OGM (eqns 1–2).

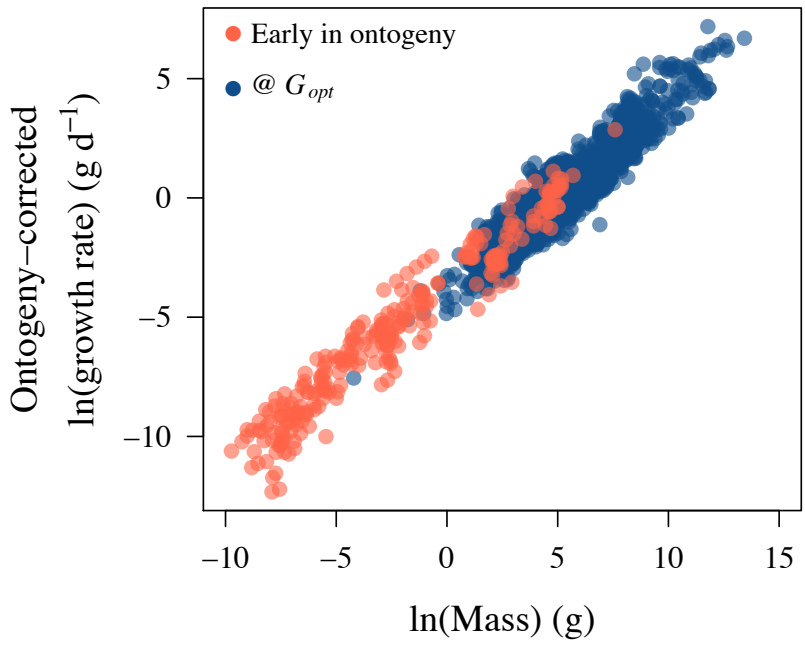

Figure 3.2. Estimates of growth rates early in ontogeny (Dataset I, red) and at optimum mass m_{opt} (Dataset II, blue). The fraction of metabolic energy allocated to maintenance increases throughout ontogeny (eqns 1–2), thus ontogenetic stage was controlled for by expressing growth rates as $(dm/dt)f(m,M)$, assuming $f(m,M) = 1$ for Dataset I and $f(m,M) = [1-(m_{opt}/M)^{(1-0.76)}] \approx 0.24$ for Dataset II (see Appendix III).

Dataset I yields an estimate for the overall temperature dependence of metabolic rate (average E_r: 0.49 eV; 95% CI: 0.38–0.59 eV) that is statistically indistinguishable from that observed for growth rate (Table 3.1), indicating that $E_m^\star$ is independent of temperature

regime. These findings are consistent with results of direct analysis of the $E_m^\star$-temperature relationship (β_1: -0.22 eV; 95% CI: -0.60–0.17 eV), and with the prediction of the OGM (West *et al.* 2001; Gillooly *et al.* 2002; Moses *et al.* 2008) (Fig. 3.3a). For Dataset II, however, the temperature dependence of metabolic rate (average E_r: 0.48 eV; 95% CI: 0.36–0.60 eV; see Table AIII.1) is significantly steeper than that of growth rate (Figs. 3.1b,d; Table 3.1), suggesting that the E_m estimates obtained for different families by combining the growth rate and metabolic rate models (Fig. 3.3b) may exhibit temperature dependence (i.e. $\propto e^{\frac{E_r - E_g}{kT}}$, where $E_r - E_g = 0.25$). Despite these discrepancies, the geometric mean estimates of E_m obtained for Datasets I and II are of similar magnitude (3,779 J g^{-1} versus 5,999 J g^{-1}). These mean estimates are also comparable in magnitude to values reported for other groups of animals (Moses *et al.* 2008). Also noteworthy, the estimates of E_m vary >10-fold among the taxa depicted in Fig. 3.3, highlighting substantial variation in the amount of energy an organism must expend in producing biomass.

Understanding how and why E_m varies is of fundamental importance to predicting constraints on the efficiency of energy transfer between trophic levels. Previous work has demonstrated that this efficiency is generally higher if the prey individual is consumed at an earlier life-history stage by the predator (Jones 1976; Andersen *et al.* 2009). The OGM quantitatively predicts this result because the fraction of metabolic energy allocated to growth ($=f(m, M)$) is higher at earlier life history stages, indexed by m/M. Thus, if a prey individual is consumed at an earlier life history stage (corresponding to lower m/M), a larger fraction of its assimilated energy will have been allocated to biomass (as opposed to respiration) prior to consumption by the predator. In fact, the rate of energy assimilation by an individual of size m, $A(m)$, is

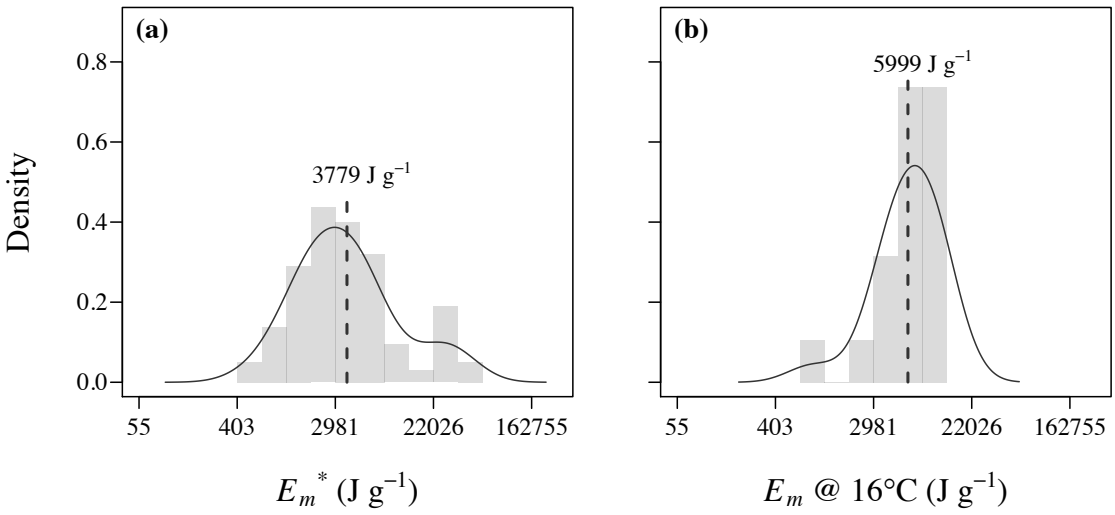

Figure 3.3. Distributions of values for E_m (J g^{-1}), the amount of energy necessary to produce biomass (g), across species (a) and families (b). In (a), values are upper-bound estimates of $E_m^\star$ obtained from 275 direct measurements of growth rates and metabolic rates in Dataset I (assuming $f(m, M) = 1$, eqn 7). In (b), values of E_m were standardised to 16˚C, and were indirectly estimated for the 19 families with growth rate data in Dataset II and metabolic rate data in the database analysed by Barneche *et al.* (2014). Family-specific estimates of $\ln g_o(T_s)$, $\ln b_o(T_s)$, E_g and E_r (Tables 3.1,AIII.1, Dataset II) were employed to calculate E_m, assuming mass invariance (i.e. $m^{\gamma-\alpha} = m^0$), following the formula (eqn 6): $E_m = [\ln b_o(T_s) - \ln g_o(T_s) + (E_r - E_g)/(8.62 \times 10^{-5})(1/T_s - 1/T) + \ln\overline{f(m,M)}]c_1$, where T_s = 15°C, T = 289.15 K (16˚C) (17 out of the 19 families had rates estimated at temperature ranges encompassing 16˚C), $\overline{f(m,M)}$ is the average fraction of energy $f(m, M)$ allocated to growth among all observations within a given family using estimates of m_{opt} and M (Appendix III), and c_1 = 39,000 J g C^{-1} is the conversion factor between g C to Joules. In (a) and (b), solid lines represent fitted density curves, and dashed lines represent average estimates of $E_m^\star$ and E_m, respectively.

$$A(m) = B + E_c \frac{dm}{dt} \quad , \tag{11}$$

where E_c is the combustion energy of biomass (Hou *et al.* 2008). Given that only the energy contained in prey biomass can be transferred to a higher trophic level, we can use eqns 1–11 to obtain estimates for the efficiency of energy transfer between trophic levels given different values for ontogenetic stage, m/M, and E_m (see Appendix III). These efficiencies represent

upper-bound estimates because they incorporate only energy losses due to respiration, and thus exclude losses attributable to other processes (e.g. biomass and faeces that are consumed by detritivores). Results of these calculations demonstrate that the maximum efficiency of energy transfer varies considerably with E_m over the empirically observed range of E_m values (Fig. 3.4). In fact, the effects of E_m are of comparable magnitude to those of ontogenetic stage, highlighting the quantitative importance of this variable for understanding energy transfers between trophic level.

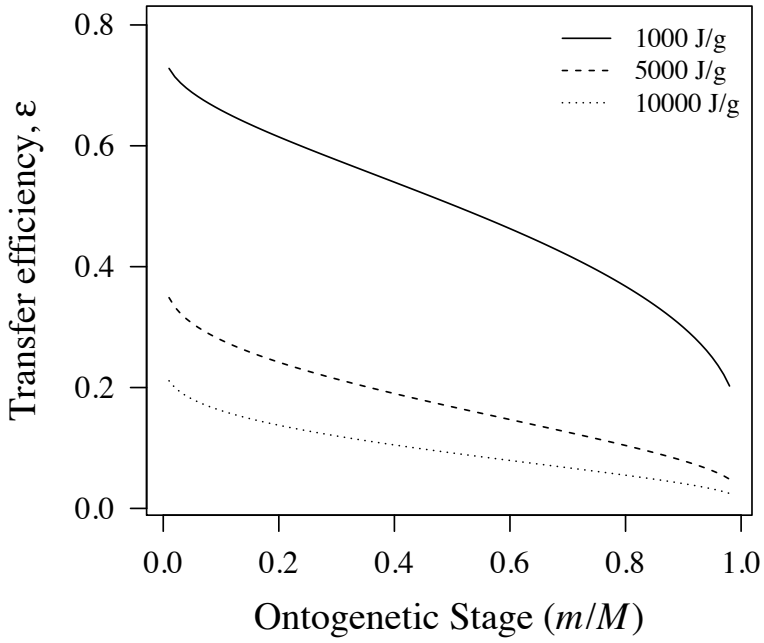

Figure 3.4. Upper-bound estimates for the efficiency of energy transfer given different values for different ontogenetic stages, m/M, and E_m (J g^{-1}) (eqns 1–11, Appendix III). Efficiencies only incorporate energy losses due to respiration, and thus exclude losses attributable to other processes (see text). Lines depict different values of E_m.

We can also use our model to expand theoretical predictions obtained from size-spectrum theory. This theory predicts a specific relationship between total community biomass, Y, and individual body mass, M,

$$Y \propto M^{1-\alpha} M^{\frac{\ln(\varepsilon)}{\ln(PPMR)}}, \quad (12)$$

based on the size-scaling of metabolic rate (α) and the assumptions that the predator-prey body-mass ratio, $PPMR$, and the efficiency of energy transfer between trophic levels, ε, are held constant moving between trophic levels (Brown & Gillooly 2003). Both assumptions appear reasonable for many marine pelagic communities (Jennings & Mackinson 2003; Trebilco *et al*. 2013). By combining this model with our expression for transfer efficiency, we can show how the predicted size structure changes with the energy required to produce biomass, E_m, through its effects on the transfer efficiency, ε (Fig. 3.5).

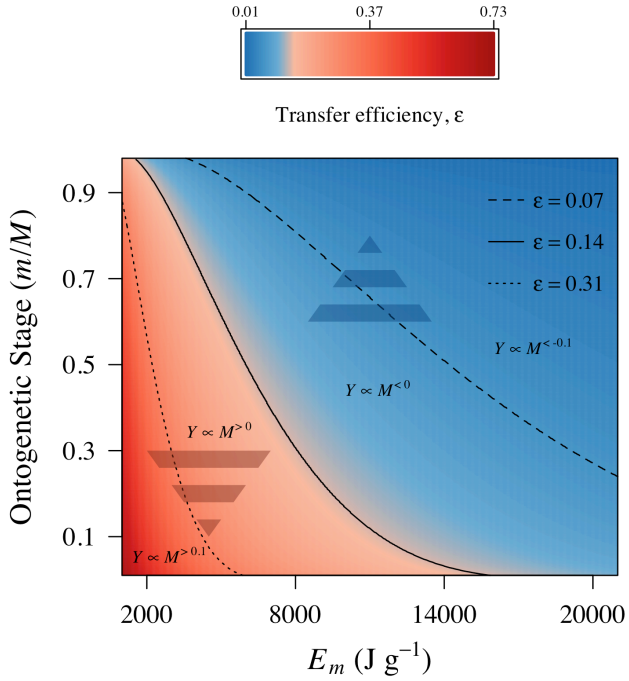

Figure 3.5. Relationship between ontogenetic stage of prey at time of predation and energy necessary to produce a unit of biomass E_m, and the resulting effects on the size structuring of biological communities and the energy transfer efficiency between trophic levels. Different colours indicate different resulting biomass – body mass scaling relationships, with blue areas depicting bottom-heavy pyramids and red areas depicting top-heavy pyramids. The black solid line represents an area where $Y \propto M^0$, i.e. a biomass stack (see Trebilco *et al*. 2013), which corresponds to an average energy transfer efficiency of 0.14. The values in the figure were calculated assuming a predatory-prey mass ratio of 2327:1 (following Al-Habsi *et al*. 2008), and a value of α = 0.75 for the size scaling of metabolic rate.

The relationships depicted in Fig. 3.5 yield new insights into how biological communities can be structured depending on species-specific physiology (e.g. changes in

E_m), as well as behaviour (e.g. preferred prey size). For instance, in coastal communities such as coral reefs, eggs produced during mass-spawning events represent an important resource for many groups (Harrison *et al*. 1984; Domeier & Colin 1997; Pratchett *et al*. 2001). Our model may help to explain the existence of top-heavy pyramids (red area in Fig. 3.5) in some reef-fish communities (Sandin *et al*. 2008; Trebilco *et al*. 2013) because egg consumption represents the most efficient form of energy transfer between trophic levels. For the illustrative $PPMR$ adopted here, an average cut-off energy transfer efficiency of 0.14 dictates whether pyramids are bottom or top heavy (Fig 3.5). Refinement of these predictions will require an assessment of ontogenetic stage of prey items in diets of different species.

Our findings might also yield important insights in terms of fisheries management. For example, our model predictions suggest that preserving large individuals that produce more (and larger) eggs in aquatic communities (Birkeland & Dayton 2005) may be key to the maintenance of high-efficiency energy transfers between trophic levels. This insight may be particularly relevant in oligotrophic communities because high-efficiency recycling of energy and nutrients is vital to the maintenance of such systems (Depczynski *et al*. 2007). Taken altogether, these results indicate that understanding the energetics of growth across different trophic levels (and/or functional groups) might help establish baselines of recovery potential in coastal fisheries (e.g. MacNeil *et al*. 2015).

Overall, our study demonstrates how growth rate and metabolic rate data can be synthesised within a theoretical framework to obtain a deeper understanding of the energetics of growth. Results of this analysis highlight general trends, but also important differences among datasets, as well as among species, particularly with regard to E_m. Reconciling these differences will require more and better data on growth rates and metabolic rates of fishes over wide temperature gradients. In this regard, it is notable that nearly 60% of the studies

from which we obtained data for Dataset I were conducted at least 20 years ago, emphasising the need for more data collection. The collection and analysis of such data may eventually aid in managing and rehabilitating economically important fisheries stocks (MacNeil *et al*. 2015), which are declining in many parts of the world (Pauly *et al.* 2002), and may also help in understanding how warming temperatures affect the distributions, developmental rates and maximum sizes of fishes (Pörtner & Knust 2007; Daufresne *et al.* 2009), ultimately affecting ecosystem dynamics in both ecological and evolutionary time scales.

3.5 ACKNOWLEDGEMENTS

I would like to thank A.P. Allen for the insightful contributions and comments on this chapter.

3.6 REFERENCES

Al-Habsi, S.H., Sweeting, C.J., Polunin, N.V.C. & Graham, N.A.J. (2008). $\delta^{15}N$ and $\delta^{13}C$ elucidation of size-structured food webs in a Western Arabian Sea demersal trawl assemblage. *Marine Ecology Progress Series*, 353, 55–6.

Andersen, K., Beyer, J. & Lundberg, P. (2009). Trophic and individual efficiencies of size-structured communities. *Proceedings of the Royal Society of London B: Biological Sciences*, 276, 109–114.

Ashworth, A. (1969). Metabolic rates during recovery from protein–calorie malnutrition: the need for a new concept of specific dynamic action. *Nature*, 223, 407–409.

Atkinson, D. (1994). Temperature and organism size—a biological law for ectotherms? *Advances in Ecological Research*, 25, 1–58.

Banavar, J.R., Damuth, J., Maritan, A. & Rinaldo, A. (2002). Ontogenetic growth (communication arising): modelling universality and scaling. *Nature*, 420, 626.

Barneche, D.R., Kulbicki, M., Floeter, S.R., Friedlander, A.M., Maina, J. & Allen, A.P. (2014). Scaling metabolism from individuals to reef-fish communities at broad spatial scales. *Ecology Letters*, 17, 1067–1076.

von Bertalanffy, L. (1938). A quantitative theory of organic growth (Inquiries on growth laws. II). *Human Biology*, 10, 181–213.

von Bertalanffy, L. (1957). Quantitative laws in metabolism and growth. *The Quarterly Review of Biology*, 32, pp. 217–231.

Birkeland, C. & Dayton, P.K. (2005). The importance in fishery management of leaving the big ones. *Trends in Ecology & Evolution*, 20, 356–358.

Brown, J.H. & Gillooly, J.F. (2003). Ecological food webs: high-quality data facilitate theoretical unification. *Proceedings of the National Acadamy of Sciences*, 100, 1467–1468.

Brown, J.H., Gillooly, J.F., Allen, A.P., Savage, V.M. & West, G.B. (2004). Toward a metabolic theory of ecology. *Ecology*, 85, 1771–1789.

Brown, J.H., Marquet, P.A. & Taper, M.L. (1993). Evolution of body size: Consequences of an energetic definition of fitness. *The American Naturalist*, 142, 573–584.

Burel, C., Ruyet, J.P.-L., Gaumet, F., Roux, A.L., Sévère, A. & Boeuf, G. (1996). Effects of temperature on growth and metabolism in juvenile turbot. *Journal of Fish Biology*, 49, 678–692.

Calbet, A. & Saiz, E. (2005). The ciliate-copepod link in marine ecosystems. *Aquatic Microbial Ecology*, 38, 157–167.

Campana, S.E. (2001). Accuracy, precision and quality control in age determination, including a review of the use and abuse of age validation methods. *Journal of Fish Biology*, 59, 197–242.

Charnov, E.L. & Gillooly, J.F. (2004). Size and temperature in the evolution of fish life histories. *Integrative and Comparative Biology*, 44, 494–497.

Chassot, E., Bonhommeau, S., Dulvy, N.K., Mélin, F., Watson, R., Gascuel, D. *et al.* (2010). Global marine primary production constrains fisheries catches. *Ecology Letters*, 13, 495–505.

Clarke, A. & Johnston, I.A. (1996). Evolution and adaptive radiation of Antarctic fishes. *Trends in Ecology & Evolution*, 11, 212–218.

Clarke, A. & Johnston, N.M. (1999). Scaling of metabolic rate with body mass and temperature in teleost fish. *Journal of Animal Ecology*, 68, pp. 893–905.

Clarke, G.L., Edmondson, W.T. & Ricker, W.E. (1946). Dynamics of production in a marine area. *Ecological Monographs*, 16, 321–337.

Conti, L. & Scardi, M. (2005). Fisheries yield and primary productivity in large marine ecosystems. *Marine Ecology Progress Series*, 410, 233–244.

Daufresne, M., Lengfellner, K. & Ulrich, S. (2009). Global warming benefits the small in aquatic ecosystems. *Proceedings of the National Academy of Sciences*, 106, 12788–12793.

Depczynski, M., Fulton, C.J., Marnane, M.J. & Bellwood, D.R. (2007). Life history patterns shape energy allocation among fishes on coral reefs. *Oecologia*, 153, 111–120.

Domeier, M.L. & Colin, P.L. (1997). Tropical Reef Fish Spawning Aggregations: Defined and Reviewed. *Bulletin of Marine Science*, 60, 698–726.

Elton, C.S. (1927). *Animal ecology*. Macmillan Co., New York, pp. 2060.

Finn, R., Rønnestad, I. & Fyhn, H. (1995). Respiration, nitrogen and energy metabolism of developing yolk-sac larvae of Atlantic halibut (*Hippoglossus hippoglossus* L.). *Comparative Biochemistry and Physiology Part A: Physiology*, 111, 647–671.

Froese, R. & Pauly, D. (2012). FishBase. World Wide Web electronic publication. Available at http://www.fishbase.org, (Version 12/2012). Last accessed 20 February 2015.

Gardiner, N.M., Munday, P.L. & Nilsson, G.E. (2010). Counter-gradient variation in respiratory performance of coral reef fishes at elevated temperatures. *PLoS ONE*, 5, e13299.

Gillooly, J.F., Brown, J.H., West, G.B., Savage, V.M. & Charnov, E.L. (2001). Effects of size and temperature on metabolic rate. *Science*, 293, 2248–2251.

Gillooly, J.F., Charnov, E.L., West, G.B., Savage, V.M. & Brown, J.H. (2002). Effects of size and temperature on developmental time. *Nature*, 417, 70–73.

Handeland, S.O., Imsland, A.K. & Stefansson, S.O. (2008). The effect of temperature and fish size on growth, feed intake, food conversion efficiency and stomach evacuation rate of Atlantic salmon post-smolts. *Aquaculture*, 283, 36–42.

Hansen, S.L. & Herbing, I.H.V. (2009). Aerobic scope for activity in age 0 year Atlantic cod *Gadus morhua*. *Journal of Fish Biology*, 74, 1355–1370.

Harrison, P.L., Babcock, R.C., Bull, G.D., Oliver, J.K., Wallace, C.C. & Willis, B.T. (1984). Mass Spawning in Tropical Reef Corals. *Science*, 223, 1186–1189.

Hawkins, A.J.S., Widdows, J. & Bayne, B.L. (1989). The relevance of whole-body protein metabolism to measured costs of maintenance and growth in *Mytilus edulis*. *Physiological Zoology*, 62, 745–763.

Hogendoorn, H. (1983). Growth and production of the African catfish, *Clarias lazera* (C. & V.): III. Bioenergetic relations of body weight and feeding level. *Aquaculture*, 35, 1–17.

Hou, C., Zuo, W., Moses, M.E., Woodruff, W.H., Brown, J.H. & West, G.B. (2008). Energy uptake and allocation during ontogeny. *Science*, 322, 736–739.

Houde, E.D. (1989). Comparative growth, mortality, and energetics of marine fish larvae: temperature and implied latitudinal effects. *Fishery Bulletin*, 87, 471–495.

Imsland, A.K., Folkvord, A. & Stefansson, S. (1995). Growth, oxygen consumption and activity of juvenile turbot (*Scophthalmus maximus* L.) reared under different temperatures and photoperiods. *Netherlands Journal of Sea Research*, 34, 149–159.

Irigoien, X., Klevjer, T.A., Røstad, A., Martinez, U., Boyra, G., Acuña, J.L. *et al.* (2013). Large mesopelagic fishes biomass and trophic efficiency in the open ocean. *Nature Communications*, 5, 1–10.

Iverson, R.L. (1990). Control of marine fish production. *Limnology and Oceanography*, 35, 1593–1604.

Jennings, S. & Mackinson, S. (2003). Abundance-body mass relationships in size-structured food webs. *Ecology Letters*, 6, 971–974.

Jones, R. (1976). Growth of fishes. In: *The ecology of the seas* (eds. Cushing, D.H. & Walsh, J.J.). Blackwell Scientific Publications, San Diego, pp. 251–279.

Kinne, O. (1960). Growth, food intake, and food conversion in a euryplastic fish exposed to different temperatures and salinities. *Physiological Zoology*, 33, 288–317.

Kiørboe, T., Munk, P. & Richardson, K. (1987). Respiration and growth of larval herring *Clupea harengus*: relation between specific dynamic action and growth efficiency. *Marine Ecology Progress Series*, 40, 1–10.

Kruschke, J.K. (2014). *Doing Bayesian data analysis: A tutorial with R, JAGS, and stan*. 2nd edn. Academic Press, pp. 776.

Laurence, G. (1975). Laboratory growth and metabolism of the winter flounder *Pseudopleuronectes americanus* from hatching through metamorphosis at three temperatures. *Marine Biology*, 32, 223–229.

Laurence, G. (1978). Comparative growth, respiration and delayed feeding abilities of larval cod (*Gadus morhua*) and haddock (*Melanogrammus aeglefinus*) as influenced by temperature during laboratory studies. *Marine Biology*, 50, 1–7.

Lindeman, R.L. (1942). The trophic-dynamic aspect of ecology. *Ecology*, 23, 399–417.

MacNeil, M.A., Graham, N.A.J., Cinner, J.E., Wilson, S.K., Williams, I.D., Maina, J. *et al*. (2015). Recovery potential of the world's coral reef fishes. *Nature*, 520, 341–344.

Makarieva, A.M., Gorshkov, V.G. & Li, B.-L. (2004). Ontogenetic growth: models and theory. *Ecological Modelling*, 176, 15–26.

Millward, D.J., Garlick, P.J. & Reeds, P.J. (1976). The energy cost of growth. *Proceedings of the Nutrition Society*, 35, 339–349.

Moses, M.E., Hou, C., Woodruff, W.H., West, G.B., Nekola, J.C., Zuo, W., *et al.* (2008). Revisiting a model of ontogenetic growth: estimating model parameters from theory and data. *The American Naturalist*, 171, pp. 632–645.

Neuheimer, A.B., Thresher, R.E., Lyle, J.M. & Semmens, J.M. (2011). Tolerance limit for fish growth exceeded by warming waters. *Nature Climate Change*, 1, 110–113.

Nixon, S.W., Oviatt, C.A., Frithsen, J. & Sullivan, B. (1986). Nutrients and the productivity of estuarine and coastal marine ecosystems. *Journal of the Limnological Society of Southern Africa*, 12, 43–71.

O'Connor, M.I., Bruno, J.F., Gaines, S.D., Halpern, B.S., Lester, S.E., Kinlan, B.P. *et al.* (2007). Temperature control of larval dispersal and the implications for marine ecology, evolution, and conservation. *Proceedings of the National Academy of Sciences*, 104, 1266–1271.

Parry, G. (1983). The influence of the cost of growth on ectotherm metabolism. *Journal of Theoretical Biology*, 101, 453–477.

Pauly, D. (1980). On the interrelationships between natural mortality, growth parameters, and mean environmental temperature in 175 fish stocks. *Journal du Conseil*, 39, 175–192.

Pauly, D. & Christensen, V. (1995). Primary production required to sustain global fisheries. *Nature*, 374, 255–257.

Pauly, D. & Palomares, M.-L. (2005). Fishing down marine food web: it is far more pervasive than we thought. *Bulletin of Marine Science*, 76, 197–212.

Pauly, D. & Pullin, R.S.V. (1988). Hatching time in spherical, pelagic, marine fish eggs in response to temperature and egg size. *Environmental Biology of Fishes*, 22, 261–271.

Pauly, D., Christensen, V., Guenette, S., Pitcher, T.J., Sumaila, U.R., Walters, C.J. *et al.* (2002). Towards sustainability in world fisheries. *Nature*, 418, 689–695.

Pörtner, H.O. & Knust, R. (2007). Climate change affects marine fishes through the oxygen limitation of thermal tolerance. *Science*, 315, 95–97.

Pratchett, M.S. Gust, N., Goby, G. & Klanten S.O. (2001). Consumption of coral propagules represents a significant trophic link between corals and reef fish. *Coral Reefs*, 20, 13–17.

Sandin, S.A., Smith, J.E., DeMartini, E.E., Dinsdale, E.A., Donner, S.D., Friedlander, A.M. *et al.* (2008). Baselines and degradation of coral reefs in the northern Line Islands. *PLoS ONE*, 3, e1548.

Savage, V.M., Gillooly, J.F., Brown, J.H., West, G.B. & Charnov, E.L.(2004a). Effects of body size and temperature on population growth. *The American Naturalist*, 163, 429–441.

Savage, V.M., Gillooly, J.F., Woodruff, W.H., West, G.B., Allen, A.P., Enquist, B.J. *et al.* (2004b). The predominance of quarter-power scaling in biology. *Functional Ecology*, 18, 257–282.

Secor, D.H. & Gunderson, T.E. (1998). Effects of hypoxia and temperature on survival, growth and respiration of juvenile Atlantic sturgeon, *Acipenser oxyrinchus*. *Fishery Bulletin*, 96, 603–613.

Su, Y.-S. & Yajima, M. (2015). *R2jags:* A package for running *JAGS* from R. R package version 0.05-03.

Trebilco, R., Baum, J.K., Salomon, A.K. & Dulvy, N.K. (2013). Ecosystem ecology: size-based constraints on the pyramids of life. *Trends in Ecology & Evolution*, 28, 423–431.

Weatherley, A.H., Gill, H.S. & Casselman, J.M. (1987). *The biology of fish growth*. Academic Press, pp. 443.

West, G.B., Brown, J.H. & Enquist, B.J. (1997). A general model for the origin of allometric scaling laws in biology. *Science*, 276, 122–126.

West, G.B., Brown, J.H. & Enquist, B.J. (2001). A general model for ontogenetic growth. *Nature*, 413, 628–631.

West, G.B., Enquist, B.J. & Brown, J.H. (2002). Ontogenetic growth (communication arising): modelling universality and scaling. *Nature*, 420, 626–627.

Wood, A.H. (1932). The effect of temperature on the growth and respiration of fish embryos (*Salmo fario*). *Journal of Experimental Biology*, 9, 271–276.

SYNTHESIS

In this PhD dissertation, I use the Metabolic Theory of Ecology (MTE; Brown *et al.* 2004) as a framework to derive and test predictions about how individual metabolic rates and growth rates scale with body mass and temperature, and how these scaling relationships in turn influence populations, communities, and ecosystems. The overarching goal of this work was to advance our understanding of how higher level, ecological phenomena are constrained by physiological processes. Models at the individual level were tested using data on all fishes for which we could obtain data, while the models at higher levels of organisation were tested using a comprehensive dataset of tropical and subtropical reef-fish community structure.

I now discuss the theoretical, empirical and analytical contributions of my thesis, while pointing out some important limitations of this work given the data currently available and the theory as it currently stands. I also comment on what I believe to be fruitful avenues for future research.

The generality of metabolic-rate scaling relationships has long been a matter of debate in Ecology and Physiology (Kleiber 1961; Peters 1983; Schmidt-Nielsen 1984; Gillooly *et al.* 2001; Agutter & Wheatley 2004; Savage *et al.* 2004; Yvon-Durocher *et al.* 2012; Hirst *et al.* 2014). The hierarchical models and model selection approaches adopted throughout this dissertation hold great promise for helping to resolve this debate. In particular, they can aid in assessing the consistency of scaling phenomena within and across taxa (e.g. Glazier 2005; Isaac & Carbone 2010; Hirst *et al.* 2014; Barneche & Allen 2015) by partitioning the variance into general trends, represented by 'fixed' factors, and taxon-specific idiosyncrasies, represented by 'random' factors. While the variance captured by random factors does not by itself identify particular driving mechanisms, it does highlight areas for future work.

With regards to the individual-level scaling relationships in Chapter 1, using a database that spans > 6 orders of magnitude in fish body mass, I was able to corroborate that the scaling of metabolic rates for fish is remarkably close to the canonical value of 0.75 predicted by MTE (Brown *et al.* 2004; Barneche *et al.* 2014). Interestingly, however, in Chapter 3, I showed that this scaling seems to be slightly steeper very early in ontogeny, which is consistent to previous estimates of metabolic rates estimated from for fish larvae (Clarke & Johnston 1999). These findings highlight that we still have much to learn about scaling of rates throughout ontogeny.

With regard to temperature, the data in Chapter 1 yield compelling evidence for the existence of a general temperature optimum in fish. These findings are directly relevant to understanding how organisms respond to effects of future climate change (Rezende *et al.* 2014). The estimation of this optimum was made possible by extending the Metabolic Theory formulation of Gillooly *et al.* model (Gillooly *et al.* 2001; Barneche *et al.* 2014). Still, this work represents only a preliminary step in assessing the capacities of fish to adapt to warmed thermal regimes. It highlights the need for work evaluating species' capacities for thermal adaptation, which will require long-term studies encompassing multiple generations (Donelson *et al.* 2012).

To what extent does individual-level energetics dictate large-scale patterns of abundance, biomass production, and energy flux at higher organisational scales? This question has been central to many critiques of the Metabolic Theory of Ecology (e.g. Cyr & Walker 2004; Tilman *et al.* 2004), and it has inspired researchers to derive and test theoretical predictions at the population, community and ecosystem levels (e.g. Allen & Gillooly 2007; O'Connor *et al.* 2007). All three of my chapters address this question directly. First, in Chapter 1, I use a new Bayesian approach (Yvon-Durocher & Allen 2012; Barneche *et al.* 2014) to simultaneously estimate uncertainties in the scaling parameters used to characterise

individual-level metabolic rates, and to account for those uncertainties to predict quantities such as population- and community-level size-corrected body mass, and averaged temperature kinetics. Second, in Chapter 2, I present empirical evidence that energetics limits the density and biomass of abundant populations, but that this constraint appears less pronounced than that imposed by ecological factors, as indexed by community species richness. Finally, in Chapter 3, I show theoretically how the energetics of individual-level growth and respiration combine to place important constraints on the efficiency of energy transfer between entire trophic levels in a food web. In general, I believe that these findings highlight the importance of individual energetics at higher levels of biological organization, from populations to ecosystems. More specifically, I believe it highlights the potential for a more community-focused approach to energy and nutrient fluxes in ecosystems.

This thesis also makes interesting and pertinent contributions to our understanding of the ecology of reef ecosystems by using data on reef-fish community structure to test MTE predictions. For instance, calculations of size-correcting body mass for different species and trophic groups reveals striking differences in community structure among fish assemblages in different biogeographic regions (Barneche *et al.* 2014). Moreover, by characterising community-level energy fluxes, this thesis highlights the need to better understand and quantify total reef net primary production (NPP). For example, while findings of Chapter 1 suggest that satellite-estimated near-pelagic NPP constrains the abundance of planktivores, comparison of these NPP estimates with estimated total respiratory fluxes of reef fish communities indicate that pelagic NPP represents only a small fraction of total resource available on reefs, and therefore should not be used as an index to total energy availability on reefs. Also, the fact that piscivores are respiring only ~2.38-fold less than herbivores, as opposed to the 100-fold expectation of Lindeman's efficiency, strongly suggests that reef piscivores are strongly subsidised by resources from outside the reef (Trebilco *et al.* 2013).

Part of these subsidies may come from high-efficient predation events on reefs during periods of spawning (Fig. 3.5 in Chapter 3). Development of a more refined understanding of the sources of these energy subsidies may be achieved through stable-isotope approaches that treat diet as a continuous variable (i.e. trophic level; e.g. Hussey *et al*. 2014), and in part through the collection of more and better data on reef NPP. Progress is being made towards estimating total reef NPP using approaches that explicitly link ecosystem-level fluxes to individual energetics (Naumann *et al.* 2013). Thus, the hierarchical statistical approach adopted for this thesis may prove useful for estimating overall rates of net primary production on reefs.

The analyses in this thesis are limited by a lack of data on reef-fish harvesting and other potential anthropogenic effects (e.g. habitat destruction, pollution and coastal eutrophication). For instance, it is unknown the extent to which the striking differences in trophic structure observed in Chapter 1 and Chapter 2 are influenced by human-related factors. In coral reefs, overfishing has largely affected the abundance and biomass of both herbivores (e.g. parrotfish) and top predators (e.g. sharks, groupers, snappers) (Jackson *et al*. 2001; Donaldson & Dulvy 2004; Mumby *et al*. 2004; Anderson *et al*. 2014), thus affecting key processes such as bioerosion of reef substrates (Bellwood *et al*. 2012), and resilience of reef systems around the world (MacNeil *et al*. 2015). Overfishing might also be correlated with coastal pollution, as demand for food sources is often related to coastal development (Sadovy 2005), thus increasing sedimentation and possibly eutrophication. As a consequence, other parts of the ecosystem are affected, particularly the microbiota, which seems to respire proportionally more carbon than reef fish along a human-impact gradient in the Pacific (McDole *et al.* 2012). I hope that the approaches adopted in this thesis will foster the consideration of the roles of energetics in coral reef science, not only at the community, but

also at the ecosystem level, in order to better understand how these human impacts will affect the dynamics of net primary production and carbon sequestration.

Overall, this thesis recognizes and addresses limitations of the Metabolic Theory of Ecology. However, more importantly, it raises important questions that should pave the way to research that is directly relevant to macrophysiology, macroecology and climate change biology. Therefore, to finish up, I would like to raise questions that I believe can be informed and pursued following the lines of research present throughout this thesis. (1) What are the adaptation capacities of different species to increasing temperatures? This has been a long quest in ecophysiology, and recent laboratory experiments are tackling this issue head on for tropical reef-fish species (e.g. Gardiner *et al*. 2010; Rummer *et al*. 2014). The models presented here should provide an integrative framework to refine and expand such experiments by allowing data from multiple species with distinct temperature regimes and body sizes to be combined. (2) What are the mechanisms that explain the existence of temperature optima in ectothermic species? Although our expansion of the Schoolfield-Sharpe equation (Schoolfield *et al*. 1981) provides an interesting way of testing the existence of temperature optima in fishes, the true mechanism remains elusive. Many possible explanations have been proposed, including not only protein denaturation (e.g. Gillooly *et al*. 2001; 2002), but also temperature-mediated oxygen limitation (Pörtner *et al*. 2007). (3) How do overfishing and pollution affect energetic fluxes in reef ecosystems? An interesting new study indicating that bacteria garner more energy, relative to fish, along a gradient of increasing human disturbance (McDole *et al*. 2012). However, it is as yet unclear how much of this imbalance can be attributed to loss of energy in the fish component of the food chain or simply increase in nutrient load promoting a higher respiration from the bacterial component of the community. (4) What are the consequences of overfishing to trophic cascades? Could invertebrates at the community level and omnivores at the population level

be the most important groups in terms of energy utilisation on reefs due to prey-release effects? Or could it be that invertebrates play a large role that has been relatively overlooked in reef food webs? Would it be possible that mass spawning events contribute to a more efficient energy transfer on coral-reef systems? (5) How can stoichiometry, together with physiological constraints, better inform us of rates of net primary production on reefs? Important studies are already on their way to help fill this gap (Naumann *et al*. 2013) after 50 years of paucity in the reef literature (Odum & Odum 1955). Similar to what we did with the heterotroph data in Chapters 1 and 2 (i.e. reef fishes), similar analyses should be conducted with autotrophs considering the different temperature dependence of photosynthetic rates relative to respiration rates (Allen *et al*. 2005; López-Urrutia *et al*. 2006, O'Connor *et al*. 2009). Finally, how much energy different reef ecosystems (e.g. islands, atolls) provide for humans to flux?

REFERENCES

Agutter, P. & Wheatley, D. (2004). Metabolic scaling: consensus or controversy? *Theoretical Biology and Medical Modelling*, 1, 13.

Allen, A.P., Gillooly, J.F. & Brown, J.H. (2005). Linking the global carbon cycle to individual metabolism. *Functional Ecology*, 19, 202–213.

Allen, A.P. & Gillooly, J.F. (2007). The mechanistic basis of the metabolic theory of ecology. *Oikos*, 116, 1073–1077.

Anderson, A.B., Bonaldo, R.M., Barneche, D.R., Hackradt, C.W., Félix-Hackradt, F.C., García-Chartón, J.A. *et al.* (2014). Recovery of grouper assemblages indicates effectiveness in a Marine Protected Area in Southern Brazil. *Marine Ecology Progress Series*, 514, 207–215.

Barneche, D.R. & Allen, A.P. (2015). Embracing general theory and taxon-level idiosyncrasies to explain nutrient recycling. *Proceedings of the National Academy of Sciences*, in press.

Barneche, D.R., Kulbicki, M., Floeter, S.R., Friedlander, A.M., Maina, J. & Allen, A.P. (2014). Scaling metabolism from individuals to reef-fish communities at broad spatial scales. *Ecology Letters*, 17, 1067–1076.

Bellwood, D.R., Hoey, A.S. & Hughes, T.P. (2012). Human activity selectively impacts the ecosystem roles of parrotfishes on coral reefs. *Proceedings of the Royal Society of London B: Biological Sciences*, 279, 1621–1629.

Brown, J.H., Gillooly, J.F., Allen, A.P., Savage, V.M. & West, G.B. (2004). Toward a metabolic theory of ecology. *Ecology*, 85, 1771–1789.

Clarke, A. & Johnston, N.M. (1999). Scaling of metabolic rate with body mass and temperature in teleost fish. *Journal of Animal Ecology*, 68, pp. 893–905.

Cyr, H. & Walker, S.C. (2004). An illusion of mechanistic understanding. *Ecology*, 85, pp. 1802–1804.

Donaldson, T.J. & Dulvy, N.K. (2004). Threatened Fishes of the World: Bolbometopon muricatum (Valenciennes 1840) (Scaridae). *Environmental Biology of Fishes*, 70, 373–373.

Donelson, J.M., Munday, P.L., McCormick, M.I. & Pitcher, C.R. (2012). Rapid transgenerational acclimation of a tropical reef fish to climate change. *Nature Climate Change*, 2, 30–32.

Gardiner, N.M., Munday, P.L. & Nilsson, G.E. (2010). Counter-gradient variation in respiratory performance of coral reef fishes at elevated temperatures. *PLoS ONE*, 5, e13299.

Gillooly, J.F., Brown, J.H., West, G.B., Savage, V.M. & Charnov, E.L. (2001). Effects of size and temperature on metabolic rate. *Science*, 293, 2248–2251.

Gillooly, J.F., Charnov, E.L., West, G.B., Savage, V.M. & Brown, J.H. (2002). Effects of size and temperature on developmental time. *Nature*, 417, 70–73.

Glazier, D.S. (2005). Beyond the '3/4-power law': variation in the intra-and interspecific scaling of metabolic rate in animals. *Biological Reviews*, 80, 611–662.

Hirst, A.G., Glazier, D.S. & Atkinson, D. (2014). Body shape shifting during growth permits tests that distinguish between competing geometric theories of metabolic scaling. *Ecology Letters*, 17, 1274–1281.

Hussey, N.E., MacNeil, M.A., McMeans, B.C., Olin, J.A., Dudley, S.F., Cliff, G. *et al.* (2014). Rescaling the trophic structure of marine food webs. *Ecology Letters*, 17, 239–250.

Isaac, N.J.B. & Carbone, C. (2010). Why are metabolic scaling exponents so controversial? Quantifying variance and testing hypotheses. *Ecology Letters*, 13, 728–735.

Jackson, J.B.C., Kirby, M.X., Berger, W.H., Bjorndal, K.A., Botsford, L.W., Bourque, B.J. *et al.* (2001). Historical overfishing and the recent collapse of coastal ecosystems. *Science*, 293, 629–637.

Kleiber, M. (1961). *The fire of life: An introduction to animal energetics*. John Wiley & Sons, New York, pp. 454.

López-Urrutia, Á., San Martin, E., Harris, R.P. & Irigoien, X. (2006). Scaling the metabolic balance of the oceans. *Proceedings of the National Academy of Sciences*, 103, 8739–8744.

MacNeil, M.A., Graham, N.A.J., Cinner, J.E., Wilson, S.K., Williams, I.D., Maina, J. *et al*. (2015). Recovery potential of the world's coral reef fishes. *Nature*, 520, 341–344.

McDole, T., Nulton, J., Barott, K.L., Felts, B., Hand, C., Hatay, M. *et al.* (2012). Assessing coral reefs on a Pacific-wide scale using the microbialization score. *PLoS ONE*, 7, e43233.

Mumby, P.J., Edwards, A.J., Arias-González, J.E., Lindeman, K.C., Blackwell, P.G., Gall, A. *et al*. (2004). Mangroves enhance the biomass of coral reef fish communities in the Caribbean. *Nature*, 427, 533–536.

Naumann, M.S., Jantzen, C., Haas, A.F., Iglesias-Prieto, R. & Wild, C. (2013). Benthic primary production budget of a Caribbean reef lagoon (Puerto Morelos, Mexico). *PLoS ONE*, 8, e82923.

O'Connor, M.I., Piehler, M.F., Leech, D.M., Anton, A. & Bruno, J.F. (2009). Warming and resource availability shift food web structure and metabolism. *PLoS Biol*ogy, 7, e1000178.

O'Connor, M.P., Kemp, S.J., Agosta, S.J., Hansen, F., Sieg, A.E. & Wallace, B.P. (2007). Reconsidering the mechanistic basis of the metabolic theory of ecology. *Oikos*, 116, 1058–1072.

Odum, H.T. & Odum, E.P. (1955). Trophic structure and productivity of a windward coral reef community on Eniwetok Atoll. *Ecological Monographs*, 25, 291–320.

Peters, R.H. (1983). *The ecological implications of body size*. Cambridge University Press, Cambridge, pp. 329.

Pörtner, H.O. & Knust, R. (2007). Climate change affects marine fishes through the oxygen limitation of thermal tolerance. *Science*, 315, 95–97.

Rezende, E.L., Castañeda, L.E. & Santos, M. (2014). Tolerance landscapes in thermal ecology. *Functional Ecology*, 28, 799–809.

Rummer, J.L., Couturier, C.S., Stecyk, J.A.W., Gardiner, N.M., Kinch, J.P., Nilsson, G.E. *et al.* (2014). Life on the edge: thermal optima for aerobic scope of equatorial reef fishes are close to current day temperatures. *Global Change Biology*, 20, 1055–1066.

Sadovy, Y. (2005). Trouble on the reef: the imperative for managing vulnerable and valuable fisheries. *Fish and Fisheries*, 6, 167–185.

Savage, V.M., Gillooly, J.F., Woodruff, W.H., West, G.B., Allen, A.P. & Enquist, B.J. (2004). The predominance of quarter-power scaling in biology. *Functional Ecology*, 18, 257–282.

Schmidt-Nielsen, K. (1984). *Scaling: Why is animal size so important?* Cambridge University Press, Cambridge, pp. 256.

Schoolfield, R., Sharpe, P. & Magnuson, C. (1981). Non-linear regression of biological temperature-dependent rate models based on absolute reaction-rate theory. *Journal of Theoretical Biology*, 88, 719–731.

Tilman, D., HilleRisLambers, J., Harpole, S., Dybzinski, R., Fargione, J., Clark, C. *et al.* (2004). Does metabolic theory apply to community ecology? It's a matter of scale. *Ecology*, 85, 1797–1799.

Trebilco, R., Baum, J.K., Salomon, A.K. & Dulvy, N.K. (2013). Ecosystem ecology: size-based constraints on the pyramids of life. *Trends in Ecology & Evolution*, 28, 423–431.

Ward-Paige, C., Mills Flemming J. & Lotze H.K. (2010). Overestimating Fish Counts by Non-Instantaneous Visual Censuses: Consequences for Population and Community Descriptions. *PLoS ONE*, 5, e11722.

Yvon-Durocher, G. & Allen, A.P. (2012). Linking community size structure and ecosystem functioning using metabolic theory. *Philosophical Transactions of the Royal Society B: Biological Sciences*, 367, 2998–3007.

Yvon-Durocher, G., Caffrey, J.M., Cescatti, A., Dossena, M., Giorgio, P. del, Gasol, J.M. *et al.* (2012). Reconciling the temperature dependence of respiration across timescales and ecosystem types. *Nature*, 487, 472–476.

APPENDIX I

SUPPLEMENTARY INFORMATION:

SCALING METABOLISM FROM INDIVIDUALS TO REEF-FISH COMMUNITIES AT BROAD SPATIAL SCALES

1 INDIVIDUAL-LEVEL ANALYSES

1.1 Data sources

Our analysis of routine metabolic rates was performed using 2,036 measurements taken from 207 species and 43 families (Table AI.1). The majority of these data (1,918 measurements) were obtained by downloading data (March 2015) from FishBase (Froese & Pauly 2012). FishBase includes routine and standard metabolic-rate measurements from > 400 studies (http://www.fishbase.org/manual/English/PDF/ FB_Book_ATorres_Oxygen_11Jul11.pdf). In these studies, metabolic rates are generally measured by placing fish into aquaria and measuring gas exchanges in respirometry chambers. The majority of these measurements were originally assembled by Thurston & Gehrke (Thurston & Gehrke 1993) in the OXYREF database, which includes data from studies published between 1969 and 1986 (http://sdi.odu.edu/mbin/oxyref/ dos/oxyref_manual.pdf). This dataset contains only primary data from studies that report all of the following: species identity, sample size, fish weight and temperature, activity level, and oxygen consumption. To increase the number of reef-fish species included in our analysis, we compiled additional data (118 measurements from 33 species and 6 families) from 15 recent studies (data table available at http://onlinelibrary.wiley.com/doi/10.1111/ele.12309/suppinfo). The metabolic-rate measurements were converted from units of mass-specific O_2 uptake (mg O_2 kg^{-1} body mass h^{-1}) to daily rates of whole-organism carbon flux, B_i (g C d^{-1}), using estimates of wet mass, M_i (g), assuming a respiratory quotient of 1, implying that 1 mg O_2 kg^{-1} body mass h^{-1} = 0.009 g C kg^{-1} body mass d^{-1}.

Table AI.1. Summary table of metabolic-rate data used in the present study. Taxonomy follows FishBase (Froese & Pauly 2012).

Family	Species	Observations
Acipenseridae	*Acipenser gueldenstaedtii*	8
	Acipenser nudiventris	1
	Acipenser ruthenus	4
	Acipenser stellatus	22
Anguillidae	*Anguilla anguilla*	28
	Anguilla australis australis	1
	Anguilla japonica	1
	Anguilla rostrata	9
Bagridae	*Mystus armatus*	2
	Mystus gulio	1
	Mystus vittatus	51
Bathylagidae	*Bathylagoides wesethi*	1
	Bathylagus antarcticus	1
	Leuroglossus stilbius	1
	Lipolagus ochotensis	1
	Pseudobathylagus milleri	1
Callionymidae	*Callionymus lyra*	5
Catostomidae	*Catostomus commersonii*	2
	Catostomus tahoensis	3
	Erimyzon oblongus	1
Centrarchidae	*Lepomis cyanellus*	3
	Lepomis gibbosus	7
	Lepomis macrochirus	70
	Micropterus salmoides	16
	Pomoxis annularis	1
Channichthyidae	*Chaenocephalus aceratus*	3
	Channichthys rhinoceratus	2
	Pagetopsis macropterus	1
	Pseudochaenichthys georgianus	2
Cichlidae	*Andinoacara pulcher*	1
	Cichlasoma bimaculatum	8
	Hemichromis bimaculatus	1
	Oreochromis aureus	1
	Oreochromis mossambicus	126
	Oreochromis niloticus	12
	Pterophyllum scalare	31
	Sarotherodon galilaeus	1
	Thorichthys meeki	2

Table AI.1. (continued)

Family	Species	Observations
Cichlidae	*Tilapia rendalli*	3
	Tilapia zillii	17
Clupeidae	*Brevoortia tyrannus*	18
	Dorosoma cepedianum	48
	Gilchristella aestuaria	20
Congridae	*Conger conger*	5
Cottidae	*Clinocottus analis*	1
	Cottus gobio	1
	Myoxocephalus octodecemspinosus	16
	Myoxocephalus scorpius	4
Cyprinidae	*Abramis brama*	40
	Alburnus alburnus	4
	Campostoma anomalum	1
	Carassius auratus	52
	Carassius carassius	16
	Cirrhinus cirrhosus	65
	Ctenopharyngodon idella	5
	Cyprinus carpio	64
	Esomus danricus	20
	Gobio gobio	6
	Labeo calbasu	8
	Labeo capensis	41
	Labeo rohita	4
	Labeobarbus aeneus	28
	Leucaspius delineatus	1
	Leuciscus idus	7
	Leuciscus leuciscus	1
	Pimephales promelas	3
	Rhodeus amarus	1
	Rhodeus sericeus	3
	Rutilus rutilus	11
	Scardinius erythrophthalmus	1
	Squalius cephalus	4
	Tinca tinca	12
Cyprinodontidae	*Aphanius dispar dispar*	5
	Cyprinodon variegatus variegatus	14
Esocidae	*Esox lucius*	8
	Esox masquinongy	9
Fundulidae	*Fundulus grandis*	18
	Fundulus heteroclitus	18

Table AI.1. (continued)

Family	Species	Observations
Fundulidae	*Fundulus parvipinnis*	10
	Fundulus similis	18
Gadidae	*Boreogadus saida*	6
	Gadus morhua	34
	Gadus ogac	1
	Pollachius pollachius	2
	Theragra chalcogramma	23
Gasterosteidae	*Gasterosteus aculeatus*	22
	Spinachia spinachia	2
Gobiidae	*Amblygobius phalaena*	1
	Amblygobius rainfordi	3
	Asteropteryx semipunctatus	1
	Gillichthys mirabilis	54
	Glossogobius giuris	18
	Gobiodon acicularis	1
	Gobiodon axillaris	1
	Gobiodon ceramensis	1
	Gobiodon erythrospilus	1
	Gobiodon histrio	2
	Gobiodon okinawae	1
	Gobiodon unicolor	1
	Gobius paganellus	1
	Oligolepis acutipennis	12
	Paragobiodon xanthosomus	1
	Rhinogobiops nicholsii	9
	Typhlogobius californiensis	17
	Valenciennea strigata	1
Haemulidae	*Pomadasys commersonnii*	30
Heteropneustidae	*Heteropneustes fossilis*	11
Ictaluridae	*Ameiurus melas*	1
	Ameiurus natalis	6
	Ameiurus nebulosus	8
	Ictalurus punctatus	3
Labridae	*Halichoeres melanurus*	1
	Labroides dimidiatus	1
	Labrus bergylta	4
	Tautogolabrus adspersus	2
Lutjanidae	*Lutjanus campechanus*	2
	Lutjanus griseus	4
Mastacembelidae	*Macrognathus aculeatus*	31

Table AI.1. (continued)

Family	Species	Observations
Melamphaidae	*Melamphaes acanthomus*	2
	Poromitra crassiceps	2
	Scopelogadus mizolepis	1
Mugilidae	*Chelon macrolepis*	1
	Liza dumerili	45
	Liza richardsonii	22
	Mugil cephalus	35
	Mugil curema	4
Myctophidae	*Diaphus theta*	2
	Electrona antarctica	1
	Gymnoscopelus braueri	1
	Gymnoscopelus opisthopterus	1
	Nannobrachium regale	1
	Nannobrachium ritteri	2
	Parvilux ingens	1
	Stenobrachius leucopsarus	2
	Symbolophorus californiensis	1
	Tarletonbeania crenularis	2
	Triphoturus mexicanus	2
Nototheniidae	*Gobionotothen gibberifrons*	1
	Notothenia coriiceps	3
	Notothenia cyanobrancha	1
	Notothenia rossii	12
	Pagothenia borchgrevinki	1
	Paranotothenia magellanica	2
	Trematomus bernacchii	1
	Trematomus hansoni	1
	Trematomus pennellii	1
Percidae	*Etheostoma blennioides*	1
	Gymnocephalus cernua	2
	Perca fluviatilis	17
	Sander vitreus	12
Petromyzontidae	*Ichthyomyzon fossor*	1
	Lampetra fluviatilis	1
	Petromyzon marinus	3
Pleuronectidae	*Limanda limanda*	1
	Parophrys vetulus	1
	Platichthys stellatus	1
	Pleuronectes platessa	10
	Pseudopleuronectes americanus	12

Table AI.1. (continued)

Family	Species	Observations
Poeciliidae	*Gambusia affinis*	9
	Gambusia holbrooki	16
	Poecilia latipinna	14
	Xiphophorus hellerii	3
Pomacentridae	*Acanthochromis polyacanthus*	4
	Chromis atripectoralis	4
	Chromis chromis	4
	Chromis viridis	1
	Chrysiptera flavipinnis	1
	Dascyllus aruanus	1
	Neoglyphidodon melas	1
	Neoglyphidodon nigroris	1
	Neopomacentrus azysron	1
	Pomacentrus ambionensis	4
	Pomacentrus bankanensis	1
	Pomacentrus coelestis	1
	Pomacentrus lepidogenys	1
	Pomacentrus moluccensis	1
	Pomacentrus philippinus	2
Salmonidae	*Coregonus autumnalis*	3
	Coregonus fera	2
	Coregonus sardinella	3
	Oncorhynchus mykiss	66
	Oncorhynchus nerka	6
	Oncorhynchus tshawytscha	1
	Salmo salar	15
	Salmo trutta	34
	Salvelinus fontinalis	1
Scorpaenidae	*Caracanthus unipinna*	1
	Parascorpaena mossambica	1
	Scorpaena porcus	2
	Sebastapistes cyanostigma	1
Scyliorhinidae	*Scyliorhinus canicula*	2
	Scyliorhinus stellaris	7
Serrasalmidae	*Colossoma macropomum*	80
Sparidae	*Acanthopagrus schlegelii*	21
	Diplodus sargus sargus	2
	Lagodon rhomboides	14
	Sparus aurata	2
Sphyrnidae	*Sphyrna lewini*	70

Table AI.1. (continued)

Family	Species	Observations
Stomiidae	*Aristostomias lunifer*	1
	Borostomias panamensis	2
	Stomias atriventer	1
	Stomias danae	1
Syngnathidae	*Hippocampus hippocampus*	5
	Syngnathus acus	2
Zoarcidae	*Lycodichthys dearborni*	15
	Melanostigma gelatinosum	1
	Zoarces viviparus	8

1.2 Model selection and fitting

A parsimonious model was constructed by evaluating the significance of optimum temperature — both fixed (T_{opt}) and random effects (ΔT_{opt}) — thermal regime (as fixed effect E_a), and temperature inactivation (as fixed effect E_i) (Table AI.2), based on likelihood ratio tests of significance ($P < 0.05$) (Zuur *et al.* 2009). Random-effects were characterised at the family level in order to increase statistical power in our analysis, particularly with respect to the estimation of temperature optimum. We also tested the robustness of the parsimonious model using species-level random effects; however, none of the models converged on the parameters estimates – this most likely occurred because most species had only a few observations (Table AI.1). We selected significant parameters using a top-down approach in which model complexity was successively reduced, first by dropping random-effect terms, and then by dropping fixed-effect terms (Zuur *et al.* 2009; Table AI.2). The parsimonious model was constructed using the package *lme4* version 1.1-8 (Bates *et al.* 2015) in R version 3.1.3 (R Core Team 2015) based on restricted maximum likelihood (REML) for random-effects selection and maximum likelihood (ML) for fixed-effects selection (Table AI.2), as recommended by Zuur *et al.* (2009) (R code available at https://github.com/dbarneche/ELEBarneche). We note that the variances of random effects do not have precisely

one degree of freedom, which may affect absolute estimates of their significance. However, this issue will not affect the structure of the final model given the high significance of our random effects (Table AI.2).

We assessed the goodness of fit for the parsimonious model (Fig. AI.1), which was then refitted using a Bayesian procedure by calling *JAGS* version 3.4.0 from the R package *R2jags* version 0.05-03 (Su & Yajima 2015) in order to derive posterior distributions and associated 95% credible intervals (CIs) for the fitted parameters (Table 1.1 in Chapter 1). The maximum likelihood estimates of the fitted parameters in *lme4* were very similar to the independently estimated averages of the posterior distributions of the fitted parameters in *JAGS* (Table AI.3, Fig. AI.2). Although this similarity was expected given that the fitted parameters were assigned priors that were vague (i.e. locally uniform over the region supported by the likelihood) in the Bayesian analysis (Kruschke 2014), it increases our overall confidence that model convergence was achieved. In both *JAGS* and *lme4*, rather than estimate E_r directly, we instead estimated the transformed quantity E_r', where $E_r = E_i \,/\, (1 + e^{-E_r'})$, to ensure convergence based on the assumption that T_{opt} exists, which requires that $E_i > E_r$ (Tables AI.3–AI.4). In *JAGS*, posterior distributions of model parameters were estimated using Markov chain Monte Carlo (MCMC) methods by constructing three chains of 1,000,000 steps each, including 500,000-step burn-in periods. Chains were thinned using a 250-step interval, so a total of 6,000 steps were retained to estimate posterior distributions (i.e. 3 × (1,000,000 - 500,000)/250 = 6,000). Correlation between fixed effects and analyses of traces in *JAGS* are also presented (Figs. AI.3–AI.4).

Table AI.2. The parsimonious model was constructed, using the R package *lme4*, in a two-stage procedure by successively removing non-significant random effects, followed by fixed effects, based on likelihood ratio tests of significance (Zuur *et al.* 2009). The full model contained the following fixed-effects terms: α, family-level average for size scaling; E_r', family-level average for temperature activation; $\ln\overline{b_o(T_c)}$, size- and temperature-corrected metabolic rate at T_c = 293.15 K = 20°C; E_a, variation in the size- and temperature-corrected metabolic rate attributable to adaptation to average temperature regime for a family; T_{opt}, family-level average for the temperature optimum; and E_i, inactivation parameter describing the steepness of decline with increasing temperature beyond T_{opt}. The full model also included family-level deviations for body size scaling ($\Delta\alpha$), temperature activation (ΔE_r'), the size- and temperature-corrected rate ($\Delta\ln\overline{b_o(T_c)}$), and the temperature optimum (ΔT_{opt}). In the table, χ^2 and d.f. refer to likelihood ratio test between the full model and nested model. The final parsimonious model (F2), which includes all parameters but the adaptation parameter, is indicated in bold.

Model		**d.f.**	$\boldsymbol{\chi^2}$	***P***
	Stage 1			
R1	**Full**			
R2	Full $-\Delta T_{opt}$	4	11.21	0.024
	Stage 2			
F1	Full			
F2	**Full** $\boldsymbol{-E_a}$	**1**	**1.98**	**0.160**
F3	Full $-E_i - T_{opt} - \Delta T_{opt}$	6	20.06	0.003
F4	F2 $-E_i - T_{opt} - \Delta T_{opt}$	6	21.98	0.001

Table AI.3. Average estimates and standard errors (as determined using restricted maximum likelihood in the R package *lme4*) for fitted parameters in the parsimonious model. When fitting the model, rather than estimate E_r directly, we instead estimated the transformed quantity E_r', where $E_r = E_i \,/\, (1 + e^{-E_r'})$, to ensure convergence based on the assumption that T_{opt} exists, which requires that $E_i > E_r$. Alternative estimates of parameters, as calculated using MCMC in *JAGS*, are reported in the main text (Table 1.1 in Chapter 1). Estimates obtained using the two approaches are statistically indistinguishable (see Fig. AI.2 below). Fixed-effect parameters include: α, the (family-level) average for the mass-dependence of metabolic rate; E_r', the average for the temperature dependence of metabolic rate; $\ln\overline{b_o(T_c)}$, the average for the size-corrected metabolic rate at temperature T_c = 20°C; T_{opt}, the average for the temperature optimum; and E_i, the inactivation parameter describing the steepness of decline with increasing temperature beyond T_{opt}. Random-effects parameters include standard deviations for family-level variation in size dependence ($\Delta\alpha$), temperature dependence (ΔE_r'), size-corrected rates at T_c ($\Delta\ln\overline{b_o(T_c)}$) and the temperature optimum (ΔT_{opt}) (see Table AI.2 above).

Parameter	**Estimate**	**Standard Error**	**t value**
Fixed effects			
Size, α	0.765	0.033	23.111
Activation energy, E_r' (eV)	-1.291	0.309	-4.185
Normalisation, $\ln\overline{b_o(T_c)}$ (g C g$^{-\alpha}$ d^{-1})	-5.82	0.091	-64.178
Temperature optimum, T_{opt} (K)	303.62	0.695	436.681
Deactivation energy, E_i (eV)	2.506	0.437	5.738
Random effects (representing differences between families)			
Standard deviation of $\Delta\alpha$	0.189	-	-
Standard deviation of $\Delta E_r'$	0.733	-	-
Standard deviation of $\Delta\ln b_o(T_c)$	0.46	-	-
Standard deviation of T_{opt}	0.77	-	-
Covariance of $\Delta\alpha$ and $\Delta E_r'$	0.311	-	-
Covariance of $\Delta\alpha$ and $\Delta\ln\overline{b_o(T_c)}$	-0.575	-	-
Covariance of $\Delta\alpha$ and T_{opt}	0.057	-	-
Covariance of $\Delta E_r'$ and $\Delta\ln\overline{b_o(T_c)}$	-0.399	-	-
Covariance of $\Delta E_r'$ and T_{opt}	0.097	-	-
Covariance of $\Delta\ln\overline{b_o(T_c)}$ and T_{opt}	-0.005	-	-

Table AI.4. Average estimates and 95% credible intervals (of Bayesian posterior distributions) for fitted parameters in the parsimonious model (model F2 in Table AI.2). When fitting the model, rather than estimate E_r directly, we instead estimated the transformed quantity E_r', where $E_r = E_i \,/\, (1 + e^{-E_r'})$, to ensure convergence based on the assumption that T_{opt} exists, which requires that $E_i > E_r$. Fixed-effect parameters include: α, the (family-level) average for the mass-dependence of metabolic rate; E_r', the average for the temperature dependence of metabolic rate; $\ln\overline{b_o(T_c)}$, the average for the size-corrected metabolic rate at temperature T_c = 20°C; T_{opt}, the average for the temperature optimum; and E_i, the inactivation parameter describing the steepness of decline with increasing temperature beyond T_{opt}. Random-effects parameters include standard deviations for family-level variation in size dependence ($\Delta\alpha$), temperature dependence ($\Delta E_r'$), size-corrected rates at T_c ($\Delta\ln\overline{b_o(T_c)}$) and the temperature optimum (ΔT_{opt}), as well as associated covariance terms for these random effects.

Parameter	**Estimate**	**2.5% CI**	**97.5% CI**
Fixed effects			
Size, α	0.758	0.674	0.842
Activation energy, E_r' (eV)	-0.786	-1.738	0.783
Normalisation, $\ln\overline{b_o(T_c)}$ (g C $g^{-\alpha}$ d^{-1})	-5.709	-5.967	-5.249
Temperature optimum, T_{opt} (K)	306.263	301.789	313.923
Inactivation energy, E_i (eV)	2.020	1.240	3.115
Random effects (representing differences between families)			
Variance of $\Delta\alpha$	0.064	0.040	0.100
Variance of $\Delta E_r'$	0.378	0.154	0.849
Variance of $\Delta\ln\overline{b_o(T_c)}$	0.339	0.174	0.672
Variance of T_{opt}	44.821	6.951	123.025
Covariance of $\Delta\alpha$ and $\Delta E_r'$	0.036	-0.022	0.108
Covariance of $\Delta\alpha$ and $\Delta\ln\overline{b_o(T_c)}$	-0.055	-0.123	-0.007
Covariance of $\Delta\alpha$ and T_{opt}	0.092	-0.721	0.924
Covariance of $\Delta E_r'$ and $\Delta\ln\overline{b_o(T_c)}$	-0.078	-0.260	0.117
Covariance of $\Delta E_r'$ and T_{opt}	0.009	-3.912	3.417
Covariance of $\Delta\ln\overline{b_o(T_c)}$ and T_{opt}	-1.849	-6.361	0.585

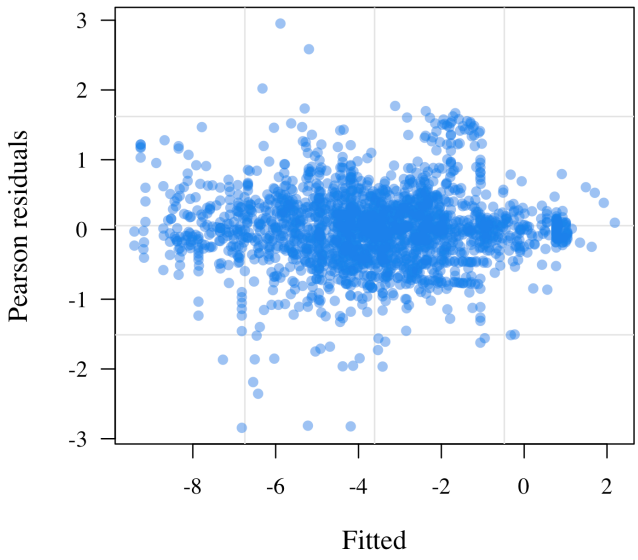

Figure AI.1. Pearson residual plot assessing the goodness of fit of the parsimonious model as fitted in *lme4* (see Table AI.3 for parameter estimates).

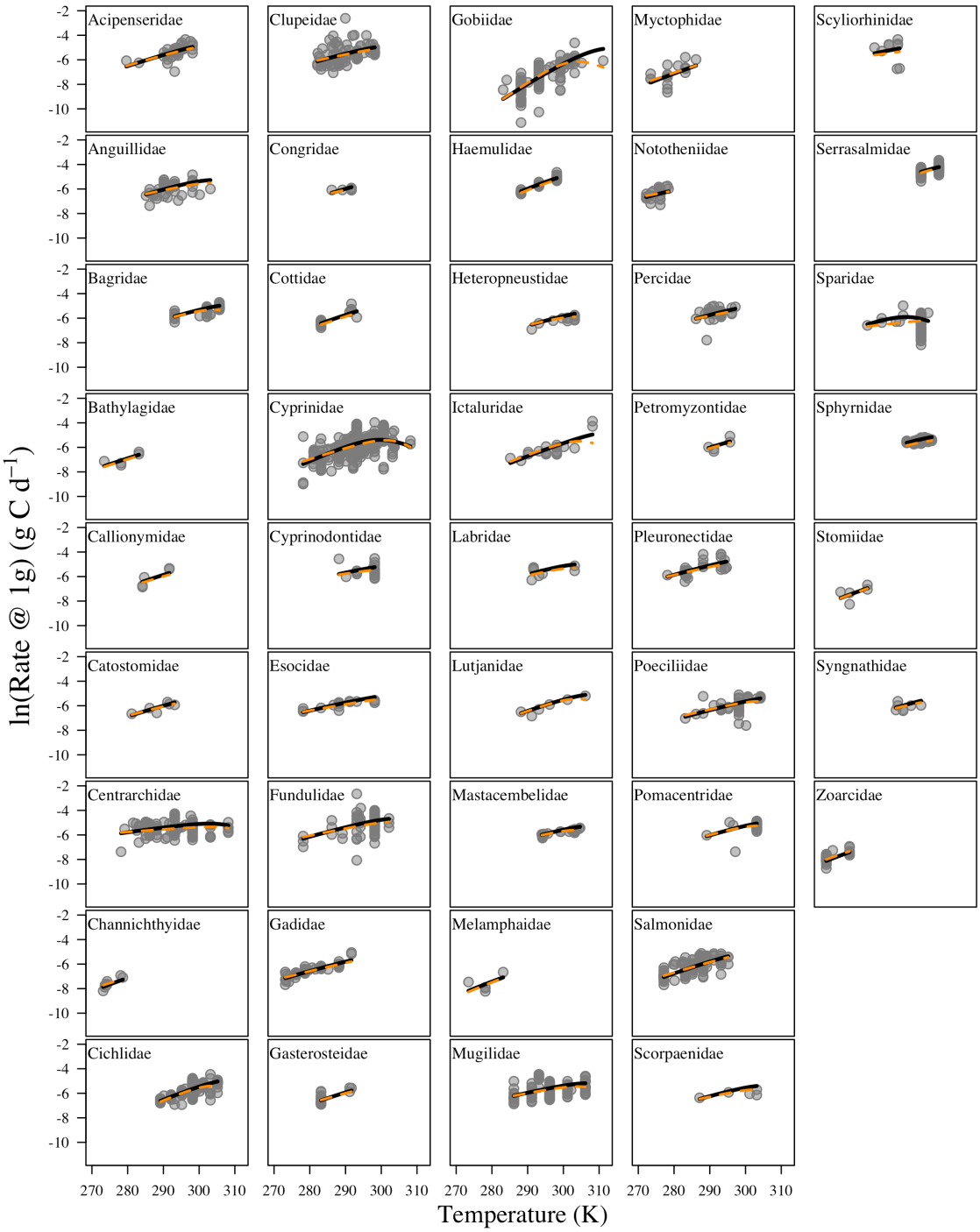

Figure AI.2. Temperature scaling of size-corrected routine rates for each of the families included in our analysis. Lines represent family-level fits obtained from *JAGS* (solid black lines, Table AI.4) and *lme4* (dashed orange, Table AI.3) for the parsimonious metabolic rate model. As shown in the figure, parameter estimates from *JAGS* and *lme4* are in most cases virtually identical.

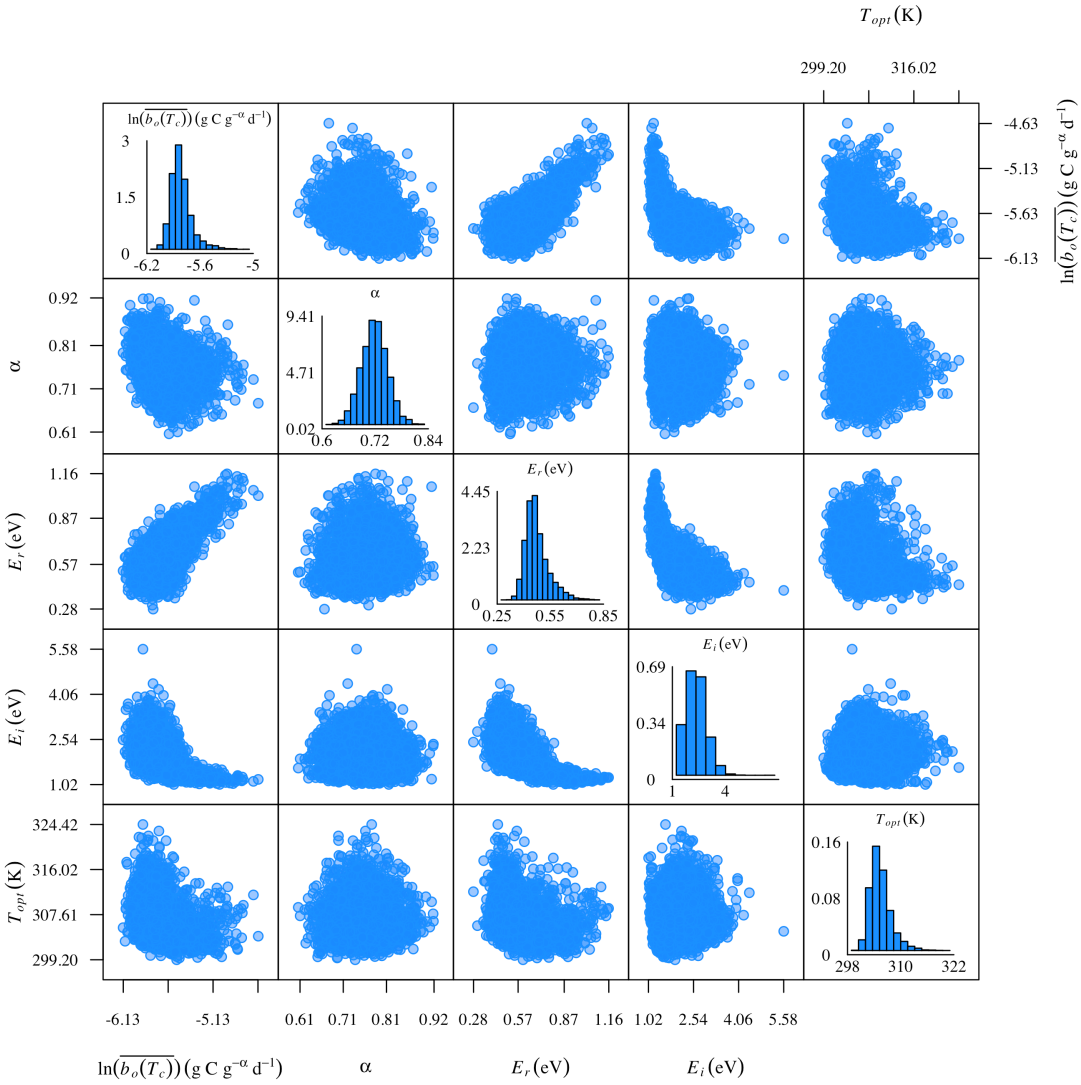

Figure AI.3. Bivariate relationships among fixed effects for the parsimonious routine metabolic rate model (Table AI.4). Blue circle represents parameter estimates for the 6,000 MCMC steps that were retained to estimate posterior distributions (see Fig. AI.4 for the traces) using *JAGS*.

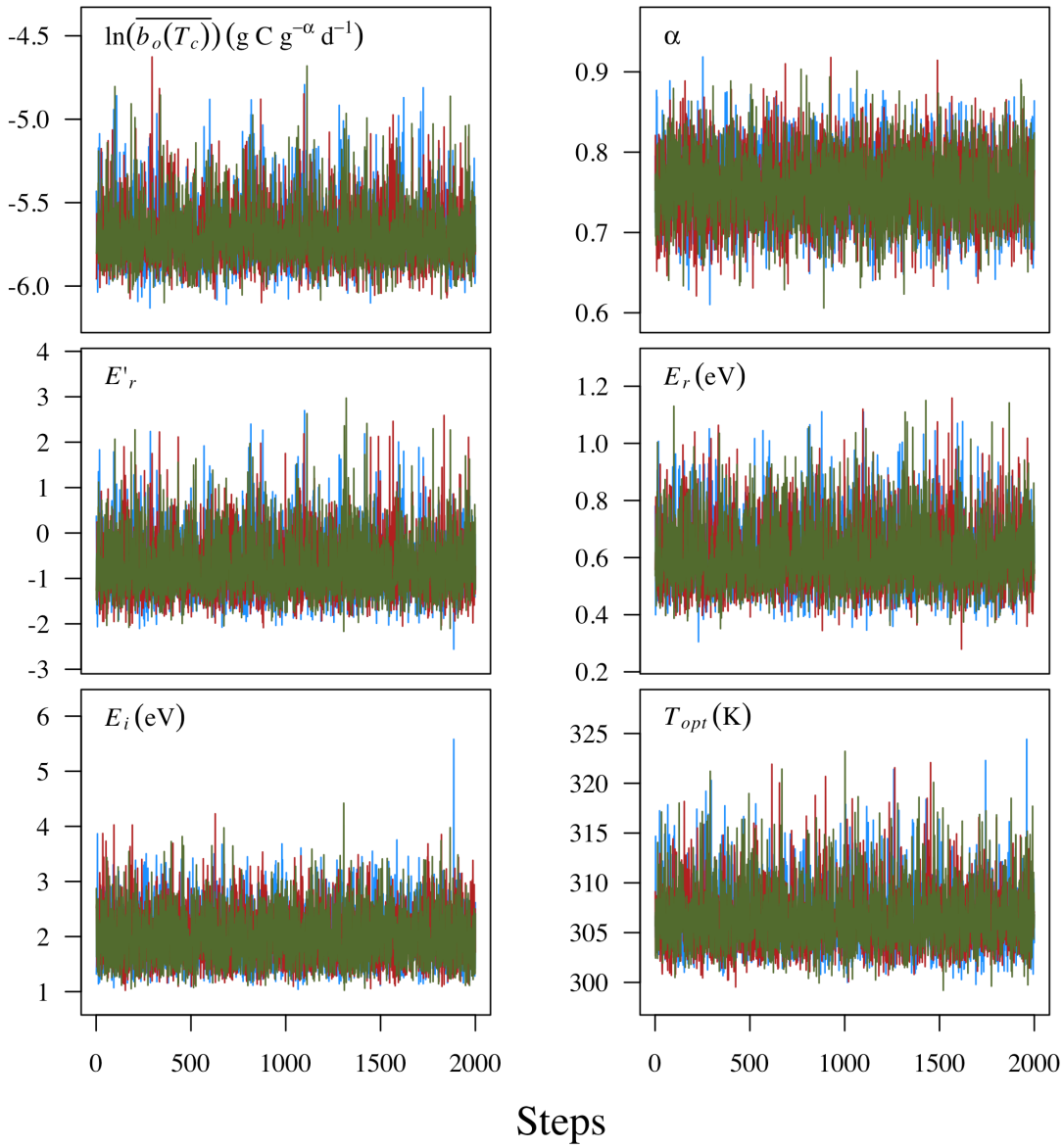

Figure AI.4. Trace analysis of fixed-effect parameters (with units in parentheses) for the parsimonious routine metabolic rate model (Table AI.4). Each MCMC chain is represented by a different colour (3 chains, 2,000 iterations each, for a total of 6,000 iterations). Model fitting in *JAGS* involved the construction of 3 MCMC chains of 1,000,000 iterations each, including initial 500,000-iteration burn-in periods. Chains were thinned by a factor of 250, so 6,000 steps were retained to estimate the posterior distributions of model parameters (i.e. 3 × (1,000,000 - 500,000)/250 = 6,000).

1.3 Characterising the temperature dependence

We characterise temperature dependence using a modified version of the Sharpe-Schoolfield formulation (Schoolfield *et al.* 1981). Our temperature expression (eqns 2–3 of Chapter 1)

differs in two substantive ways from the original formulation. First, we exclude from eqn 2 parameters used to characterise low-temperature inactivation due to insufficient data to quantify this phenomenon in our analysis. Second, rather than characterise temperature effects below T_{opt} using the Eyring relation, $(T/T_c)e^{E_r\left(\frac{1}{kT_c} - \frac{1}{kT}\right)}$, we instead use the simpler Boltzmann relation, $e^{E_r\left(\frac{1}{kT_c} - \frac{1}{kT}\right)}$, consistent with previous MTE work. This simplification facilitates expressing temperature dependence explicitly in terms of T_{opt}, and has negligible effects on model predictions ($\pm$ 6%) over the temperature range 0 to 30 ˚C (i.e. 273/288 to 303/288).

Our analysis indicates that the fitted Schoolfield model (Tables AI.3–AI.4), which incorporates temperature optima, provides a significantly better fit than the Boltzmann relationship (model F3 in Table AI.2; see Fig. AI.5), as indicated by the significant improvement in model fit (Table AI.2). Our mixed-effects modelling procedure yields a distinct estimate for the temperature optimum for each of the 43 families included in our analysis (Fig. AI.2), but clear evidence of an optimum is observed for only a subset of families with data that span a wide temperature range (e.g. Centrarchidae, Cyprinidae, Sparidae).

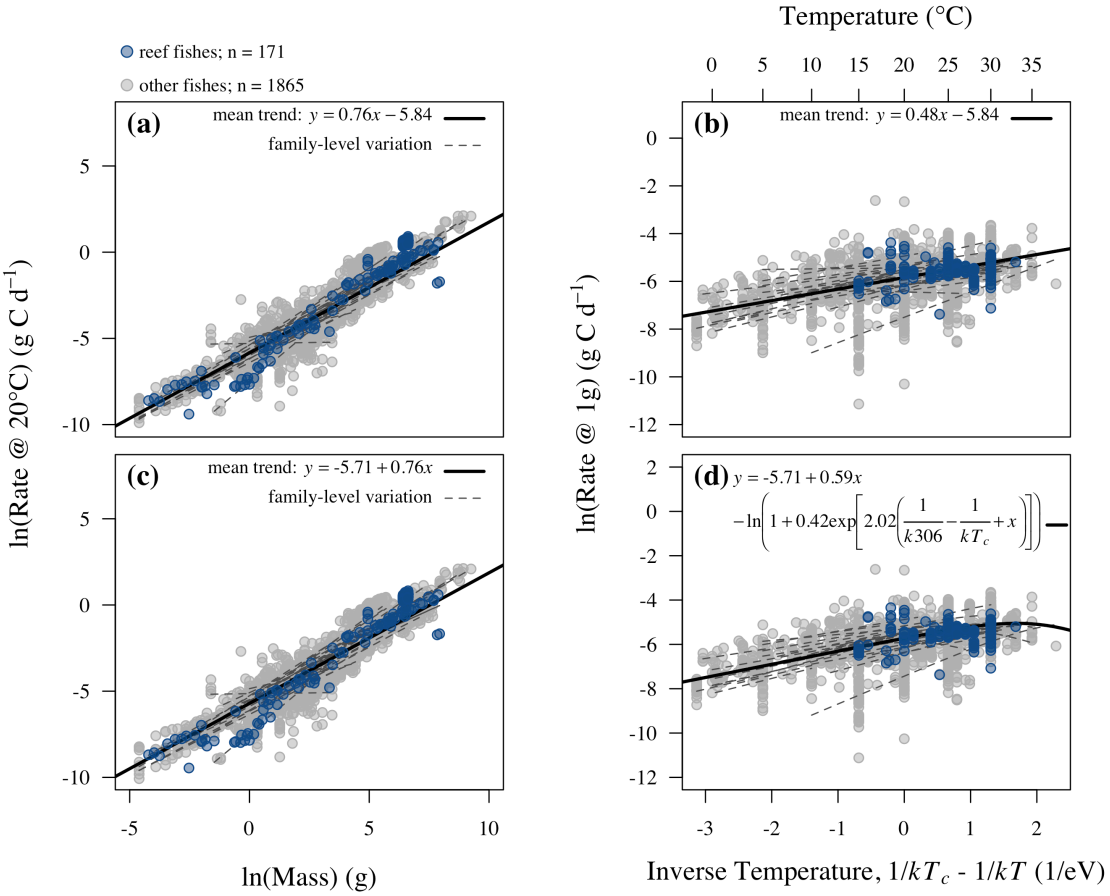

Figure AI.5. Comparison of model fits to routine metabolic rate data, assuming (a, b) the Boltzmann relationship and (a, c) the modified Schoolfield equation (eqns 2–3). The fitted lines correspond to estimates obtained from *JAGS*. The data and model depicted in panels (c) and (d), which are included here for comparison, are identical to Fig. 1.2 of Chapter 1.

1.4 Analysis of standard rates

Our analysis focuses on routine metabolic rates (rather than standard rates) because this rate corresponds more closely to energy expenditure by a fish under field conditions. Nevertheless, analyses of standard-rate data serve as a useful independent means of assessing the robustness of the size- and temperature-scaling relationships identified in Chapter 1. These analyses yield nearly identical parameter estimates (as estimated using *lme4*) that overlap with those of the routine-metabolic rate model (Table AI.3): α = 0.75, (95% CIs: 0.73–0.77), activation energy E_r = 0.62 eV (0.37–0.96 eV) and inactivation energy E_i = 2.53 eV (1.46–3.60 eV). Finally, and perhaps most importantly, these data yield further evidence

of an average temperature optimum at ~33 ˚C (T_{opt} = 34˚C, 95%CI: 32 to 37 ˚C) (Fig. AI.6). Thus, overall, these additional analyses provide additional support for the scaling relationships documented in the main text. The estimated size- and temperature-corrected rate, $\ln\overline{b_o(T_c)}$, is significantly lower for the standard metabolic-rate model ($\ln\overline{b_o(T_c)}$ = -6.21 g C $g^{-\alpha}$ d^{-1}, 95% CIs: -6.28, -6.13) than for the routine metabolic-rate model, consistent with theoretical expectations (Savage *et al.* 2004).

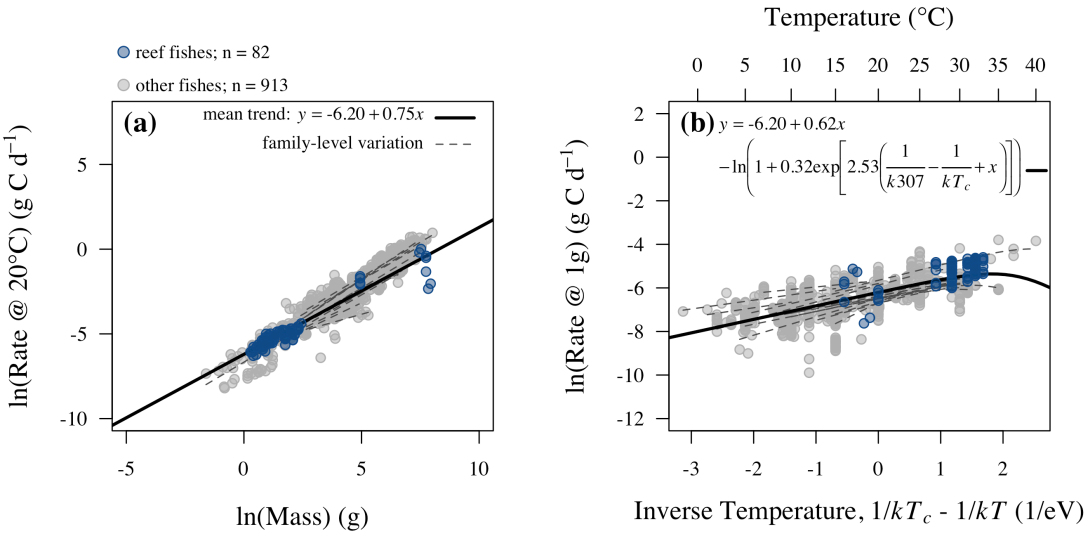

Figure AI.6. (a) Size scaling and (b) temperature scaling of standard metabolic rates in fish. The model depicted in the figure was identical in structure (in terms of fixed effects and random effects attributable to family) to the parsimonious metabolic rate model in Table 1.1 of Chapter 1. For graphing, data have been temperature corrected (in a) and size corrected (in b) based on the size-temperature scaling relationships inferred from the model. Analyses were performed using standard metabolic rate measurements in FishBase that were taken from non-stressed individuals (924 measurements, 17 families, and 64 species), along with additional data from reef fishes (71 measurements, 2 families, and 13 species). As with the routine metabolic rate analysis, the analysis here was restricted to families with 5 or more measurements taken over at least a 5 ˚C temperature range.

2 COMMUNITY-LEVEL ANALYSES

2.1 Reef-fish community structure dataset

We evaluated Hypotheses H4–H5 of Chapter 1 using community-level reef-fish data collected from 49 sites (islands, atolls and coastal contiguous reefs), including 14 sites in the South-western Atlantic (SWA) and its oceanic islands (SWO), 1 site in the Caribbean (CAR), 2 sites in the Tropical Eastern Atlantic (TEA), 1 site in the Tropical Eastern Pacific (TEP), 4 sites in the Central Pacific (CP), 2 sites in the South-eastern Pacific (SEP), and 25 sites in the South Pacific (SP) (Floeter *et al.* 2007; Friedlander *et al.* 2007a, 2007b, 2012, 2013; MacNeil *et al.* 2009; Preuss *et al.* 2009; Chabanet *et al.* 2010; Bozec *et al.* 2011; Carassou *et al.* 2012) (Table AI.5).

The first four authors, together with colleagues, collected these data using standardised belt transects of varying length and width in SWA, SWO and TEA (20 × 2 m), TEP (25 × 2 m and 50 × 2 m), SEP (25 × 2 m and 50 × 2 m), CAR (50 × 2 m), CP (25 × 5 m) and SP (50 × 4 m, 25 × 2 m and 50 × 2 m). Samples were collected by swimming ~1.5 m above the reef substrate, at fixed transect depths of < 30 m, and recording all fish observed at or below the depth of the observer that fell within the transect area. Highly mobile families such as carangids were also counted. This method is expected to yield accurate estimates of overall reef-fish density given that reef fishes are generally sedentary and remain closely associated with the reef substrate (Floeter *et al.* 2007; Chabanet *et al.* 2010). We only included transects conducted over consolidated hard-reef bottoms to allow direct comparisons between rocky and coral reef sites. Divers tallied the numbers, species identities, and body lengths of all fish simultaneously for 42 of 49 sites. For the other seven sites (Astrolab Reefs and Beautemps-Beaupré Atoll in SP, Isla del Coco in TEP, Ducie Atoll, Henderson Island, Oeno Atoll, Pitcairn Island, Rapa Nui and Salaz y Gómez in SEP), divers first counted all fish

≥ 20 cm length in each 50 × 2 m transect, and then counted all fish < 20 cm length on the way back along the same transect line, but only over a distance of 25 m. Since data for the smaller individuals were only collected over half the transect area (25 × 2 m), counts of individuals < 20 cm length were doubled for abundance calculations for these seven sites.

Species were assigned to five trophic groups: 1) herbivores: fish feeding on turf or filamentous algae and/or undefined organic material and/or fleshy algae and/or seagrass); 2) omnivores: fish for which both plant and animal material are important; 3) planktivores: fish eating small organisms in the water column; 4) invertivores: fish targeting sessile (i.e. corals, sponges, ascidians), and/or mobile invertebrates (i.e. benthic species such as crustaceans). Some of these species may at times eat fish, but it accounts for < 50% of their diet at the species level; 5) piscivores: fish eating other fish and/or cephalopods. These fish may eat other diet items, but they account for < 50% of the diet at the species level. Categorisation was performed using information in the published literature, online databases (Randall 1967; Kulbicki *et al.* 2005a; Robertson & Allen 2008; Froese & Pauly 2012), and expert judgment.

Table AI.5. Sites sampled for the present study, with respective number of transects, recorded individuals, species, family and trophic levels richness. The coordinates shown were used to extract the mean annual temperature (SST) and pelagic net primary productivity (NPP) between 1997 and 2007.

Region	Country	Site	Longitude	Latitude	Average NPP (g C/m2/yr)	Average SST (°C)	Transects	Individuals	Species richness	Families	Herbivores	Omnivores	Invertivores	Piscivores	Planktivores
SWO	Brazil	St. Paul's Rocks	-29.3430	0.9188	149.6321	27.1807	177	11601	29	15	2	2	16	4	5
		Fernando de Noronha Archipelago	-32.3902	-3.8145	115.9242	27.3379	96	3841	52	29	7	3	26	10	6
		Rocas Atoll	-33.8036	-3.8752	114.2742	27.5001	156	11500	45	26	8	2	20	10	5
		Trindade & Martim Vaz Archipelago	-29.3296	-20.4920	80.1562	25.4476	486	26737	70	34	8	5	37	12	8
SWA		Risca do Meio	-38.3917	-3.5981	315.2976	27.8580	43	11585	64	29	9	1	43	7	4
		Parrachos de Maracajaú	-35.0393	-5.9562	95.5973	27.7491	68	6693	57	24	12	3	35	3	4
		Baía de Todos os Santos	-38.5518	-13.1371	220.5056	26.8348	222	6401	80	32	13	2	47	10	8
		Abrolhos Archipelago	-38.7110	-17.9574	309.9057	26.0471	161	6197	45	24	10	2	28	5	0
		Guarapari	-40.1442	-20.7212	382.7710	24.8583	317	7467	84	33	12	5	47	13	7
		Arraial do Cabo	-41.8620	-22.9519	365.7216	23.4925	640	19085	116	43	17	8	68	14	9
		Cagarras Archipelago	-43.1617	-23.1100	452.3744	23.7218	11	313	27	18	4	3	17	2	1
		Ilha Grande	-44.1272	-23.3396	373.4355	23.9692	105	2615	59	29	11	4	32	9	3
		Laje de Santos	-46.0672	-24.3457	362.7906	23.6144	72	4317	57	23	12	3	29	8	5
		Santa Catarina	-48.3638	-27.2906	783.3477	22.2183	633	20125	97	38	14	10	49	16	8
TEA	Cape Verde	Cape Verde	-24.7097	16.8139	363.6669	23.9216	198	29594	63	32	9	5	25	16	8
	São Tomé & Príncipe	São Tomé	6.9279	0.4199	258.4411	27.0868	138	12412	53	29	7	2	26	10	8
CAR	United States	US Virgin Islands	-64.7952	18.3221	112.8840	27.6752	318	12242	138	43	20	7	84	15	12
TEP	Costa Rica	Isla del Coco	-87.0429	5.4871	150.4738	27.5311	98	33869	84	36	7	10	35	23	9
CP	United States	Hawaii	-160.8186	19.4912	91.3064	26.0852	232	17375	132	29	23	17	56	20	16

Region	Country	Site	Longitude	Latitude	Average NPP (g C/m2/yr)	Average SST (°C)	Transects	Individuals	Species richness	Families	Herbivores	Omnivores	Invertivores	Piscivores	Planktivores
		Maui	-156.6668	20.9998	127.7537	25.6804	98	5378	122	30	18	17	52	20	15
		Lanai	-156.9341	20.7346	87.3954	25.9538	52	3105	97	22	18	15	42	12	10
		Oahu	-157.6953	21.2697	99.2407	25.5081	183	13924	126	30	24	18	56	17	11
SEP	Chile	Salaz y Gómez	-105.3603	-26.4754	58.4066	22.5187	58	2970	32	18	3	3	16	7	3
		Rapa Nui	-109.3931	-27.0610	61.4820	22.8397	49	4546	35	21	3	4	17	8	3
	United Kingdom	Ducie Atoll	-124.7710	-24.6750	47.0833	24.5102	62	2110	80	23	11	11	32	18	8
		Henderson Is.	-128.3000	-24.3290	48.2599	24.7360	77	4089	105	29	12	8	44	24	17
		Pitcairn Is.	-130.1140	-25.0590	54.1832	24.4139	63	2318	76	27	10	6	39	18	3
		Oeno Atoll	-130.7270	-23.9430	54.2674	24.8917	69	3956	111	25	16	13	49	19	14
SP	French Polynesia	Kauehi	-144.9724	-15.7814	125.6064	28.0008	31	4255	131	35	21	19	50	28	13
		Taiaro	-144.9097	-15.9558	96.9421	27.9912	4	387	26	11	3	9	9	3	2
		Hiti	-144.1178	-16.7025	80.0636	27.7630	14	522	65	18	4	16	30	9	6
		Nihiru	-142.8692	-16.7347	78.8506	27.7180	18	1686	84	22	14	15	34	10	11
		Tepoto	-144.2227	-16.8263	72.0872	27.7354	4	311	57	20	12	12	26	5	2
		Tekokota	-142.4823	-17.2866	70.2295	27.5750	19	1358	76	20	8	14	37	12	5
		Haraiki	-143.4525	-17.4511	65.4375	27.5835	7	1239	74	15	11	16	34	6	7
		Hikueru	-142.4888	-17.4905	111.8448	27.5393	23	2373	85	21	15	17	35	11	7
		Marokau	-142.3842	-18.0178	103.3975	27.4533	26	2811	111	27	18	20	42	18	13
	Tonga	Vava'u	-173.9323	-18.7908	124.3600	26.6139	52	5409	225	38	26	32	103	33	31
		Ha'apai	-175.2420	-19.7301	109.6200	26.4591	52	5027	191	35	21	28	89	32	21
		Tongatapu	-175.0632	-21.0301	302.2930	25.4995	94	12192	243	40	30	32	111	32	38
	Fiji	Vanua Levu	179.0546	-16.1632	156.9139	28.0983	66	11236	234	37	28	31	106	44	25
		Viti Levu	178.7283	-18.2244	208.6284	27.0302	52	5861	198	33	26	24	98	30	20
		Lakeba	178.7958	-18.4411	121.5803	26.9631	65	9016	220	34	30	31	95	39	25
	New Caledonia	E Lagoon	166.0836	-21.3187	230.1437	25.7935	96	20483	287	39	45	38	125	44	35

Region	Country	Site	Longitude	Latitude	Average NPP (g C/m2/yr)	Average SST (°C)	Transects	Individuals	Species richness	Families	Herbivores	Omnivores	Invertivores	Piscivores	Planktivores
		SW Lagoon	166.3503	-22.4483	136.8116	24.6057	556	65227	461	58	53	55	215	85	53
		W Lagoon	164.5745	-21.0508	128.8918	25.2692	71	8553	234	33	25	32	120	33	24
		Lifou	168.1517	-21.3815	130.5719	25.4439	26	2162	147	27	22	25	67	16	17
		Astrolab Reefs	165.8284	-19.8943	128.5678	26.0366	36	6577	183	26	23	20	78	28	34
		Beautemps-Beaupré Atoll	166.1606	-20.3981	132.9146	25.9417	20	2768	141	23	19	17	51	20	34

The lengths and species identities of all fish observed within the transect areas were estimated at 10-cm resolution for the 16 sites at SWA, SWO and TEA (length classes: 10–20 cm, 20–30 cm, etc.), and at 1-cm resolution for the 33 remaining sites. Wet weights of individuals were estimated from lengths using power-function length-weight conversion formulas compiled from the literature and online databases for each species (Kulbicki *et al.* 2005b; Froese & Pauly 2012). For species without published formulas, conversions were performed based on the formula of the phylogenetic and ecologically closest species available or a formula drawn from typical mass of an adult of a given genus.

Three procedures were implemented to ensure maximum consistency among sites in our calculations of size-corrected biomass. First, individuals with estimated lengths in the 0–10 cm size class (SWA, SWO and TEA), or with estimated lengths < 10 cm (remaining sites), were excluded from analyses. Second, for all sites, including the 33 sites where sizes were estimated at 1-cm resolution, size-corrected biomass was estimated using 10-cm resolution length estimates. Third, we conducted a sensitivity analysis to assess how differences among sites in length resolution affected our estimates of size-corrected community biomass (Table AI.6). Results of this sensitivity analysis indicated that errors in estimating $M_T\langle M_i^{\alpha-1}\rangle_T$ were minimised by assigning individuals to the geometric mean of 10-cm bins (e.g. all individuals in the 10–20 cm length range were assigned a value of $\sqrt{10 \times 20} = 14.14$ cm). Using this method of calculation, the average discrepancy in size-corrected biomass was only 7.21% for the community as a whole, and 2.58–19.42% for the separate trophic groups (14.70%, 9.42%, 19.42%, 9.56% and 2.58% for herbivores, omnivores, planktivores, invertivores, and piscivores respectively).

To perform the sensitivity analysis, we used the 1-cm resolution data to calculate five different estimates of size-corrected community biomass, $M_T\langle M_i^{\alpha-1}\rangle_T$, assuming α = 0.76: 1)

1-cm-resolution lengths (e.g. 17 cm); 2) arithmetic mean lengths in 10-cm-resolution bins, e.g. 17 cm is assigned a value of 15 cm in the 10–20 cm bin; 3) geometric mean lengths in 10-cm-resolution bins, e.g. all individuals in the 10–20 cm length range were assigned a value of $\sqrt{10 \times 20} = 14.14$ cm; 4) lower bounds of 10-cm-resolution bins, e.g. 17 cm is assigned a value of 10 cm; 5) upper bounds of 10-cm-resolution bins, e.g. 17 cm is assigned a value of 20 cm.

Table AI.6. Mean deviations (in percentages) in size-corrected biomass yielded by different length-averaging methods. Deviations are relative to the 1-cm-resolution data. The best method is highlighted in bold.

Method	**Mean deviation (%)**					
	Overall	**Herbivores**	**Omnivores**	**Planktivores**	**Invertivores**	**Piscivores**
Arithmetic mean	14.79	22.67	14.41	27.07	20.06	2.53
Geometric mean	**7.21**	**14.7**	**9.42**	**19.42**	**9.56**	**2.58**
Lower bound	39.63	40.54	41.74	44.88	42.71	27.79
Maximum bound	93.82	108.31	90.71	132.25	112.12	39.26

We deliberately excluded individuals with estimated lengths in the 0–10 cm size class (SWA, SWO and TEA), or with estimated lengths < 10 cm (remaining sites), for consistency among sites, because these individuals tend to be underestimated by visual census techniques (Willis 2001). However, given that the smaller individuals have higher mass-specific metabolic rates, they may contribute substantially size-corrected biomass in reef systems. Inclusion of individuals < 10cm length results in estimates of size-corrected biomass that are ~25% higher (Fig. AI.7), indicating that our estimates of size-corrected biomass and hence energy flux are conservative.

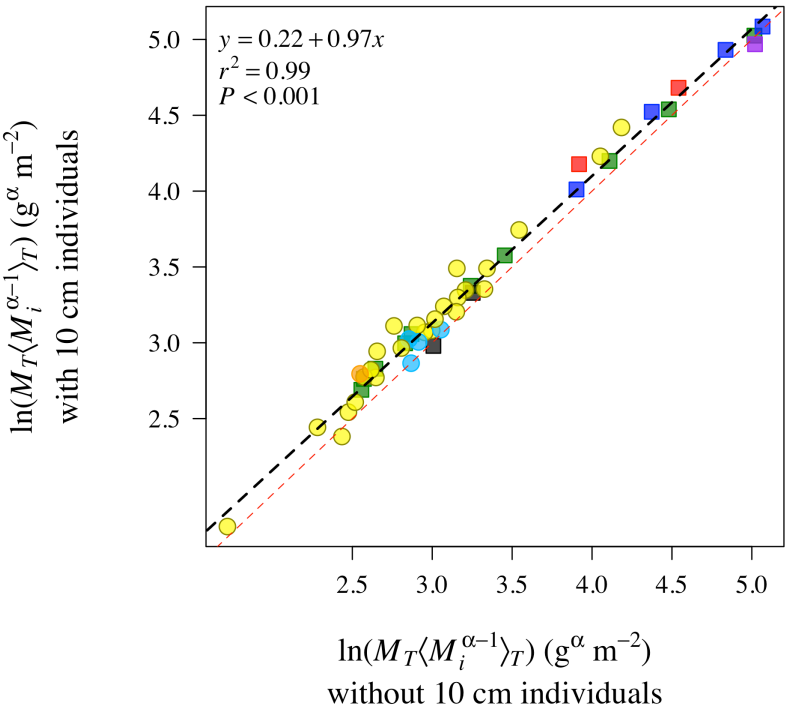

Figure AI.7. Relationship between size-corrected biomass including and excluding individuals smaller than 10 cm. The fit line (black dashed) and r^2 and P values were obtained by applying standard OLS regression to the log-transformed variables. Red dashed line represents a 1:1 fit. The slope of this relationship is ~1, with an intercept of 0.22, which implies that estimates that include individuals < 10cm length are ~25% higher ($= e^{0.22}$ - 1). South Pacific sites are represented by yellow, Tropical Eastern Pacific by purple, South-western Atlantic by green, South-western Atlantic oceanic islands by blue and Tropical Eastern Atlantic by red. Coral-dominated reefs are depicted as circles, and rock-dominated reefs are depicted as squares.

2.2 Size-corrected biomass estimates per trophic group

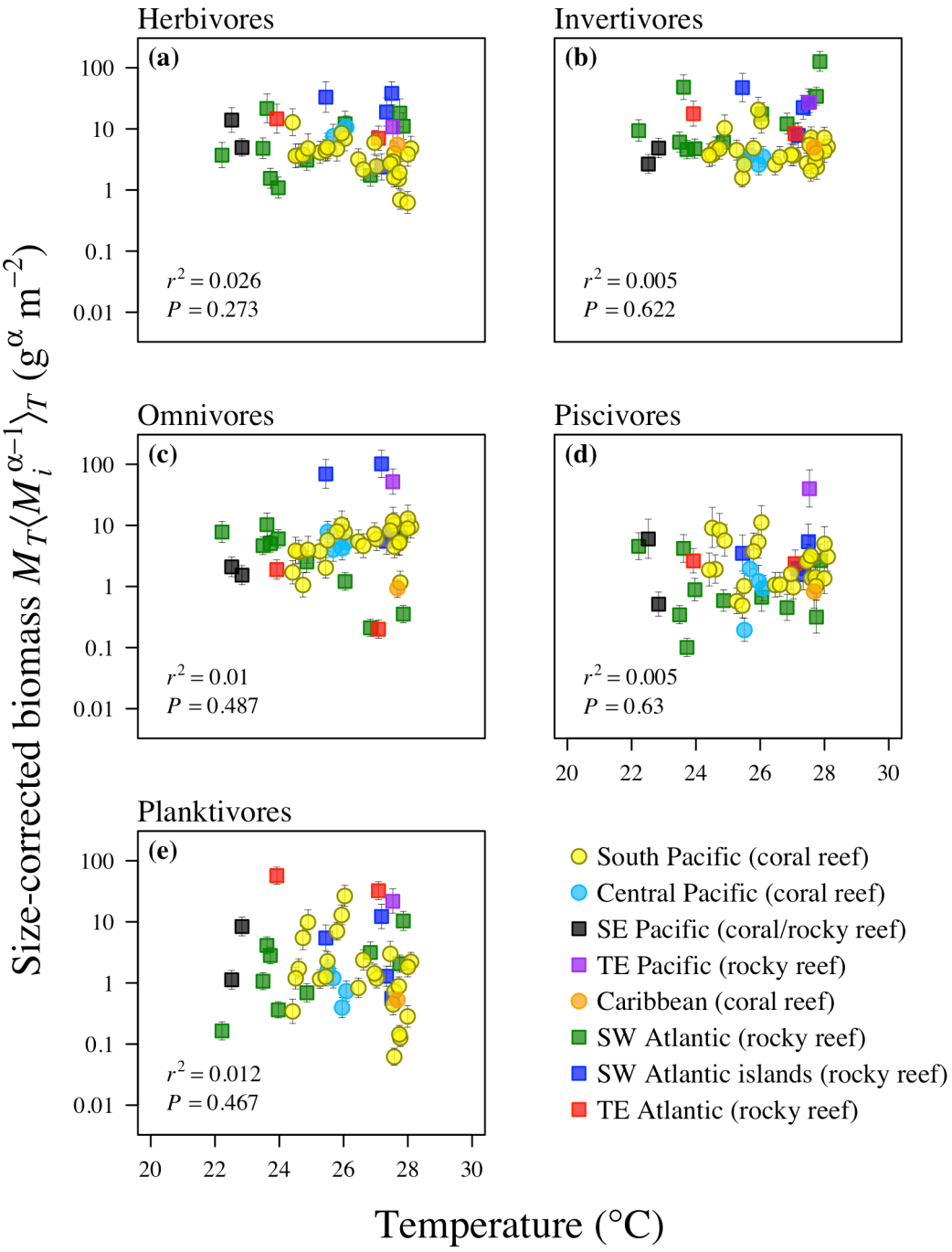

Figure AI.8. Relationship between size-corrected biomass and mean annual temperature for different trophic levels. The r^2 and P values correspond to standard Pearson product-moment correlation tests. Statistical uncertainties in our estimates for the size- and temperature-scaling of fish metabolic rates introduced errors of negligible magnitude into our community-level estimates of size-corrected biomass (represented by 95% CI bars in the figure).

2.3 Turbidity data

We used ocean-colour derived estimates of total suspended matter (TSM) as proxies for turbidity (Ouillon *et al.* 2008). To estimate TSM, we carried out a series of analyses with satellite-derived ocean colour observations from the SeaWIFS, MODIS, and Medium Resolution Imaging Spectrometer Instrument (MERIS) sensors, following the methodology of Maina *et al.* (2011). Briefly, the Globcolour processor at the European Space Agency's Globcolour project (http://hermes.acri.fr/ GlobColour) was used to process satellite-derived Level 2 data from three sensors to extract monthly level-3 binned products i.e. case I and case II TSM concentrations with their respective flags, at a spatial resolution of ~4.63 km at the equator (http://www.globcolour.info/products_description.html). MERIS Case II algorithm was used to retrieve TSM monthly aggregated data from the three sensors — for the time period 2002–2010 (Schroeder *et al.* 2007). In clear shallow bottoms that are highly complex or reflective, as in coral reefs and atolls, bottom reflection can induce an increase in marine reflectance, which is wrongly interpreted as ocean colour constituents (Boss & Zaneveld 2003; Mumby *et al.* 2004). To address this issue, we used depth flags (< 30 m) derived from the processing of level 2 products, in a logical expression designed to exclude shallow water (< 30 m) pixels. Having masked shallower depths using the depth flags, we assumed similar water column properties in masked areas to those found in adjacent deeper (> 30 m) water pixels, and extrapolated the deeper water pixels to these areas. To achieve this for each layer, we applied 3 × 3 spatial filter, which calculates the median value of 8 pixels adjacent to the pixel being considered. In effect, pixels adjacent to the missing value maintained their original values while the missing pixel was assigned the resulting value from the filter.

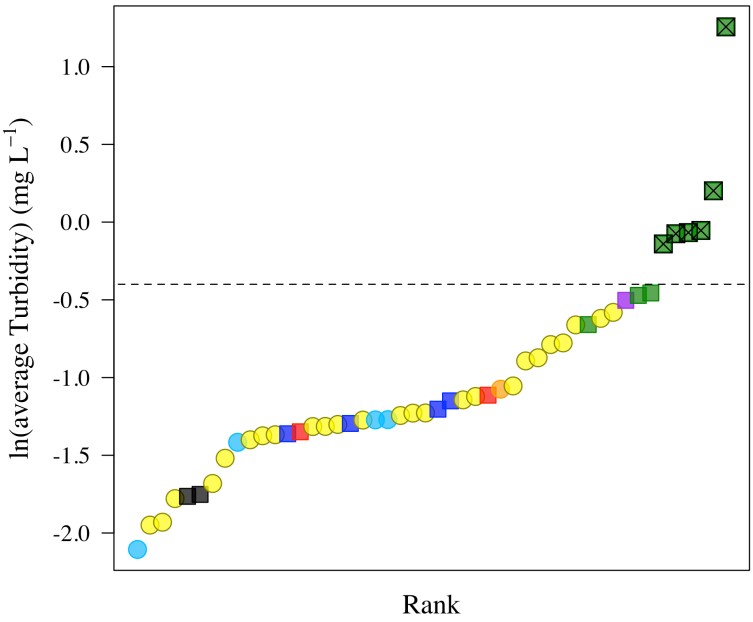

Figure AI.9. The average natural logarithm of total suspended matter. For each site at each time step, we calculated the average total suspended matter available within a 5-km radius from the site coordinate. Dashed line indicates maximum cut-off point above which sites were excluded to re-evaluate hypothesis H4 of Chapter 1. Data for Arraial do Cabo are not represented due to lack of turbidity data.

A recent study demonstrated that turbidity could decrease planktivorous fish ability to find food at higher turbidity levels (Johansen & Jones 2013). The sites with the highest turbidity in our dataset all occur along the Brazilian coast at latitudes below 17 ˚S (sites above dashed line in Fig. AI.9). It was not possible to obtain turbidity data for one site along the Brazilian coast, Arraial do Cabo, due to its harbor location. These sites all occur along the coast in a zone where the continental shelf is particularly broad. Coastal upwelling from the central waters of the South Atlantic are significant below the Abrolhos Archipelago platform, resulting not only in an increase in the amount of nutrients, but also a decrease in water temperature (Piola *et al.* 2005, 2008; Möller *et al.* 2008). The Brazilian coast also receives substantial nutrient inputs from rivers. Thus, environmental characteristics of these sites are distinct from all of the other sites in our database.

2.4 Linear-mixed models for total community respiration

Linear mixed-model analyses were used to assess the statistical significance of variation in respiratory flux in relation to temperature within and among regions. Three nested models were evaluated: (*i*) a model with fixed and random effects (by region) on the slope and intercept of the flux-temperature relationship; (*ii*) a model with a fixed effect on the slope and fixed and random effects on the intercept; (*iii*) a model with fixed and random effects on the intercept, but no (fixed) temperature effect. A comparison of Models (*i*) and (*ii*), fitted using restricted maximum likelihood, yields no evidence that the slope of the size-corrected-biomass-temperature relationship varies among regions (likelihood ratio test: χ^2 = 2.22; d.f. = 2; P = 0.329). Comparisons of Model (*ii*) and (*iii*), using maximum likelihood, indicate that temperature is not significant (likelihood ratio test: χ^2 = 1.90; d.f. = 1; P = 0.169), implying that respiratory fluxes do not vary significantly with temperature after controlling for regional differences. Average respiratory fluxes did however vary significantly among regions (likelihood ratio test: χ^2 = 13.33; d.f. = 1; P < 0.001).

3 REFERENCES

Bates, D., Maechler, M., Bolker, B. & Walker, S. (2015). *lme4:* Linear mixed-effects models using Eigen and S4. R package version 1.1-8. Available at http://www.CRAN.R-project.org/package=lme4.

Boss, E. & Zaneveld, J.R.V. (2003). The effect of bottom substrate on inherent optical properties: evidence of biogeochemical processes. *Limnology and Oceanography*, 48, 346–354.

Bozec, Y.-M., Kulbicki, M., Laloë, F., Mou-Tham, G. & Gascuel, D. (2011). Factors affecting the detection distances of reef fish: implications for visual counts. *Marine Biology*, 158, 969–981.

Carassou, L., Wantiez, L., Ponton, D. & Kulbicki, M. (2012). Can differences in the structure of larval, juvenile and adult coral-reef fish assemblages be detected at the family level? *Austral Ecology*, 37, 374–382.

Chabanet, P., Guillemot, N., Kulbicki, M., Vigliola, L. & Sarramegna, S. (2010). Baseline study of the spatio-temporal patterns of reef fish assemblages prior to a major mining project in New Caledonia (South Pacific). *Marine Pollution Bulletin*, 61, 598–611.

Floeter, S.R., Krohling, W., Gasparini, J.L., Ferreira, C.E. & Zalmon, I.R. (2007). Reef fish community structure on coastal islands of the southeastern Brazil: the influence of exposure and benthic cover. *Environmental Biology of Fishes*, 78, 147–160.

Friedlander, A.M., Ballesteros, E., Beets, J., Berkenpas, E., Gaymer, C.F., Gorny, M. *et al.* (2013). Effects of isolation and fishing on the marine ecosystems of Easter Island and Salas y Gómez, Chile. *Aquatic Conservation: Marine and Freshwater Ecosystems*, 23, 515–531.

Friedlander, A.M., Brown, E. & Monaco, M.E. (2007a). Defining reef fish habitat utilisation patterns in Hawaii: comparisons between marine protected areas and areas open to fishing. *Marine Ecology Progress Series*, 351, 221–233.

Friedlander, A.M., Brown, E.K. & Monaco, M.E. (2007b). Coupling ecology and GIS to evaluate efficacy of marine protected areas in Hawaii. *Ecological Applications*, 17, 715–730.

Friedlander, A.M., Zgliczynski, B.J., Ballesteros, E., Aburto-Oropeza, O., Bolaños, A. & Sala, E. (2012). The shallow-water fish assemblage of Isla del Coco National Park, Costa Rica: structure and patterns in an isolated, predator-dominated ecosystem. *Revista de Biología Tropical*, 60, 321–338.

Froese, R. & Pauly, D. (2012). FishBase. World Wide Web electronic publication. Available at http://www.fishbase.org, (Version 12/2012). Last accessed 20 February 2015.

Johansen, J.L. & Jones, G.P. (2013). Sediment-induced turbidity impairs foraging performance and prey choice of planktivorous coral reef fishes. *Ecological Applications*, 23, 1504–1517.

Kruschke, J.K. (2014). *Doing Bayesian data analysis: A tutorial with R, JAGS, and stan*. 2nd edn. Academic Press, pp. 776.

Kulbicki, M., Bozec, Y.-M., Labrosse, P., Letourneur, Y., Mou-Tham, G. & Wantiez, L. (2005a). Diet composition of carnivorous fishes from coral reef lagoons of New Caledonia. *Aquatic Living Resources*, 18, 231–250.

Kulbicki, M., Guillemot, N. & Amand, M. (2005b). A general approach to length-weight relationships for New Caledonian lagoon fishes. *Cybium*, 29, 235–252.

MacNeil, M.A., Graham, N.A.J., Polunin, N.V.C., Kulbicki, M., Galzin, R., Harmelin-Vivien, M. *et al.* (2009). Hierarchical drivers of reef-fish metacommunity structure. *Ecology*, 90, pp. 252–264.

Maina, J., McClanahan, T.R., Venus, V., Ateweberhan, M. & Madin, J. (2011). Global gradients of coral exposure to environmental stresses and implications for local management. *PLoS ONE*, 6, e23064.

Möller, J.O.O., Piola, A.R., Freitas, A.C. & Campos, E.J.D. (2008). The effects of river discharge and seasonal winds on the shelf off southeastern South America. *Continental Shelf Research*, 28, 1607–1624.

Mumby, P.J., Skirving, W., Strong, A.E., Hardy, J.T., LeDrew, E.F., Hochberg, E.J. *et al.* (2004). Remote sensing of coral reefs and their physical environment. *Marine Pollution Bulletin*, 48, 219–228.

Ouillon, S., Douillet, P., Petrenko, A., Neveux, J., Dupouy, C., Froidefond, J.-M. *et al.* (2008). Optical algorithms at satellite wavelengths for total suspended matter in tropical coastal waters. *Sensors*, 8, 4165–4185.

Piola, A.R., Möller, J.O.O., Guerrero, R.A. & Campos, E.J.D. (2008). Variability of the subtropical shelf front off eastern South America: winter 2003 and summer 2004. *Continental Shelf Research*, 28, 1639–1648.

Piola, A.R., Matano, R.P., Palma, E.D., Möller, J.O.O. & Campos, E.J.D. (2005). The influence of the Plata river discharge on the western South Atlantic shelf. *Geophysical Research Letters*, 32, L01603.

Preuss, B., Pelletier, D., Wantiez, L., Letourneur, Y., Sarramégna, S., Kulbicki, M. *et al.* (2009). Considering multiple-species attributes to understand better the effects of successive changes in protection status on a coral reef fish assemblage. *ICES Journal of Marine Science: Journal du Conseil*, 66, 170–179.

R Core Team (2015). *R: a language and environment for statistical computing*. R Foundation for Statistical Computing, Vienna, Austria.

Randall, J.E. (1967). Food habits of reef fishes of the West Indies. *Studies in Tropical Oceanography Miami*, 5, 665–847.

Robertson, D.R. & Allen, G.R. (2008). Shorefishes of the Tropical Eastern Pacific online information system.

Savage, V.M., Gillooly, J.F., Woodruff, W.H., West, G.B., Allen, A.P., Enquist, B.J. *et al.* (2004). The predominance of quarter-power scaling in biology. *Functional Ecology*, 18, 257–282.

Schoolfield, R., Sharpe, P. & Magnuson, C. (1981). Non-linear regression of biological temperature-dependent rate models based on absolute reaction-rate theory. *Journal of Theoretical Biology*, 88, 719–731.

Schroeder, T., Behnert, I., Schaale, M., Fischer, J. & Doerffer, R. (2007). Atmospheric correction algorithm for MERIS above case-2 waters. *International Journal of Remote Sensing*, 28, 1469–1486.

Su, Y.-S. & Yajima, M. (2015). *R2jags:* A package for running *JAGS* from R. R package version 0.05-03.

Thurston, R.V. & Gehrke, P.C. (1993). Respiratory oxygen requirements of fishes: description of OXYREF, a data file based on test results reported in the published literature. In: *Fish physiology, toxicology, and water quality management. Proceedings of an International Symposium* (eds. Russo, R.C. & Thurston, R.V.). Sacramento, California, USA, pp. 95–108.

Willis, T.J. (2001). Visual census methods underestimate density and diversity of cryptic reef fishes. *Journal of Fish Biology*, 59, 1408–1411.

Zuur, A.F., Ieno, E.N., Walker, N.J., Saveliev, A.A. & Smith, G.M. (2009). *Mixed effects models and extensions in ecology with R*. Springer, New York, pp. 574.

APPENDIX II

SUPPLEMENTARY INFORMATION:

ENERGETIC AND ECOLOGICAL

CONSTRAINTS ON POPULATION DENSITY

1 BAYESIAN MODEL FITTING

Estimates of population density, D_p ($\equiv J_p/A_c$), were calculated for each population at each site using a reef-fish abundance and body mass database (described below), where J_p was taken to be the total number of individuals counted over the entire transect area sampled for the community, A_c. Estimates of temperature kinetics, $\langle K(T)\rangle_c$, and average size-corrected body mass, $\langle M_i^{\alpha}\rangle_p$, were calculated by combining the reef-fish community data with weekly estimates of mean annual sea-surface temperature for each site that were obtained from the CorTAD database between 1997 and 2007 (Selig *et al.* 2010), and the metabolic-rate model of Barneche *et al.* (2014). The metabolic-rate model was fitted using a Markov chain Monte Carlo (MCMC) procedure to 2,036 measurements of routine metabolic rate taken from 43 fish families and 207 species of marine and freshwater species. The metabolic-rate model yielded a Bayesian joint posterior distribution for all of the parameters in eqns 1–3, including α (average of 0.76), E_r (average of 0.59 eV), E_i (average of 2.03 eV), and T_{opt} (average of 306 K). Overall estimates of $\langle M_i^{\alpha}\rangle_p$ for each population and $\langle K(T)\rangle_c$ (standardised to T_s = 20˚C) for each community were calculated by integrating over this joint posterior distribution. Methodologically, this entailed estimating $\langle M_i^{\alpha}\rangle_p$ and $\langle K(T)\rangle_c$ based on the parameter estimates for each MCMC trial, and then averaging the different estimates of $\langle M_i^{\alpha}\rangle_p$ and $\langle K(T)\rangle_c$ across all MCMC trials.

We fit the log-transformed population density data, $\ln D_p$, to our model (eqns 6 and 8) using as predictors population-level estimates of $\langle M_i^{\alpha}\rangle_p$, community-level estimates of $\langle K(T)\rangle_c$, S_c and A_c, and the species-level trophic-group variable (categories: herbivore, omnivore, planktivore, invertivore, piscivore). We fit a total of 30 quantile regression models, which correspond to 30 distinct values of q (0.15, 0.18, …, 0.92, 0.95), by calling *JAGS* version 3.4.0 from the R package *R2jags* version 0.5-6 (Su & Yajima 2015) in R version 3.2.1

(R Core Team 2015). For each model, we estimated posterior distributions of the model parameters – $\langle \ln \widetilde{D_p} \rangle$, $\Delta_c \langle \ln \widetilde{D_p} \rangle$, $\ln \Delta_g$, β_M, β_K, β_S and β_A – using Markov chain Monte Carlo (MCMC) methods by constructing three chains of 100,000 steps each, including 50,000-step burn-in periods. Chains were thinned using a 50-step interval, so a total of 6,000 steps were retained to estimate posterior distributions (i.e. 3 × 100,000/50 = 6,000).

2 JAGS (.BUG) CODE

Mixed-effects quantile regression models were implemented in a Bayesian framework using the Asymmetric Laplace Distribution (ALD) to calculate a likelihood (Yu & Moyeed 2001). The ALD is not built into *JAGS*, so it was coded using the "zeroes trick" (see pp. 204–206 of Lunn *et al.* 2012). Briefly, implementation of this trick involves first coding up a fictitious set of 0s (lines 1–6 in the code below), corresponding to the set of observations, that are assumed to be Poisson distributed (line 33). Given that the likelihood of obtaining a 0 count is equal to $e^{-\lambda}$ for a Poisson distribution with a mean and variance of λ, we will obtain the correct likelihood contribution for each observation, i, up to a multiplicative constant, if its corresponding fictitious 0 is assumed to be Poisson distributed with $\lambda_i = C - \ln L_i$ (line 37), where L_i is the likelihood of obtaining the actual value for observation i under the distribution of interest (in this case, ALD; lines 39–41), and C is an arbitrary constant that is added to ensure that $\lambda_i > 0$ for every observation i. The fixed-effect parameters – $\langle \ln \widetilde{D_p} \rangle$, $\ln \Delta_g$, β_M, β_K, β_S and β_A – were assigned normally-distributed priors with high variance (=1000) (lines 11-19) so that the resulting posterior distributions would be governed by the likelihood (Gelman *et al.* 2013). To enforce the constraint that $\Delta_g = 1$ for the categorical variable used to characterise trophic-group effects, the coefficient for the fifth trophic group (out of 5) was set equal to -1 times the sum of the first four coefficients on the log scale (lines 20-21). Random

effects, $\Delta_c\langle \ln\widetilde{D_p}\rangle$, for the communities, c, were assumed to be normally distributed with a mean of 0 (lines 25-27), so $\langle \ln\widetilde{D_p}\rangle$ corresponds to a mean across communities for the normalised density.

```
1  data {
2      #set up vector for zeros trick
3      for(i in 1:length(lnSizeCorrectedBodyMass)) {
4          zeroes[i] <- 0
5      }
6  }
7
8  model {
9      #priors for fixed effects
10     lSig         ~ dunif(-10000, 10000) #log of ALD scale parameter
11     lnMedianD_p  ~ dnorm(0, 0.001)      #density normalisation
12     beta_M       ~ dnorm(0, 0.001)      #size effect
13     beta_K       ~ dnorm(0, 0.001)      #temperature effect
14     beta_S       ~ dnorm(0, 0.001)      #species effect
15     beta_A       ~ dnorm(0, 0.001)      #area effect
16     #priors for trophic-group fixed effects; sum to 0 on a log scale
17     for(z in 1:4) {
18         lnDelta_g[z] ~ dnorm(0, 1.0E-6)
19     }
20     lnDelta_g[5]  <-  -1*(lnDelta_g[1] + lnDelta_g[2] +
21                           lnDelta_g[3] + lnDelta_g[4])
22
23     #priors for community-level random effects on density normalisation (intercept)
24 lnMedianD_p
25     for(j in 1:max(SiteNumber)) {
26         deltaLnMedianD_p_c[j] ~ dnorm(0, tauR)
27     }
28     tauR    ~  dgamma(1.0E-3, 1.0E-3)
29     sigma2R <- 1/tauR
30
31     #quantile regression using ALD for likelihood calculation
32     for (i in 1:length(lnSizeCorrectedBodyMass)) {
33         zeroes[i]  ~ dpois(phi[i])
34         #value of 10000 is arbitrary
35         #just needs to be big enough to
36         #ensure phi[i] is always > 0
37         phi[i]    <- 10000 - LL[i]
38         #pdf of ALD
39         LL[i]     <- log(densityQuantile*(1-densityQuantile)) -
40                      lSig - (D_p[i]-mu[i]) / exp(lSig) *
41                      (densityQuantile - step(-1*(D_p[i]-mu[i])))
42         mu[i]     <- (lnMedianD_p + lnDelta_g[trophicGroupNumber[i]] +
43                       deltaLnMedianD_p_c[SiteNumber[i]]) +
44                       beta_M*lnSizeCorrectedBodyMass[i] +
45                       beta_K*lnKinetics[i] +
46                       beta_S*lnRichness[i] +
47                       beta_A*lnArea[i]
48     }
49 }
```

3 REEF-FISH COMMUNITY DATABASE

We analysed the same community-level database as in Barneche *et al.* (2014). Data were collected from 49 sites (islands, atolls and coastal contiguous reefs), including 14 sites in the South-western Atlantic (SWA) and its oceanic islands (SWO), 1 site in the Caribbean (CAR), 2 sites in the Tropical Eastern Atlantic (TEA), 1 site in the Tropical Eastern Pacific (TEP), 4 sites in the Central Pacific (CP), 2 sites in the South-eastern Pacific (SEP), and 25 sites in the South Pacific (SP) (Floeter *et al.* 2007; Friedlander *et al.* 2007a, 2007b, 2012, 2013; MacNeil *et al.* 2009; Preuss *et al.* 2009; Chabanet *et al.* 2010; Bozec *et al.* 2011; Carassou *et al.* 2012). The first four authors, together with colleagues, collected these data using standardised belt transects of varying length and width in SWA, SWO and TEA (20 × 2 m), TEP (25 × 2 m and 50 × 2 m), SEP (25 × 2 m and 50 × 2 m), CAR (50 × 2 m), CP (25 × 5 m) and SP (50 × 4 m, 25 × 2 m and 50 × 2 m). Divers tallied the numbers, species identities, and body lengths of all fish simultaneously for 42 of 49 sites. For the other seven sites (Astrolab Reefs and Beautemps-Beaupré Atoll in SP, Isla del Coco in TEP, Ducie Atoll, Henderson Island, Oeno Atoll, Pitcairn Island, Rapa Nui and Salaz y Gómez in SEP), divers first counted all fish ≥ 20 cm length in each 50 × 2 m transect, and then counted all fish < 20 cm length on the way back along the same transect line, but only over a distance of 25 m. Since data for the smaller individuals were only collected over half the transect area (25 × 2 m), counts of individuals < 20 cm length were doubled for density calculations for these seven sites. Community-level estimates of richness, S_c, were calculated as the total numbers of species sampled over the entire sampling area, A_c.

Each species was assigned to one of five trophic groups (herbivores, omnivores, planktivores, invertivores, piscivores) using information in the published literature, online databases (Randall 1967; Kulbicki *et al.* 2005a; Robertson & Allen 2008; Froese & Pauly

2012), and expert judgment. Body masses were inferred from body lengths by estimating the wet weights of individuals using length-weight conversion formulas compiled from the literature and online databases (Kulbicki *et al.* 2005b; Froese & Pauly 2012; see Appendix I). The lengths and species identities of all fish counted within the transect areas were estimated at 10-cm resolution for sites in the South-western Atlantic (including islands) and Tropical Eastern Atlantic (length bins: $<$ 10 cm, 10–20 cm, 20–30 cm, etc.), and at 1-cm resolution for the remaining sites. Individuals $<$ 10 cm in length were excluded from analyses. For sites with 10-cm resolution length data, errors in estimating $\langle {M_i}^{\alpha} \rangle_p$ were minimised by assigning individuals lengths equal to the geometric mean of the bounds of the corresponding 10-cm bin (e.g. all individuals in the 10–20 cm bin were assigned a value of $\sqrt{10 * 20} = 14.14$ cm), as demonstrated by the sensitivity analysis of Barneche *et al.* (2014).

4 RELATIONSHIP OF BODY SIZE TO TROPHIC GROUP

Our reef-fish database yields little evidence that size-corrected body mass increases dramatically with trophic level (Fig. AII.1), contrary to expectations based on pelagic systems (Kerr & Dickie 2001; Jennings & Mackinson 2003; Reuman *et al.* 2009). Fitting a linear mixed-model model to the log-transformed size-corrected body mass data (5609 populations), with trophic group as a fixed effect, and species as a random effect (1169 species), the averages for size-corrected body mass vary only $\leq$ 2.5-fold between planktivores (27 $g^{0.76}$), invertivores (31 $g^{0.76}$), omnivores (33 $g^{0.76}$), herbivores (43 $g^{0.76}$), and piscivores (68 $g^{0.76}$). Overall, these findings suggest the existence of complex relationships between body size and trophic level for reef-fish communities.

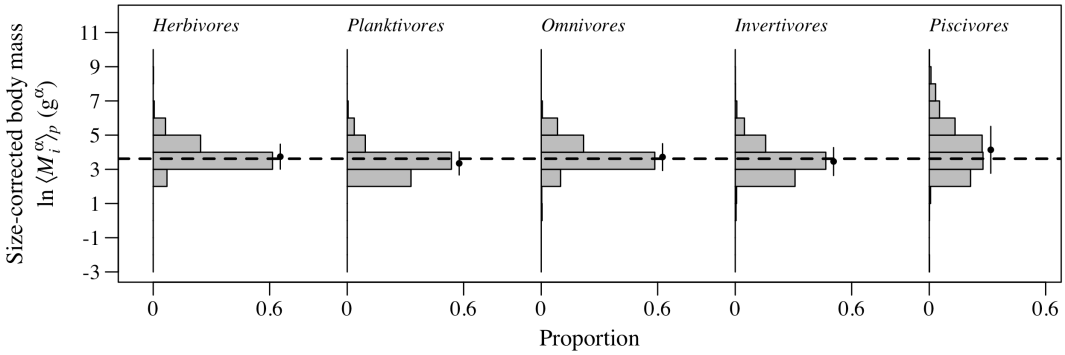

Figure AII.1. Distributions of log-transformed population-level size-corrected body mass values, $\langle M_i^{\alpha} \rangle_p$, for different trophic groups. The dashed line represents the average size-corrected body mass across all populations, and the points represent average size-corrected biomass values ($\pm$ standard deviation) for each trophic group, as directly calculated from the dataset.

5 EFFECT OF AVERAGING ON POPULATION ESTIMATES OF BODY MASS

The Energetic Equivalence Rule is often evaluated using raw arithmetic averages for body mass – an approximation that becomes less accurate as variation in body size increases. In Fig. AII.2 we show the magnitude of the error introduced by this approximation compared to the proper averaging of body mass presented in eqn 5 – see main text.

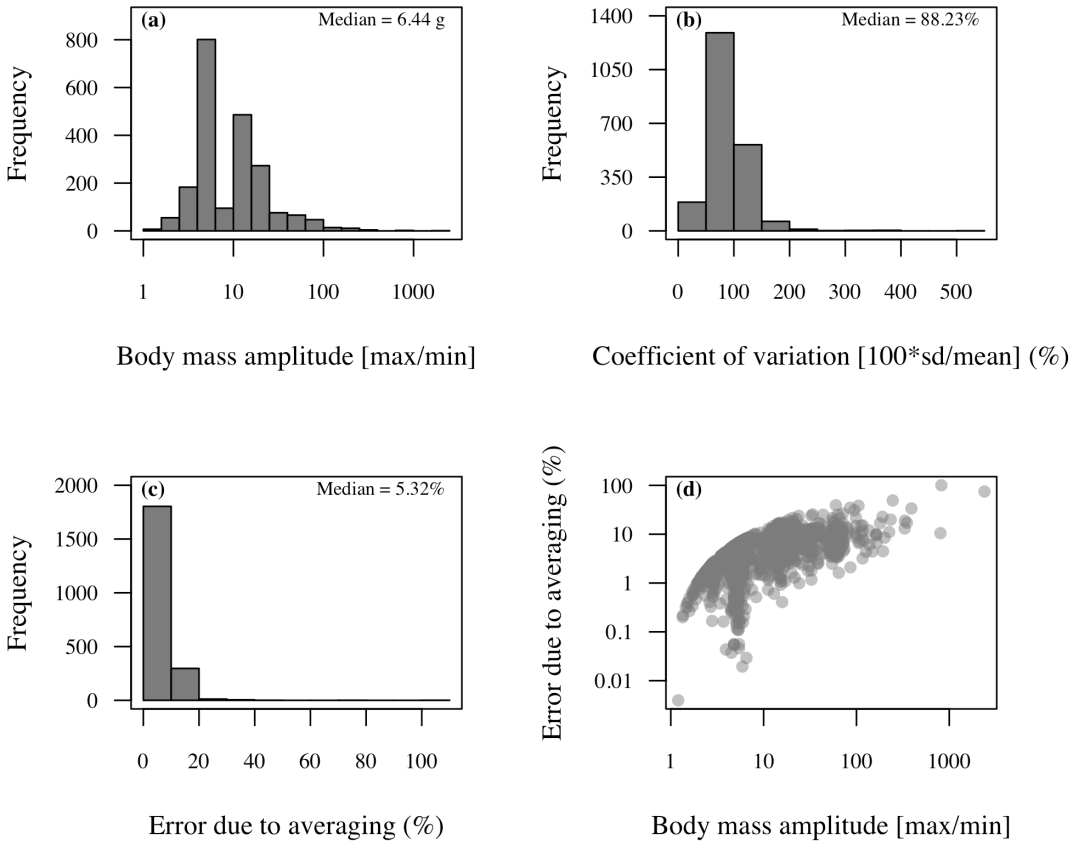

Figure AII.2. The magnitudes of variation in body size within species populations: (a) Body size amplitude (max size/min size), (b) coefficient of variation of individual body size (100 × SD/mean). (c) quantifies the magnitudes of the error introduced by simple arithmetic averaging as $100 \times \langle M \rangle^{3/4} / \langle M^{3/4} \rangle$, where $\langle M \rangle$ is arithmetic average mass. (d) demonstrates that the error attributed to simple arithmetic averaging increases systematically with the body size amplitude. Data shown for the 2121 populations (i.e. 37.8% of the 5609) that had individuals with more than one sampled body size.

We note that: (1) the ratio $\langle M \rangle^{3/4} / \langle M^{3/4} \rangle > 0$, i.e. the error is always additional, and that (2) Fig. AII.2 demonstrates quite convincingly why it is necessary to perform body-size averaging following eqn 5.

6 GOODNESS OF FIT

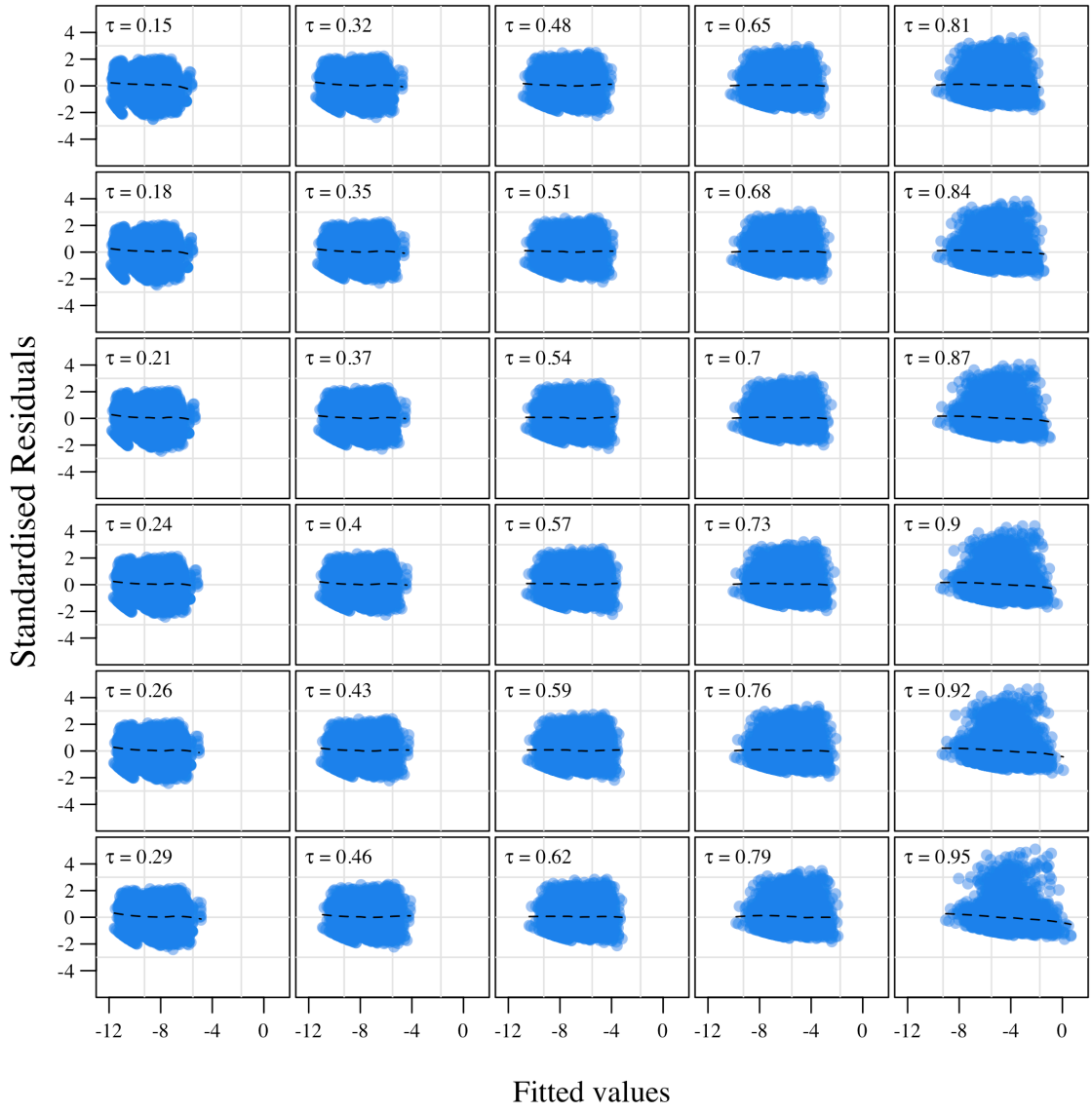

Figure AII.3. Standardised residual plots of the quantile regression model (eqns 6 and 8) across a range of quantiles (τ). Standardised residuals were obtained by transforming the Asymmetric Laplace Distribution quantiles into z-scores in order to normalise them around zero. Dashed lines represent *loess* fits.

7 VARIATION IN POPULATION DENSITY AMONG COMMUNITIES

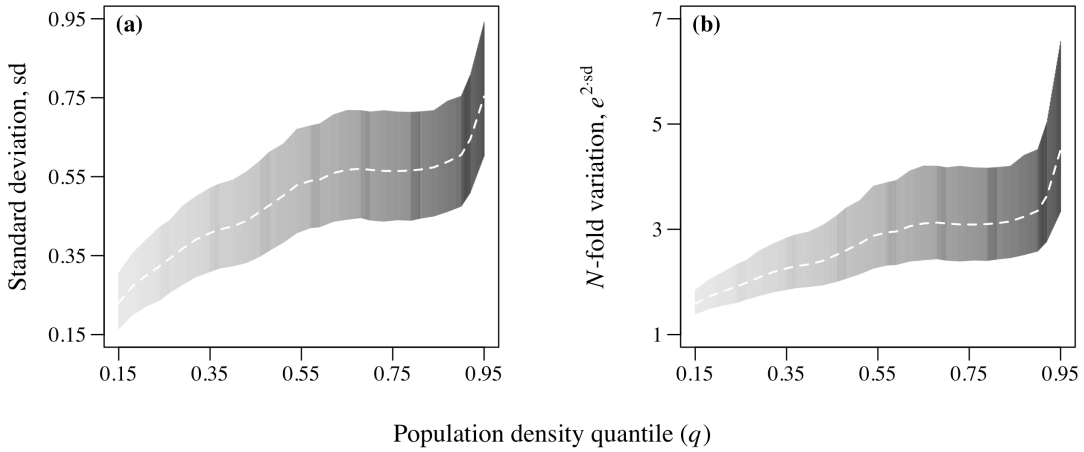

Figure AII.4. (a) Variation in normalised population density among communities, as indexed by the standard deviation of the community-level random effects, $\mathrm{sd}[\Delta_c\langle \ln \widetilde{D_p} \rangle]$, after accounting for the fixed effects of our model (eqns 6 and 8 of the main text). This variation is characterised for a range of population density quantiles, q, which encompasses rare (q = 0.15) to abundant taxa (q = 0.95) (see sections 1 and 2, above). In (b), this variability is expressed as the expected N-fold difference in normalised density for two communities picked at random. Shading represent 95% credible intervals.

8 SENSITIVITY TO MEASURES OF SPECIES RICHNESS

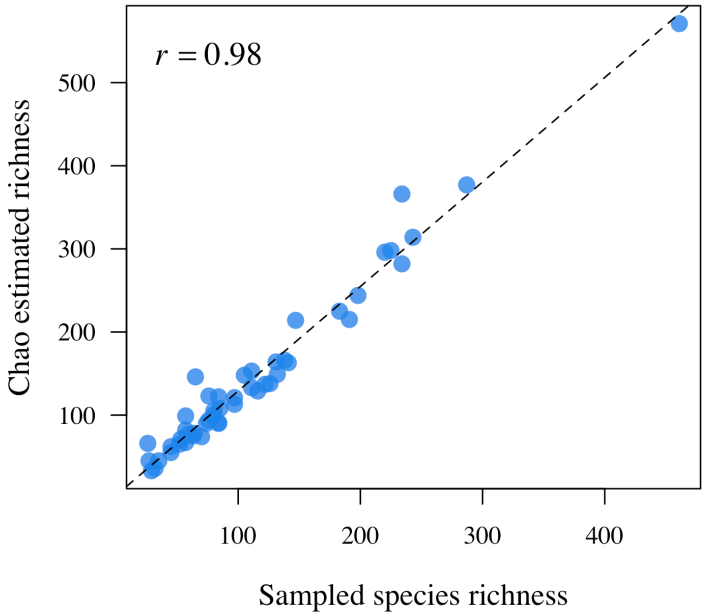

Figure AII.5. Relationships between Chao diversity estimator and 'raw' sampled species richness. *r* represents the Pearson correlation (d.f. = 47, $t = 37.27$, $P < 0.0001$).

9 MODEL WITH RANDOM INTERCEPTS AND SLOPES

In order to assess whether size-density relationships varied within versus across communities, we fit a modified version our model (eqns 6 and 8), treating the size-scaling parameter β_M as having both a fixed and a random effect. Because the size-scaling parameter was allowed to vary among communities, unlike the GSDR model in the main text (see Introduction), this alternative formulation represents an LSDR model. Community-level random effects on β_M were assumed to be normally distributed with a mean of 0. Due the limited sample sizes at the community level, we considered only three population density quantiles, q (0.25, 0.50, 0.75). For these quantiles, community-level estimates for β_M are statistically indistinguishable from the overall estimate of β_M for the GSDR model presented in the main text (Fig. AII.6). Thus,

for the communities in our database, the local relationships between population density and body size are largely consistent with the global relationship.

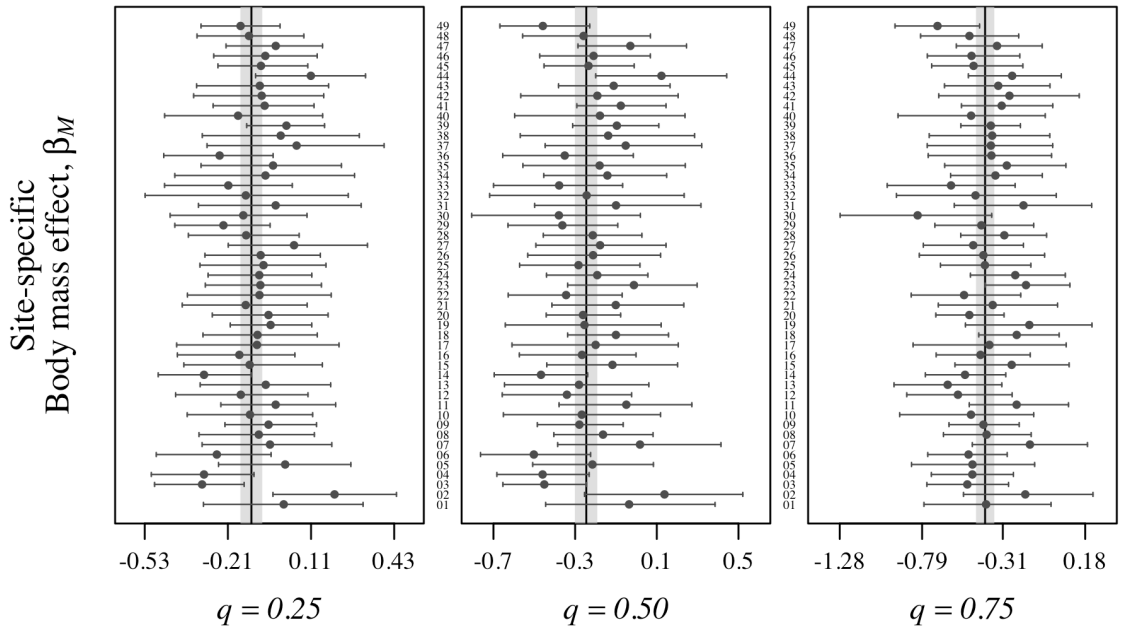

Figure AII.6. Community-level posterior distributions for β_M, at three different density quantiles, for the LSDR model. Points and horizontal lines represent averages and 95% CIs for these posterior distributions. The grey stripe represent the 95% CIs for β_M at the corresponding quantiles, q, for the GSDR model (see eqns 6 and 8 of the main text).

10 SPECIES ABUNDANCE DISTRIBUTIONS

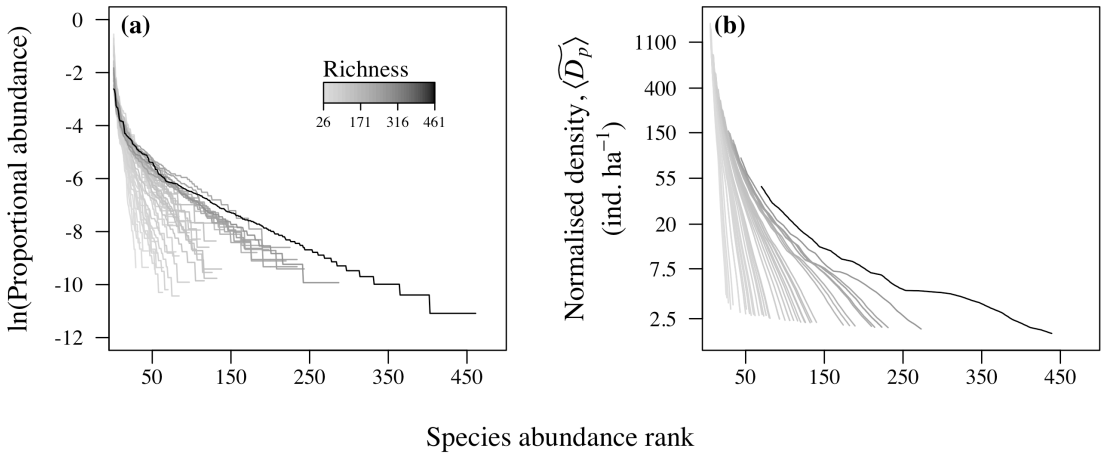

Figure AII.7. Species abundance distributions for the 49 communities of reef fishes sampled in the present study. (a) Abundances are expressed as proportions of the total numbers of individuals counted in each community. (b) Predicted normalised densities as obtained from the quantile regression analyses presented in the main text. Densities were normalised to the median estimates of population-level size-corrected body mass, and community-level temperature kinetics, species richness and sampling area.

9 REFERENCES

Barneche, D.R., Kulbicki, M., Floeter, S.R., Friedlander, A.M., Maina, J. & Allen, A.P. (2014). Scaling metabolism from individuals to reef-fish communities at broad spatial scales. *Ecology Letters*, 17, 1067–1076.

Bozec, Y.-M., Kulbicki, M., Laloë, F., Mou-Tham, G. & Gascuel, D. (2011). Factors affecting the detection distances of reef fish: implications for visual counts. *Marine Biology*, 158, 969–981.

Carassou, L., Wantiez, L., Ponton, D. & Kulbicki, M. (2012). Can differences in the structure of larval, juvenile and adult coral-reef fish assemblages be detected at the family level? *Austral Ecology*, 37, 374–382.

Chabanet, P., Guillemot, N., Kulbicki, M., Vigliola, L. & Sarramegna, S. (2010). Baseline study of the spatio-temporal patterns of reef fish assemblages prior to a major mining project in New Caledonia (South Pacific). *Marine Pollution Bulletin*, 61, 598–611.

Floeter, S.R., Krohling, W., Gasparini, J.L., Ferreira, C.E. & Zalmon, I.R. (2007). Reef fish community structure on coastal islands of the southeastern Brazil: the influence of exposure and benthic cover. *Environmental Biology of Fishes*, 78, 147–160.

Friedlander, A.M., Ballesteros, E., Beets, J., Berkenpas, E., Gaymer, C.F., Gorny, M. *et al.* (2013). Effects of isolation and fishing on the marine ecosystems of Easter Island and Salas y Gómez, Chile. *Aquatic Conservation: Marine and Freshwater Ecosystems*, 23, 515–531.

Friedlander, A.M., Brown, E. & Monaco, M.E. (2007a). Defining reef fish habitat utilisation patterns in Hawaii: comparisons between marine protected areas and areas open to fishing. *Marine Ecology Progress Series*, 351, 221–233.

Friedlander, A.M., Brown, E.K. & Monaco, M.E. (2007b). Coupling ecology and GIS to evaluate efficacy of marine protected areas in Hawaii. *Ecological Applications*, 17, 715–730.

Friedlander, A.M., Zgliczynski, B.J., Ballesteros, E., Aburto-Oropeza, O., Bolaños, A. & Sala, E. (2012). The shallow-water fish assemblage of Isla del Coco national park, Costa Rica: structure and patterns in an isolated, predator-dominated ecosystem. *Revista de Biología Tropical*, 60, 321–338.

Froese, R. & Pauly, D. (2012). FishBase. World Wide Web electronic publication. Available at http://www.fishbase.org, (Version 12/2012). Last accessed 20 February 2015.

Gelman, A., Carlin, J.B., Stern, H.S., Dunson, D.B., Vehtari, A. & Rubin, D.B. (2013). *Bayesian data analysis*. Chapman & hall/CRC texts in Statistical Science. 3rd edn. Chapman & Hall / CRC, London, pp. 675.

Jennings, S. & Mackinson, S. (2003). Abundance-body mass relationships in size-structured food webs. *Ecology Letters*, 6, 971–974.

Kerr, S.R. & Dickie, L.M. (2001). *The biomass spectrum: a predator-prey theory of aquatic production*. Columbia University Press, New York, pp. 352.

Kulbicki, M., Bozec, Y.-M., Labrosse, P., Letourneur, Y., Mou-Tham, G. & Wantiez, L. (2005a). Diet composition of carnivorous fishes from coral reef lagoons of New Caledonia. *Aquatic Living Resources*, 18, 231–250.

Kulbicki, M., Guillemot, N. & Amand, M. (2005b). A general approach to length-weight relationships for New Caledonian lagoon fishes. *Cybium*, 29, 235–252.

Lunn, D., Jackson, C., Best, N., Thomas, A. & Spiegelhalter, D. (2012). *The BUGS book: A practical introduction to Bayesian analysis*. Chapman & hall/CRC texts in statistical science. 1st edn. Chapman & Hall / CRC, London, pp. 399.

MacNeil, M.A., Graham, N.A.J., Polunin, N.V.C., Kulbicki, M., Galzin, R., Harmelin-Vivien, M. *et al.* (2009). Hierarchical drivers of reef-fish metacommunity structure. *Ecology*, 90, pp. 252–264.

Preuss, B., Pelletier, D., Wantiez, L., Letourneur, Y., Sarramégna, S., Kulbicki, M. *et al.* (2009). Considering multiple-species attributes to understand better the effects of successive changes in protection status on a coral reef fish assemblage. *ICES Journal of Marine Science: Journal du Conseil*, 66, 170–179.

R Core Team (2015). *R: a language and environment for statistical computing*. R Foundation for Statistical Computing, Vienna, Austria.

Randall, J.E. (1967). Food habits of reef fishes of the West Indies. *Studies in Tropical Oceanography Miami*, 5, 665–847.

Reuman, D.C., Mulder, C., Banasek-Richter, C., Blandenier, M.-F.C., Breure, A.M., Hollander, H.D. *et al.* (2009). Allometry of body size and abundance in 166 food webs. *Advances in Ecological Research*, 41, 1–44.

Robertson, D.R. & Allen, G.R. (2008). Shorefishes of the Tropical Eastern Pacific online information system.

Selig, E.R., Casey, K.S. & Bruno, J.F. (2010). New insights into global patterns of ocean temperature anomalies: implications for coral reef health and management. *Global Ecology and Biogeography*, 19, 397–411.

Su, Y.-S. & Yajima, M. (2015).*:* A package for running *JAGS* from R. R package version 0.5-6.

Yu, K. & Moyeed, R.A. (2001). Bayesian quantile regression. *Statistics & Probability Letters*, 54, 437–447.

APPENDIX III

SUPPLEMENTARY INFORMATION:

QUANTIFYING THE ENERGETICS OF

FISH GROWTH AND ITS IMPLICATIONS FOR

ENERGY TRANSFER BETWEEN TROPHIC LEVELS

1 ESTIMATING THE MASS OF MAXIMUM GROWTH RATE FOR DIFFERENT ONTOGENETIC GROWTH MODELS

The West *et al.* (2001) growth model (OGM) and the mass-based model of von Bertalanffy (1938) (VBGM) make fundamentally different assumptions. Nevertheless, for both models, ontogenetic changes in individual mass, m (g), through time, t (d), adhere to an expression of the same general form:

$$\frac{dm}{dt} = xm^{\alpha} - ym^{\beta} = xm^{\alpha}\left(1 - \left(\frac{m}{M}\right)^{\beta-\alpha}\right) \quad , \qquad \text{(AIII.1)}$$

where

$$M = \left(\frac{x}{y}\right)^{\left(\frac{1}{\beta-\alpha}\right)} \quad , \qquad \text{(AIII.2)}$$

is the asymptotic adult mass, meaning that $dm/dt = 0$ (see also Pauly 1980; Moses *et al.* 2008). Also, both models assume that the exponent $\beta = 1$, so it is possible to integrate eqn AIII.1 in order to derive an explicit theoretical expression for the mass of an individual at age t, $m_1(t)$,

$$m_1(t) = M\left(1 - \left(1 - \left(\frac{m_o}{M}\right)^{1-\alpha}\right)e^{-x(1-\alpha)M^{\alpha-1}t}\right)^{1/(\alpha-1)} \quad , \qquad \text{(AIII.3)}$$

where m_o is the mass at birth ($t = 0$). We denote this function by a subscript "1" to allow for comparisons with a different ontogenetic growth curve presented below.

Despite the fact that the OGM and the mass-based VBGM both adhere to eqns AIII.1–AIII.3, their underlying assumptions differ, so the parameters take different values and have different interpretations. The OGM is derived based on energy- and mass-balance constraints (West *et al.* 2001). It partitions the total rate of energy expenditure by an individual, that is its metabolic rate, B, into two components, maintenance of existing biomass and growth of new biomass. The OGM assumes that metabolic rate increases with body mass, m (g), according to a power function of the form $B = B_o m^{\alpha}$, where B_o is metabolic normalization (g C $g^{-\alpha}$ d^{-1}), and α = 3/4, following to the prediction of the model of West *et al.* (1997). Consequently, in the OGM, $x \equiv B_o/E_m$ in the first term of eqn AIII.1, and $y \equiv B_m/E_m$ in the second term, where E_m is the amount of energy required to produce biomass (J g^{-1}) and B_m is the metabolic energy required to maintain biomass (g C d^{-1}). By contrast, the mass-based VBGM assumes that the first term reflects anabolism, and that anabolism scales as $\propto M^{2/3}$, implying that α = 2/3 rather than α = 3/4, as in the OGM. Moreover, while the mass-based VBGM and OGM models both assume that β = 1 for the second term, the mass-based VBGM assumes that this term reflects catabolism rather than maintenance, as in the OGM.

Fisheries scientists generally infer growth rates based on ontogenetic increases in length, $l(t)$ (cm), rather than mass, using a length-based version of the VBGM

$$l(t) = L_{\infty}\left(1 - e^{-k(t-t_0)}\right) = L_{\infty}\left(1 - \left(1 - \frac{l_o}{L_{\infty}}\right)e^{-kt}\right) \quad , \qquad \text{(AIII.4)}$$

where L_{∞} is asymptotic adult length (i.e. length when growth rate is 0), and k is a growth rate parameter (d^{-1}) (Froese & Pauly 2012). In the middle expression, $t_0 < 0$ is a parameter that is fitted to allow length at birth to exceed 0; this parameter corresponds to "negative" ages and therefore has no direct biological interpretation. While this middle expression is the one

typically fitted to data (Froese & Pauly 2012), the last expression is arguably more biologically informative because it directly characterises l_o, the length at birth.

The length-based VBGM in eqn AIII.4 corresponds to the mass-based VBGM model outlined above when specific assumptions about length-weight relationships are upheld. To demonstrate this point, we first note that weight-length relationships for fish are generally expressed using power functions of the form (Froese & Pauly 2012)

$$m = a\, l^b \quad , \qquad \text{(AIII.5)}$$

where a is a normalization (g cm^{-b}) and b is an exponent that characterises any changes in shape over ontogeny. The *a priori* expectation is that $b = 3$ in this equation because this corresponds to a shape that is unchanging as the organism grows in size. Empirical data are largely consistent with this expectation (Fig. AIII.1). Substituting eqn AIII.5 into eqn AIII.4 yields an alternative expression for the ontogenetic growth curve in terms of mass, $m_2(t)$,

$$m_2(t) = a\left(L_\infty\left(1-\left(1-\frac{l_0}{L_\infty}\right)e^{-kt}\right)\right)^b = M\left(1-\left(1-\left(\frac{m_0}{M}\right)^{1/b}\right)e^{-kt}\right)^b \quad . \qquad \text{(AIII.6)}$$

Comparison of the expression for $m_2(t)$ above with the ontogenetic growth curve in eqn AIII.3 demonstrates that, if $\alpha = 2/3$ (corresponding to the mass-based VBGM in eqns AIII.1–AIII.3), and if $b = 3$ (corresponding to the expectation for the weight-length scaling in eqn AIII.5), then eqns AIII.3 and AIII.6 are identical in form such that $k = x(1-\alpha)M^{\alpha-1}$. The equivalence of these two expressions demonstrates that length- and mass-based VBGMs are equivalent provided that $b = 3$ for the weight-length relationship.

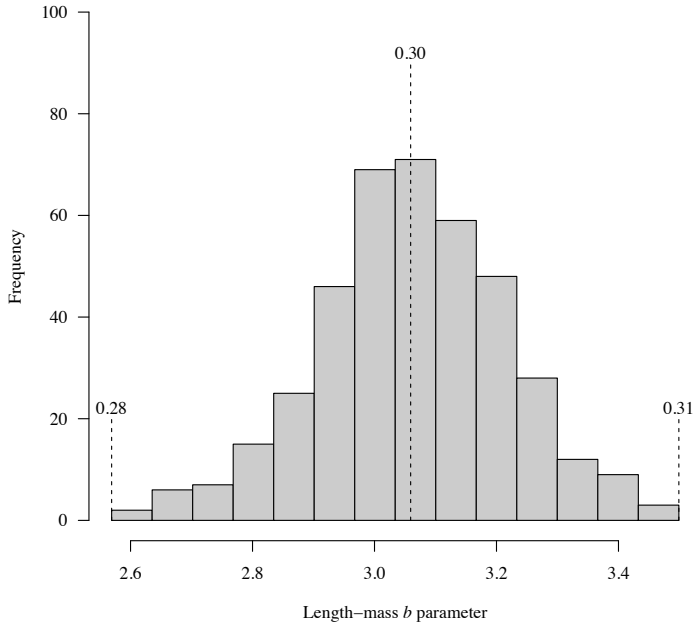

Figure AIII.1. Distribution of 400 species-specific estimates of the length-weight parameter b (eqn AIII.5) for growth-rate Dataset II (described below). The values are centred near 3, as would be if species exhibit negligible changes in shape over ontogeny. Values on top of the dashed lines (2.5%, 50% and 97.5% quantiles) correspond to the estimated ratio of the mass at maximum growth rate ($m_{opt(2)}$) to the asymptotic adult mass (M), i.e. $m_{opt(2)}/M$, as calculated from b using eqn AIII.8.

Using the equations above, the mass at maximum growth rate, m_{opt}, can be estimated for the OGM and mass-based VBGM (eqns AIII.1–AIII.3),

$$m_{opt(1)} = \left(\frac{\alpha x}{\beta y}\right)^{\left(\frac{1}{\beta-\alpha}\right)} = M\left(\frac{\alpha}{\beta}\right)^{\left(\frac{1}{\beta-\alpha}\right)} \quad , \qquad \text{(AIII.7)}$$

and for the length-based VBGM (eqns AIII.4–AIII.6),

$$m_{opt(2)} = a\left(L_\infty\left(1-\frac{1}{b}\right)\right)^b = M\left(1-\frac{1}{b}\right)^b \quad . \qquad \text{(AIII.8)}$$

Eqns AIII.7 and AIII.8 were obtained by taking the second derivatives of mass with respect to time in eqns AIII.3 and AIII.6, respectively, and then setting these derivatives equal to 0 in order to determine the age of maximum growth rate. These ages were then plugged back into eqns AIII.3 and AIII.6 to determine the corresponding masses.

Of particular relevance, the OGM, the mass-based VBGM, and the length-based VBGM all yield nearly identical predictions for the ontogenetic stage at which maximum growth rate is achieved, defined as m_{opt}/M. For example, for the OGM, $m_{opt}/M = (3/4)^4 \approx 0.32$, whereas for the mass-based VBGM and length-based VBGM (with $b = 3$), $m_{opt}/M = (2/3)^3 \approx 0.30$. Moreover, the values of m_{opt}/M appear largely insensitive to empirically observed variation in b (Fig. AIII.1). Thus, the age at which growth rate is maximal, and hence the estimated maximal growth rate, g_{opt}, appears to be relatively insensitive to the specific values of α and b. These results justify our use of m_{opt} and g_{opt} to compare growth rates across species for our analysis of Dataset II (described below). For this analysis, g_{opt} was calculated as

$$g_{opt} = akL_\infty \left(L_\infty \left(1 - \frac{1}{b} \right) \right)^{b-1} \quad \text{(AIII.9)}$$

by substituting the calculated mass in eqn AIII.8 into the derivative of eqn AIII.6 with respect to time.

2 DATA SOURCES

2.1 Dataset I

We compiled a dataset of paired growth and metabolic rates measurements for individual fish at early-life stage, from eggs to juveniles (and one point for a young adult). We searched for data sources on Google Scholar using the key words *fish*, *respiration*, *oxygen consumption* and *growth*. The initial dataset was compiled primarily from tables and figures (one data point was collected from an abstract) in 34 studies published between 1932 and 2010. Prior to analysis, we excluded data corresponding to negative growth-rate estimates (i.e. individuals that were stressed and shrunk in size), and estimates for $\ln E_m^\star$ that fell outside the 95% quantiles from the standardised z-score values (see eqn 7 of the main text for the calculation of $E_m^\star$). The final dataset contains 275 observations from 30 species. For 23 of those studies, data from different figures and tables were combined based on matched body mass and temperature estimates. For 2 studies, growth rates were estimated based on the model parameters provided in the paper. For 8 studies, data were directly obtained from one unique source (i.e. a table or figure) within a given study (Appendix IV). All measurements of growth rates were standardised to g of wet mass d^{-1}, assuming a dry-mass-wet-mass ratio of 15%. Metabolic rate measurements were standardised to g C d^{-1} (see Table AIII.1 below for complete set of unit conversions). For all the studies where growth rates were not explicitly reported, we calculated growth rates as $[\ln(M_1/M_0)M_1]/(t_1 - t_0)$ at mass M_1, assuming an exponential increase in mass from M_0 to M_1 over the time interval t_0 to t_1.

Table AIII.1. Conversion factors used to transform units of metabolism to mg O_2 h^{-1}. Units were then transformed to g C d^{-1} assuming a respiratory quotient of 1.0, implying that 1 mg O_2 h^{-1} = 0.009 g C d^{-1}.

Original units	Multiplication factor to yield mg O_2 h^{-1}
joules d^{-1}	2.84×10^{-3}
nL O_2 h^{-1}	1.429×10^{-6}
µL O_2 h^{-1}	1.429×10^{-3}
mL O_2 h^{-1}	1.429
µg O_2 h^{-1}	1×10^{-3}
nmol O_2 h^{-1}	32×10^{-6}
µmol O_2 h^{-1}	32×10^{-3}
mg O_2 d^{-1}	41.7×10^{-3}

2.2 Dataset II

Growth data in Dataset II were obtained from FishBase (Froese & Pauly 2012), which includes measurements from ~2,000 primary and secondary sources. Growth rates in this database were generally estimated by aging individuals using counting otolith annuli, scale annuli, other annual rings, daily otolith rings, tagging/recaptures, length-frequencies, direct observations. Dataset II contains only data from studies that report all of the following: species identity; L_∞ (cm), and k (yr^{-1}) from the length-based VGBM (eqn AIII.4); mean environmental temperature (K) where the specimen was found; captivity category (captivity-bred or wild); and length-mass conversion parameters (a, b).

Using these parameter estimates, masses and growth rates were calculated as m_{opt} (eqn AIII.8) and g_{opt} (eqn AIII.9). Estimates of a and b were only included if the length-weight function was calibrated using data that encompassed $m_{opt(2)}$, that had quality scores of 0.9 or higher for the function fit, and that had length-weight scaling exponents in the range $2.5 < b < 3.5$ (Froese *et al.* 2014). For species with multiple estimates of a and b, the arithmetic mean of a and geometric mean of b were used, consistent with the fact that most length-mass parameters are estimated by fitted functions of the form $\log m = \log a + b \log l$. The final merged Dataset II contained 2,211 paired estimates of m_{opt} and g_{opt} from 400

species and 52 families at the time we downloaded the datasets from FishBase (February 2015).

3 ESTIMATING THE TEMPERATURE DEPENDENCE OF BIOLOGICAL RATES USING THE BOLTZMANN RELATIONSHIP

Barneche *et al.* (2014) accounted for the existence of optimum temperature, T_{opt}, in metabolic rates of fish, using the Schoolfield-Sharpe equation (Schoolfield *et al.* 1981) to describe the effects of temperature on the mass-normalized metabolic rate, b_o

$$b_o = b_o(T_s)e^{\frac{E_r}{k}\left(\frac{1}{T_s}-\frac{1}{T}\right)}I(T) \quad , \tag{AIII.10}$$

where

$$I(T) = \left(1 + \left(\frac{E_r}{E_i - E_r}\right)e^{\frac{E_i}{k}\left(\frac{1}{T_{opt}}-\frac{1}{T}\right)}\right)^{-1} \quad . \tag{AIII.11}$$

characterises declines in metabolic rates above T_{opt} (K) using an inactivation parameter, E_i (eV). While incorporating a general temperature optimum resulted in a significant improvement in the model, different optima were clearly evident for only a subset of families (Fig. AI.1 in Appendix I). By contrast, for the growth rate data in Datasets I and II, we found no clear evidence of temperature optima (Fig. 3.1 in the main text, Figs. AIII.2–AIII.3), justifying the use of the simple Boltzmann relationship. Because a primary goal of Chapter 3 was to compare the temperature dependence of growth rates from Dataset II and with the temperature dependence of metabolic rate, we refit the metabolic-rate data analysed in

Barneche *et al.* (2014) using a simple exponential Boltzmann relationship (i.e., dropping the $I(T)$ term from eqn AIII.10). Although this refitting decreased the mean estimate of E_r, the 95% credible intervals still overlap the 0.6–0.7 eV range (Table AIII.2).

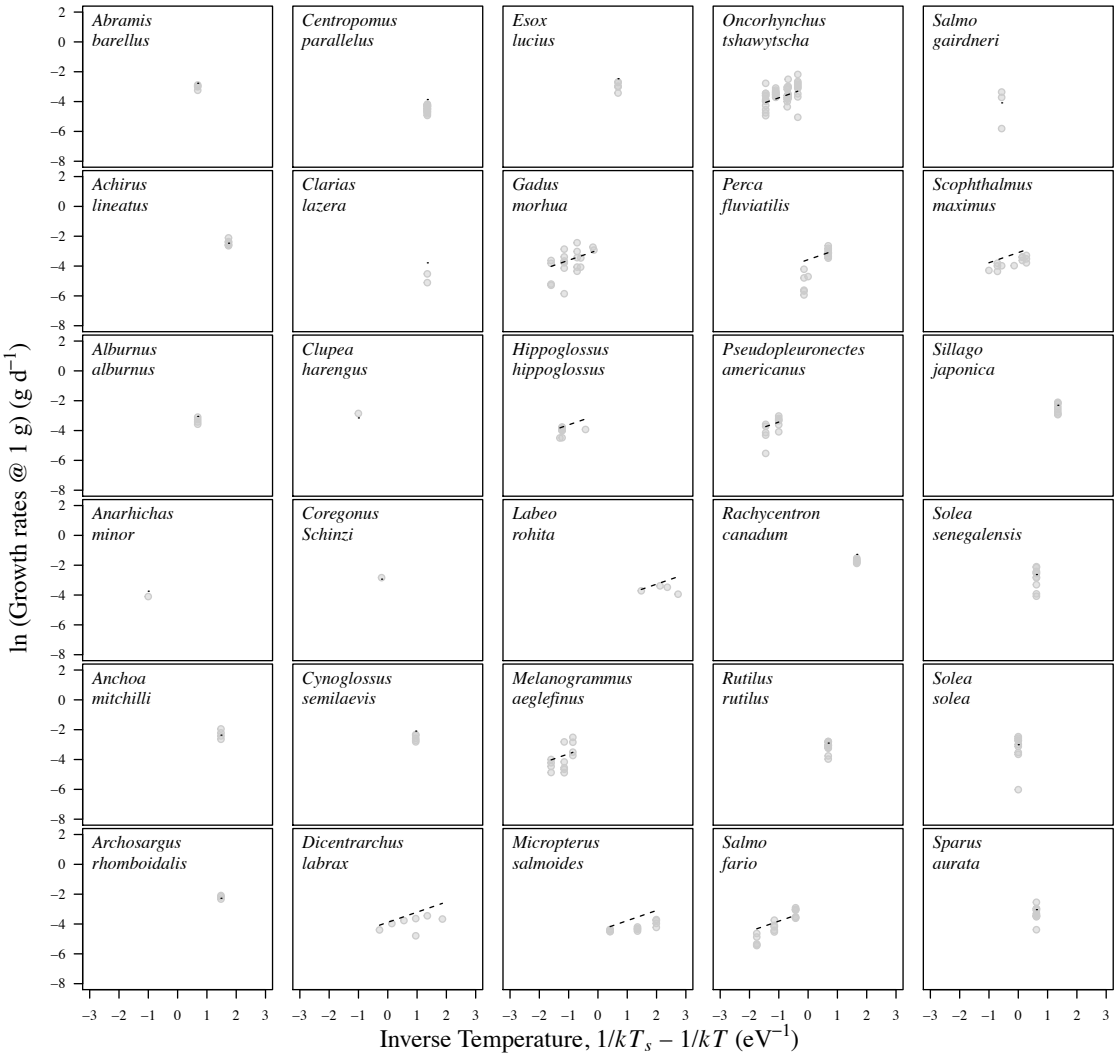

Figure AIII.2. Temperature scaling of size-corrected growth rates for each of the species in Dataset I. Data were size-corrected using the size-scaling parameter, α, from *JAGS* (α = 0.82).

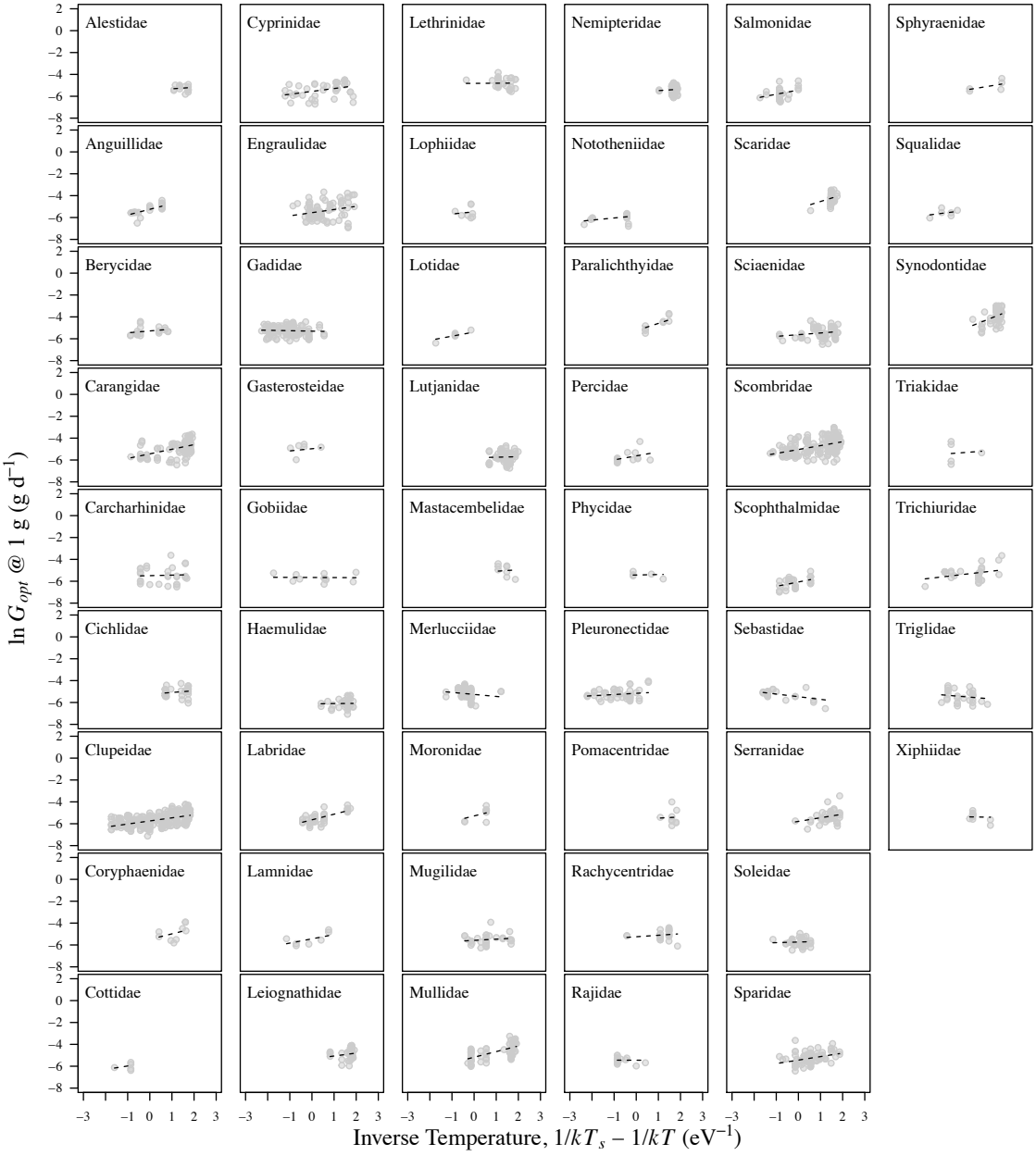

Figure AIII.3. Temperature scaling of size-corrected growth rates for each of the families in Dataset II. Data were size-corrected using family-specific parameter estimates obtained from *JAGS*.

Table AIII.2. Point estimates and 95% credible intervals (as determined using Bayesian methods) for fitted parameters in the metabolic rate models. Fixed-effect parameters include: α, the average for the mass-dependence of metabolic rate; E_r, the average for the temperature dependence of metabolic rate; $\ln b_o(T_s)$, the average for the mass-corrected metabolic rate at temperature T_s = 15 ˚C; $\Delta\theta$ (Dataset I only), deviations from $\ln b_o(T_s)$ for different ontogenetic stages. Random-effects include the variance for species- (Dataset I) and family-level (Dataset II) variation in mass-corrected rates at T_s ($\Delta\ln b_o(T_s)$) as well as variance for family-level size dependence ($\Delta\alpha$) and temperature dependence ΔE_r.

	Dataset I			Dataset II		
Parameter	**Mean**	**2.5% CI**	**97.5% CI**	**Mean**	**2.5% CI**	**97.5% CI**
Fixed effects						
Mass, α	0.83	0.80	0.87	0.76	0.68	0.85
Activation energy, E_r (eV)	0.49	0.38	0.59	0.48	0.36	0.60
Normalisation, $\ln b_o(T_s)$ (g C $g^{-\alpha}$ d^{-1})	-5.94	-6.26	-5.62	-5.84	-6.04	-5.63
$\Delta\theta$ eggs	-0.57	-1.11	-0.02	-	-	-
$\Delta\theta$ yolk-sac larvae	-0.07	-0.57	0.45	-	-	-
$\Delta\theta$ larvae without yolk	-0.26	-0.58	0.05	-	-	-
$\Delta\theta$ larvae undefined	0.68	0.27	1.08	-	-	-
$\Delta\theta$ juveniles	0.06	-0.28	0.42	-	-	-
$\Delta\theta$ adult	0.16	-0.56	0.89	-	-	-
Random effects						
Variance of $\Delta\alpha$	-	-	-	0.06	0.04	0.10
Variance of ΔE_r	-	-	-	0.10	0.06	0.17
Variance of $\Delta\ln b_o(T_s)$	0.42	0.22	0.75	0.31	0.17	0.52
Covariance of $\Delta\alpha$ and ΔE_r	-	-	-	0.01	-0.01	0.04
Covariance of $\Delta\alpha$ and $\Delta\ln b_o(T_s)$	-	-	-	-0.06	-0.13	-0.01
Covariance of $\Delta\ln b_o(T_s)$ and ΔE_r	-	-	-	-0.03	-0.10	0.04

4 PREDICTING MAXIMUM TRANSFER EFFICIENCY

The rate of energy assimilation by an organism of size m, $A(m)$, is equal to the sum of the energy assimilated as respiration, B, and biomass, $E_c(dm/dt)$,

$$A(m) = B + E_c\frac{dm}{dt} =$$

$$B + E_c\frac{B}{E_m}\left[1 - \left(\frac{m}{M}\right)^{1-\alpha}\right] = B_o m^{\alpha}\left(1 + \frac{E_c}{E_m}\left[1 - \left(\frac{m}{M}\right)^{1-\alpha}\right]\right) \quad , \qquad \text{(AIII.12)}$$

where E_c is the combustion energy content of biomass, which is ~24,000 J g^{-1} on a dry mass (Hou *et al.* 2008). Only the energy assimilated by the prey organism as biomass, $E_c m$, when it

is consumed at size m is transferred to the next trophic level. Hence, the efficiency of energy transfer, ε, to the next trophic level is constrained to be less than or equal to the following ratio

$$\varepsilon = \frac{E_c m}{\int_{t=0}^{t=-4E_m/B_o M^{1-\alpha} \ln\left[1-\left(\frac{m}{M}\right)^{1-\alpha}\right]} A\left(m_1(t)\right) dt} \quad \text{(AIII.13)}$$

for a prey organism consumed at size m. The corresponding age at which the prey item was consumed, $-4E_m/B_o M^{1-\alpha} \ln\left[1-\left(\frac{m}{M}\right)^{1-\alpha}\right]$, is obtained by solving for t in eqn AIII.3. The denominator represents the total amount of energy the organism has assimilated over its lifetime. This quantity is calculated by inserting the function for the time-dependence of mass over ontogeny (eqn AIII.3) into the function for the mass-dependence of assimilation rate (eqn AIII.12), and then integrating the resulting expression with respect to time. This integral is readily integrated numerically, as was done to calculate the curves for Fig. 3.4 of the main text. Curves were calculated for different values of E_m (wet mass basis), assuming that m_o= 0 g, α = 0.75, B_o= 132 J $g^{-0.75}$ d^{-1} for fish at 20°C (Barneche *et al.* 2014), and E_c = (24,000 J g^{-1} dry mass)(0.15 g dry mass g^{-1} wet mass) = 3,600 J g^{-1} wet mass (Hou *et al.* 2008). The values for m (size at the time of consumption) and M (asymptotic adult size of the prey individual) are arbitrary because ε depends only on their ratio.

5 REFERENCES

Barneche, D.R., Kulbicki, M., Floeter, S.R., Friedlander, A.M., Maina, J. & Allen, A.P. (2014). Scaling metabolism from individuals to reef-fish communities at broad spatial scales. *Ecology Letters*, 17, 1067–1076.

von Bertalanffy, L. 1938. A quantitative theory of organic growth. (Inquiries on growth laws II). Hum. Biol. 10:181-213.

Froese, R. & Pauly, D. (2012). FishBase. World Wide Web electronic publication. Available at http://www.fishbase.org, (Version 12/2012). Last accessed 20 February 2015.

Froese, R., Thorson, J.T. & Reyes, R.B. (2014). A Bayesian approach for estimating length-weight relationships in fishes. *Journal of Applied Ichthyology*, 30, 78–85.

Hou, C., Zuo, W., Moses, M.E., Woodruff, W.H., Brown, J.H. & West, G.B. (2008). Energy uptake and allocation during ontogeny. *Science*, 322, 736–739.

Moses, M.E., Hou, C., Woodruff, W.H., West, G.B., Nekola, J.C. & Zuo, W. (2008). Revisiting a model of ontogenetic growth: estimating model parameters from theory and data. *The American Naturalist*, 171, pp. 632–645.

Pauly, D. (1980). On the interrelationships between natural mortality, growth parameters, and mean environmental temperature in 175 fish stocks. *Journal du Conseil*, 39, 175–192.

Schoolfield, R., Sharpe, P. & Magnuson, C. (1981). Non-linear regression of biological temperature-dependent rate models based on absolute reaction-rate theory. *Journal of Theoretical Biology*, 88, 719–731.

West, G.B., Brown, J.H. & Enquist, B.J. (1997). A general model for the origin of allometric scaling laws in biology. *Science*, 276, 122–126.

West, G.B., Brown, J.H. & Enquist, B.J. (2001). A general model for ontogenetic growth. *Nature*, 413, 628–631.

APPENDIX IV

DATASET:

DATASET COMPILED FOR CHAPTER THREE

Species	Ontogenetic stage	Growth rate (g wet mass / d)	Metabolic rate (g C /d)	Body wet mass (g)	Temperature (K)	Em* (J / g)	Reference	Growth rate source	Metabolic rate source
Perca fluviatilis	Juvenile	0.0269800	0.0198360	3.8000000	288.15	28673.24	1	Table 3; Page 141	Fig. 1; Page 141
Gadus morhua	NoYolkLarvae	0.0000380	0.0000038	0.0005787	283.98	3862.39	2	Fig. 1; Page 221	Fig. 4; Page 224
Gadus morhua	NoYolkLarvae	0.0001277	0.0000075	0.0011987	284.02	2300.11	2	Fig. 1; Page 221	Fig. 4; Page 224
Gadus morhua	NoYolkLarvae	0.0005104	0.0000237	0.0034160	287.17	1812.73	2	Fig. 1; Page 221	Fig. 4; Page 224
Gadus morhua	NoYolkLarvae	0.0016281	0.0000747	0.0111000	286.93	1790.30	2	Fig. 1; Page 221	Fig. 4; Page 224
Clarias lazera	Juvenile	0.0690154	0.0186780	9.5800000	298.15	10554.80	3	Table 1; Page 4	Table 1; Page 4
Clarias lazera	Juvenile	0.2788758	0.1744980	108.0000000	298.15	24403.06	3	Table 1; Page 4	Table 1; Page 4
Anchoa mitchilli	YolkLarvae	0.0000246	0.0000009	0.0000593	299.15	1427.36	4	Table 3; Page 288	Table 2; Page 287
Anchoa mitchilli	YolkLarvae	0.0000861	0.0000031	0.0002087	299.15	1398.63	4	Table 3; Page 288	Table 2; Page 287
Anchoa mitchilli	YolkLarvae	0.0002705	0.0000073	0.0006567	299.15	1057.00	4	Table 3; Page 288	Table 2; Page 287
Anchoa mitchilli	YolkLarvae	0.0011648	0.0000466	0.0028293	299.15	1558.78	4	Table 3; Page 288	Table 2; Page 287
Archosargus rhomboidalis	YolkLarvae	0.0000601	0.0000023	0.0001207	299.15	1501.22	4	Table 4; Page 288	Table 2; Page 287
Archosargus rhomboidalis	YolkLarvae	0.0001395	0.0000057	0.0002793	299.15	1581.57	4	Table 4; Page 288	Table 2; Page 287
Archosargus rhomboidalis	YolkLarvae	0.0002206	0.0000080	0.0004413	299.15	1409.63	4	Table 4; Page 288	Table 2; Page 287
Achirus lineatus	YolkLarvae	0.0000364	0.0000017	0.0000953	301.15	1793.32	4	Table 5; Page 288	Table 2; Page 287
Achirus lineatus	YolkLarvae	0.0000462	0.0000046	0.0001207	301.15	3912.57	4	Table 5; Page 288	Table 2; Page 287
Achirus lineatus	YolkLarvae	0.0000590	0.0000042	0.0001540	301.15	2803.85	4	Table 5; Page 288	Table 2; Page 287
Achirus lineatus	YolkLarvae	0.0001268	0.0000085	0.0003293	301.15	2610.83	4	Table 5; Page 288	Table 2; Page 287
Achirus lineatus	YolkLarvae	0.0001631	0.0000134	0.0004233	301.15	3197.82	4	Table 5; Page 288	Table 2; Page 287
Achirus lineatus	YolkLarvae	0.0006395	0.0000197	0.0016560	301.15	1199.98	4	Table 5; Page 288	Table 2; Page 287
Clupea harengus	NoYolkLarvae	0.0001799	0.0000030	0.0008733	281.15	655.85	5	Fig. 1; Page 199	Table 5; Page 203
Gadus morhua	LarvaeUnk	0.0000080	0.0000027	0.0003828	277.15	13046.26	6	Fig. 1; Page 3	Fig. 3; Page 4
Gadus morhua	LarvaeUnk	0.0000097	0.0000116	0.0004373	277.15	46492.58	6	Fig. 1; Page 3	Fig. 3; Page 4
Gadus morhua	LarvaeUnk	0.0000886	0.0000083	0.0009417	277.15	3663.74	6	Fig. 1; Page 3	Fig. 3; Page 4
Gadus morhua	LarvaeUnk	0.0001166	0.0000101	0.0016615	277.15	3371.63	6	Fig. 1; Page 3	Fig. 3; Page 4
Gadus morhua	LarvaeUnk	0.0000044	0.0000033	0.0003694	280.15	29066.27	6	Fig. 1; Page 3	Fig. 3; Page 4

Species	Ontogenetic stage	Growth rate (g wet mass / d)	Metabolic rate (g C /d)	Body wet mass (g)	Temperature (K)	Em* (J / g)	Reference	Growth rate source	Metabolic rate source
Gadus morhua	LarvaeUnk	0.0000352	0.0000056	0.0005719	280.15	6262.03	6	Fig. 1; Page 3	Fig. 3; Page 4
Gadus morhua	LarvaeUnk	0.0000943	0.0000134	0.0010622	280.15	5525.05	6	Fig. 1; Page 3	Fig. 3; Page 4
Gadus morhua	LarvaeUnk	0.0001267	0.0000075	0.0017624	280.15	2303.23	6	Fig. 1; Page 3	Fig. 3; Page 4
Gadus morhua	LarvaeUnk	0.0003502	0.0000531	0.0037628	280.15	5912.56	6	Fig. 1; Page 3	Fig. 3; Page 4
Gadus morhua	LarvaeUnk	0.0011429	0.0000872	0.0084530	280.15	2974.63	6	Fig. 1; Page 3	Fig. 3; Page 4
Gadus morhua	LarvaeUnk	0.0000233	0.0000046	0.0004470	283.15	7633.26	6	Fig. 1; Page 3	Fig. 3; Page 4
Gadus morhua	LarvaeUnk	0.0000426	0.0000380	0.0006622	283.15	34801.04	6	Fig. 1; Page 3	Fig. 3; Page 4
Gadus morhua	LarvaeUnk	0.0002889	0.0000408	0.0019143	283.15	5501.71	6	Fig. 1; Page 3	Fig. 3; Page 4
Gadus morhua	LarvaeUnk	0.0003199	0.0000428	0.0035868	283.15	5217.61	6	Fig. 1; Page 3	Fig. 3; Page 4
Gadus morhua	LarvaeUnk	0.0026223	0.0001759	0.0138009	283.15	2616.10	6	Fig. 1; Page 3	Fig. 3; Page 4
Melanogrammus aeglefinus	LarvaeUnk	0.0000308	0.0000175	0.0005369	277.15	22152.58	6	Fig. 2; Page 3	Fig. 4; Page 4
Melanogrammus aeglefinus	LarvaeUnk	0.0000566	0.0000466	0.0008582	277.15	32093.22	6	Fig. 2; Page 3	Fig. 4; Page 4
Melanogrammus aeglefinus	LarvaeUnk	0.0000274	0.0000323	0.0010304	277.15	45915.85	6	Fig. 2; Page 3	Fig. 4; Page 4
Melanogrammus aeglefinus	LarvaeUnk	0.0000515	0.0000534	0.0013493	277.15	40470.12	6	Fig. 2; Page 3	Fig. 4; Page 4
Melanogrammus aeglefinus	LarvaeUnk	0.0000311	0.0000202	0.0005055	280.15	25275.97	6	Fig. 2; Page 3	Fig. 4; Page 4
Melanogrammus aeglefinus	LarvaeUnk	0.0000234	0.0000164	0.0006504	280.15	27313.81	6	Fig. 2; Page 3	Fig. 4; Page 4
Melanogrammus aeglefinus	LarvaeUnk	0.0000217	0.0000186	0.0007880	280.15	33528.10	6	Fig. 2; Page 3	Fig. 4; Page 4
Melanogrammus aeglefinus	LarvaeUnk	0.0000372	0.0000416	0.0010139	280.15	43552.91	6	Fig. 2; Page 3	Fig. 4; Page 4
Melanogrammus aeglefinus	LarvaeUnk	0.0005570	0.0000390	0.0033251	280.15	2732.55	6	Fig. 2; Page 3	Fig. 4; Page 4
Melanogrammus aeglefinus	LarvaeUnk	0.0000536	0.0000164	0.0005806	282.15	11906.96	6	Fig. 2; Page 3	Fig. 4; Page 4
Melanogrammus aeglefinus	LarvaeUnk	0.0001201	0.0000534	0.0011825	282.15	17355.24	6	Fig. 2; Page 3	Fig. 4; Page 4
Melanogrammus aeglefinus	LarvaeUnk	0.0005881	0.0000914	0.0036485	282.15	6060.62	6	Fig. 2; Page 3	Fig. 4; Page 4
Melanogrammus aeglefinus	LarvaeUnk	0.0022713	0.0001516	0.0127118	282.15	2602.90	6	Fig. 2; Page 3	Fig. 4; Page 4
Solea senegalensis	NoYolkLarvae	0.0000586	0.0000013	0.0002109	292.65	835.74	7	Fig. 1a; Page 2177	Fig. 5a; Page 2179
Solea senegalensis	NoYolkLarvae	0.0000839	0.0000055	0.0003413	292.65	2539.61	7	Fig. 1a; Page 2177	Fig. 5a; Page 2179

Species	Ontogenetic stage	Growth rate (g wet mass / d)	Metabolic rate (g C /d)	Body wet mass (g)	Temperature (K)	Em* (J / g)	Reference	Growth rate source	Metabolic rate source
Solea senegalensis	NoYolkLarvae	0.0001784	0.0000124	0.0006070	292.65	2707.94	7	Fig. 1a; Page 2177	Fig. 5a; Page 2179
Solea senegalensis	NoYolkLarvae	0.0001175	0.0000064	0.0009029	292.65	2120.94	7	Fig. 1a; Page 2177	Fig. 5a; Page 2179
Solea senegalensis	NoYolkLarvae	0.0004569	0.0000108	0.0016060	292.65	923.61	7	Fig. 1a; Page 2177	Fig. 5a; Page 2179
Solea senegalensis	NoYolkLarvae	0.0013039	0.0000187	0.0041277	292.65	559.08	7	Fig. 1a; Page 2177	Fig. 5a; Page 2179
Solea senegalensis	NoYolkLarvae	0.0013056	0.0000208	0.0063138	292.65	621.81	7	Fig. 1a; Page 2177	Fig. 5a; Page 2179
Solea senegalensis	NoYolkLarvae	0.0002957	0.0000152	0.0071440	292.65	2010.99	7	Fig. 1a; Page 2177	Fig. 5a; Page 2179
Solea senegalensis	NoYolkLarvae	0.0003888	0.0000336	0.0082373	292.65	3365.53	7	Fig. 1a; Page 2177	Fig. 5a; Page 2179
Solea senegalensis	NoYolkLarvae	0.0045329	0.0001995	0.0178665	292.65	1716.76	7	Fig. 1a; Page 2177	Fig. 5a; Page 2179
Sparus aurata	NoYolkLarvae	0.0000239	0.0000026	0.0001663	292.65	4250.70	7	Fig. 1b; Page 2177	Fig. 5b; Page 2179
Sparus aurata	NoYolkLarvae	0.0000380	0.0000022	0.0002589	292.65	2285.67	7	Fig. 1b; Page 2177	Fig. 5b; Page 2179
Sparus aurata	NoYolkLarvae	0.0000158	0.0000041	0.0002891	292.65	10172.02	7	Fig. 1b; Page 2177	Fig. 5b; Page 2179
Sparus aurata	NoYolkLarvae	0.0000529	0.0000064	0.0004221	292.65	4703.19	7	Fig. 1b; Page 2177	Fig. 5b; Page 2179
Sparus aurata	NoYolkLarvae	0.0001056	0.0000105	0.0005994	292.65	3871.57	7	Fig. 1b; Page 2177	Fig. 5b; Page 2179
Sparus aurata	NoYolkLarvae	0.0001518	0.0000104	0.0008198	292.65	2666.00	7	Fig. 1b; Page 2177	Fig. 5b; Page 2179
Sparus aurata	NoYolkLarvae	0.0001231	0.0000186	0.0011426	292.65	5899.32	7	Fig. 1b; Page 2177	Fig. 5b; Page 2179
Sparus aurata	NoYolkLarvae	0.0002915	0.0000193	0.0018295	292.65	2588.39	7	Fig. 1b; Page 2177	Fig. 5b; Page 2179
Sparus aurata	NoYolkLarvae	0.0002731	0.0000493	0.0025263	292.65	7040.91	7	Fig. 1b; Page 2177	Fig. 5b; Page 2179
Sparus aurata	NoYolkLarvae	0.0008363	0.0000810	0.0038992	292.65	3777.63	7	Fig. 1b; Page 2177	Fig. 5b; Page 2179
Oncorhynchus tshawytscha	Egg	0.0012177	0.0000229	0.0081899	278.15	732.62	8	Fig. 1; Page 181	Fig. 3; Page 182
Oncorhynchus tshawytscha	Egg	0.0016460	0.0000503	0.0330409	278.15	1191.72	8	Fig. 1; Page 181	Fig. 3; Page 182
Oncorhynchus tshawytscha	Egg	0.0009979	0.0000537	0.0394425	278.15	2099.21	8	Fig. 1; Page 181	Fig. 3; Page 182
Oncorhynchus tshawytscha	Egg	0.0029193	0.0000599	0.0544192	278.15	800.70	8	Fig. 1; Page 181	Fig. 3; Page 182
Oncorhynchus tshawytscha	Egg	0.0020831	0.0000841	0.0675343	278.15	1575.32	8	Fig. 1; Page 181	Fig. 3; Page 182
Oncorhynchus tshawytscha	Egg	0.0010674	0.0001093	0.0784392	278.15	3994.04	8	Fig. 1; Page 181	Fig. 3; Page 182
Oncorhynchus tshawytscha	YolkLarvae	0.0046746	0.0001790	0.1135987	278.15	1493.47	8	Fig. 1; Page 181	Fig. 3; Page 182
Oncorhynchus tshawytscha	YolkLarvae	0.0064307	0.0002229	0.1423801	278.15	1351.75	8	Fig. 1; Page 181	Fig. 3; Page 182

Species	Ontogenetic stage	Growth rate (g wet mass / d)	Metabolic rate (g C /d)	Body wet mass (g)	Temperature (K)	Em* (J / g)	Reference	Growth rate source	Metabolic rate source
Oncorhynchus tshawytscha	YolkLarvae	0.0047048	0.0003078	0.1838915	278.15	2551.13	8	Fig. 1; Page 181	Fig. 3; Page 182
Oncorhynchus tshawytscha	YolkLarvae	0.0079430	0.0004637	0.3027344	278.15	2276.97	8	Fig. 1; Page 181	Fig. 3; Page 182
Oncorhynchus tshawytscha	YolkLarvae	0.0030953	0.0006154	0.3622375	278.15	7753.77	8	Fig. 1; Page 181	Fig. 3; Page 182
Oncorhynchus tshawytscha	YolkLarvae	0.0057331	0.0008849	0.4684042	278.15	6019.76	8	Fig. 1; Page 181	Fig. 3; Page 182
Oncorhynchus tshawytscha	Egg	0.0006651	0.0000215	0.0077072	280.45	1263.17	8	Fig. 1; Page 181	Fig. 3; Page 182
Oncorhynchus tshawytscha	Egg	0.0011300	0.0000305	0.0129891	280.45	1052.89	8	Fig. 1; Page 181	Fig. 3; Page 182
Oncorhynchus tshawytscha	Egg	0.0021607	0.0000534	0.0242410	280.45	963.72	8	Fig. 1; Page 181	Fig. 3; Page 182
Oncorhynchus tshawytscha	Egg	0.0025250	0.0001037	0.0606136	280.45	1601.43	8	Fig. 1; Page 181	Fig. 3; Page 182
Oncorhynchus tshawytscha	Egg	0.0035576	0.0001418	0.0793283	280.45	1554.24	8	Fig. 1; Page 181	Fig. 3; Page 182
Oncorhynchus tshawytscha	YolkLarvae	0.0051739	0.0002673	0.1062479	280.45	2014.96	8	Fig. 1; Page 181	Fig. 3; Page 182
Oncorhynchus tshawytscha	YolkLarvae	0.0074806	0.0003080	0.1559483	280.45	1605.99	8	Fig. 1; Page 181	Fig. 3; Page 182
Oncorhynchus tshawytscha	YolkLarvae	0.0083317	0.0004682	0.2067668	280.45	2191.72	8	Fig. 1; Page 181	Fig. 3; Page 182
Oncorhynchus tshawytscha	YolkLarvae	0.0134321	0.0010935	0.3943469	280.45	3174.87	8	Fig. 1; Page 181	Fig. 3; Page 182
Oncorhynchus tshawytscha	YolkLarvae	0.0133304	0.0013063	0.4791352	280.45	3821.85	8	Fig. 1; Page 181	Fig. 3; Page 182
Oncorhynchus tshawytscha	Egg	0.0030627	0.0000916	0.0407966	283.15	1165.88	8	Fig. 1; Page 181	Fig. 3; Page 182
Oncorhynchus tshawytscha	Egg	0.0021809	0.0001060	0.0540982	283.15	1896.15	8	Fig. 1; Page 181	Fig. 3; Page 182
Oncorhynchus tshawytscha	Egg	0.0028043	0.0001223	0.0619649	283.15	1701.24	8	Fig. 1; Page 181	Fig. 3; Page 182
Oncorhynchus tshawytscha	Egg	0.0020243	0.0001345	0.0677738	283.15	2591.98	8	Fig. 1; Page 181	Fig. 3; Page 182
Oncorhynchus tshawytscha	Egg	0.0027240	0.0003032	0.0803013	283.15	4340.68	8	Fig. 1; Page 181	Fig. 3; Page 182
Oncorhynchus tshawytscha	YolkLarvae	0.0096376	0.0004133	0.1395375	283.15	1672.34	8	Fig. 1; Page 181	Fig. 3; Page 182
Oncorhynchus tshawytscha	YolkLarvae	0.0053874	0.0007314	0.3450898	283.15	5294.62	8	Fig. 1; Page 181	Fig. 3; Page 182
Oncorhynchus tshawytscha	Egg	0.0030302	0.0000767	0.0359207	283.35	986.78	8	Fig. 1; Page 181	Fig. 3; Page 182
Oncorhynchus tshawytscha	Egg	0.0044295	0.0000997	0.0508829	283.35	878.20	8	Fig. 1; Page 181	Fig. 3; Page 182
Oncorhynchus tshawytscha	Egg	0.0028406	0.0001270	0.0636122	283.35	1743.32	8	Fig. 1; Page 181	Fig. 3; Page 182
Oncorhynchus tshawytscha	Egg	0.0031111	0.0001707	0.0802670	283.35	2139.75	8	Fig. 1; Page 181	Fig. 3; Page 182

Species	Ontogenetic stage	Growth rate (g wet mass / d)	Metabolic rate (g C /d)	Body wet mass (g)	Temperature (K)	Em* (J / g)	Reference	Growth rate source	Metabolic rate source
Oncorhynchus tshawytscha	YolkLarvae	0.0060888	0.0004716	0.1408176	283.35	3020.76	8	Fig. 1; Page 181	Fig. 3; Page 182
Oncorhynchus tshawytscha	YolkLarvae	0.0233303	0.0005475	0.2166393	283.35	915.19	8	Fig. 1; Page 181	Fig. 3; Page 182
Oncorhynchus tshawytscha	YolkLarvae	0.0108695	0.0010843	0.3161974	283.35	3890.61	8	Fig. 1; Page 181	Fig. 3; Page 182
Oncorhynchus tshawytscha	YolkLarvae	0.0105054	0.0012665	0.3918391	283.35	4701.85	8	Fig. 1; Page 181	Fig. 3; Page 182
Oncorhynchus tshawytscha	Egg	0.0028878	0.0000709	0.0257564	285.65	957.54	8	Fig. 1; Page 181	Fig. 3; Page 182
Oncorhynchus tshawytscha	Egg	0.0038971	0.0000939	0.0412893	285.65	939.97	8	Fig. 1; Page 181	Fig. 3; Page 182
Oncorhynchus tshawytscha	Egg	0.0023478	0.0001251	0.0555145	285.65	2077.81	8	Fig. 1; Page 181	Fig. 3; Page 182
Oncorhynchus tshawytscha	Egg	0.0079399	0.0001929	0.0697156	285.65	947.35	8	Fig. 1; Page 181	Fig. 3; Page 182
Oncorhynchus tshawytscha	Egg	0.0092027	0.0002230	0.0936255	285.65	945.24	8	Fig. 1; Page 181	Fig. 3; Page 182
Oncorhynchus tshawytscha	YolkLarvae	0.0212373	0.0004446	0.1298528	285.65	816.52	8	Fig. 1; Page 181	Fig. 3; Page 182
Oncorhynchus tshawytscha	YolkLarvae	0.0123397	0.0006754	0.2084897	285.65	2134.69	8	Fig. 1; Page 181	Fig. 3; Page 182
Oncorhynchus tshawytscha	YolkLarvae	0.0170000	0.0009897	0.2818702	285.65	2270.39	8	Fig. 1; Page 181	Fig. 3; Page 182
Oncorhynchus tshawytscha	YolkLarvae	0.0023312	0.0012883	0.2916402	285.65	21552.37	8	Fig. 1; Page 181	Fig. 3; Page 182
Oncorhynchus tshawytscha	YolkLarvae	0.0122463	0.0011434	0.3247164	285.65	3641.39	8	Fig. 1; Page 181	Fig. 3; Page 182
Cynoglossus semilaevis	Juvenile	0.6417834	0.0328077	15.9503000	295.15	1993.66	9	Fig. 1; Page 125	Fig. 3a; Page 127
Cynoglossus semilaevis	Juvenile	1.0692688	0.0394475	19.7969000	295.15	1438.79	9	Fig. 1; Page 125	Fig. 3a; Page 127
Cynoglossus semilaevis	Juvenile	1.5849523	0.0599328	30.1477000	295.15	1474.73	9	Fig. 1; Page 125	Fig. 3a; Page 127
Cynoglossus semilaevis	Juvenile	2.0060041	0.0949565	54.3913000	295.15	1846.11	9	Fig. 1; Page 125	Fig. 3a; Page 127
Cynoglossus semilaevis	Juvenile	3.0502226	0.1634698	121.4758000	295.15	2090.12	9	Fig. 1; Page 125	Fig. 3a; Page 127
Rutilus rutilus	NoYolkLarvae	0.0001395	0.0000228	0.0025000	293.15	6362.37	10	Table 1; Page 502	Table 1; Page 502
Rutilus rutilus	NoYolkLarvae	0.0006761	0.0000303	0.0041000	293.15	1750.54	10	Table 1; Page 502	Table 1; Page 502
Rutilus rutilus	NoYolkLarvae	0.0010528	0.0000540	0.0073000	293.15	2001.52	10	Table 1; Page 502	Table 1; Page 502
Rutilus rutilus	NoYolkLarvae	0.0010930	0.0000800	0.0101000	293.15	2854.18	10	Table 1; Page 502	Table 1; Page 502
Rutilus rutilus	NoYolkLarvae	0.0021749	0.0000983	0.0169000	293.15	1762.98	10	Table 1; Page 502	Table 1; Page 502
Rutilus rutilus	NoYolkLarvae	0.0008914	0.0001184	0.0186000	293.15	5179.60	10	Table 1; Page 502	Table 1; Page 502
Centropomus parallelus	Juvenile	0.0870000	0.0495000	8.2500000	298.15	22189.66	11	Table 3; Page 36	Table 3; Page 36

Species	Ontogenetic stage	Growth rate (g wet mass / d)	Metabolic rate (g C /d)	Body wet mass (g)	Temperature (K)	Em* (J / g)	Reference	Growth rate source	Metabolic rate source
Centropomus parallelus	Juvenile	0.0650000	0.0506250	8.5500000	298.15	30375.00	11	Table 3; Page 36	Table 3; Page 36
Centropomus parallelus	Juvenile	0.0900000	0.0521250	9.1600000	298.15	22587.50	11	Table 3; Page 36	Table 3; Page 36
Centropomus parallelus	Juvenile	0.0590000	0.0585000	11.4500000	298.15	38669.49	11	Table 3; Page 36	Table 3; Page 36
Centropomus parallelus	Juvenile	0.0390000	0.0495000	7.8400000	298.15	49500.00	11	Table 3; Page 36	Table 3; Page 36
Centropomus parallelus	Juvenile	0.0870000	0.0513750	9.1800000	298.15	23030.17	11	Table 3; Page 36	Table 3; Page 36
Centropomus parallelus	Juvenile	0.0650000	0.0510000	8.6400000	298.15	30600.00	11	Table 3; Page 36	Table 3; Page 36
Centropomus parallelus	Juvenile	0.0930000	0.0555000	10.7100000	298.15	23274.19	11	Table 3; Page 36	Table 3; Page 36
Centropomus parallelus	Juvenile	0.0650000	0.0577500	11.3100000	298.15	34650.00	11	Table 3; Page 36	Table 3; Page 36
Centropomus parallelus	Juvenile	0.0620000	0.0547500	9.9900000	298.15	34439.52	11	Table 3; Page 36	Table 3; Page 36
Centropomus parallelus	Juvenile	0.0650000	0.0540000	9.7400000	298.15	32400.00	11	Table 3; Page 36	Table 3; Page 36
Centropomus parallelus	Juvenile	0.0790000	0.0517500	9.0700000	298.15	25547.47	11	Table 3; Page 36	Table 3; Page 36
Centropomus parallelus	Juvenile	0.0840000	0.0570000	11.1700000	298.15	26464.29	11	Table 3; Page 36	Table 3; Page 36
Centropomus parallelus	Juvenile	0.1040000	0.0592500	12.1700000	298.15	22218.75	11	Table 3; Page 36	Table 3; Page 36
Perca fluviatilis	Juvenile	0.0291725	0.0168482	18.7500000	287.15	22523.99	12	Table 2; Page 708	Table 2; Page 708
Perca fluviatilis	Juvenile	0.0758038	0.0128903	7.3500000	287.15	6631.90	12	Table 2; Page 708	Table 2; Page 708
Perca fluviatilis	Juvenile	0.0421109	0.0103071	7.2900000	287.15	9545.71	12	Table 2; Page 708	Table 2; Page 708
Perca fluviatilis	Juvenile	0.0249982	0.0147794	11.3000000	287.15	23057.58	12	Table 2; Page 708	Table 2; Page 708
Perca fluviatilis	Juvenile	0.0172736	0.0140600	6.7000000	287.15	31744.32	12	Table 2; Page 708	Table 2; Page 708
Salmo gairdneri	Juvenile	0.0093628	0.0113715	4.0200000	284.15	47366.93	13	Table 3; Page 32	Fig. 5; Page 37
Salmo gairdneri	Juvenile	2.5669763	0.3342769	297.0000000	284.15	5078.66	13	Table 3; Page 32	Fig. 5; Page 37
Salmo gairdneri	Adult	17.4382741	1.8847998	1982.0000000	284.15	4215.28	13	Table 3; Page 32	Fig. 5; Page 37
Esox lucius	Juvenile	0.1530134	0.0111926	3.7920000	293.15	2852.76	14	Table 1; Page 502	Table 1; Page 502
Esox lucius	Juvenile	0.0814179	0.0088344	3.0690000	293.15	4231.77	14	Table 1; Page 502	Table 1; Page 502
Esox lucius	Juvenile	0.1980599	0.0122280	3.8100000	293.15	2407.82	14	Table 1; Page 502	Table 1; Page 502
Esox lucius	Juvenile	0.0997320	0.0084690	2.3700000	293.15	3311.78	14	Table 1; Page 502	Table 1; Page 502

Species	Ontogenetic stage	Growth rate (g wet mass / d)	Metabolic rate (g C /d)	Body wet mass (g)	Temperature (K)	Em* (J / g)	Reference	Growth rate source	Metabolic rate source
Esox lucius	Juvenile	0.1795824	0.0106272	3.2940000	293.15	2307.91	14	Table 1; Page 502	Table 1; Page 502
Perca fluviatilis	Juvenile	0.0841968	0.0055967	2.1850000	293.15	2592.39	14	Table 1; Page 502	Table 1; Page 502
Perca fluviatilis	Juvenile	0.0859364	0.0059025	2.2760000	293.15	2678.70	14	Table 1; Page 502	Table 1; Page 502
Perca fluviatilis	Juvenile	0.0803928	0.0083134	2.8560000	293.15	4032.98	14	Table 1; Page 502	Table 1; Page 502
Perca fluviatilis	Juvenile	0.0819977	0.0089399	3.2610000	293.15	4252.01	14	Table 1; Page 502	Table 1; Page 502
Perca fluviatilis	Juvenile	0.0851233	0.0085658	2.8560000	293.15	3924.48	14	Table 1; Page 502	Table 1; Page 502
Perca fluviatilis	Juvenile	0.1183541	0.0085747	3.1860000	293.15	2825.53	14	Table 1; Page 502	Table 1; Page 502
Perca fluviatilis	Juvenile	0.1426966	0.0091061	2.8540000	293.15	2488.77	14	Table 1; Page 502	Table 1; Page 502
Perca fluviatilis	Juvenile	0.2034870	0.0104511	3.6010000	293.15	2003.05	14	Table 1; Page 502	Table 1; Page 502
Perca fluviatilis	Juvenile	0.2145797	0.0178144	5.4090000	293.15	3237.78	14	Table 1; Page 502	Table 1; Page 502
Perca fluviatilis	Juvenile	0.1469795	0.0149285	4.5910000	293.15	3961.17	14	Table 1; Page 502	Table 1; Page 502
Coregonus Schinzi	NoYolkLarvae	0.0135604	0.0010521	0.1670000	286.65	3025.86	15	abstract; Page 333	Fig. 1c; Page 336
Solea solea	NoYolkLarvae	0.0001022	0.0000013	0.0005168	288.15	492.40	16	Fig. 1; Page 833	Fig. 3; Page 836
Solea solea	NoYolkLarvae	0.0000050	0.0000009	0.0005219	288.15	7333.70	16	Fig. 1; Page 833	Fig. 3; Page 836
Solea solea	NoYolkLarvae	0.0000574	0.0000014	0.0005742	288.15	935.28	16	Fig. 1; Page 833	Fig. 3; Page 836
Solea solea	NoYolkLarvae	0.0000784	0.0000023	0.0007204	288.15	1148.93	16	Fig. 1; Page 833	Fig. 3; Page 836
Solea solea	NoYolkLarvae	0.0002450	0.0000028	0.0011175	288.15	447.81	16	Fig. 1; Page 833	Fig. 3; Page 836
Solea solea	NoYolkLarvae	0.0003626	0.0000045	0.0014527	288.15	481.94	16	Fig. 1; Page 833	Fig. 3; Page 836
Solea solea	NoYolkLarvae	0.0004232	0.0000087	0.0034315	288.15	802.58	16	Fig. 1; Page 833	Fig. 3; Page 836
Solea solea	Juvenile	0.0026591	0.0000285	0.0145861	288.15	417.66	16	Fig. 1; Page 833	Fig. 3; Page 836
Solea solea	Juvenile	0.0059630	0.0001420	0.0514725	288.15	928.91	16	Fig. 1; Page 833	Fig. 3; Page 836
Hippoglossus hippoglossus	NoYolkLarvae	0.0000737	0.0000036	0.0011150	279.65	1909.21	17	Fig. 5; Page 652	Fig. 1; Page 650
Hippoglossus hippoglossus	NoYolkLarvae	0.0000860	0.0000040	0.0014302	279.65	1832.36	17	Fig. 5; Page 652	Fig. 1; Page 650
Hippoglossus hippoglossus	NoYolkLarvae	0.0001139	0.0000046	0.0017593	279.65	1577.77	17	Fig. 5; Page 652	Fig. 1; Page 650
Hippoglossus hippoglossus	NoYolkLarvae	0.0000698	0.0000046	0.0019998	279.65	2587.66	17	Fig. 5; Page 652	Fig. 1; Page 650
Hippoglossus hippoglossus	NoYolkLarvae	0.0001698	0.0000057	0.0024625	279.65	1317.16	17	Fig. 5; Page 652	Fig. 1; Page 650

Species	Ontogenetic stage	Growth rate (g wet mass / d)	Metabolic rate (g C /d)	Body wet mass (g)	Temperature (K)	Em* (J / g)	Reference	Growth rate source	Metabolic rate source
Hippoglossus hippoglossus	NoYolkLarvae	0.0001590	0.0000081	0.0030447	279.65	1990.41	17	Fig. 5; Page 652	Fig. 1; Page 650
Hippoglossus hippoglossus	NoYolkLarvae	0.0002211	0.0000115	0.0036856	279.65	2019.53	17	Fig. 5; Page 652	Fig. 1; Page 650
Hippoglossus hippoglossus	NoYolkLarvae	0.0002866	0.0000153	0.0049218	279.65	2076.38	17	Fig. 5; Page 652	Fig. 1; Page 650
Alburnus alburnus	NoYolkLarvae	0.0003040	0.0000205	0.0040000	293.15	2628.95	18	Table 7; Page 40	Table 7; Page 40
Alburnus alburnus	NoYolkLarvae	0.0009467	0.0000564	0.0133333	293.15	2321.62	18	Table 7; Page 40	Table 7; Page 40
Alburnus alburnus	NoYolkLarvae	0.0034667	0.0001870	0.0533333	293.15	2103.67	18	Table 7; Page 40	Table 7; Page 40
Alburnus alburnus	NoYolkLarvae	0.0183333	0.0009196	0.3333333	293.15	1956.23	18	Table 7; Page 40	Table 7; Page 40
Abramis barellus	NoYolkLarvae	0.0015200	0.0000717	0.0133333	293.15	1840.27	18	Table 7; Page 40	Table 7; Page 40
Abramis barellus	NoYolkLarvae	0.0050667	0.0002587	0.0533333	293.15	1991.43	18	Table 7; Page 40	Table 7; Page 40
Abramis barellus	NoYolkLarvae	0.0200000	0.0014012	0.3333333	293.15	2732.27	18	Table 7; Page 40	Table 7; Page 40
Abramis barellus	NoYolkLarvae	0.0280000	0.0026538	0.6666667	293.15	3696.31	18	Table 7; Page 40	Table 7; Page 40
Rutilus rutilus	NoYolkLarvae	0.0004440	0.0000205	0.0040000	293.15	1800.00	18	Table 7; Page 40	Table 7; Page 40
Rutilus rutilus	NoYolkLarvae	0.0013333	0.0000589	0.0133333	293.15	1723.28	18	Table 7; Page 40	Table 7; Page 40
Rutilus rutilus	NoYolkLarvae	0.0044800	0.0002177	0.0533333	293.15	1895.43	18	Table 7; Page 40	Table 7; Page 40
Rutilus rutilus	NoYolkLarvae	0.0190000	0.0011911	0.3333333	293.15	2444.93	18	Table 7; Page 40	Table 7; Page 40
Rutilus rutilus	NoYolkLarvae	0.0280000	0.0022695	0.6666667	293.15	3161.13	18	Table 7; Page 40	Table 7; Page 40
Sillago japonica	LarvaeUnk	0.0000555	0.0000053	0.0002297	298.15	3732.13	19	model Fig. 2 Page 60 of ref. 32	Fig. 1; Page 208
Sillago japonica	LarvaeUnk	0.0000707	0.0000072	0.0002925	298.15	3996.51	19	model Fig. 2 Page 60 of ref. 32	Fig. 1; Page 208
Sillago japonica	LarvaeUnk	0.0001460	0.0000133	0.0006041	298.15	3563.59	19	model Fig. 2 Page 60 of ref. 32	Fig. 1; Page 208
Sillago japonica	LarvaeUnk	0.0003841	0.0000238	0.0015889	298.15	2415.90	19	model Fig. 2 Page 60 of ref. 32	Fig. 1; Page 208
Sillago japonica	LarvaeUnk	0.0010104	0.0000856	0.0041791	298.15	3302.95	19	model Fig. 2 Page 60 of ref. 32	Fig. 1; Page 208
Sillago japonica	LarvaeUnk	0.0033845	0.0002268	0.0139986	298.15	2613.30	19	model Fig. 2 Page 60 of ref. 32	Fig. 1; Page 208
Sillago japonica	LarvaeUnk	0.0043101	0.0002089	0.0178273	298.15	1890.03	19	model Fig. 2 Page 60 of ref. 32	Fig. 1; Page 208
Sillago japonica	LarvaeUnk	0.0054890	0.0002388	0.0227031	298.15	1696.89	19	model Fig. 2 Page 60 of ref. 32	Fig. 1; Page 208
Rachycentron canadum	Juvenile	0.0210400	0.0005638	0.0578000	300.55	1045.07	20	Table 1; Page 229	Table 1; Page 229

Species	Ontogenetic stage	Growth rate (g wet mass / d)	Metabolic rate (g C /d)	Body wet mass (g)	Temperature (K)	Em* (J / g)	Reference	Growth rate source	Metabolic rate source
Rachycentron canadum	Juvenile	0.0303733	0.0009080	0.1021333	300.55	1165.83	20	Table 1; Page 229	Table 1; Page 229
Rachycentron canadum	Juvenile	0.0419467	0.0013611	0.1652667	300.55	1265.47	20	Table 1; Page 229	Table 1; Page 229
Rachycentron canadum	Juvenile	0.0550667	0.0022222	0.2506667	300.55	1573.84	20	Table 1; Page 229	Table 1; Page 229
Rachycentron canadum	Juvenile	0.0700400	0.0026198	0.3620667	300.55	1458.76	20	Table 1; Page 229	Table 1; Page 229
Rachycentron canadum	Juvenile	0.0868933	0.0031457	0.5030000	300.55	1411.87	20	Table 1; Page 229	Table 1; Page 229
Scophthalmus maximus	Juvenile	0.1345569	0.0152512	17.6552000	283.15	4420.42	21	Fig. 1; Page 151	Fig. 5a; Page 155
Scophthalmus maximus	Juvenile	0.2203220	0.0211424	20.5979000	283.15	3742.50	21	Fig. 1; Page 151	Fig. 5c; Page 155
Scophthalmus maximus	Juvenile	0.3009680	0.0231959	24.2716000	283.15	3005.77	21	Fig. 1; Page 151	Fig. 5e; Page 155
Scophthalmus maximus	Juvenile	1.3225335	0.1332860	87.9298000	289.15	3930.45	21	Fig. 1; Page 151	Fig. 5b; Page 155
Scophthalmus maximus	Juvenile	1.1954342	0.1534077	103.8049000	289.15	5004.79	21	Fig. 1; Page 151	Fig. 5d; Page 155
Scophthalmus maximus	Juvenile	1.7154018	0.1478917	124.5598000	289.15	3362.35	21	Fig. 1; Page 151	Fig. 5f; Page 155
Labeo rohita	NoYolkLarvae	0.2271899	0.0079894	15.3000000	299.14	1371.47	22	Table 3; Page 382	Table 2; Page 381
Labeo rohita	NoYolkLarvae	0.3755629	0.0111977	18.8400000	304.15	1162.82	22	Table 3; Page 382	Table 2; Page 381
Labeo rohita	NoYolkLarvae	0.3196388	0.0119317	17.3800000	306.15	1455.82	22	Table 3; Page 382	Table 2; Page 381
Labeo rohita	NoYolkLarvae	0.1714214	0.0120122	14.3100000	309.15	2732.90	22	Table 3; Page 382	Table 2; Page 381
Scophthalmus maximus	Juvenile	1.5447280	0.3433012	172.8498000	290.15	8667.38	23	Fig. 2a; Page 107	Fig. 3a; Page 109
Scophthalmus maximus	Juvenile	2.2832170	0.3175848	151.3152000	290.15	5424.72	24	Fig. 1a; Page 878	Fig. 2a; Page 879
Dicentrarchus labrax	Juvenile	0.3176253	0.2505505	85.5056400	295.15	30764.14	24	Fig. 1b; Page 878	Fig. 2b; Page 879
Scophthalmus maximus	Juvenile	0.4460979	0.0476575	70.4370000	281.15	4166.45	25	Fig. 1e; Page 683	Fig. 3; Page 688
Scophthalmus maximus	Juvenile	0.7019520	0.0777247	83.6155000	284.15	4318.33	25	Fig. 1e; Page 683	Fig. 3; Page 688
Scophthalmus maximus	Juvenile	0.7638030	0.1456280	92.0172000	287.15	7435.81	25	Fig. 1e; Page 683	Fig. 3; Page 688
Scophthalmus maximus	Juvenile	1.3276605	0.1861624	103.5478000	290.15	5468.52	25	Fig. 1e; Page 683	Fig. 3; Page 688
Anarhichas minor	Juvenile	0.7306699	0.0739879	102.0760000	281.15	3949.16	26	Table 1; Page 110	Fig. 2; Page 112
Dicentrarchus labrax	Juvenile	0.5701465	0.1382784	108.1089000	286.15	9458.72	27	Fig. 1; Page 274	Fig. 3b; Page 277
Dicentrarchus labrax	Juvenile	0.9749234	0.1853710	123.3526000	289.15	7415.42	27	Fig. 1; Page 274	Fig. 3b; Page 277
Dicentrarchus labrax	Juvenile	1.3501658	0.2906800	143.6775000	292.15	8396.39	27	Fig. 1; Page 274	Fig. 3b; Page 277

Species	Ontogenetic stage	Growth rate (g wet mass / d)	Metabolic rate (g C /d)	Body wet mass (g)	Temperature (K)	Em* (J / g)	Reference	Growth rate source	Metabolic rate source
Dicentrarchus labrax	Juvenile	1.6729191	0.3524031	158.9213000	295.15	8215.41	27	Fig. 1; Page 274	Fig. 3b; Page 277
Dicentrarchus labrax	Juvenile	2.2033787	0.4525389	177.0686000	298.15	8009.98	27	Fig. 1; Page 274	Fig. 3b; Page 277
Dicentrarchus labrax	Juvenile	1.7671806	0.4896414	176.3427000	302.15	10805.92	27	Fig. 1; Page 274	Fig. 3b; Page 277
Salmo fario	NoYolkLarvae	0.0012043	0.0001759	0.0201300	285.13	5697.73	28	Table 1; Page 272	Table 2; Page 273
Salmo fario	NoYolkLarvae	0.0036968	0.0003733	0.0433600	285.13	3938.29	28	Table 1; Page 272	Table 2; Page 273
Salmo fario	NoYolkLarvae	0.0052095	0.0004538	0.0570300	285.13	3397.34	28	Table 1; Page 272	Table 2; Page 273
Salmo fario	NoYolkLarvae	0.0050273	0.0004675	0.0663600	285.13	3626.30	28	Table 1; Page 272	Table 2; Page 273
Salmo fario	NoYolkLarvae	0.0032732	0.0005115	0.0726200	285.13	6095.08	28	Table 1; Page 272	Table 2; Page 273
Salmo fario	NoYolkLarvae	0.0068683	0.0005345	0.0910600	285.13	3035.23	28	Table 1; Page 272	Table 2; Page 273
Salmo fario	NoYolkLarvae	0.0044678	0.0005808	0.1113000	285.13	5069.45	28	Table 1; Page 272	Table 2; Page 273
Salmo fario	NoYolkLarvae	0.0015842	0.0002601	0.0632900	280.13	6402.20	28	Table 1; Page 272	Table 2; Page 273
Salmo fario	NoYolkLarvae	0.0027205	0.0002917	0.0710000	280.13	4182.30	28	Table 1; Page 272	Table 2; Page 273
Salmo fario	NoYolkLarvae	0.0012508	0.0002968	0.0722400	280.13	9255.79	28	Table 1; Page 272	Table 2; Page 273
Salmo fario	NoYolkLarvae	0.0024373	0.0002370	0.0956200	280.13	3792.17	28	Table 1; Page 272	Table 2; Page 273
Salmo fario	NoYolkLarvae	0.0020102	0.0002051	0.1123300	280.13	3980.04	28	Table 1; Page 272	Table 2; Page 273
Salmo fario	NoYolkLarvae	0.0003981	0.0001488	0.0518400	276.13	14576.11	28	Table 1; Page 272	Table 2; Page 273
Salmo fario	NoYolkLarvae	0.0010346	0.0001860	0.0648200	276.13	7012.42	28	Table 1; Page 272	Table 2; Page 273
Salmo fario	NoYolkLarvae	0.0004807	0.0001968	0.0685600	276.13	15962.07	28	Table 1; Page 272	Table 2; Page 273
Salmo fario	NoYolkLarvae	0.0009598	0.0001655	0.0792800	276.13	6723.68	28	Table 1; Page 272	Table 2; Page 273
Salmo fario	NoYolkLarvae	0.0006964	0.0001604	0.0946000	276.13	8984.40	28	Table 1; Page 272	Table 2; Page 273
Micropterus salmoides	Juvenile	0.0600000	0.0081000	8.0000000	291.15	5265.00	29	Table 3; Page 454	Table 3; Page 454
Micropterus salmoides	Juvenile	0.0700000	0.0090000	8.0000000	298.15	5014.29	29	Table 3; Page 454	Table 3; Page 454
Micropterus salmoides	Juvenile	0.0800000	0.0108000	8.0000000	303.15	5265.00	29	Table 3; Page 454	Table 3; Page 454
Micropterus salmoides	Juvenile	0.3100000	0.0387000	50.0000000	291.15	4868.71	29	Table 3; Page 454	Table 3; Page 454
Micropterus salmoides	Juvenile	0.3700000	0.0387000	50.0000000	298.15	4079.19	29	Table 3; Page 454	Table 3; Page 454

Species	Ontogenetic stage	Growth rate (g wet mass / d)	Metabolic rate (g C /d)	Body wet mass (g)	Temperature (K)	Em* (J / g)	Reference	Growth rate source	Metabolic rate source
Micropterus salmoides	Juvenile	0.4700000	0.0585000	50.0000000	303.15	4854.26	29	Table 3; Page 454	Table 3; Page 454
Micropterus salmoides	Juvenile	0.5500000	0.0684000	100.0000000	291.15	4850.18	29	Table 3; Page 454	Table 3; Page 454
Micropterus salmoides	Juvenile	0.5900000	0.0765000	100.0000000	298.15	5056.78	29	Table 3; Page 454	Table 3; Page 454
Micropterus salmoides	Juvenile	1.0700000	0.1395000	100.0000000	303.15	5084.58	29	Table 3; Page 454	Table 3; Page 454
Micropterus salmoides	Juvenile	0.6800000	0.0837000	150.0000000	291.15	4800.44	29	Table 3; Page 454	Table 3; Page 454
Micropterus salmoides	Juvenile	0.6900000	0.0900000	150.0000000	298.15	5086.96	29	Table 3; Page 454	Table 3; Page 454
Micropterus salmoides	Juvenile	1.3900000	0.1809000	150.0000000	303.15	5075.61	29	Table 3; Page 454	Table 3; Page 454
Hippoglossus hippoglossus	Juvenile	0.6473136	0.0784378	71.2035000	285.15	4725.80	30	Fig. 2; Page 222	Table 1; Page 223
Hippoglossus hippoglossus	Juvenile	0.1778380	0.0229087	29.4267000	279.15	5023.89	30	Fig. 2; Page 222	Table 1; Page 223
Pseudopleuronectes americanus	NoYolkLarvae	0.0000146	0.0000020	0.0001970	278.15	5332.86	31	Fig. 1; Page 224	Fig. 2b; Page 226
Pseudopleuronectes americanus	NoYolkLarvae	0.0000386	0.0000069	0.0003807	278.15	6931.48	31	Fig. 1; Page 224	Fig. 2b; Page 226
Pseudopleuronectes americanus	NoYolkLarvae	0.0000805	0.0000202	0.0007967	278.15	9771.00	31	Fig. 1; Page 224	Fig. 2b; Page 226
Pseudopleuronectes americanus	NoYolkLarvae	0.0000451	0.0000334	0.0042437	278.15	28842.54	31	Fig. 1; Page 224	Fig. 2b; Page 226
Pseudopleuronectes americanus	NoYolkLarvae	0.0002250	0.0000227	0.0067648	278.15	3930.66	31	Fig. 1; Page 224	Fig. 2b; Page 226
Pseudopleuronectes americanus	NoYolkLarvae	0.0000123	0.0000022	0.0001482	281.15	6909.73	31	Fig. 1; Page 224	Fig. 2c; Page 226
Pseudopleuronectes americanus	NoYolkLarvae	0.0001073	0.0000149	0.0005722	281.15	5411.43	31	Fig. 1; Page 224	Fig. 2c; Page 226
Pseudopleuronectes americanus	NoYolkLarvae	0.0001582	0.0000251	0.0013493	281.15	6176.32	31	Fig. 1; Page 224	Fig. 2c; Page 226
Pseudopleuronectes americanus	NoYolkLarvae	0.0003057	0.0000583	0.0028240	281.15	7437.48	31	Fig. 1; Page 224	Fig. 2c; Page 226
Pseudopleuronectes americanus	NoYolkLarvae	0.0003346	0.0000481	0.0046919	281.15	5601.49	31	Fig. 1; Page 224	Fig. 2c; Page 226
Pseudopleuronectes americanus	NoYolkLarvae	0.0009057	0.0000494	0.0093610	281.15	2128.19	31	Fig. 1; Page 224	Fig. 2c; Page 226

REFERENCES

1. Collvin, L. (1984). The effects of copper on maximum prespiration rate and growth rate of perch, *Perca fluviatilis* L. *Water Research* 18, 139–144.
2. Finn, R.N., Rønnestad, I., van der Meeren, T. & Fyhn, H.J. (2002). Fuel and metabolic scaling during the early life of Atlantic cod *Gadus morhua*. *Marine Ecology Progress Series*, 243, 217–234.
3. Hogendoorn, H. (1983). Growth and production of the African catfish, *Clarias lazera* (C. & V.) III. Bioenergetic relations of body weight and feeding level. *Aquaculture*, 35, 1–17.
4. Houde, E.D. & Schekter, R.C. (1983). Oxygen uptake and comparative energetics among eggs and larvae of three subtropical marine fishes. *Marine Biology*, 72, 283–293.
5. Houlihan, D.F., Pedersen, B.H., Steffensen, J.F. & Brechin, J. (1995). Protein synthesis, growth and energetics in larval herring (*Clupea harengus*) at different feeding regimes. *Fish Physiology and Biochemistry*, 14, 195–208.
6. Laurence, G.C. (1978). Comparative growth, respiration and delayed feeding abilities of larval cod (*Gauds morhua*) and Haddock (*Melanogrammus aeglefinus*) as influenced by temperature during laboratory studies. *Marine Biology*, 50, 1–7.
7. Parra, G. & Yúfera, M. (2001). Comparative energetics during early development of two marine fish species, *Solea senegalensis* (Kaup) and *Sparus aurata* (L.). *The Journal of Experimental Biology*, 204, 2175–2183.
8. Rombough, P.J. (1994). Energy partitioning during fish development: additive or compensatory allocation of energy to support growth? *Functional Ecology*, 8, 178–186.
9. Tian, X., Fang, J. & Dong, S. (2010). Effects of starvation and recovery on the growth, metabolism and energy budget of juvenile tongue sole (*Cynoglossus semilaevis*). *Aquaculture*, 310, 122–129.
10. Wieser, W., Forstner, H., Medgyesy, N. & Hinterleitner, S. (1988). To switch or not to switch: partitioning of energy between growth and activity in larval cyprinids (Cyprinidae: Teleostei). *Functional Ecology*, 2, 499–507.
11. Lemos, D., Netto, B. & Germano, A. (2006). Energy budget of juvenile fat snook *Centropomus parallelus* fed live food. *Comparative Biochemistry and Physiology, Part A*, 144, 33–40.12

12. Solomon, D.J., Brafield, A.E. (1972). The energetics of feeding, metabolism and growth of perch (*Perca fluviatilis* L.). *Journal of Animal Ecology*, 41, 699–718.
13. Staples, D.J. & Nomura, M. (1976). Influence of body size and food ration on the energy budget of rainbow trout *Salmo gairdneri* Richardson. *Journal of Fish Biology*, 9, 29–43.
14. Wieser, W. & Medgyesy, N. (1991). Metabolic rate and cost of growth in juvenile pike (*Esox lucius* L.) and perch (*Perca fluviatilis* L.): the use of energy budgets as indicators of environmental change. *Oecologia*, 87, 500–505.
15. Dabrowski, K. & Kaushik S.J. (1984). Rearing of coregonid (*Coregonus schinzi palea* Cuv. et Val.) larvae using dry and live food. II. Oxygen consumption and nitrogen excretion. *Aquaculture*, 41, 333–344.
16. Day, O.J. & Jones, D.A. (1996). Food consumption, growth and respiration of sole, *Solea solea* (L.), during early ontogeny in a hatchery environment. *Aquaculture Research*, 27, 831–839.
17. Finn, R.N., Rønnestad, I & Fyhn, H.J. (1995). Respiration, nitrogen and energy metabolism of developing yolk-sac larvae of Atlantic halibut (*Hippoglossus hippoglossus* L.). *Comparative Biochemistry and Physiology*, 111, 647–671.
18. Keckeis, H. & Schiemer, F. (1992). Food consumption and growth of larvae and juveniles of three cyprinid species at different food levels. *Environmental Biology of Fishes*, 33, 33–45.
19. Oozeki, Y. & Hirano, R. (1994). Changes in oxygen consumption rate during development of larval Japanese whiting, *Sillago japonica*. *Japanese Journal of Ichthyology*, 41, 207–214.
20. Watson, A.M. & Holt, G.J (2010). Energy budget of early juvenile cobia, *Rachycentron canadum*. *Journal of the World Aquaculture Society*, 41, 224–234.
21. Imsland, A.K., Folkvord, A. & Stefansson, S. (1995). Growth, oxygen consumption and activity of juvenile turbot (scophthalmus maximus l.) reared under different temperatures and photoperiods. *Netherlands Journal of Sea Research*, 34, 149–159.
22. Dasa, T., Pal, A.K., Chakraborty, S.K., Manush, S.M., Sahu, N.P. & Mukherjee, S.C. (2005). Thermal tolerance, growth and oxygen consumption of *Labeo rohita* fry (Hamilton, 1822) acclimated to four temperatures. *Journal of Thermal Biology*, 30, 378–383.

23. Pichavant, K., Person-Le-Ruyet, J., Le Bayon, N. Sévère, A., Le Roux, A., Quéméner, L. Maxime, V., Nonnotte, G. & Boeuf, G. (2000). Effect of hypoxia on growth and metabolism of juvenile turbot. *Aquaculture*, 188, 103–114.

24. Pichavant, K., Person-Le-Ruyet, J., Le Bayon, N. Sévère, A., Le Roux, A. & Boeuf, G. (2001). Comparative effects of long-term hypoxia on growth, feeding and oxygen consumption in juvenile turbot and European sea bass. *Journal of Fish Biology*, 59, 875–883.

25. Burel, C., Ruyet, J.P.-L., Gaumet, F., Roux, A.L., Sévère, A. & Boeuf, G. (1996). Effects of temperature on growth and metabolism in juvenile turbot. *Journal of Fish Biology*, 49, 678–692.

26. Foss, A., Vollen, T. & Øiestad, V. (2003). Growth and oxygen consumption in normal and O_2 supersaturated water, and interactive effects of O_2 saturation and ammonia on growth in spotted wolffish (*Anarhichas minor* Olafsen). *Aquaculture*, 224, 105–116.

27. Person-Le Ruyet, J., Mahé, K., Le Bayon, N. & Le Delliou, H. (2004). Effects of temperature on growth and metabolism in a Mediterranean population of European sea bass, *Dicentrarchus labrax*. *Aquaculture*, 237, 269–280.

28. Wood, A.H. (1932). The effect of temperature on the growth and respiration of fish embryos (*Salmo fario*). *Journal of Experimental Biology*, 9, 271–276.

29. Niimi, A.J. & Beamish, F.W.H. (1974). Bioenergetics and growth of largemouth bass (*Micropterus salmoides*) in relation to body weight and temperature. *Canadian Journal of Zoology*, 52, 447–456.

30. Jonassen, T.M., Imsland, A.K., Kadowaki, S. & Stefansson, S.O. (2000). Interaction of temperature and photoperiod on growth of Atlantic halibut *Hippoglossus hippoglossus* L. Aquaculture Research, 31, 219–227.

31. Laurence, G. (1975). Laboratory growth and metabolism of the winter flounder *Pseudopleuronectes americanus* from hatching through metamorphosis at three temperatures. *Marine Biology*, 32, 223–229.

32. Oozeki, Y., Pung-Pung, H. & Hirano, R. (1994). Larval development of the Japanese whiting, *Sillago japonica*. *Japanese Journal of Ichthyology*, 39, 59–66.